OPTIMAL LIMIT DESIGN OF REINFORCED CONCRETE FRAMES

by

C.S. KRISHNAMOORTHY, B.E., M.Sc.(Eng.)

A Thesis submitted for the degree of Doctor of Philosophy

in the Faculty of Engineering of the University of London

Imperial College of Science and Technology

London

October 1972

ABSTRACT

The simplified limit method of Baker for ultimate load analysis of reinforced concrete frames is discussed and a modified computer oriented procedure by adjustment of rotations is suggested for frames which present problems for convergence of solution. A computer program is presented for the analysis of reinforced concrete frames for five different cases of hinge pattern under two ultimate loading conditions. Three multi-storey frames have been designed to illustrate the use of this program. The salient details of design and the results of analysis are described. The amount of moment redistribution in these frames is discussed. It is concluded that the ultimate load analysis program is useful to determine the distribution of moment for any desired plastic hinge pattern.

A linear programming model is proposed for the optimal limit design of reinforced concrete frames with the compatibility and limited ductility, equilibrium and serviceability criteria as the governing constraints. The requirement of minimum volume of steel reinforcement for the frame is selected as the optimality criterion. Expressions are derived for the constraints associated with the above criteria of the frame. The optimal limit design problem is formulated in the standard form of linear programming so that simplex algorithm can be applied for solution.

A computer program has been developed for the formulation and solution of optimal limit design problem. The program analyses a frame for three cases of hinge pattern, under each of the two loading conditions, to satisfy specific design requirements. The optimal reinforced concrete frame design program is described with the aid of flow chart. The computational aspects of the problem are also explained along with the input and output details of the program.

Tests conducted on T-beams subjected to negative moments at the ends and positive moment near midspan are described. The moment-curvature relations for various sections and the EI distribution along the beam are discussed. Based on this investigation a simplified design procedure is suggested to determine the equivalent EI value for T-beams to be used in the calculation of end rotations in frame analysis.

The application of the proposed optimal limit design method to practical designs is illustrated by the examples of six reinforced concrete multi-storey frames. The results of analysis for the distribution of

moments and the plastic hinge pattern for optimal solution are discussed. Comparisons are made with ultimate strength design based on elastic analysis for factored loads.

It is concluded that the proposed optimal limit design using linear programming presents a unified approach to the limit design of reinforced concrete frames and the method offers significant savings in the requirement of steel reinforcement.

ACKNOWLEDGEMENTS

The work described in this thesis was carried out in the Concrete Structures and Technology Section of the Civil Engineering Department of Imperial College of Science and Technology, London, under the supervision of Professor A.L.L. Baker. His guidance, help and encouragement are gratefully acknowledged.

The author expresses his gratitude to Dr. C.W. Yu for his advice, willing help and guidance given throughout the work.

The author is grateful to Dr. J. Munro for his valuable comments and discussions on the application of linear programming to optimal design of frames.

Thanks are due to the staff of the Concrete Structures Laboratories and in particular to Messrs. R.W. Loveday, H. Wilson, and F. Turner for their assistance in the experimental work, to Mrs. B. Gray for typing the manuscript and to Mrs. S.A. Boreham for tracing the drawings.

The author also thanks the Commonwealth Scholarship Commission in the United Kingdom for the award of a scholarship and the Indian Institute of Technology, Madras, India for grant of study leave, which made this work possible.

TABLE OF CONTENTS

		PAGE
Title Page		1
Abstract		2
Acknowledgements		4
Table of Contents		5
List of Figures		10
List of Tables		16
Notation		18
CHAPTER 1	INTRODUCTION	
1.1	Limit Design of Reinforced Concrete Frames	25
1.2	Plastic Analysis and Design of Steel Frames Using Linear Programming	27
1.3	Optimal Limit Design of Reinforced Concrete Frames	28
1.4	Object and Scope of the Present Work	30
CHAPTER 2	SIMPLIFIED COMPUTER APPROACH TO THE ULTIMATE LOAD ANALYSIS AND DESIGN OF REINFORCED CONCRETE FRAMES	
2.1	Introduction	33
2.2	Simplified Limit Method of Baker	33
2.2.1	Moment-Curvature/Rotation Relations for Reinforced Concrete Members	33
2.2.2	Idealised Limits, L_1 and L_2	35
2.2.3	Flexural Rigidity of Reinforced Concrete Members in Limit Design	36
2.2.4	Inelastic Rotation Capacity of Reinforced Concrete Members	38
2.2.5	Method of Analysis by Trial and Adjustment Procedure	41
2.2.6	Discussion on Trial and Adjustment Procedure.	44
2.3	General Limit Method of Munro	44

PAGE

2.4 Proposed Procedure by Adjustment of Rotations for Simplified Limit Method 49

2.5 Computer Program for Ultimate Load Analysis of Reinforced Concrete Frames.. 50

2.5.1 Sequence of Operations 53

2.5.2 Input 54

2.5.3 Output 58

2.6 Design Examples 58

2.6.1 General Description.. 58

2.6.2 Results of Ultimate Load Analysis 70

2.6.3 Inelastic Analysis of Reinforced Concrete Frames.. 70

2.6.4 Discussion 82

2.7 Recommended Procedure for Ultimate Load Design of Reinforced Concrete Frames 83

CHAPTER 3 A LINEAR PROGRAMMING FORMULATION FOR OPTIMAL LIMIT DESIGN OF REINFORCED CONCRETE FRAMES

3.1 Introduction 85

3.2 The Optimal Limit Design Problem 86

3.2.1 Definition of Design Moment.. 86

3.3 Compatibility and Limited Ductility Criteria .. 89

3.4 Equilibrium Criteria 93

3.5 Serviceability Criteria 94

3.5.1 Introduction 94

3.5.2 No Plastic Hinges at Working Load 95

3.5.3 Control of Deflections 95

3.5.4 Control of Cracking.. 96

3.5.5 Control of Steel Stresses 97

3.5.6 Serviceability Criteria.. 97

3.6 Mechanism Criteria 98

		PAGE
3.7	Objective Function and Optimality Criterion ..	98
	3.7.1 Introduction	98
	3.7.2 Area of Reinforcement	99
	3.7.3 Formulation of the Objective Function ..	99
3.8	Linear Programming Formulation..	100
	3.8.1 Lower Bound Restrictions	101
	3.8.2 Additional Design Constraints	103
	3.8.3 Change in Sign of Moment	103
3.9	Solution of the Optimal Design Problem..	104
CHAPTER 4	COMPUTER PROGRAM FOR OPTIMAL LIMIT DESIGN	
4.1	Introduction	105
4.2	Flexibility Matrix..	105
4.3	Static and Kinematic Matrices	110
4.4	Transformation of Basis	111
4.5	Cases of Hinge Pattern for the Analysis of Frames..	113
4.6	Computer Program for Optimal Limit Design	121
	4.6.1 Sequence of Operations	121
	4.6.2 Input	129
	4.6.3 Output	130
	4.6.4 Discussion	130
CHAPTER 5	EXPERIMENTAL INVESTIGATION OF FLEXURAL RIGIDITY OF T-BEAMS FOR FRAME DESIGN	
5.1	Introduction	133
5.2	Test Specimens..	133
5.3	Materials and Fabrication	134
	5.3.1. Concrete Mix	134
	5.3.2 Reinforcing Steel	144

		PAGE
	5.3.3 Casting and Curing	144
	5.3.4 Control Specimens	144
5.4	Description of Tests	146
	5.4.1 Test Set-up..	146
	5.4.2 Instrumentation..	146
	5.4.3 Test Procedure	146
	5.4.4 Behaviour of Test Beams..	151
5.5	Moment-Curvature Relations..	151
	5.5.1 Basic Assumptions	154
	5.5.2 Stress-Strain Relations..	154
	5.5.3 Derivation of Expressions	156
	5.5.4 Computer Program for Moment-Curvature Calculations..	162
	5.5.5 Design Charts for Values of EI	167
	5.5.6 Comparison of Experimental and Theoretical Moment-Curvature Relations	167
5.6	Curvature and EI Distribution	189
5.7	Equivalent EI value	209
	5.7.1 Proposed Models..	209
	5.7.2 Derivation of Expressions	212
	5.7.3 Comparison of Experimental Results	217
	5.7.4 Proposed Design Procedure	221
CHAPTER 6	OPTIMAL LIMIT DESIGN EXAMPLES	
6.1	Introduction	229
6.2	Objective Function..	229
	6.2.1 Area of Reinforcement	230
6.3	Inelastic Rotation Capacity of R.C. Members ..	231
6.4	Notes on Design and Analysis	232

PAGE

6.5 Results of Analysis and Discussion.. 238

6.6 Effect of Variation of Flexural Rigidity of Beams 263

6.7 Instability Consideration in O.L.D.. 276

CHAPTER 7 SUMMARY AND CONCLUSIONS

7.1 Summary 285

7.2 Conclusions 287

7.3 Recommendations for Future Research 289

REFERENCES 291

LIST OF FIGURES

FIGURE	TITLE	PAGE
2.1(a)	Typical Moment-Curvature Diagram	34
2.1(b)	Typical Moment-Rotation Diagrams	34
2.2	Idealised Stress-Strain Relations	37
2.3	Idealised Plastic Rotation Capacity of Reinforced Concrete Members	40
2.4	Hinge Pattern for Loading Condition I	42
2.5	Influence Diagrams for a Frame	46
2.6	Discontinuity at a Non-Basic Hinge	47
2.7	Release System for a Frame and Sign Conventions	48
2.8	Five Cases of Ultimate Load Analysis	52
2.9	Flow Chart - Ultimate Load Analysis Program	55
2.10	Design Example 1	59
2.11	Design Example 2	60
2.12	Design Example 3	61
3.1	Release Systems for a Frame	91
3.2	Sign Conventions	91
4.1	Typical Moment Diagrams for Unit Actions at Basic Hinges and for Loads	106
4.2	Influence Diagrams (S)	109
4.3	Influence Diagrams (D)	109
4.4	Release Systems and m_o Diagram for a Frame	112
4.5	Loading Conditions	114
4.6	Position of Hinges	117
4.7	Example of Position of Hinges for Case 3	118
4.8	Position of Hinges	119
4.9	Position of Hinges for Case 3	120

FIGURE	TITLE	PAGE
4.10	Flow Chart-Optimal Reinforced Concrete Frame Design Program	124
5.1	Reinforcement Details for Beam A1	135
5.2	Reinforcement Details for Beam A2	136
5.3	Reinforcement Details for Beam A3	137
5.4	Reinforcement Details for Beam A4	138
5.5	Reinforcement Details for Beam A5	139
5.6	Reinforcement Details for Beam A6	140
5.7	Reinforcement Details for Beam B1	141
5.8	Reinforcement Details for Beam B2	142
5.9	Typical Stress-Strain Curves for Reinforcement	145
5.10	General Layout for Beam Tests	149
5.11	Instrumentation..	150
5.12(a)	Stress-Strain Curve for Steel in Compression and Tension	155
5.12(b)	Stress-Strain Curve for Concrete in Compression.. ..	155
5.13	Rectangular Beam: Distribution of Strain and Stress	157
5.14	T-Beam: Distribution of Strain and Stress	157
5.15	Flow Chart - Computer Program for Moment-Curvature Calculations	163
5.16	Design Chart for Values of EI (Rectangular Sections)	164
5.17	Design Chart for Values of EI (T-Sections)	165
5.18	Design Chart for Values of EI (T-Sections)	166
5.19(a)	Moment-Curvature Diagrams. Beam A1 - Sections 2, 3, 4, 5..	168
5.19(b)	Moment-Curvature Diagrams. Beam A1 - Sections 7, 8, 9	169
5.20(a)	Moment-Curvature Diagrams. Beam A2 - Sections 2, 3, 4, 5..	170

FIGURE	TITLE	PAGE
5.20(b)	Moment-Curvature Diagrams. Beam A2 - Sections 8, 9, 10	171
5.20(c)	Moment-Curvature Diagrams. Beam A2 - Sections 13, 14, 15, 16	172
5.21(a)	Moment-Curvature Diagrams. Beam A3 - Sections 2, 3, 4, 5	173
5.21(b)	Moment-Curvature Diagrams. Beam A3 - Sections 8, 9, 10	174
5.22(a)	Moment-Curvature Diagrams. Beam A4 - Sections 2, 3, 4, 5	175
5.22(b)	Moment-Curvature Diagrams. Beam A4 - Sections 8, 9, 10	176
5.22(c)	Moment-Curvature Diagrams. Beam A4 - Sections 13, 14, 15,16	177
5.23(a)	Moment-Curvature Diagrams. Beam A5 - Sections 2, 3, 4	178
5.23(b)	Moment-Curvature Diagrams. Beam A5 - Sections 7, 8, 9, 10	179
5.24(a)	Moment-Curvature Diagrams. Beam A6 - Sections 2, 3, 4	180
5.24(b)	Moment-Curvature Diagrams. Beam A6 - Sections 7, 8, 9, 10, 11	181
5.24(c)	Moment-Curvature Diagrams. Beam A6 - Sections 14, 15, 16	182
5.25(a)	Moment-Curvature Diagrams. Beam B1 - Sections 2, 3, 4, 5	183
5.25(b)	Moment-Curvature Diagrams. Beam B1 - Sections 8, 9, 10	184
5.25(c)	Moment-Curvature Diagrams. Beam B1 - Sections 13, 14, 15, 16	185
5.26(a)	Moment-Curvature Diagrams. Beam B2 - Sections 2, 3, 4	186

FIGURE	TITLE	PAGE
5.26(b)	Moment-Curvature Diagrams. Beam B2 - Sections 8, 9, 10	187
5.26(c)	Moment-Curvature Diagrams. Beam B2 - Sections 13, 14, 15, 16..	188
5.27	Curvature Distribution. Beam A1 - Load Stages 6, 8, 11	190
5.28	Curvature Distribution. Beam A2 - Load Stages 6, 8, 10	191
5.29	Curvature Distribution. Beam A3 - Load Stages 6, 8, 10	192
5.30	Curvature Distribution. Beam A4 - Load Stages 6, 9, 10	193
5.31	Curvature Distribution. Beam A5 - Load Stages 4, 7, 9	194
5.32	Curvature Distribution. Beam A6 - Load Stages 6, 8, 9	195
5.33	Curvature Distribution. Beam B1 - Load Stages 6, 8, 9	196
5.34	Curvature Distribution. Beam B2 - Load Stages 6, 8, 9	197
5.35(a)	Bending Moment Distribution for Test Beams	199
5.35(b)	Bending Moment Distribution for Test Beams	200
5.36	EI Distribution. Beam A1 - Load Stages 6, 8, 11 ..	201
5.37	EI Distribution. Beam A2 - Load Stages 6, 8, 10 ..	202
5.38	EI Distribution. Beam A3 - Load Stages 6, 8, 10 ..	203
5.39	EI Distribution. Beam A4 - Load Stages 6, 9, 10 ..	204
5.40	EI Distribution. Beam A5 - Load Stages 4, 7, 9 ..	205
5.41	EI Distribution. Beam A6 - Load Stages 6, 8, 9 ..	206
5.42	EI Distribution. Beam B1 - Load Stages 6, 8, 9 ..	207
5.43	EI Distribution. Beam B2 - Load Stages 6, 8, 9 ..	208

FIGURE	TITLE	PAGE
5.44	Proposed Models for EI Distribution	211
5.45	Design Chart for Equivalent EI	223
5.46	Design Chart for Equivalent EI	224
5.47	Design Chart for Equivalent EI	225
5.48	Design Chart for Equivalent EI	226
5.49	Design Chart for Equivalent EI	227
6.1	Optimal Design Examples..	233
6.2	EI values for Members of the Frames..	234
6.3	Equivalent Lengths of Reinforcement..	237
6.4	B.M. Diagrams. Example 1	247
6.5	B.M. Diagrams. Example 2	248
6.6	B.M. Diagrams. Example 3	249
6.7	B.M. Diagrams. Example 4	250
6.8(a)	B.M. Diagrams. Example 5	251
6.8(b)	B.M. Diagrams. Example 5	252
6.9(a)	B.M. Diagrams. Example 6	253
6.9(b)	B.M. Diagrams. Example 6	254
6.10	Example 1	255
6.11	Example 2	256
6.12	Example 3	257
6.13	Example 4	258
6.14	Example 5	259
6.15(a)	Example 6	260
6.15(b)	Example 6	261
6.16	EI Values for Beams	265
6.17(a)	B.M. Diagrams. Example 5	266
6.17(b)	B.M. Diagrams. Example 5	267

FIGURE	TITLE	PAGE
6.18(a)	B.M. Diagrams. Example 6	268
6.18(b)	B.M. Diagrams. Example 6	269
6.19	Example 5	270
6.20(a)	Example 6	271
6.20(b)	Example 6	272
6.21	B.M. Diagrams. Example 5	279
6.22	B.M. Diagrams. Example 6	280
6.23	Example 5	281
6.24(a)	Example 6	282
6.24(b)	Example 6	283

LIST OF TABLES

TABLE	TITLE	PAGE
2.1	Details of Loadings and Strengths of Concrete and steel	62
2.2	Design Details of Example 1..	63
2.3	Design Details of Example 2..	64
2.4	Design Details of Example 3..	67
2.5	Results of Analysis - Example 1	72
2.6	Results of Analysis - Example 2	73
2.7	Results of Analysis - Example 3	75
2.8	Ratio of Moments for Ultimate Load Analysis to Elastic Analysis for Factored Loads - Example 1 ..	77
2.9	Ratio of Moments for Ultimate Load Analysis to Elastic Analysis for Factored Loads - Example 2 ..	78
2.10	Ratio of Moments for Ultimate Load Analysis to Elastic Analysis for Factored Loads - Example 3 ..	80
5.1	Properties of Test Beams	143
5.2	Values of Tensile Steel Strains	198
5.3	Ratio of EI Values and Moments..	218
5.4	Results of Observed and Calculated Rotations	219
5.5	Comparison of Observed and Calculated Rotations using Equivalent EI	220
6.1	Loading, Serviceability and Strength Details of Frames..	235
6.2	Design Solutions: Example 1	239
6.3	Design Solutions: Example 2	240
6.4	Design Solutions: Example 3	241
6.5	Design Solutions: Example 4	242
6.6	Design Solutions: Example 5	243
6.7	Design Solutions: Example 6	245

TABLE	TITLE	PAGE
6.8	Comparison of Ultimate Strength and Optimal Designs..	262
6.9(a)	Ratio of Moments $\frac{M^j_{dT}}{M^j_{dR}}$. Example 5	273
6.9(b)	Ratio of Moments $\frac{M^j_{dT}}{M^j_{dR}}$. Example 6	274
6.10	Comparison of Designs for the Effect of Variation of Flexural Rigidity of Beams	275
6.11	Calculation of Magnification Factors	278
6.12	Instability Consideration in O.L.D...	284

NOTATION

A_j	Area of reinforcement for section j
A_{st}	Area of tensile reinforcement
A_{sc}	Area of compression reinforcement
b	Breadth of rectangular section or of flange of T-section
b_r	Breadth of rib of T-section
c	Total number of critical sections
d	Effective depth of section
d_1	Depth to compression steel from top
d_s	Depth of flange in T-section
e_c	Strain in concrete
e_{c1}	Strain in concrete at Limit L_1. Limiting value = 0.002
e_{c2}	Strain in concrete at Limit L_2. Limiting value = 0.0035 (unbound)
e_{s1}	Strain in steel at Limit L_1
e_{sc}	strain in compression steel
e_{st}	strain in tension steel
E_c	Modulus of elasticity of concrete
E_s	Modulus of elasticity of steel
EI	Flexural rigidity
EI_{be}	Flexural rigidity of exterior beam in a storey
EI_{bi}	Flexural rigidity of interior beam in a storey
EI_c	Flexural rigidity of column
RI_{ce}	Flexural rigidity of exterior column in a storey
EI_{ci}	Flexural rigidity of interior column in a storey
EI_e	Equivalent EI for T-beam
EI_G	$= E_c \times I_G$
EI_1, EI_2, EI_3	Value of EI at Limit L_1 for sections 1, 2 and 3 respectively

EI_4 — Value of EI in between sections 1 and 3, and 2 and 3 (Fig. 5.44)

f_c — Characteristic cylinder strength of concrete

f_m — Maximum ordinate of stress-strain curve for concrete

f_{sc} — Stress in compression steel

f_{st} — Stress in tension steel

f_{sw} — Allowable stress in tension steel

f_y — Characteristic yield strength of reinforcement

F_2, F_3, F_4 — Ratio of EI values of sections 2, 3 and 4 to EI value of critical section 1 (Fig. 5.44)

$$F_2 = \frac{EI_2}{EI_1}; \quad F_3 = \frac{EI_3}{EI_1}; \quad F_4 = \frac{EI_4}{EI_1}$$

[G] — Flexibility matrix for the frame

$$g_{ij} = \int \frac{k_i k_j}{EI} \, ds$$

$[G^A]$, $[G^B]$ — Flexibility matrix for release systems A and B respectively

[H] — Static matrix, $h_{iq} = k_{qi}$

$[H^A]$, $[H^B]$ — Static matrix for release systems A and B respectively

H — Height of column

I_G — Gross moment of inertia of rectangular section $= \frac{1}{12} b_r t^3$

[K] — Kinematic matrix

k_{iq} = ordinate at q of the influence diagram due to unit value of moment m^i

k_i — Influence diagram due to unit value of moment m^i

K_1 — $\frac{\text{Average compression stress}}{\text{Maximum compression stress}}$

$= K_6 \left(1 - \frac{K_6}{3}\right)$ when $K_6 \leq 1$

$1 - \frac{1}{3K_6}$ when $1 \leq K_6 \leq 1.75$

K_2 — $\frac{\text{Depth of resultant compression}}{\text{Depth of neutral axis}}$

$= \frac{4 - K_6}{12 - 4K_6}$ when $K_6 \leq 1$

$= \frac{\frac{1}{2} - \frac{1}{3}\left(\frac{1}{K_6}\right) + \frac{1}{12}\left(\frac{1}{K_6}\right)^2}{K_1}$ when $1 \leq K_6 \leq 1.75$

$K_1^1 = K_8\left(1 - \frac{1}{3} K_8\right)$

$K_2^1 = \frac{4 - K_8}{12 - 4 K_8}$

$K_3 = = \frac{f_m}{\sigma_b}$

$K_6 = \frac{e_c}{e_{cl}}$

$K_8 e_{cl}$ Strain in concrete at the bottom of flange of T-section,

$\overline{K_b} = \frac{EI_{bi}}{L_{bi}} \cdot \frac{L_{be}}{EI_{be}}$

L^j Lower bound values of x^j for section j $= \frac{\lambda_*^j}{\lambda_u}$

L Length of beam

L_1, L_2, L_3 Lengths of constant EI regions (Fig.5.44)

L_{bi} Length of internal beam in a storey

L_{be} Length of external beam in a storey

l^j Equivalent length of reinforcement for a critical section j

m Number of storey, counting from top

m^r Moment at a section r

$\{m_b\}$ Column vector $\{m^1, m^2, \ldots, m^\alpha\}$

$\{m_b^A\}, \{m_b^B\}$ Column vectors $\{m_b\}$ for release systems A and B respectively

m_o^q Bending moment at a section q in the reduced structure due to loads

$\{m_o^A\}, \{m_o^B\}$ Column vectors $\{m_o\}$ for release systems A and B respectively

M	Moment, generally
M_1, M_2, M_3	Moments at three critical sections, 1, 2, 3 of a T-beam (Fig. 5.44)
M^j	Moment at a section j under working load
M_d^j	Design moment at a section j under ultimate load
M_{dR}^j	Design moment at a section j by analysis using uniform EI value for beams (T-beam action not considered)
M_{dT}^j	Design moment at a section j by analysis using equivalent EI value for T-beams
M_{du}^j	Design moment at section j by ultimate load analysis
M_r	Moment of resistance
M_{ru}	Moment of resistance at Limit L_2
M_{ry}	Moment of resistance at Limit L_1
M_u^j	Factored elastic moment at a section j
M_y^j	Yield moment for section j
nd	Depth to neutral axis
$n_1 d$	Depth to neutral axis at Limit L_1
$n_2 d$	Depth to neutral axis at Limit L_2
P	Axial load in a column
P_T	Sum of axial loads in columns of a storey
$\bar{p}_T$	$= \dfrac{P_T H^2}{\Sigma EI_c}$
p_j	Reinforcement ratio for a section j $= \dfrac{A_j}{bd}$
p	$= \dfrac{A_{st}}{bd}$
p^1	$= \dfrac{A_{sc}}{bd}$
q_{sc}	$= \dfrac{A_{sc}}{bd} \cdot \dfrac{f_y}{f_m}$
q_{st}	$= \dfrac{A_{st}}{bd} \cdot \dfrac{f_y}{f_m}$

r_f $= \frac{EI_{ci}}{EI_{ce}}$

R_2, R_3 Ratio of moments of sections 2 and 3 to moment at section 1 (Fig. 5.44)

$R_2 = \frac{M_2}{M_1}$; $R_3 = \frac{M_3}{M_1}$

R_{3e} $= R_3 - \frac{5}{6}(R_2 - 1)$

s $= \frac{d_s}{d_1}$

t Total depth of section

v_i Angular discontinuity at a basic hinge section i

v_{io} Angular discontinuity at a basic hinge section i due to loads $= \int \frac{k_i m_o}{EI} ds$

$\{v_o\}$ Column vector $\{v_{1o}, v_{2o}, \ldots, v_{\alpha o}\}$

V_j Volume of reinforcement for section j

V Total volume of reinforcement for the frame

V_0 Total volume of reinforcement for O.L.D.

V_U Total volume of reinforcement for U.S.D.

$(V_0)_T$ Total volume of reinforcement for O.L.D. using equivalent EI value for T-beam

$(V_U)_T$ Total volume of reinforcement for U.S.D. using equivalent EI value for T-beam

$(V_0)_S$ Total volume of reinforcement for O.L.D. with consideration for instability effects

$(V_U)_S$ Total volume of reinforcement for U.S.D. with consideration for instability effects

W Working load

W_1 Yield load of the frame

W_D, W_L, W_W Dead, live and wind working loads

W_u Ultimate load

x^j Yield safety parameter for section j $= \frac{\lambda^j}{\lambda_u}$

x_d^j Design moment parameter

y $= \frac{EI_{be}}{L_{be}} \cdot \frac{H}{EI_{ce}}$

α Indeterminacy number for a frame

β_e Elastic magnification factor for lateral loads

β_p Plastic magnification factor for lateral loads

β_d Magnification factor for lateral loads at design ultimate load

θ^r Inelastic rotation at a hinge r

θ_b^i Inelastic rotation at a basic hinge i

θ_n^j Inelastic rotation at a non-basic hinge j

θ_p^r Permissible rotation for a hinge r

$\{\theta_b\}$ Column vector $\{\theta_b^1, \theta_b^2, \ldots, \theta_b^\alpha\}$

$\{\theta_n\}$ Column vector $\{\theta_n^{\alpha+1}, \theta_n^{\alpha+2}, \ldots, \theta_n^c\}$

θ_1, θ_2 Rotation at end sections 1 and 2 for T-beam (Fig. 5.44)

θ_{cal} Calculated value of rotation

θ_{obs} Observed value of rotation

θ_{UEI_1} Calculated value of rotation based on uniform EI_1

ϕ Curvature

ϕ_1 $= \phi d$

λ^j Yield moment factor for section j $= \frac{M_y^j}{M^j}$

$\lambda_D, \lambda_L, \lambda_C$ Load factors for dead, live and combined loads

σ_{al} Design strength of steel

σ_b Design strength of concrete

ABBREVIATIONS

CLD	Compatibility and Limited Ductility
E	Equilibrium
LC	Loading Condition
LP	Linear Programming
O	Optimality
O.L.D.	Optimal Limit Design
PHI	Plastic Hinge Indicator
S	Serviceability
U.S.D.	Ultimate Strength Design

CHAPTER ONE

INTRODUCTION

1.1. LIMIT DESIGN OF REINFORCED CONCRETE FRAMES

The classical methods of plastic analysis and design (1) assume moment-curvature relations of unlimited ductility. These methods have had ready application to the design of steel structures (1, 2, 3, 4, 5, 6). The limit design of reinforced concrete frames require additional consideration due to the inelastic behaviour of reinforced concrete memebers under various stages of loading, limited ductility of the sections and the serviceability requirements under working loads. A variety of limit design methods have been proposed for reinforced concrete structures and each method has been developed within the framework of some particular assumptions, criteria and experimental evidence.

Baker (7) has proposed a Simplified Limit Method for the design of reinforced concrete frames. In this method a simple bi-linear moment-rotation relation with limited ductility characteristics for reinforced concrete sections is considered satisfactory for use in deformation calculations. A frame is reduced to a statically determinate form by the introduction of sufficient hinges. These hinges may be chosen from a knowledge of approximate elastic moment distribution, at positions where the bending moments are critical for the members. The moments at the hinges are solved by a trial and adjustment procedure such that the inelastic rotations at the hinges are less than the permissible values. The final design is to be checked separately for serviceability conditions. The techniques proposed for carrying out the design by this method are fully described in References (7, 8, 9, 10, 11, 12). The possibility of extending its application to space frames has been outlined in Reference (13). The results of an extensive programme of experimental investigation on the flexural behaviour of reinforced concrete members have been used to determine the safe limiting values for the parameters used in the simplified limit method (10, 12, 14). These are described in Chapter 2.

The method of ultimate load analysis by "imposed rotations" suggested by Macchi (15) uses a tri-linear moment-rotation diagram for the calculations. The bending moment distribution corresponding to the failure stage is obtained by the superposition of the elastic moments due to loads and the "redistribu-

tion moments" due to plastic rotations imposed at critical sections. The analysis is carried out in successive trials. First a complete redistribution is considered, assuming that all the critical sections developed their limiting moments. The load corresponding to this moment distribution is calculated and the elastic moment distribution corresponding to this load is determined. The redistribution moments due to the plastic rotations imposed at all the critical sections is calculated and superimposed on the elastic moment distribution. If the final moment values coincide with the initially assumed values the moment distribution is complete and in equilibrium with the load. Otherwise several trials are made to achieve the above condition. This trial and error method of analysis involves tedious calculations and becomes almost prohibitive for multi-storey frames.

A Bi-Linear Design of reinforced concrete frames has been suggested by Sawyer (16). In this method two stages of failure are considered in design; (i) wide cracking and (ii) crushing and spalling. The procedure of design is summarized as follows. Based on elastic analysis for all combinations of ultimate load, assume a statically admissible bending moment distribution within the envelope and calculate the corresponding inelastic rotations. Then analyse the frame elastically for the moments induced by the loads and the inelastic rotations. If the totals of these moments are also within the envelope the design is satisfactory for the loading with respect to crushing and spalling. The design is also satisfactory against failure stage of wide cracking if the calculated stresses in reinforcement for the moment distribution based on elastic analysis do not exceed the allowable values.

Petcu (17) and Cohn (18, 19) have proposed limit design methods which emphasize the serviceability requirements under working load. A design solution for the frame is found such that the following criteria are satisfied:

(i) Limit equilibrium: The condition of the limit equilibrium is that no collapse mechanism may form prior to the specified ultimate load for the structure. For each possible mechanism one limit equilibrium equation can be written to express the condition that the energy dissipated in the plastic hinge rotations is at least equal to the external work done by the load.

(ii) Serviceability: The critical sections of the frame will remain well within the elastic range for any combination of service loads and hence will have a safety against yield above a specified minimum value of λ^j.

Solving the system of equations and inequalities provided by the adopted limit equilibrium and serviceability criteria the values of the design moments at all the critical sections of the structure can be found. A solution is optimal in the sense that of the number of solutions satisfying the limit equilibrium condition, it is the best in relation to a convenient set of serviceability constraints. Depending on the emphasis placed on either the equilibrium or the serviceability criteria involved in the formulation of the problem Full and Limited Redistribution Designs are obtained. Limited Redistribution Design assumes the ultimate stage corresponds to a mechanism collapse and that at least one collapse mode is possible at the specified ultimate Load. Other collapse modes are possible only at load factors larger than the design load factor. Full Redistribution Design is based on similar assumption to L.R.D. The main difference lies in the attempt to produce designs with a higher degree of moment redistribution. If a full redistribution design can be achieved, the number of possible collapse mechanisms at the specified ultimate load equals the number of independent equations of equilibrium for the structure. These methods are illustrated with design examples elsewhere (19, 20, 21, 22).

1.2. PLASTIC ANALYSIS AND DESIGN OF STEEL FRAMES USING LINEAR PROGRAMMING

The main object of plastic analysis is to determine the collapse load of a frame when the resisting capacities of its members are known; the object of optimal plastic design is to determine the member resistances that minimize the objective function representing the total weight of the structure when the ultimate design loads are applied.

The plastic analysis of framed structures has been identified as a linear programming problem by Charnes and Greenberg (23) and several other earlier studies (24, 25) have been devoted to this problem. In an attempt to make the analysis more automatic for computer programming Grierson and Gladwell (26) presented a kinematic approach to the plastic analysis using linear programming. The method uses the concept due to Neal and Symmonds (27) that every possible mechanism can be constructed as a combination of independent elementary mechanisms. Thus a set of independent mechanisms are combined to form other mechanisms until the mechanism with the smallest load factor has been found. Cohn, Ghosh and Parimi (28) have illustrated in a recent publication that all problems of plastic analysis and design can be formulated as linear programming problems and therefore, can be solved in a unified way with standard algorithms.

The minimum weight design of frames has been formulated as a linear programming problem by Foulkes (29, 30) and has been the subject of subsequent work (31, 32, 33). It has been assumed that the relationship between the weight per unit length of the frame members and their fully plastic moments is linear. A computer-aided design system for optimal design of steel frames has been developed by Toakley (34), and, Horne and Morris (35). A linearised weight function has been used. In dealing with the optimisation problem a 'force method' approach has been adopted by taking an arbitrary set of redundants. The bending moment at any point can then be expressed as a linear function of the redundants. This enables to establish the constraints which satisfy both the equilibrium and yield criteria of the plastic theory. An iterative process has been employed to satisfy instability and other practical considerations.

A general limit analysis of skeletal structures has been developed by Munro (36, 37) without using work or energy principle but based on the contragredience relation which link the kinematic and static transformations. First the frame is reduced to a determinate form by the insertion of hinges at suitable set of critical sections. A 'basic mechanism' is created by inserting an additional hinge in one other critical section. These basic mechanisms can be suitably combined to generate all other 'non-basic mechanisms'. A tabular method (36) has been presented to calculate the collapse load of a structure. The method can also be used to calculate the displacements and plastic hinge angular discontinuities at collapse. The above concepts of this limit analysis have recently been extended by Munro and Smith (38). The plastic analysis and synthesis of frames have been formulated in a unified manner through safe and unsafe linear programs. The primal-dual relations of the programs have been rigorously established.

1.3. OPTIMAL LIMIT DESIGN OF REINFORCED CONCRETE FRAMES

The optimal design of reinforced concrete frames has recently attracted increasing attention. Cohn and Grierson have illustrated in their contributions (39, 40) that the techniques adopted for steel structures are not strictly applicable to reinforced concrete frames. The major difficulties arise from the limit design requirements to satisfy all the three basic conditions: (1) Compatibility and limited

ductility (2) Equilibrium and (3) Serviceability. Also in the case of concrete structures the design of each member is essentially unique and the relationship between weight and moment capacity is not known beforehand. Further, unlike standard steel members, the weight and moment capacity of a reinforced concrete member vary along the length of the member depending on the detailing of reinforcement. It may also be noted that minimum structural weight need not be the only decisive optimality criterion of design. Thus the choice of an objective function is not as straightforward as for steel frames.

Cohn and Grierson (39, 40) have proposed a linear programming model for the optimal limit design of reinforced concrete frames. The method of limit design due to Cohn (18, 19), described in section 1.1, is used as the basis of design. Thus the limit equilibrium and serviceability requirements of the frame are considered as the governing constraints of the problem. The compatibility condition is to be checked separately being not incorporated in the formulation. In this method the design bending moment at any section is expressed as the yield safety parameter (explained in section 3.2.1) times the value of factored elastic moment envelope. The optimal design problem consists of determining the values of the yield safety parameter, treated as design variables, subject to the optimality, limit equilibrium and serviceability conditions.

The limit equilibrium criteria specifies that no collapse mechanism may form prior to the design load of the structure. A computer program developed for the combination of mechanisms (41) is used to determine the governing collapse mechanisms for the frames. The limit equilibrium requirement is then expressed by the condition that for each possible mechanism the energy dissipated in the plastic hinge rotations is greater than or equal to the external work done by the load.

The serviceability criteria adopted is that at working loads, no plastic behaviour may occur and widths of cracks, steel stresses and deflections must be within allowable limits. These serviceability conditions have been investigated (40) and found that they would be satisfied by placing lower limits on the yield safety parameters.

The optimality criterion used is that the total volume of steel reinforcement required is a minimum. A linear objective function is chosen to express the volume of steel in terms of the design variables.

The optimal design problem is thus formulated as a linear programming problem with the linear objective function and the constraints associated with limit equilibrium and serviceability conditions of the frame. The method is illustrated by examples of continuous beams and simple cases of frames (39, 40).

A very general formulation of the optimal frame design problem has been presented by Grierson and Cohn (42) in which the design moments, the relative member stiffnesses and also the relative member lengths are all treated as variables and the volume of reinforcement is minimised subject to constraints associated with equilibrium, serviceability, compatibility and limited ductility for several loading schemes. This is a non-linear programming problem of considerable complexity and Grierson and Cohn illustrated the expected trends for a simple two-span beam example in which various approximations were made in order to linearise the problem.

1.4. OBJECT AND SCOPE OF THE PRESENT WORK

It can be seen from the above discussion that existing limit design methods for reinforced concrete frames can be classified into two classes, depending on the way they satisfy the compatibility, equilibrium and serviceability conditions of the frame. Compatibility methods (7, 15, 16) satisfy the compatibility and equilibrium criteria of the frame and the final design is checked for serviceability. Serviceability methods (17, 18, 19) are based on the satisfaction of limit equilibrium conditions of the governing collapse mechanisms and the serviceability requirements of the frame. A subsequent check is necessary for the compatibility conditions and this aspect is discussed below.

Reinforced concrete members exhibit inelastic behaviour even at the early stages of loading and this effect is more pronounced at the ultimate load stages. Hence limit design methods for reinforced concrete structures must take into account this deformational behaviour of the members. Unlike steel structures the rotation capacity of a reinforced concrete hinging section is limited and this is specially so in the case of over-reinforced beam sections and in columns carrying heavy axial loads (10, 14, 52). Consequently premature failure of section may occur (68) before the formation of a plastic collapse mechanism as assumed in the serviceability methods.

The simplified limit method due to Baker considers the deformational behaviour of reinforced concrete members through the use of bi-linear moment-rotation characteristics for the critical sections. This is incorporated in the method by the use of appropriate values for the flexural rigidity of the members in compatibility calculations. Also the inelastic rotation of the plastic hinge sections is limited to the safe limiting values based on experimental investigations.

With increasing use of computers in the analysis and design of reinforced concrete frames it is useful to examine the simplified limit method in the light of this development. It has been found that in the case of large frames, the trial and adjustment procedure suggested by Baker may present problems for convergence. Also there may be situations in design where different cases of hinge pattern (53, 54) have to be considered. Hence a computer oriented approach is necessary for the method to be practical in actual designs. In the present investigation, such a computer program has been developed for the ultimate load analysis of reinforced concrete frames.

There has been growing interest in the application of mathematical programming techniques to the study of optimisation of structural designs. Of the various methods, the use of linear programming techniques for optimal designs has the advantage of wider application as standard algorithm (58) for solution is readily available. The optimal design method due to Cohn and Grierson (39, 40) is based on the serviceability method and does not consider the limited rotation capacity of reinforced concrete sections. The present work is, therefore, concerned with the development of an optimal limit design method for reinforced concrete frames that simultaneously satisfies the optimality, compatibility and limited ductility, equilibrium and serviceability criteria.

In the limit design of reinforced concrete structures, the flexural rigidity, EI, of the members forms an important factor in the deformation calculations. Experimental investigations show that there is considerable reduction in the stiffness of reinforced concrete members at ultimate load stages. Hence the need to use appropriate values of EI consistent with the behaviour of members at relevant load stages has been emphasized by various authors (7, 10, 14, 43, 44, 45, 46, 47). These earlier investigations were confined to rectangular beam and column sections. In building frames the beams are subject to varying sectional behaviour; T-section in the positive

moment region and rectangular section in negative moment regions. The flexural rigidity of these beams can not be assumed to be uniform of magnitude equal to that of one of the critical sections. The present work, therefore, includes an experimental investigation on T-beams subject to varying nature of moments, to study the EI values of beams to be used in limit design calculations.

The object of the present work outlined in the above discussion can be summarized as follows:

1. a) To propose a modified procedure oriented to computer programming for simplified limit method.

   b) To develop a computer program for the ultimate load analysis of reinforced concrete frames for different cases of hinge pattern and to study the use of the program through design examples of multi-storey frames.

2. a) To propose a linear programming method for optimal limit design of reinforced concrete plane frames that satisfies the optimality, compatibility and limited ductility, equilibrium and serviceability criteria.

   b) To develop a computer program for the formulation and solution of optimal limit design problem.

3. To study through an experimental investigation the flexural rigidity of T-beams subjected to negative moment at the ends and positive moment near midspan and to propose a design procedure for the calculation of equivalent EI value for beams to be used in limit design calculations.

4. To apply the proposed optimal limit design method to practical examples of frames and to study the merits of the proposed method.

CHAPTER TWO

SIMPLIFIED COMPUTER APPROACH TO THE ULTIMATE LOAD ANALYSIS AND DESIGN OF REINFORCED CONCRETE FRAMES

2.1 INTRODUCTION

The simplified limit method of Baker (7, 9, 10, 12) for the analysis of moments under ultimate load by trial and adjustment procedure is first described. For the case of large frames it has been found that the procedure suggested in the method may present problems for convergence. Also in certain cases of sway frames susceptible to instability effects a recent investigation (53, 54) has shown that it is desirable to avoid plastic hinges in columns and to allow only beam hinges to form at the ultimate load stage. These problems will be discussed. A modified procedure by adjustment of rotations is proposed to the simplified limit method and this procedure is shown through examples to provide rapid convergence of solution.

A computer program based on the generalised compatibility equation of Munro (36) is presented for the analysis of reinforced concrete frames for five cases of hinge pattern under two ultimate loading conditions. The program includes the proposed modified procedure to the simplified limit method. The use of this program will be illustrated through the design of three examples of multi-storey frames. The amount of moment redistribution in these frames will be discussed. These frames have been tested analytically for the actual load factor by a separate program developed (53) for a rigorous inelastic stage-by-stage analysis of reinforced concrete frames. The results of the analysis will be discussed.

Based on this investigation a design procedure is recommended for the ultimate load design of reinforced concrete frames.

2.2 SIMPLIFIED LIMIT METHOD OF BAKER

2.2.1. Moment-Curvature/Rotation Relations For Reinforced Concrete Members

The behaviour of reinforced concrete members is best represented by the moment-curvature relations of the cross sections. Typical moment-curvature relation for a reinforced concrete section is shown in Fig.2.1(a).

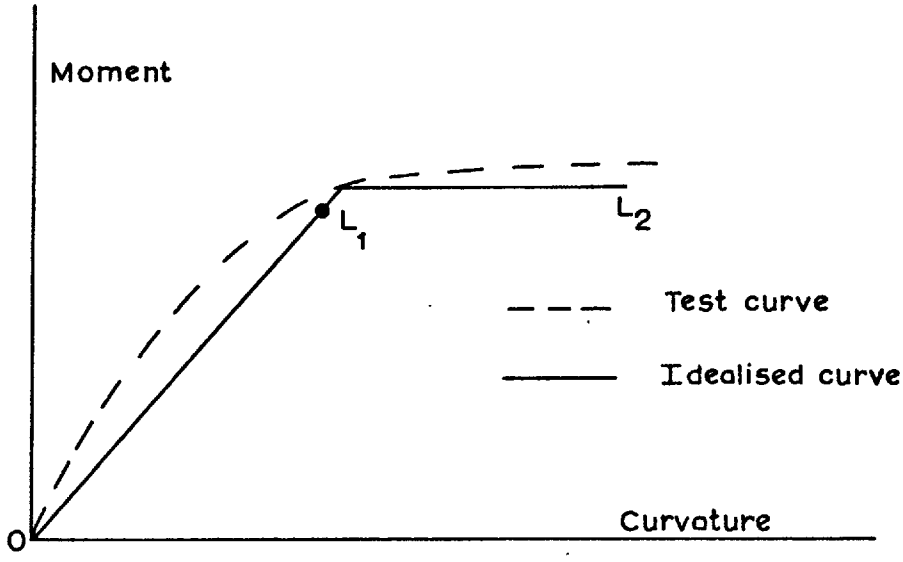
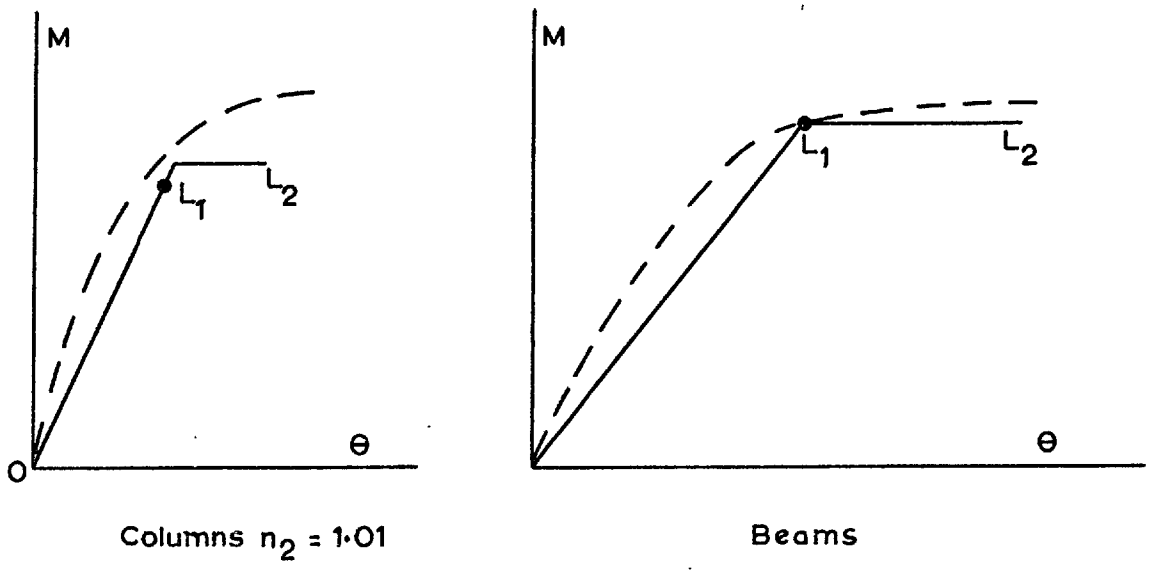


FIG. 2.1 (a) TYPICAL MOMENT – CURVATURE DIAGRAM



Columns $n_2 = 1{\cdot}01$ Beams

FIG. 2.1 (b) TYPICAL MOMENT – ROTATION DIAGRAMS

One of the main objectives in methods of analysis has been to relate the total deformation, usually rotations, to various bending moment values. If the moment-curvature relations of sections are known, it is theoretically possible to analyse the structure for any loading up to and including the ultimate load (43, 46). But this approach using moment-curvature relation will lead to complicated and cumbersome calculations due to the non-linear nature of the above relations.

Since the primary calculation to be carried out in the ultimate load analysis is the calculation of total inelastic rotations at the specified sections it is assumed in this analysis that the inelastic rotations are concentrated at these critical sections. It is, therefore, logical to use the moment-rotation relation for a critical section and thus avoid the disadvantages inherent in using the moment-curvature relation. The inelastic rotation is not a sectional property but is the cumulative effect of the behaviour of the reinforced concrete member in the vicinity of the critical section; it is not a discontinuous effect. This concept of moment-rotation relation is convenient for the analysis (7, 9, 44, 46). Extensive experimental investigations carried out on the moment-rotation characteristics of beams and columns are reported in references (10, 14). Typical moment-rotation diagrams are shown in Fig.2.1(b).

It can be seen from Fig.2.1. that the moment-rotation relation curve is non-linear even at the early stages of loading. The slope of the curve at the origin is influenced by the uncracked flexural rigidity of the member. As the load increases the flexural rigidity decreases but does not have a constant value throughout the member. After yield the rotation is made of the contribution from that portion of the member acting elastically and the contribution from that portion of the member in the vicinity of the critical section undergoing inelastic deformation.

2.2.2. Idealised Limits, L_1 and L_2

To simplify the analysis Baker (7) has suggested that the moment-rotation diagram of reinforced concrete member may be assumed to have the form OL_1L_2 as shown in Fig.2.1. The limits L_1 and L_2 are so chosen that they are on the safe side yet as close to the actual diagram as possible. The limit L_1 can be termed the idealised elastic limit and L_2 the idealised plastic limit. These limits are defined by specifying the stress-strain relation for concrete and the limiting strain conditions at the critical

section. Experimental evidence shows that the idealised elastic limit L_1 is associated with the yield stress of tension reinforcement or decided by the concrete reaching the maximum stress. Baker has suggested that the limit L_1 can be defined by the attainment of a strain of 0.002 in concrete or an off-set strain of 0.001 in steel according to the condition whichever is attained first. The limit L_2 is defined by the attainment of a maximum strain of 0.0035 for unbound concrete or 0.01 in steel. These limits are shown in Fig.2.2 for the assumed stress-strain curves for concrete and steel.

2.2.3 Flexural Rigidity of Reinforced Concrete Members in Limit Design

In the stress and deformation analysis of reinforced concrete structures, the flexural rigidity, EI, of members forms an important factor influencing the calculated stress state. For the elastic analysis of reinforced concrete structures the Code of Practice (62) suggests that the relative stiffnesses may be calculated using any one of the following throughout:

(a) the concrete section - the entire concrete cross-section ignoring the reinforcement.

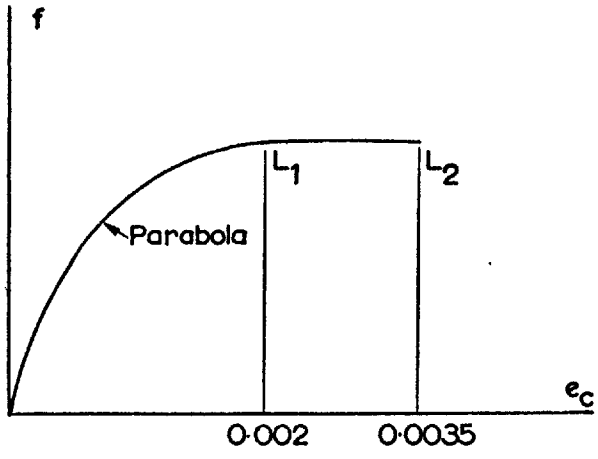
(b) the gross section - the entire concrete cross-section including the reinforcement on the basis of modular ratio.

(c) the transformed section - the compression area of the concrete cross-section combined with the reinforcement on the basis of modular ratio.

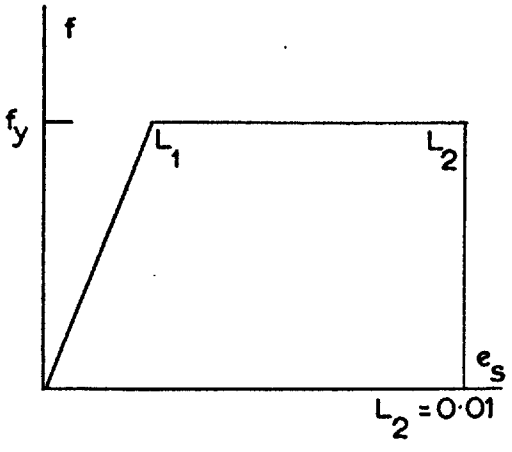
The differences in the EI values calculated by different assumptions are quite large (14, 47). In the analysis of frames the basic assumptions for the determination of EI values may give rise to large differences in the design values. For certain frames under extreme conditions the error in the analysis of moments, due to different assumptions for the EI values could be as much as 30 per cent.

Experimental investigations (10, 14) show that there is a considerable reduction in stiffness of reinforced concrete members at ultimate load stage. This can also be seen from the moment-curvature diagram of Fig.2.1. In the ultimate load analysis, where the degree of safety is more critical, it is therefore, important to base the calculation of EI values consistent with the behaviour of the members at the relevant load stage.

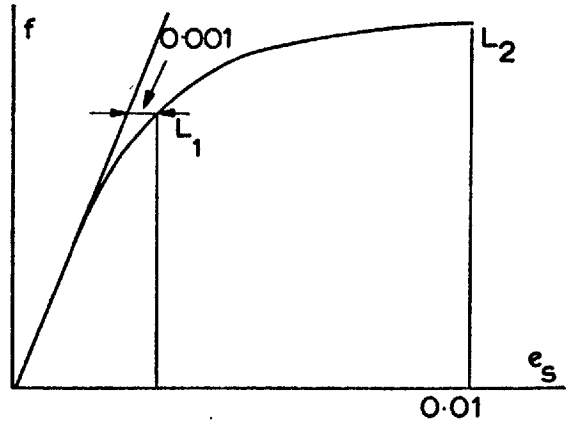
As discussed earlier, Baker in introducing the ultimate load analysis of frames (7) has suggested a bi-linear moment-rotation relation for



(a) CONCRETE



(b) MILD STEEL



(c) COLD-WORKED STEEL

FIG. 2.2 IDEALISED STRESS - STRAIN RELATIONS

reinforced concrete members (Fig.2.1). This assumption simplifies the analysis and experimental investigations show that it leads to safe results (14).

The assumption of the moment-rotation diagram to follow the bi-linear diagram OL_1L_2 (Fig.2.1) leads to the result that the EI value is idealised to be constant from 0 to L_1 and between the critical sections of the member. The value of EI to be assumed for the member in compatibility calculations with respect to the ultimate load stage is, therefore, assumed to be the value at limit L_1.

$$\text{At } L_1 \text{ limit,} \quad \phi = \frac{M_{ry}}{EI} = \frac{e_{cl}}{n_1 d}$$

$$\text{Hence,} \quad EI = \frac{M_{ry} n_1 d}{e_{cl}} \qquad (2.1)$$

$$\text{or alternatively,} \quad EI = \frac{M_{ry}(1-n_1)d}{e_{sl}}$$

Thus it can be seen that the EI value specified by equation (2.1) is based, not just on the property of the material and dimensions of the sections, but on the integrated curvature at a particular limit state and depends on the distribution of stress in concrete and cracking and the corresponding strain values.

The values of moments M_{ry}, n_1, e_{cl} and e_{sl} corresponding to limit L_1 are calculated using the stress-strain relations shown in Fig.2.2. Typical computation charts are presented in the book (12).

2.2.4. Inelastic Rotation Capacity of Reinforced Concrete Members

Limit design methods for reinforced concrete statically indeterminate structures require a knowledge of the rotation capacity of hinging regions in reinforced concrete members. The limit of the plastic rotation is primarily controlled by the ultimate strain in concrete or in extremely under-reinforced members the strain in reinforcement may determine the maximum plastic rotation. These limits are referred to limit L_2.

Extensive experimental investigations (7, 10, 48, 49, 50, 51, 52) on reinforced concrete members show that the plastic rotation capacity θ_p^r is subject to large fluctuations even when the members are tested under similar conditions. Hence, in calculations involving plastic rotations, it would only be possible to use approximate values of θ_p^r, which may be considered to be safe values as compared to experimental results.

In 1956, Baker (7) has suggested the following empirical formula for θ_p^r.

Tension hinges (under-reinforced beam hinges):

$$\theta_p^r = \frac{0.01}{n_2}$$

Compression hinges (column hinges or over-reinforced beam hinges):

$$\theta_p^r = 0.01 \text{ for well bound sections.}$$

$$\theta_p^r = 0.001 \text{ for unbound sections.}$$

A more comprehensive formula for θ_p^r which incorporates the influence of section parameters has been suggested in the Research Committee Report of the Institution of Civil Engineers (9).

$$\theta_p^r = \bar{k}_1 \bar{k}_2 \bar{k}_3 (0.0035 - e_{c1}) \left(\frac{Z}{d}\right)^{\frac{1}{4}} \qquad (2.2)$$

where $\bar{k}_1$, $\bar{k}_2$, $\bar{k}_3$ are factors which take into account the influence of grade of steel, axial load and grade of concrete respectively, Z refers to the length of the member between critical section and point of contra-flexure, d is the effective depth of section and e_{c1} is the concrete strain at limit L_1.

The values of θ_p^r predicted by equation (2.2) has been compared by Amarakone (14) with the moment-rotation characteristics for beam and column tests carried out under the auspices of the European Concrete Committee and a large scatter of test results was recorded. It was shown that the main parameters affecting θ_p^r were the degree of binding and the depth of concrete in compression zone at the critical section as expressed by the neutral axis depth. Based on this investigation Baker and

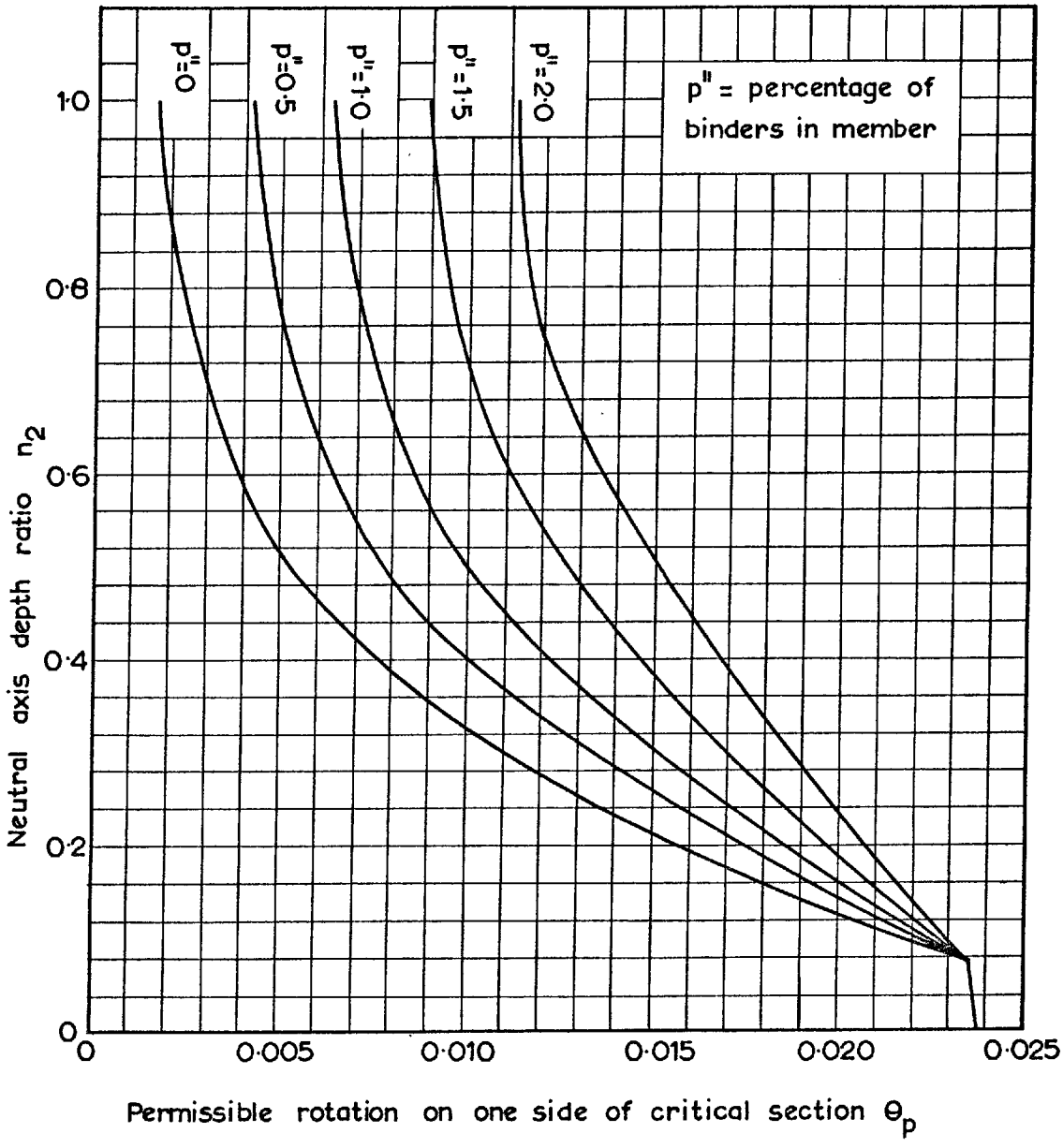


FIG. 2.3 IDEALISED PLASTIC ROTATION CAPACITY OF REINFORCED CONCRETE MEMBERS

Amarakone (10) proposed a set of curves, shown in Fig.2.3, for the calculation of rotation capacity of reinforced concrete members. This set of curves has been found suitable for use in designs as it involves minimum number of variables.

2.2.5 Method of Analysis by Trial and Adjustment Procedure

Based on the above discussion the following assumptions are made in the simplified limit method of Baker (7, 8, 9):

1. The moment-rotation diagram of reinforced concrete member is idealised to follow the bi-linear diagram as shown in Fig.2.1. The EI value is, therefore, idealised to be constant from 0 to L_1 and between the critical sections of the member.
2. The inelastic rotation is concentrated at a critical section which acts as a plastic hinge.
3. The ultimate strength of a frame is reached when sufficient number of critical sections become plastic hinges to make the structure statically determinate and stable.
4. Members between plastic hinges are assumed to behave elastically and hence are designed to develop bending moments equal to or less than the values at limit L_1 for the members.
5. The position of the first α plastic hinges are predetermined and as implied in assumption (4) that there is no plastic rotation at any other position.

The simplified limit method is essentially based on the flexibility method of analysis of any indeterminate structure. For a given frame indeterminate to α degree, α hinge releases are chosen to make it determinate and stable. These hinges may be chosen from a knowledge of approximate elastic moment distribution at positions, where the bending moments are critical for the members. Fig. 2.4 shows a suggested pattern of hinges for a frame subjected to wind, dead and live loads.

The governing compatibility equation is given as follows:

$$g_{11}m^1 + g_{12}m^2 + - - - - - + g_{1\alpha}\, m^{\alpha} + v_{10} = -\theta_b^1$$

$$g_{21}m^1 + g_{22}m^2 + - - - - - + g_{2\alpha}\, m^{\alpha} + v_{20} = -\theta_b^2$$

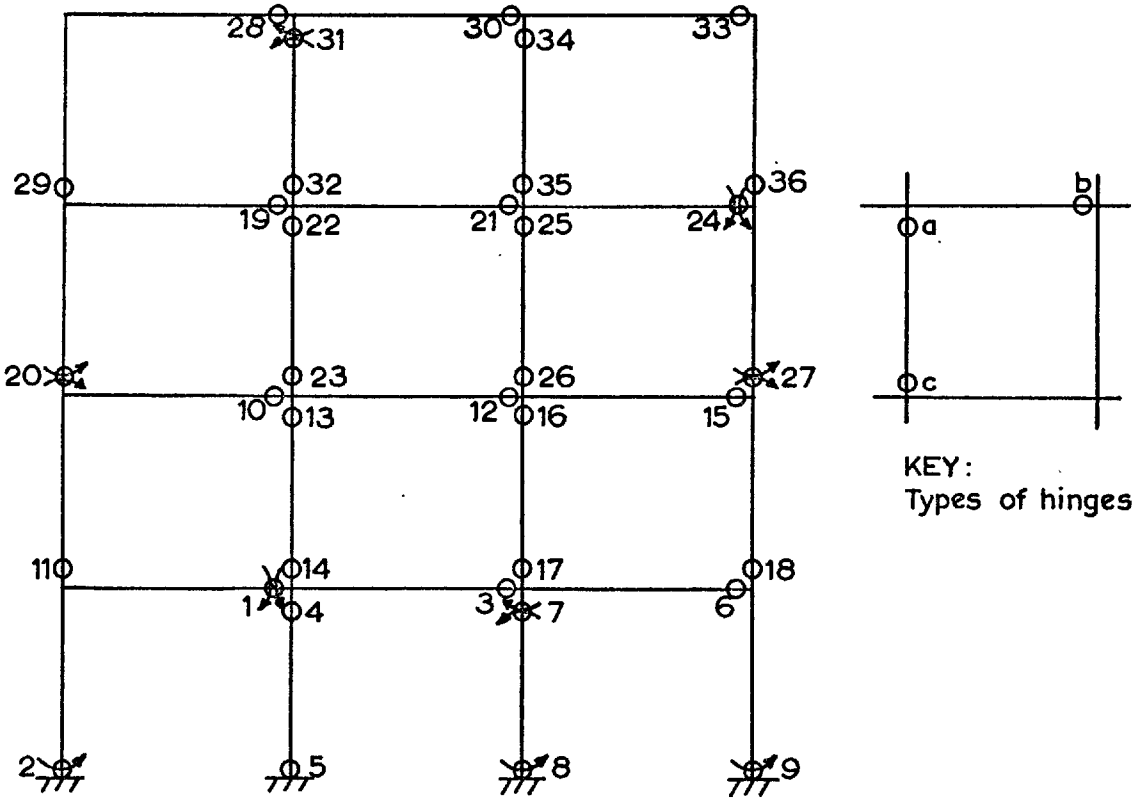


FIG. 2.4 HINGE PATTERN FOR LOADING CONDITION I

$$g_{31}m^1 + g_{32}m^2 + - - - - - - + g_{3\alpha}\, m^{\alpha} + v_{30} = -\theta_b^3$$

$$- -$$

$$- -$$

$$- -$$

$$g_{\alpha 1}m^1 + g_{\alpha 2}m^2 + - - - - - + g_{\alpha\alpha}\, m^{\alpha} + v_{\alpha 0} = -\theta_b^{\alpha} \qquad (2.3)$$

The values of the redundant moments, m^i, at the hinges are solved by the trial and adjustment procedure summarized below:

1. Determine the influence coefficients g_{ij} and v_{io} for the release system shown in Fig.2.4.
2. Choose a set of m^i values and adjust their values by a systematic procedure such that the rotations at these hinges are less than the permissible values.

The following method has been proposed (7) as a quick adjustment procedure for building frames.

(a) Adjust moments of hinges type 'b' of all storeys.

(b) Adjust moments of hinges type 'a' and 'c' except the moments at the hinge type 'c' of the first and last bay in the top storey.

(c) Adjust moments at the hinge type 'c' of the first and last bay in the top storey.

(d) Repeat steps (b) and (c) in the storey next below the top storey and so on down through the frame.

Repeat the cycle, if necessary. It is quite important that the sign of the moment and the corresponding rotations are compatible as expressed in equation (2.3) for positive values of m^i.

The guide lines for the initial choice of the values of m^i and the method of working of the trial and adjustment procedure are fully explained in Reference (7).

2.2.6. Discussion on Trial and Adjustment Procedure

The trial and adjustment procedure of the simplified limit method is a general approach suggested for the ultimate load analysis of reinforced concrete frames. A designer analysing multi-storey frames, however, may face the following problems:

1. One of the implicit assumptions in the trial and adjustment procedure is the existence of an inelastic compatibility state with the plastic hinges at the assumed positions which is not always the case. Hence in certain cases of frames the assumed hinge pattern may not be suitable for the compatibility calculations leading to difficulties for convergence of solution.

2. As the influence coefficients have to be worked out for the trial and adjustment procedure it becomes necessary to assume the sign of the moments at these hinges. Though one may, in normal cases of loading and geometry, be sure of the sign of moments in beam hinges it is difficult to guess them in some of the column hinges.

3. The choice of the initial values of moments for the trial and adjustment procedure requires sound judgement based on experience.

The above stated problems, which are interconnected to each other, make the computational aspect of the procedure difficult and cumbersome. It is, therefore, evident that a computerised procedure to adjust the rotations is necessary for the method to be practical in general. For the development of such a computer program it has been found desirable to base the analysis on the generalised compatibility equation of the limit method due to Munro (36). This compatibility equation, explained below, will give the choice of location of plastic hinges away from the release hinges.

2.3. GENERAL LIMIT METHOD OF MUNRO

A general limit analysis using a basic set of influence functions has been developed by Munro (36). The method has been developed for the computation of collapse loads and displacements and is illustrated through examples in Reference (36). A brief summary of the method is given in section 1.2. The generalised compatibility equation which is used in the present work is explained below.

A frame which is α times indeterminate can be reduced to a determinate form by the suitable insertion of α hinges. Such a reduced structure can be used as the basis of all static and kinematic analysis. The selected hinges will be termed 'basic' and will be numbered 1 to α. The remaining critical sections will be termed 'non-basic' and will be numbered $(\alpha + 1)$ to c where c is the total number of critical sections. It should be emphasized that it is not implied that the basic hinges are the actual plastic hinges at the ultimate load.

The basic influence diagrams k_i and the particular solution m_o are shown for a frame in Fig.2.5. From the property of contragredience (36) the influence diagrams k_i can also be used as the basis of kinematic analysis, and a simple illustration is indicated in Fig.2.6 where θ^i is the angular discontinuity at the i^{th} basic hinge and θ^j is the inelastic rotation at non-basic critical section j. The angular discontinuity at basic hinge 1 of Fig. 2.5 is,

$$\theta_b^1 = g_{11}m^1 + g_{12}m^2 + g_{13}m^3 + v_{10} + k_{14}\theta_n^4 + k_{15}\theta_n^5$$

The other two basic hinges can similarly be considered and the compatibility equation for the frame shown in Fig.2.5 becomes,

$$\begin{aligned}
g_{11}m^1 + g_{12}m^2 + g_{13}m^3 + v_{10} + k_{14}\theta_n^4 + k_{15}\theta_n^5 &= \theta_b^1 \\
g_{21}m^1 + g_{22}m^2 + g_{23}m^3 + v_{20} + k_{24}\theta_n^4 + k_{25}\theta_n^5 &= \theta_b^2 \\
g_{31}m^1 + g_{32}m^2 + g_{33}m^3 + v_{30} + k_{34}\theta_n^4 + k_{35}\theta_n^5 &= \theta_b^3
\end{aligned} \qquad (2.4)$$

The above result can be extended to a frame shown in Fig.2.7 indeterminate to α degree. The governing compatibility equation becomes,

$$g_{11}m^1 + g_{12}m^2 + \text{- - - - - -} + g_{1\alpha}m^\alpha + v_{10} + \sum_{j=\alpha+1}^{c} k_{1j}\theta_n^j = \theta_b^1$$

$$g_{21}m^1 + g_{22}m^2 + \text{- - - - - -} + g_{2\alpha}m^\alpha + v_{20} + \sum_{j=\alpha+1}^{c} k_{2j}\theta_n^j = \theta_b^2$$

- -

- -

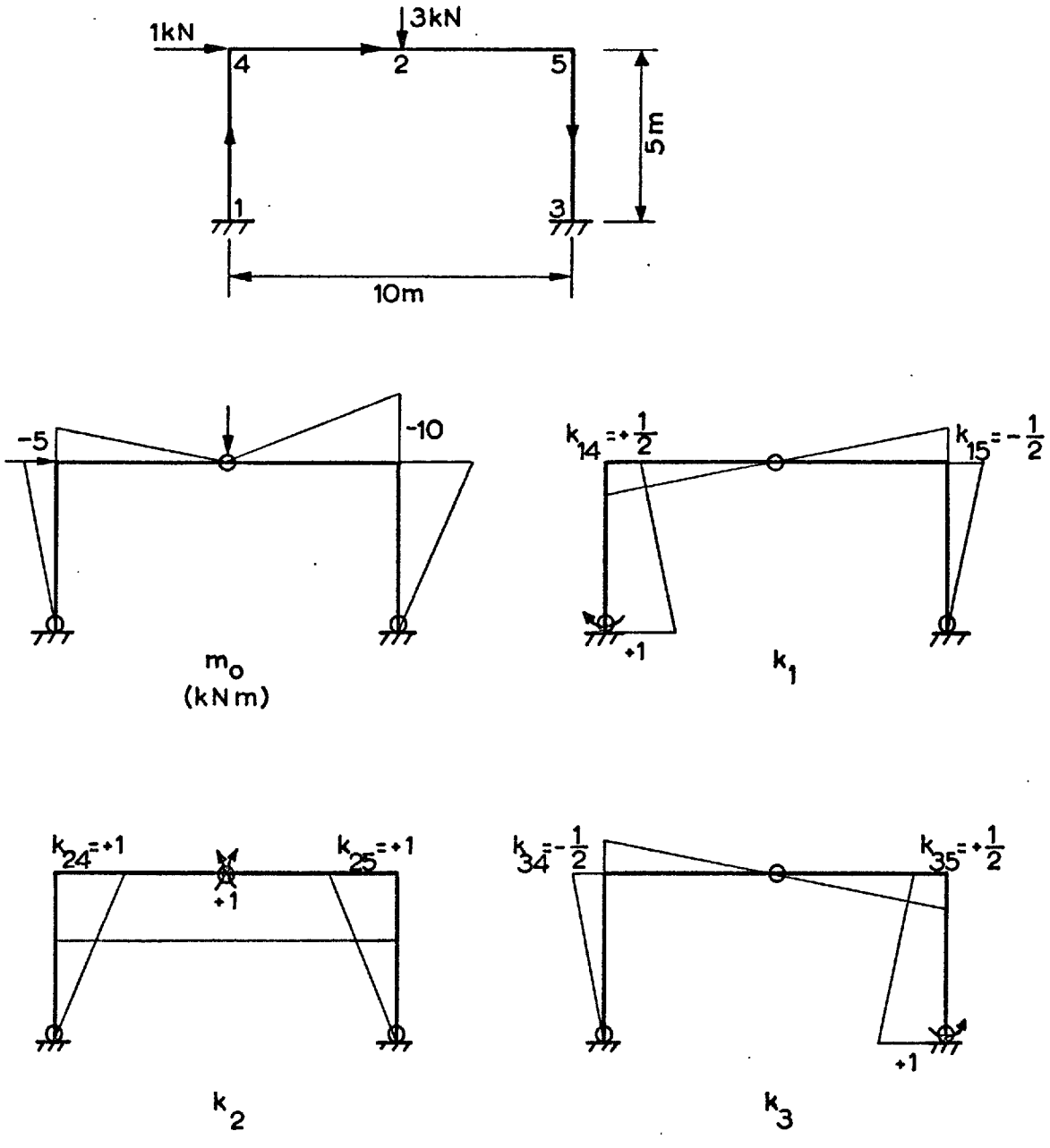
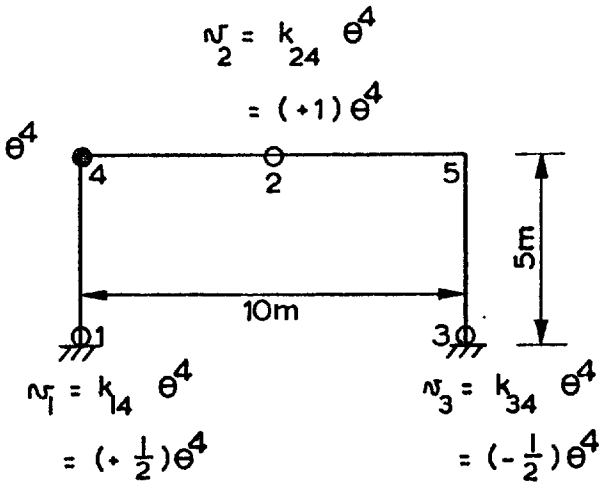
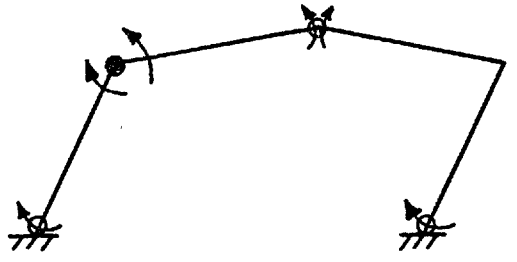


FIG. 2.5 INFLUENCE DIAGRAMS FOR A FRAME

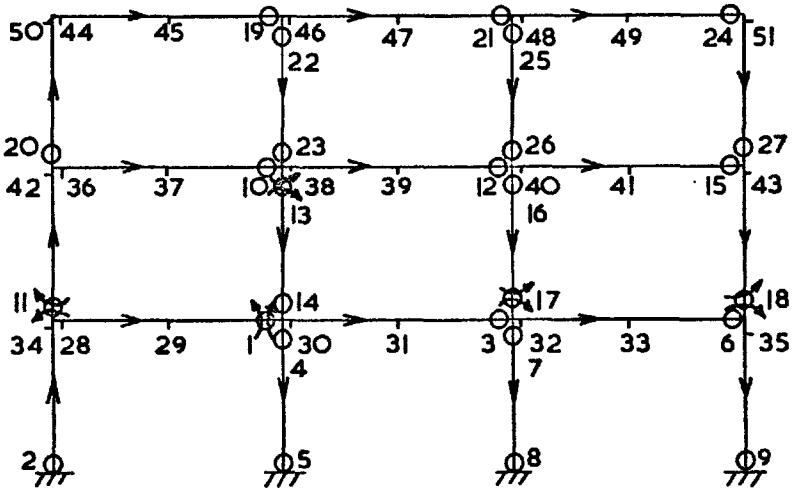


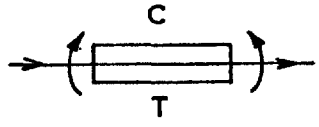
(a)



(b)

FIG. 2.6 DISCONTINUITY AT A NON-BASIC HINGE





Positive moment



Positive moment



Positive rotation

NON-BASIC HINGE



Positive rotation

BASIC HINGE

FIG. 2.7 RELEASE SYSTEM FOR A FRAME AND SIGN CONVENTIONS

$$g_{\alpha 1} m^1 + g_{\alpha 2} m^2 + - - - - + g_{\alpha\alpha}\ m^{\alpha} + v_{\alpha o} + \sum_{j=\alpha+1}^{c} k_{\alpha j} \theta_n^j = \theta_b^{\alpha} \qquad (2.5)$$

or more compactly,

$$[G]\ \{m_b\} + \{v_o\} + [K]\ \{\theta_n\} = \{\theta_b\} \qquad (2.6)$$

Parity Rule

In the ultimate load analysis of frames with some of the sections developing inelastic rotations it is necessary to establish the rule between the rotations and the moments at these sections. Fig. 2.7 shows the sign conventions employed for arbitrarily selected member directions. In order that all stress-resultants shall correspond to strain-resultants the following Parity Rule proposed by Munro (37) must be satisfied:

(a) At a basic hinge, i, developing inelastic rotation:

If m^i is positive $\quad \theta_b^i \leq 0$

If m^i is negative $\quad \theta_b^i \geq 0$ (2.7a)

(b) At a non-basic hinge, j, developing inelastic rotation:

If m^j is positive $\quad \theta_n^j \geq 0$

If m^j is negative $\quad \theta_n^j \leq 0$ (2.7b)

2.4 PROPOSED PROCEDURE BY ADJUSTMENT OF ROTATIONS FOR SIMPLIFIED LIMIT METHOD

For the cases of frames, where the computational difficulties discussed earlier are experienced in the trial and adjustment procedure of the simplified limit method, a modified procedure by adjustment of rotations is suggested below.

1. Assign the permissible rotation, θ_p^r, as the value for θ^r for beam hinges whose sign of moments are known for normal cases and zero rotation for column hinges. With these values of θ^r analyse the frame using equation (2.6) for moments, m^i, at all the hinges. The solution gives the magnitude and sign of moments for all the critical sections.

2. Since the sign of the column moments are now known, assign the sign of θ_p^r for column hinges according to Parity Rule (equation 2.7). Analyse the frame with proper values of θ_p^r as θ^r for beam and column hinges. The moments at critical beam and column sections corresponding to the permissible hinge rotations are now determined.

3(a). Compare the moments, m^r, obtained and the sign of θ^r used for the analysis in the previous step, and thus check for the Parity Rule.

3(b). If the Parity Rule is not satisfied assign the value of θ^r at that hinge as zero. Analyse the frame with the values of θ^r as zero at those hinges where Parity Rule is not satisfied and θ_p^r as the values of θ^r at the other hinges.

4. Check for Parity Rule for the analysis carried out in step (3). If Parity Rule is not satisfied at all the hinges repeat the procedure described in step 3(b) until it is satisfied at all the hinges.

The examples of the multi-storey frames presented here illustrate that the proposed procedure leads to rapid convergence for solution. It is to be noted that by this procedure one may obtain a solution for a frame with slightly less than α hinges when the values of rotation at certain of the hinges (mostly column hinges for normal cases of loading and geometry) are assigned as zero to satisfy the Parity Rule in step 3(b) of the procedure. But experience in working out the design examples shows that in actual cases of design the permissible rotation available in columns is quite small and hence the assumption of zero rotations may not introduce serious errors for practical purposes.

2.5 COMPUTER PROGRAM FOR ULTIMATE LOAD ANALYSIS OF REINFORCED CONCRETE FRAMES

A computer program developed for the ultimate load analysis of reinforced concrete frames is explained in the following. The basic flexibility matrix, [G], displacement vector $\{v_o\}$ and the kinematic

matrix, [K], for the frame with the basic hinges shown in Fig.2.7 are worked out using the influence diagrams and coefficients given in Reference (7) with the modification to the directed graph sign convention adopted here. The computational aspects of these matrices will be explained in Chapter 4. The generalised compatibility equation and Parity Rule (equations 2.5 and 2.7) due to Munro (36, 37) are used in the analysis of frames. The modified procedure by adjustment of rotations proposed in section 2.4 is used to obtain the solution of moments for the cases of hinge pattern, described below, under each of the two loading conditions.

The program analyses a frame for five different cases of hinge pattern under two ultimate loading conditions as shown in Fig.2.8.

Loading Condition I:

Case 1(a): Elastic analysis for factored loads.
This solution is useful to calculate the moment redistribution with the development of plastic hinges.

Case 1(b): Hinges at the ends of beams only.
For the cases of frames which require consideration of instability effects a recent investigation (53, 54) has shown that it is desirable to allow only beam hinges and avoid the formation of plastic hinges in columns. Hence this analysis can be used to design the frame to satisfy these requirements.

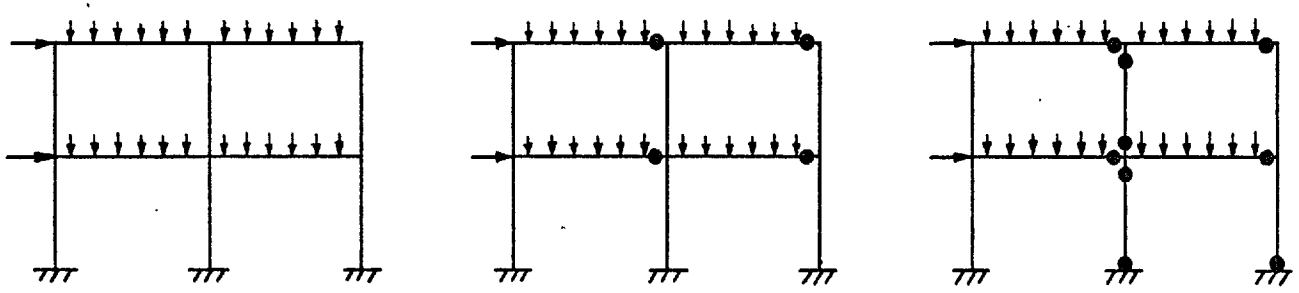
Case 2: Beam and Column hinges.
For frames where there are no such restrictions as above, hinges are allowed in beams and columns. The modified procedure by adjustment of rotations is used to obtain the solution for this case.

Loading Condition II:

Case 3(a): Elastic analysis for factored loads.

Case 3(b) and 4: Similar to cases 1(b) and 2. These two cases are included to compare the values of moments for the two loading conditions.

Case 5: Hinges at both ends of beams.
For loading condition II this hinge pattern is found to produce a maximum amount of moment redistribution and hence is included for the frames where the design is governed by this condition.

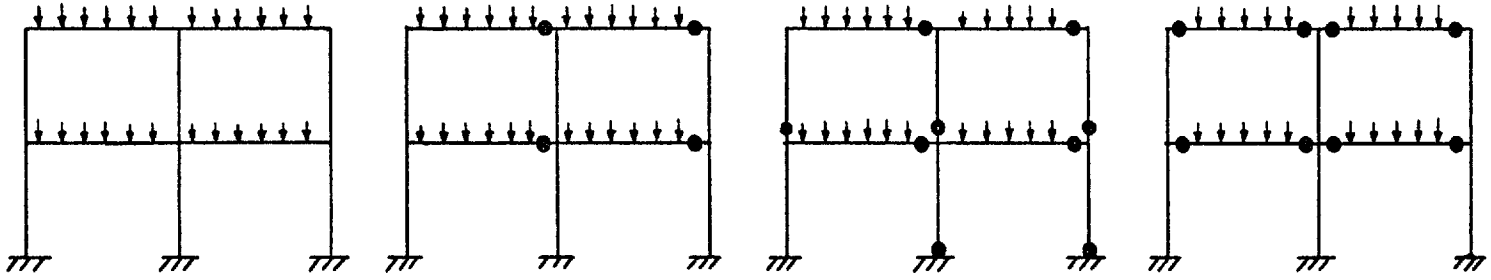


Elastic analysis — CAse 1(a)

Beam hinges only — Case 1(b)

Adjustment of rotations (an example) — Case 2

LOADING CONDITION I : $\lambda_c (W_D + W_L + W_W)$



Elastic analysis — Case 3(a)

Beam hinges only — Case 3(b)

Adjustment of rotations (an example) — Case 4

Hinges at both ends of beams only — Case 5

LOADING CONDITION II : $\lambda_D W_D + \lambda_L W_L$

FIG. 2.8 FIVE CASES OF ULTIMATE LOAD ANALYSIS

2.5.1. Sequence of Operations

The logic of the computer program is shown in the flow chart of Fig.2.9. Following is a step-by-step description of the main operations executed by the program.

1. Read and print input data. (The input data required for the program is listed separately.)

2. For a frame with hinge release system shown in Fig.2.7 calculate the influence coefficients g_{ij} of the flexibility matrix [G] through a set of subroutines. These subroutines will be explained in Chapter 4.

3. As the influence coefficients computed in step 2 follow the sign convention adopted in Reference (7) the flexibility matrix [G] is modified for the directed graph sign convention shown in Fig.2.7. This computation will be described later.

4. Calculate the displacement vector $\{v_o\}$ for each of the two loading conditions.

5. The kinematic matrix [K] used in the compatibility equation (2.6) is formulated through a subroutine for the release system and sign convention shown in Fig.2.7. This computation consists, essentially, of calculating the ordinate of the influence diagram at the non-basic hinge sections as described in section 2.3.

6. Compute the inverse of the flexibility matrix [G] using the subroutine MINV and $[G]^{-1}$ is stored in place of [G] for future calculations. The subroutine MINV uses the standard Gauss-Jordon method and has also the facility to use double precision in calculations.

7. Read the permissible rotation values for the basic and non-basic hinges for each of the loading conditions.

8. Elastic analysis of the frame (case 1(a) or case 3(a)) is carried out in this step. The moments at the non-basic hinge sections can be calculated from the equilibrium conditions and this is done through a subroutine CALMAC. The results of analysis are printed out.

9. Assign permissible rotation values at the beam hinges and zero rotation in all the column hinges (case 1(b) or case 3(b)) and analyse the frame. This also forms the step 1 of the proposed modified procedure by adjustment of rotations.

10, 11, 12 and 13. These form the steps 2 to 4 of the analysis by adjustment of rotations. The procedure in steps 11, 12 and 13 is repeated until the solution satisfies the compatibility equation and parity rule.

14. Print the position and value of rotation of plastic hinges.

15. Calculate the moments at the non-basic hinges through the sub-routine CALMAC and print the results.

16. Steps 7 through 15 are repeated for loading condition II (cases 3, 3(b) and 4).

17. For loading condition II read the values of permissible rotations for hinges at both ends of beams. Analyse the frame for this hinge pattern (case 5) and print the results.

2.5.2. Input

The input data to be supplied for the program are as follows:

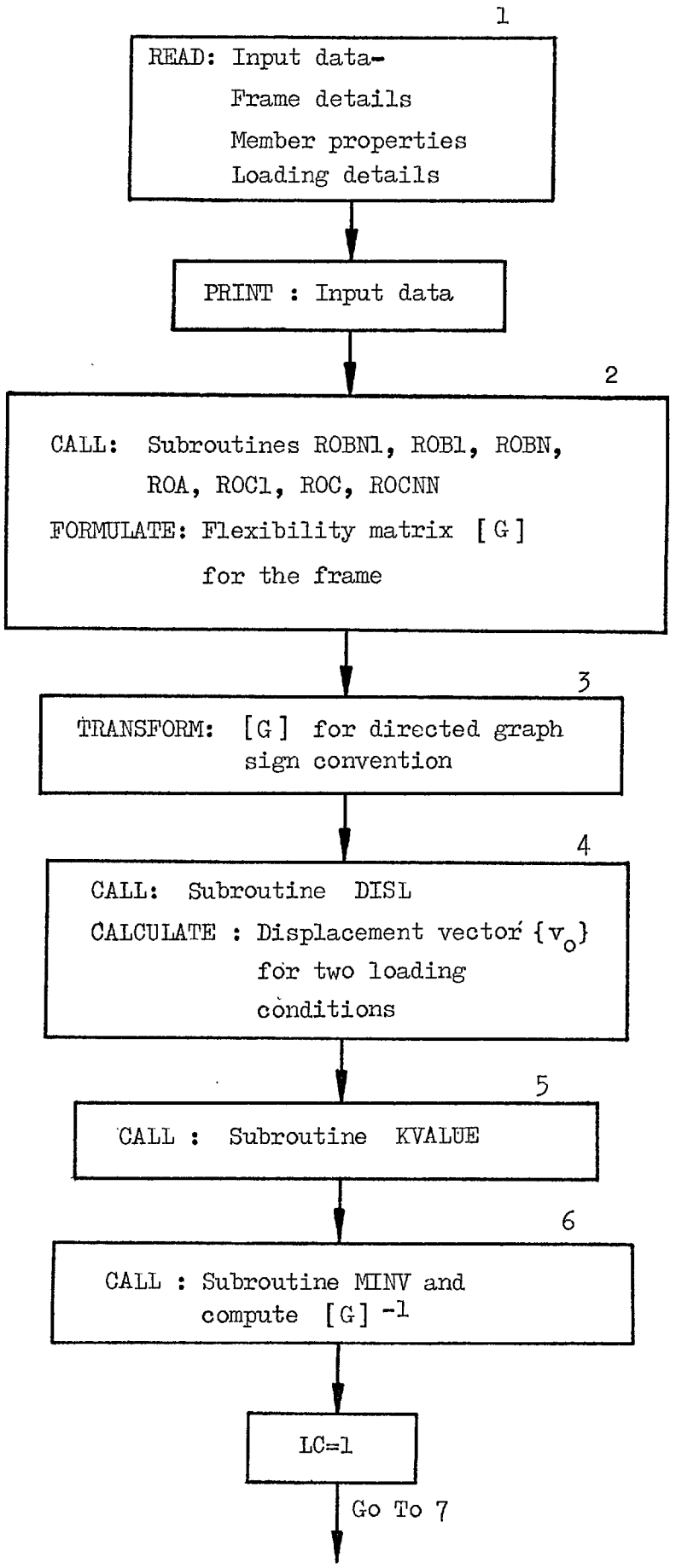
1. Number of storeys and number of bays.
2. Type of supports: These are entered as numerical integers whose value indicates whether a particular support is hinged or fixed.
3. Lengths of beams.
4. Heights of columns.
5. EI values for beams.
6. EI values for columns.
7. Simply supported bending moment values due to dead and live working loads on beams.
8. Wind load moment for each storey (= storey shear x height).
9. Load factors for loading condition I.
10. Load factors for loading condition II.
11. Permissible rotation for basic hinge sections.
12. Permissible rotation for non-basic hinge sections.

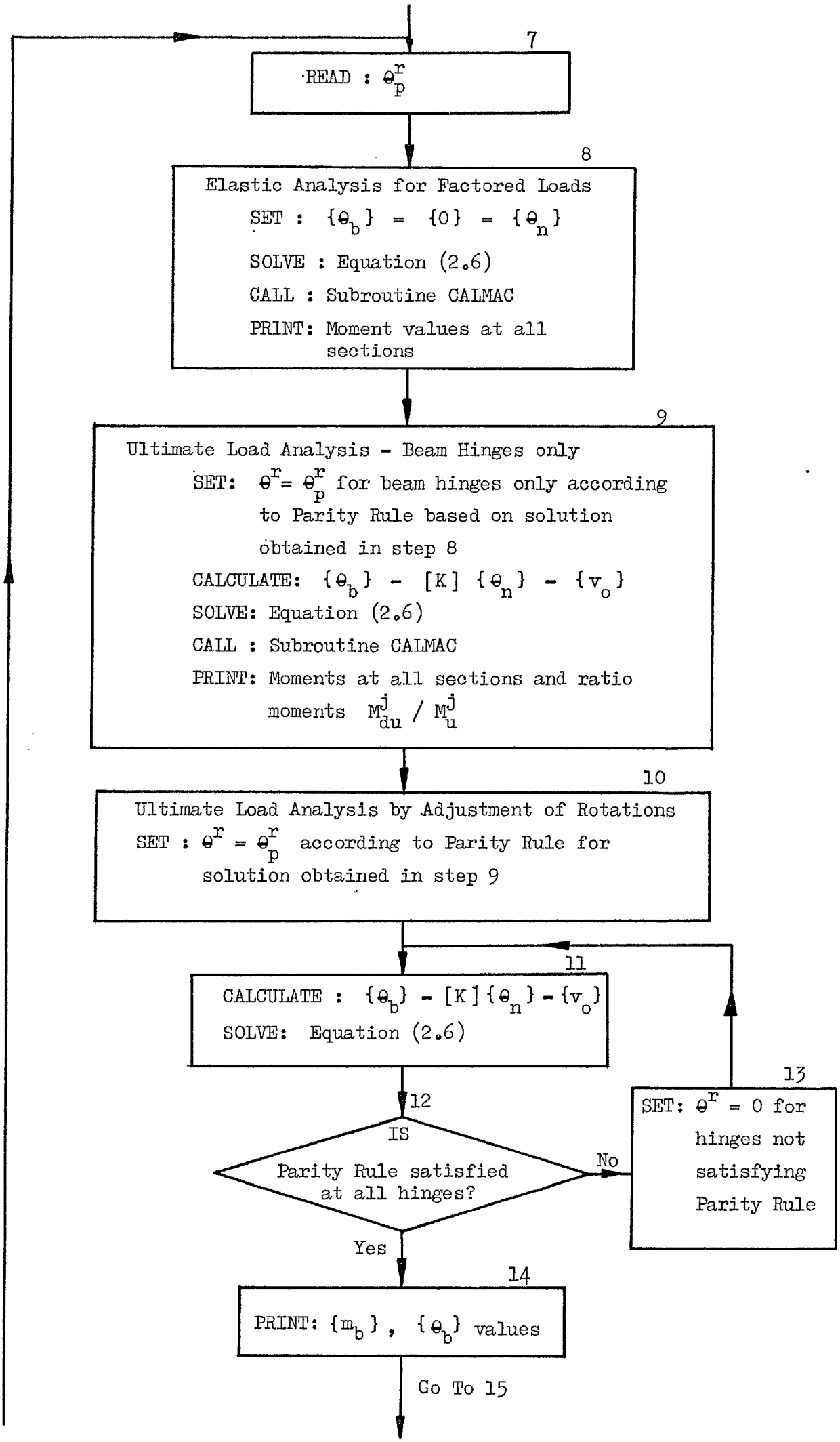
The set of data in (11) and (12) are required for two loading conditions.

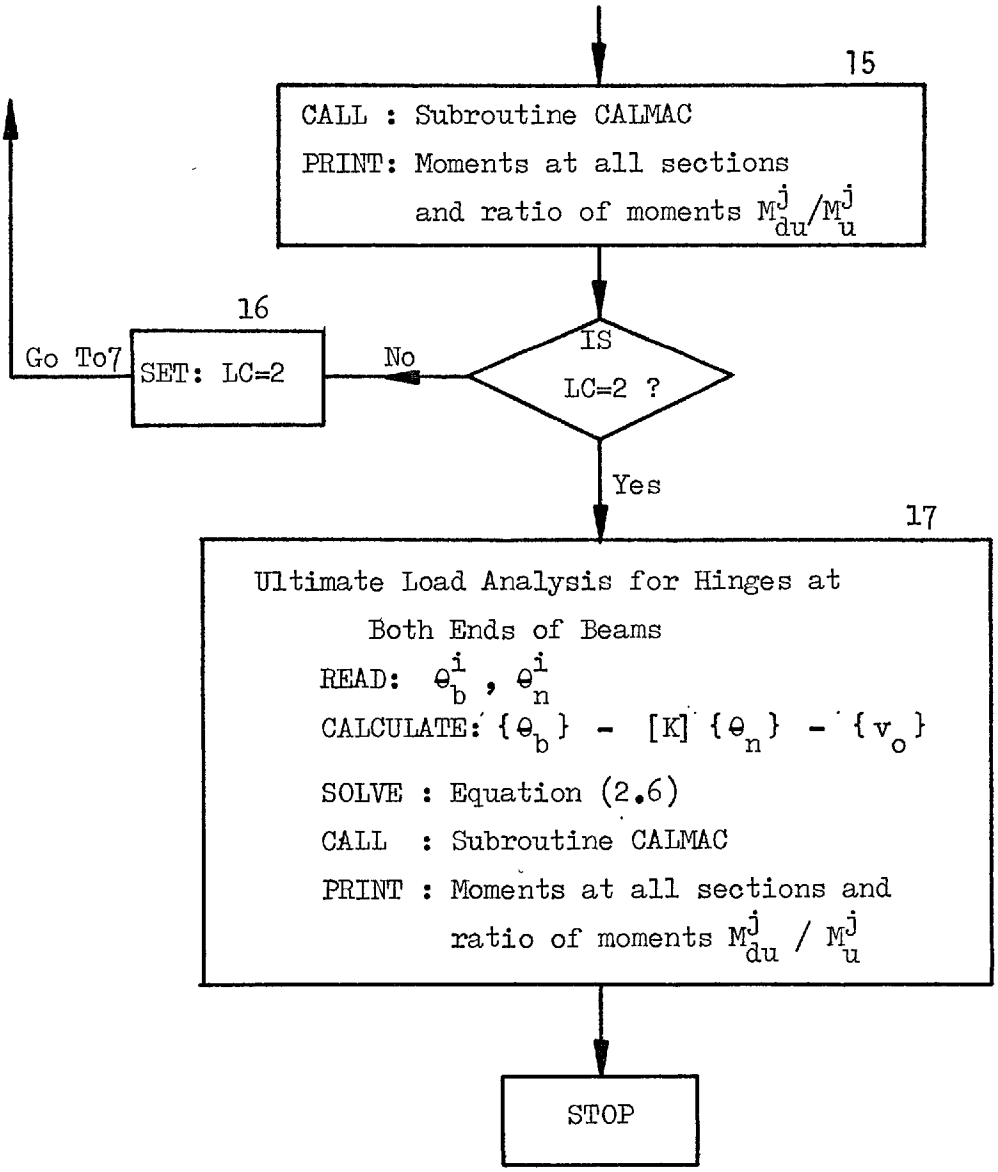
Fig.2.7 indicates the numbering system required for the preparation of input data.

FIG.2.9. FLOW CHART

ULTIMATE LOAD ANALYSIS PROGRAM




7
READ : θ_p^r
8
Elastic Analysis for Factored Loads
SET : $\{\theta_b\} = \{0\} = \{\theta_n\}$
SOLVE : Equation (2.6)
CALL : Subroutine CALMAC
PRINT: Moment values at all sections
9
Ultimate Load Analysis - Beam Hinges only
SET: $\theta^r = \theta_p^r$ for beam hinges only according to Parity Rule based on solution obtained in step 8
CALCULATE: $\{\theta_b\} - [K]\{\theta_n\} - \{v_o\}$
SOLVE: Equation (2.6)
CALL : Subroutine CALMAC
PRINT: Moments at all sections and ratio moments M_{du}^j / M_u^j
10
Ultimate Load Analysis by Adjustment of Rotations
SET : $\theta^r = \theta_p^r$ according to Parity Rule for solution obtained in step 9
11
CALCULATE : $\{\theta_b\} - [K]\{\theta_n\} - \{v_o\}$
SOLVE: Equation (2.6)
12
IS Parity Rule satisfied at all hinges?
No
13
SET: $\theta^r = 0$ for hinges not satisfying Parity Rule
Yes
14
PRINT: $\{m_b\}$, $\{\theta_b\}$ values
Go To 15


15
CALL : Subroutine CALMAC
PRINT: Moments at all sections
and ratio of moments M^j_{du}/M^j_u
16
Go To7
SET: LC=2
No
IS
LC=2 ?
Yes
17
Ultimate Load Analysis for Hinges at
Both Ends of Beams
READ: θ^i_b , θ^i_n
CALCULATE: $\{\theta_b\} - [K]\{\theta_n\} - \{v_o\}$
SOLVE : Equation (2.6)
CALL : Subroutine CALMAC
PRINT : Moments at all sections and
ratio of moments M^j_{du} / M^j_u
STOP

2.5.3. Output

The output of the program is listed below:

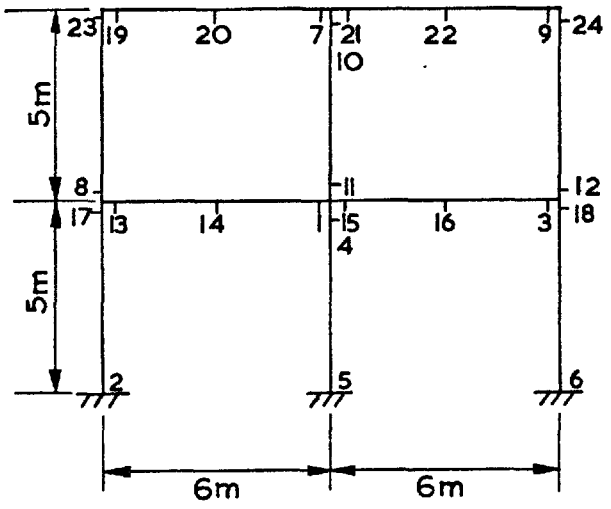
1. Frame and member properties as given in the data.
2. Results of elastic analysis for factored loads and of ultimate load analysis for five cases of hinge pattern are printed as described below:
   For each storey -
   Beams - Moments at three sections; left end, mid span and right end.
   Ratio of moments for ultimate load analysis to elastic analysis for factored loads for the three sections.
   Columns - Moments at two sections; top and bottom ends.
   Ratio of moments for ultimate load analysis to elastic analysis for factored loads for the two sections.
3. For cases 2 and 4 the hinge number, the value of moment and the rotation for each iteration. This will enable to study the convergence and to identify the hinges at which inelastic rotations have been assigned.

2.6. DESIGN EXAMPLES

In order to study the problem of ultimate load design of reinforced concrete frames in more detail and to examine the amount of moment redistribution three frames have been designed using the program presented here. The salient details of design and the results of analysis are discussed below.

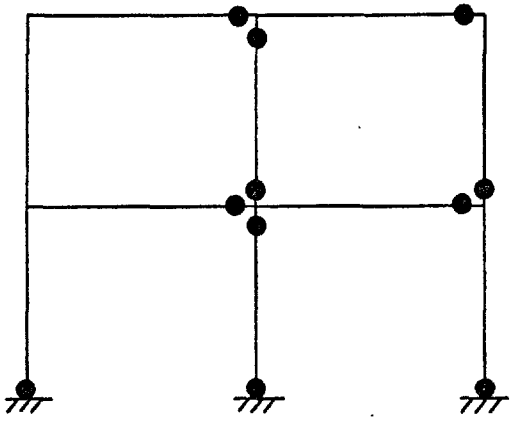
2.6.1. General Description

Figs. 2.10 to 2.12 show the geometry, the member sizes and the numbering of the basic and non-basic hinge sections for the three frames. The details of loading are given in Table 2.1. The members of the frames have been designed according to the assumptions and recommendations of the simplified limit method of Baker. Thus the critical sections which form plastic hinges at the ultimate load stage are designed for the conditions at limit L_2 and the other critical sections are designed for the conditions at limit L_1. The design charts given in Reference (12) have been used for the calculation of area of steel reinforcement and of the EI values of the members. The permissible rotations of the critical sections have been calculated using the curves given in Fig. 2.3. The final design details are given in Tables 2.2 to 2.4.



(a) Beams : 250 x 500mm

Columns : 250 x 250mm



Ultimate Load Analysis

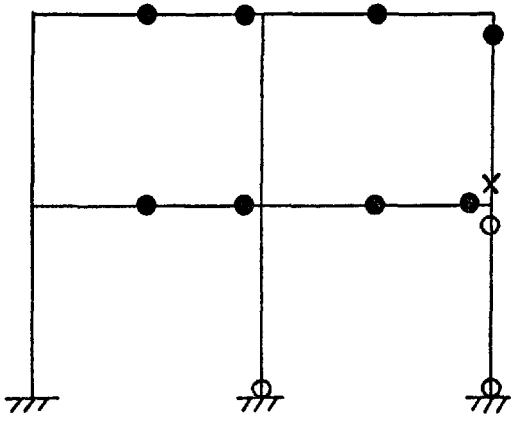
(b) Loading condition I

CASE 2

(Adjustment of rotations)

Position of plastic hinges

No of iterations : 3



Inelastic stage-by-stage analysis

(c) Loading condition I

Plastic hinge pattern

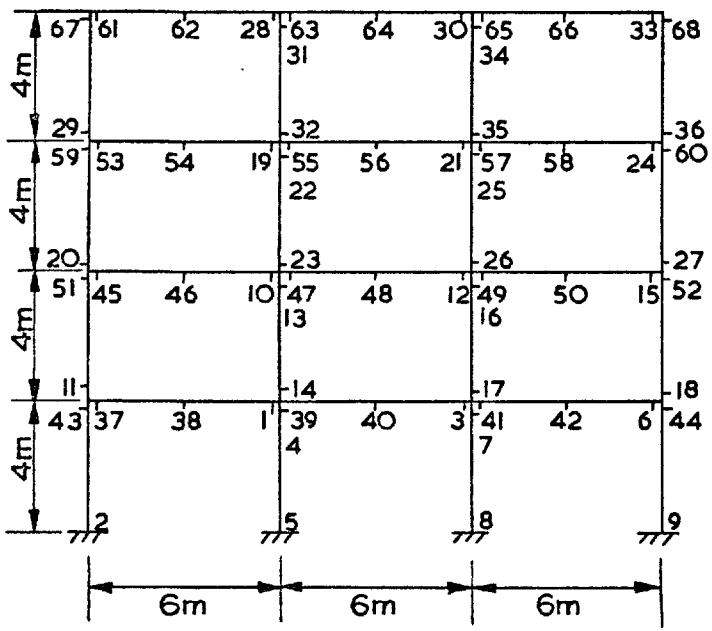
Load factor at failure , $\lambda_c = 1{\cdot}323$

● - Full plastic hinge ($M^j = M_{ru}$)

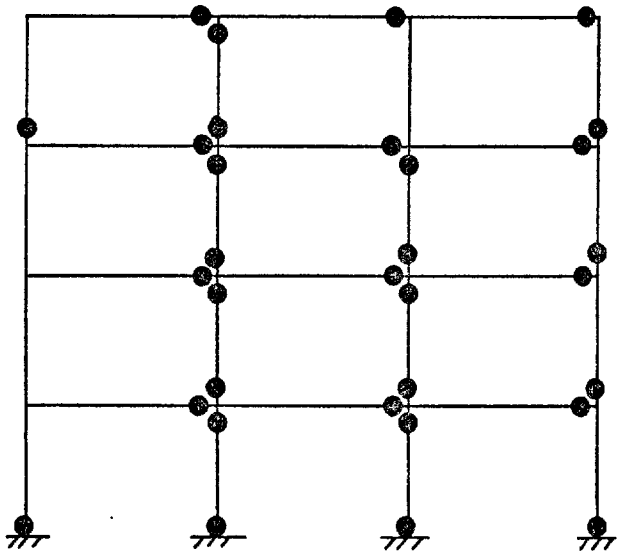
O - Partial plastic hinge ($M_{ry} < M^j < M_{ru}$)

X - About to yield

FIG.2.10 DESIGN EXAMPLE 1



(a) Beams 250 x 450 mm
Columns 250 x 250 mm



Ultimate Load Analysis

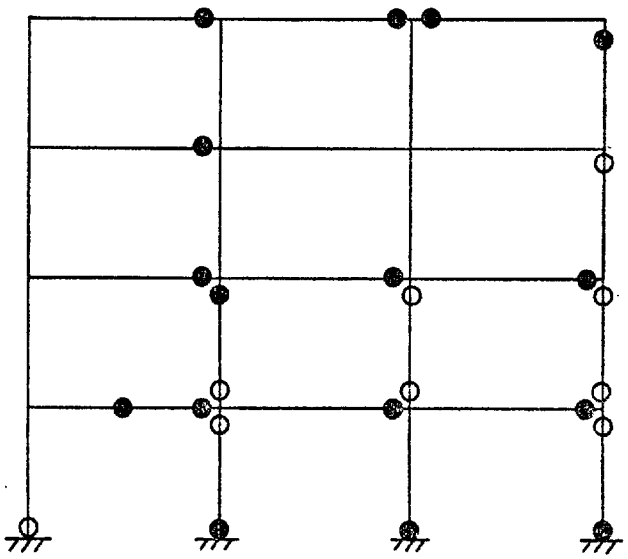
(b) Loading condition I

CASE 2

(Adjustment of rotations)

Position of plastic hinges

No. of iterations : 3



Inelastic stage - by - stage analysis

(c) Loading condition I

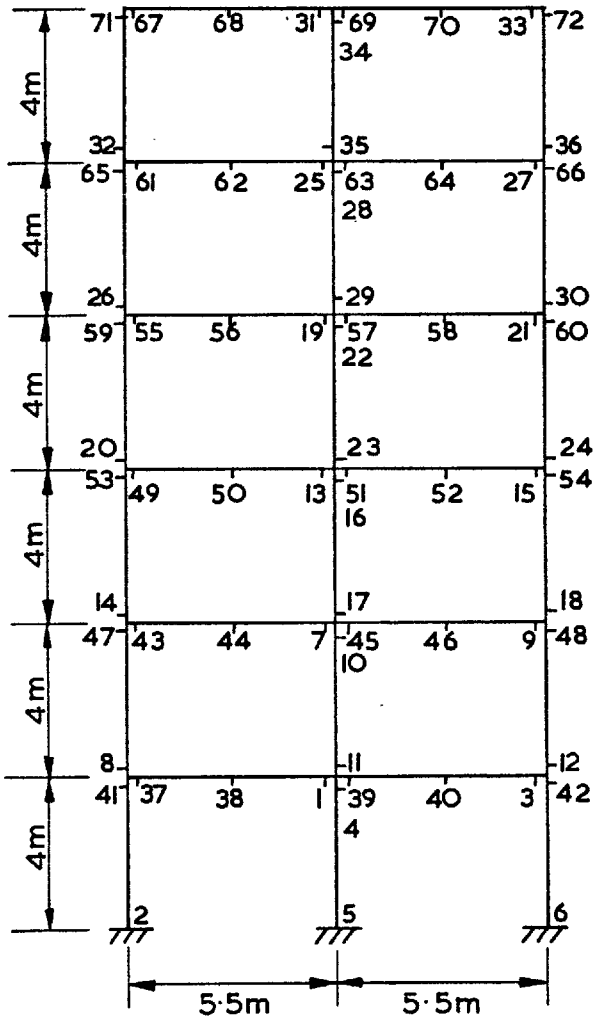
Plastic hinge pattern

Load factor at failure , $\lambda_c = 1{\cdot}436$

● – Full plastic hinge ($M^j = M_{ru}$)

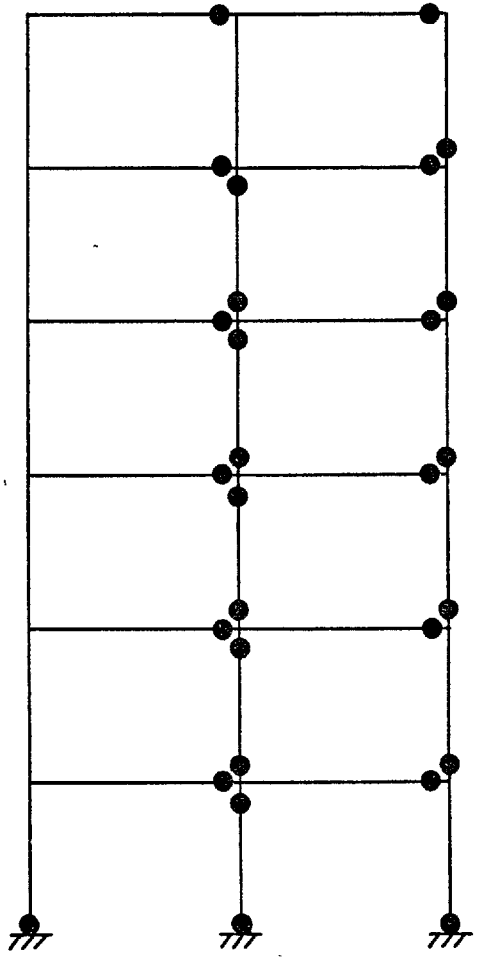
○ – Partial plastic hinge ($M_{ry} < M^j < M_{ru}$)

FIG. 2.11 DESIGN EXAMPLE 2



(a) Beams 250 x 460mm

Columns 250 x 250mm



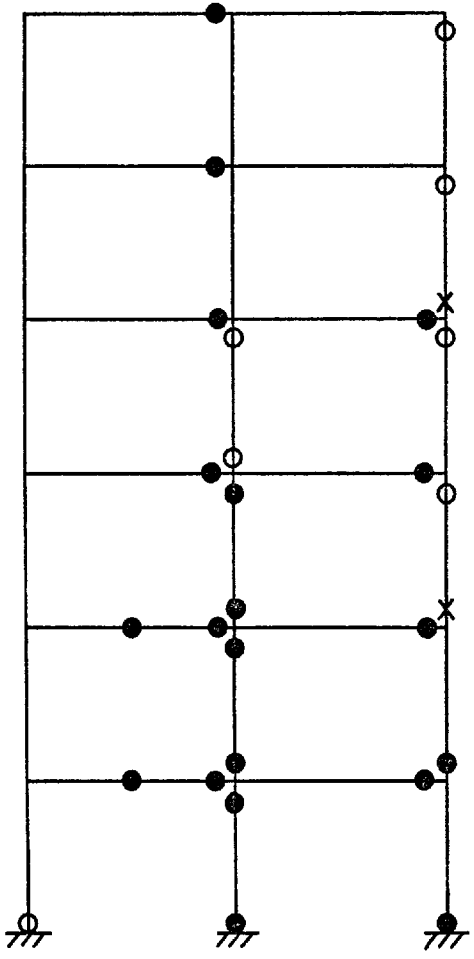
Ultimate load analysis

(b) Loading condition I

CASE 2

Position of plastic hinges

No of iterations : 3



Ine lastic stage - by - stage analysis

(c) Loading condition I

Plastic hinge pattern

Load factor at failure, $\lambda_c = 1{\cdot}267$

FIG. 2.12 DESIGN EXAMPLE 3

TABLE 2.1. DETAILS OF LOADINGS AND STRENGTHS OF CONCRETE AND STEEL

	Example 1	Example 2	Example 3
Loadings:			
Live load, kN/m^2	5.0	2.5	3.0
Floor finishes, kN/m^2	1.0	1.0	1.0
Wind load, kN/m^2	1.0	0.7	0.7
Beams:			
Live load per metre run, kN/m	20.0	9.4	12.0
Dead load per metre run, kN/m	25.0	19.5	20.0
Wind force:			
Top floor level, kN	10.0	8.4	5.6
Other floor levels, kN	20.0	16.8	11.2
Load factors:			
λ_D	1.4	1.4	1.4
λ_L	1.6	1.6	1.6
λ_C	1.25	1.25	1.25
Design strengths:			
Concrete, N/mm^2	16.0	17.0	16.0
Steel, N/mm^2	415.0	415.0	415.0

TABLE 2.2. DESIGN DETAILS OF EXAMPLE 1

Member	Section	Percentage steel p x 100	Permissible rotation	EI value of the member x 10^{12} ($N.mm^2$)
B1	1 14 13	1.20 0.75 0.40	0.009 - 0.0125	21.0
B2	3 16 15	0.40 0.75 1.20	0.0125 - -	21.0
B3	7 20 19	1.20 0.75 0.40	0.009 - 0.0125	21.0
B4	9 22 21	0.40 0.75 1.20	0.0125 - -	21.0
C1	13 2	0.5	- 0.004	3.0
C2	4 5	1.75	0.001 0.001	6.0
C3	18 6	0.50	- 0.004	3.0
C4	23 8	0.40	- 0.008	2.5
C5	10 11	0.40	0.001 0.001	4.0
C6	24 12	0.40	- 0.008	2.5

TABLE 2.3. DESIGN DETAILS OF EXAMPLE 2

Member	Section	Percentage steel p x 100	Permissible rotation	EI value of the member x 10^{12} (Nmm^2)
B1	37	0.55	0.01	12.0
	38	0.75	-	
	1	0.85	0.01	
B2	39	0.80	0.01	12.0
	40	0.75	-	
	3	0.80	0.01	
B3	41	0.85	0.01	12.0
	42	0.75	-	
	6	0.55	0.01	
B4	45	0.55	0.01	12.0
	46	0.75	-	
	10	0.85	0.01	
B5	47	0.80	0.01	12.0
	48	0.75	-	
	12	0.80	0.01	
B6	49	0.85	0.01	12.0
	50	0.75	-	
	15	0.55	0.01	
B7	53	0.50	0.01	12.0
	54	0.75	-	
	19	0.80	0.01	
B8	55	0.75	0.01	12.0
	56	0.75	-	
	21	0.75	0.01	
B9	57	0.80	0.01	12.0
	58	0.75	-	
	24	0.50	0.01	
B10	61	0.50	0.01	12.0
	62	0.75	-	
	28	0.80	0.01	

(contd.)

TABLE 2.3. (contd)

Member	Section	Percentage steel p x 100	Permissible rotation	EI value of the member x 10^{12} (Nmm^2)
B11	63 64 30	0.75 0.75 0.75	0.01 - 0.01	12.0
B12	65 66 33	0.80 0.75 0.50	0.01 - 0.01	12.0
C1	39 2	0.80	- 0.0025	4.5
C2	4 5	2.05	0.001 0.001	7.0
C3	7 8	2.05	0.001 0.001	7.0
C4	44 9	0.80	- 0.0025	4.5
C5	51 11	0.80	- 0.0025	4.0
C6	13 14	1.00	0.001 0.001	7.0
C7	16 17	1.00	0.001 0.001	7.0
C8	52 18	0.80	- 0.0025	4.0
C9	59 20	0.80	- 0.005	3.5
C10	22 23	0.80	0.002 0.002	4.5
C11	25 26	0.80	0.002 0.002	4.5

(contd)

TABLE 2.3. (contd)

Member	Section	Percentage steel p x 100	Permissible rotation	EI value of the member x 10^{12} (Nmm^2)
C12	60 27	0.80	- 0.005	3.5
C13	61 29	0.80	- 0.006	3.5
C14	31 32	0.80	0.002 0.002	4.0
C15	34 35	0.80	0.002 0.002	4.0
C16	33 36	0.80	- 0.006	3.5

TABLE 2.4. DESIGN DETAILS OF EXAMPLE 3

Member	Section	Percentage steel p x 100	Permissible rotation	EI value of the member x 10^{12} (Nmm^2)
B1	37	0.60	0.01	12.0
	38	0.62	-	
	1	0.95	0.01	
B2	39	0.95	0.01	12.0
	40	0.62	-	
	3	0.60	0.01	
B3	43	0.60	0.01	12.0
	44	0.62	-	
	7	0.95	0.01	
B4	45	0.95	0.01	12.0
	46	0.62	-	
	9	0.60	0.01	
B5	49	0.50	0.01	12.0
	50	0.62	-	
	13	0.85	0.01	
B6	51	0.85	0.01	12.0
	52	0.62	-	
	15	0.50	0.01	
B7	55	0.45	0.01	12.0
	56	0.65	-	
	19	0.75	0.01	
B8	57	0.75	0.01	12.0
	58	0.65	-	
	21	0.45	0.01	
B9	61	0.45	0.01	12.0
	62	0.65	-	
	25	0.75	0.01	
B10	63	0.75	0.01	12.0
	64	0.65	-	
	27	0.45	0.01	

(contd)

TABLE 2.4 (contd)

Member	Section	Percentage steel p x 100	Permissible rotation	EI value of the member x 10^{12} (Nmm^2)
B11	67 68 31	0.45 0.65 0.75	0.01 - 0.01	12.0
B12	69 70 33	0.75 0.65 0.45	0.01 - 0.01	12.0
C1	41 2	1.55	- 0.002	5.5
C2	4 5	3.50	0.0015 0.0015	13.0
C3	42 6	1.55	- 0.002	5.5
C4	47 8	1.55	- 0.0025	5.5
C5	10 11	2.25	0.0015 0.0015	10.0
C6	48 12	1.55	- 0.0025	5.5
C7	53 14	1.00	- 0.003	4.0
C8	16 17	1.45	0.0015 0.0015	7.0
C9	54 18	1.00	- 0.003	4.0
C10	59 20	0.60	- 0.005	3.0
C11	22 23	1.00	0.0015 0.0015	6.0

(contd)

TABLE 2.4 (contd)

Member	Section	Percentage steel p x 100	Permissible Rotation	EI value of the member x 10^{12} (Nmm^2)
C12	60 24	0.60	- 0.005	3.0
C13	65 26	0.50	- 0.005	3.0
C14	28 29	0.50	0.0025 0.0025	4.0
C15	66 30	0.50	- 0.005	3.0
C16	71 32	0.50	- 0.0075	2.5
C17	34 35	0.50	0.005 0.005	3.5
C18	72 36	0.50	- 0.0075	2.5

2.6.2. Results of Ultimate Load Analysis

The frames have been analysed for five cases of hinge pattern under two loading conditions using the computer program described in section 2.5. The values of moments at all the critical sections for the elastic analysis and for cases 2 and 5 of hinge pattern for ultimate load analysis are given in Tables 2.5 to 2.7. In order to study the variation of moments with respect to the elastic analysis, the ratio of moments for ultimate load analysis to elastic analysis for factored loads are given in Tables 2.8 to 2.10, for all the five cases of hinge pattern considered in the program.

The modified procedure by adjustment of rotations, which is incorporated in the program, has been used to solve for the case 2 of the hinge pattern. Figs. 2.10 to 2.12 show the position of plastic hinges obtained by this analysis that satisfy the compatibility (including the limited rotation capacity of sections) and parity rule requirements. The number of iterations required to obtain the final solution are also indicated in Figs. 2.10 to 2.12.

2.6.3. Inelastic Analysis of Reinforced Concrete Frames

A computer-oriented method of inelastic analysis of reinforced concrete frames has been developed by Nahhas (53). This program has been used to calculate the actual load factor for the three design examples described above. The method of analysis is summarized in the following.

The inelastic frame analysis program is based on the stiffness method of analysis (55) of framed structures and produces a loading history upto failure. The solution proceeds by increments of loading which eventually reaches the failure stage. In the calculation of stiffness coefficients of the members the moment-curvature relations derived on the basis of the behaviour of the reinforced concrete members under the stress-resultants corresponding to a particular load stage are used. These coefficients include, the effect of formation of plastic hinges in the members and the stability functions which account for column deflections. The computation involves an iterative process whereby, at any load stage, a set of axial loads and moments at

the ends of the members are proposed and the stiffness coefficients are formulated. The frame is then analysed and the stress resultants calculated. If these are close enough to the proposed values, a valid solution is reached. Otherwise a new iteration is started with the obtained stress resultants used as proposed values. When convergence is obtained, the load factor is increased by a predetermined increment and the initial proposed values of the stress resultants are linearly extrapolated. A new set of iterations is thus started.

As the load factor reaches the vicinity of the failure load, convergence increasingly requires more cycles of iterations. Eventually either convergence cannot be obtained or one of the failure criteria described below is met. In both cases this indicates that the load factor may have exceeded the failure load. The value of the load factor is reset at that corresponding to the most valid solution and the load increment is halved. The process is repeated until it is found that no solution can be obtained while the load increment has become less than a predetermined minimum limit. The frame is thus assumed to have reached its failure load and the analysis is terminated.

The failure criteria adopted in the analysis are as follows:

1. The determinant of the stiffness matrix is zero or negative indicating a condition of instability. This condition prevails whether the failure is due to the existence of an excessive number of plastic hinges (mechanism) or to overall frame instability in a mode against which the frame is unrestrained.

2. Local beam failure. This condition is attained when a beam develops a local mechanism with three hinges developed at the three critical sections.

3. Local column failure. For cases where a column is bent in single curvature, the possibility of a plastic zone occurring along the length of the column cannot be completely excluded. This condition causes local instability and therefore, complete failure.

The inelastic analysis program described above has been used to test the actual load factor at failure of the three frames, which have been designed to illustrate the use of the ultimate load analysis program developed here. Figs. 2.10 to 2.12 show the position of plastic hinges and the actual load factor at failure.

TABLE 2.5. RESULTS OF ANALYSIS - EXAMPLE 1

Section	Loading Condition I		Loading Condition II	
	Elastic analysis for factored loads M_u^j (kNm)	Ultimate load analysis Case 2 M_{du}^j (kNm)	Elastic analysis for factored loads M_u^j (kNm)	Ultimate load analysis Case 5 M_{du}^j (kNm)
13	-17.58	-3.06	-57.13	-25.30
14	115.03	139.64	136.47	191.68
1	-258.62	-223.91	-272.93	-194.35
15	-199.67	-161.70	-272.93	-194.35
16	114.11	147.67	136.47	191.68
3	-78.36	-49.20	-57.13	-25.30
17	1.72	4.47	-24.66	-10.92
2	-13.86	15.45	12.33	5.46
4	-45.48	-43.92	0.0	0.0
5	48.74	59.20	0.0	0.0
18	-43.13	-34.16	-24.66	-10.92
6	34.57	30.30	-12.33	5.46
19	-19.68	-7.83	-34.12	-15.11
20	120.09	145.19	142.22	194.22
7	-246.39	-208.04	-284.44	-199.45
21	-231.22	-187.70	-284.44	-199.45
22	118.72	147.18	142.22	194.22
9	-37.60	-24.19	-34.12	-15.11
23	-19.68	-7.83	-34.12	-15.11
8	19.30	7.53	32.47	14.38
10	-15.18	-20.34	0.0	0.0
11	13.47	18.29	0.0	0.0
24	-37.60	-24.19	-34.12	-15.11
12	35.22	15.04	32.47	14.38

TABLE 2.6. RESULTS OF ANALYSIS - EXAMPLE 2

Section	Loading Condition I		Loading Condition II	
	Elastic analysis for factored loads M_u^j (kNm)	Ultimate load analysis Case 2 M_{du}^j (kNm)	Elastic analysis for factored loads M_u^j (kNm)	Ultimate load analysis Case 5 M_{du}^j (kNm)
37	-23.05	-13.11	-74.12	-50.81
38	69.10	87.20	79.81	114.72
1	-164.37	-138.11	-147.96	-101.44
39	-75.74	-59.14	-131.12	-89.90
40	50.95	71.42	59.73	100.95
3	-147.98	-123.63	-131.12	-89.90
41	-88.07	-69.26	-147.96	-101.44
42	67.07	85.01	79.81	114.72
6	-103.41	-86.33	-74.12	-50.82
43	-3.60	-3.28	-32.07	-21.99
2	-18.00	-21.34	16.03	10.99
4	-46.32	-38.42	-6.81	-4.67
5	53.95	62.83	3.40	2.33
7	-34.71	-28.45	6.81	4.67
8	48.15	57.85	-3.40	-2.33
44	-51.11	-43.60	-32.07	-21.99
9	45.35	44.78	16.03	10.99
45	-35.76	-19.15	-76.72	-52.60
46	68.23	87.41	78.90	114.16
10	-153.41	-131.65	-146.99	-100.78
47	-85.32	-66.38	-130.90	-89.75
48	51.14	71.61	59.95	101.10
12	-138.03	-116.03	-130.90	-89.75
49	-97.38	-76.57	-146.99	-100.78
50	66.56	84.69	78.90	114.16
15	95.13	79.68	-76.72	-52.60
51	-17.04	-8.90	-41.35	-28.35
11	19.45	9.83	42.05	28.83
13	-44.98	-42.55	-9.83	-6.74
14	42.30	40.55	10.02	6.87
16	-28.21	-28.25	9.83	6.74
17	25.20	25.92	-10.02	-6.87
52	-53.50	-48.73	-41.35	-28.35

(contd)

TABLE 2.6 (contd)

Section	Loading Condition I		Loading Condition II	
	Elastic analysis for factored loads M_u^j (kNm)	Ultimate load analysis Case 2 M_{du}^j (kNm)	Elastic analysis for factored loads M_u^j (kNm)	Ultimate load analysis Case 5 M_{du}^j (kNm)
18	52.29	42.73	42.05	28.83
53	-49.98	-22.99	-77.69	-53.27
54	68.30	91.90	78.83	114.05
19	-139.05	-118.82	-146.34	-100.33
55	-99.66	-83.73	-131.01	-89.82
56	51.05	69.37	59.84	101.03
21	-123.87	-103.16	-131.01	-89.82
57	-110.64	-89.25	-146.34	-100.33
58	66.20	86.84	78.83	114.05
24	-82.58	-62.70	-77.69	-53.27
59	-16.67	-11.01	-35.18	-24.12
20	18.73	10.26	35.37	24.25
22	-25.83	-26.81	-6.31	-4.33
23	23.11	22.72	6.25	4.29
25	-15.06	-12.78	6.31	4.33
26	12.44	11.21	-6.25	-4.29
60	- 43.35	-42.80	-35.18	-24.12
27	41.62	30.95	35.37	24.25
61	-37.85	-23.85	-50.03	-34.30
62	77.83	96.98	90.79	122.24
28	-132.11	-107.81	-150.10	-102.91
63	-114.21	-96.00	-137.72	-94.43
64	45.37	64.92	53.13	96.42
30	-120.77	-99.78	-137.72	-94.43
65	-124.00	-99.58	-150.10	-102.91
66	77.06	94.76	90.79	122.24
33	-47.51	-36.53	-50.03	-34.30
67	-37.85	-23.85	-50.03	-34.30
29	33.30	11.99	42.51	29.15
31	-17.90	-11.81	-12.38	-8.49
32	13.56	8.28	-9.02	6.18
34	3.22	-0.20	12.38	8.49
35	1.83	1.12	9.02	-6.18
68	-47.51	-36.53	-50.03	-34.30
36	39.23	19.90	42.51	29.15

TABLE 2.7. RESULTS OF ANALYSIS - EXAMPLE 3

Section	Loading Condition I		Loading Condition II	
	Elastic analysis for factored loads M_u^j (kNm)	Ultimate load analysis Case 2 M_{du}^j (kNm)	Elastic analysis for factored loads M_u^j (kNm)	Ultimate load analysis Case 5 M_{du}^j (kNm)
37	0.31	12.05	-72.46	-45.89
38	59.77	81.75	71.11	110.49
1	-183.26	-151.04	-142.23	-90.06
39	-57.82	-40.42	-142.23	-90.06
40	60.77	79.43	71.11	110.49
3	-123.14	-103.22	-72.46	-45.89
41	4.58	4.85	-29.31	-18.56
2	-29.76	-36.23	14.66	9.28
4	-66.58	-51.92	0.0	0.0
5	98.21	110.73	0.0	0.0
42	-54.27	-46.98	-29.31	18.56
6	54.60	57.29	14.66	9.28
43	-6.88	-11.50	-75.04	-47.52
44	60.78	82.92	70.47	110.08
7	-174.06	-148.16	-140.94	-89.25
45	-64.85	-42.65	-140.94	-89.25
46	58.67	77.94	70.47	110.08
9	-120.32	-103.97	-75.04	-47.52
47	-3.19	6.82	-42.34	-26.81
8	4.28	-7.20	43.15	27.33
10	-63.15	-60.70	0.0	0.0
11	58.86	58.70	0.0	0.0
48	-68.58	-62.33	-42.34	-26.81
12	68.87	56.24	43.15	27.33
49	-11.80	5.20	-64.16	-40.63
50	62.43	83.52	73.19	111.80
13	-165.84	-140.66	-146.38	-92.69
51	-82.29	-58.62	-146.38	-92.69
52	61.63	81.58	73.19	111.80
15	-96.95	-80.71	-64.16	-40.63
53	-3.45	5.46	-35.19	-22.28
14	3.69	-4.67	32.70	20.71
16	-49.14	-47.13	0.0	0.0
17	46.06	44.81	0.0	0.0
54	-56.21	-52.30	-35.19	-22.28

(contd)

TABLE 2.7 (contd)

Section	Loading Condition I		Loading Condition II	
	Elastic analysis for factored loads M_u^j (kNm)	Ultimate load analysis Case 2 M_{du}^j (kNm)	Elastic analysis for factored loads M_u^j (kNm)	Ultimate load analysis Case 5 M_{du}^j (kNm)
18	51.73	41.63	32.70	20.71
55	-22.10	-4.49	-60.09	-38.05
56	63.56	85.26	74.21	112.45
19	-153.28	-127.50	-148.42	-93.98
57	-98.30	-75.08	-148.42	-93.98
58	62.23	81.48	74.21	112.45
21	-79.74	-64.45	-60.09	-38.05
59	-7.43	0.45	-29.66	-18.78
20	8.36	0.26	28.96	18.34
22	-37.80	-38.73	0.0	0.0
23	34.40	34.91	0.0	0.0
60	-42.85	-37.76	-29.66	-18.78
24	40.74	28.42	28.96	18.34
61	-35.18	-17.60	-59.75	-37.83
62	64.21	84.66	74.29	112.50
25	-138.89	-115.58	-148.59	-94.09
63	-112.97	-89.01	-148.59	-94.09
64	61.72	83.09	74.29	112.50
27	-66.10	-47.30	-59.75	-37.83
65	-13.32	-3.30	-30.48	-19.30
26	14.67	4.94	30.42	19.26
28	-19.58	-15.32	0.0	0.0
29	17.18	13.69	0.0	0.0
66	-38.34	-36.53	-30.48	-19.30
30	36.90	26.70	30.42	19.26
67	-23.83	-14.89	-33.09	-20.95
68	68.89	86.38	80.96	116.72
31	-140.90	-114.86	-161.92	-102.53
69	-133.56	-103.06	-161.92	-102.53
70	68.34	88.03	80.96	116.72
33	-32.25	-23.38	-33.09	-20.95
71	-23.83	-14.89	-33.09	-20.95
32	21.86	14.31	29.27	18.53
34	-7.33	-11.80	0.0	0.0
35	6.35	11.25	0.0	0.0
72	-32.25	-23.38	-33.09	-20.95
36	27.75	10.77	29.27	18.53

TABLE 2.8. RATIO OF MOMENTS FOR ULTIMATE LOAD ANALYSIS TO ELASTIC ANALYSIS FOR FACTORED LOADS - EXAMPLE 1

Section	$\frac{M^j_{du}}{M^j_u}$				
	Case 1	Case 2	Case 3	Case 4	Case 5
1	0.846	0.866	0.855	0.881	0.712
14	1.217	1.214	1.183	1.211	1.405
15	0.805	0.810	0.858	0.881	0.712
16	1.265	1.294	1.222	1.244	1.405
3	0.724	0.628	0.622	0.404	0.443
4	0.915	0.966	-	-	-
5	1.153	1.215	-	-	-
18	0.740	0.792	0.546	0.549	0.443
6	0.974	0.877	0.927	0.460	0.443
7	0.834	0.844	0.856	0.863	0.701
20	1.203	1.209	1.172	1.190	1.366
21	0.810	0.812	0.845	0.860	0.701
22	1.232	1.240	1.194	1.198	1.366
9	0.703	0.643	0.672	0.523	0.443
10	1.201	1.340	-	-	-
11	1.226	1.357	-	-	-
24	0.703	0.643	0.672	0.523	0.443
12	0.704	0.427	0.679	0.294	0.443

TABLE 2.9. RATIO OF MOMENTS FOR ULTIMATE LOAD ANALYSIS TO ELASTIC ANALYSIS FOR FACTORED LOADS - EXAMPLE 2

Section	$\frac{M^j_{du}}{M^j_u}$				
	Case 1	Case 2	Case 3	Case 4	Case 5
1	0.833	0.840	0.815	0.800	0.686
3	0.835	0.835	0.814	0.854	0.686
40	1.405	1.402	1.345	1.305	1.690
39	0.778	0.781	0.872	0.868	0.686
6	0.844	0.835	0.782	0.740	0.686
42	1.263	1.268	1.221	1.262	1.437
41	0.783	0.786	0.871	0.848	0.686
4	0.796	0.829	-	-	0.686
5	1.139	1.165	3.199	2.289	0.686
7	0.790	0.820	2.071	1.512	0.686
8	1.178	1.202	-	-	0.686
44	0.804	0.853	0.687	0.678	0.686
9	1.062	0.987	1.176	0.695	0.686
10	0.848	0.858	0.841	0.841	0.686
12	0.849	0.841	0.840	0.866	0.686
48	1.402	1.400	1.343	1.302	1.687
47	0.763	0.778	0.845	0.858	0.686
15	0.871	0.838	0.840	0.752	0.686
50	1.264	1.272	1.222	1.270	1.445
49	0.766	0.786	0.845	0.840	0.686
13	0.951	0.946	0.777	0.508	0.686
14	0.972	0.959	0.880	0.546	0.686
16	1.032	1.001	0.909	0.353	0.686
17	1.077	1.029	0.806	0.312	0.686
52	0.874	0.911	0.837	0.907	0.686
18	0.884	0.817	0.855	0.788	0.686
19	0.835	0.855	0.843	0.830	0.686
21	0.834	0.833	0.843	0.882	0.686
56	1.403	1.359	1.344	1.258	1.688
55	0.793	0.840	0.843	0.882	0.686

(contd)

TABLE 2.9. (contd)

Section	$\frac{M^j_{du}}{M^j_u}$				
	Case 1	Case 2	Case 3	Case 4	Case 5
24	0.852	0.759	0.843	0.694	0.686
58	1.266	1.312	1.223	1.309	1.447
57	0.792	0.807	0.843	0.830	0.686
22	0.961	1.038	0.840	0.545	0.686
23	0.959	0.983	0.849	1.008	0.686
25	1.065	0.849	0.846	0.565	0.686
26	1.082	0.901	0.836	1.060	0.686
60	0.872	0.987	0.842	0.861	0.686
27	0.866	0.755	0.843	0.570	0.686
28	0.821	0.816	0.843	0.823	0.686
30	0.821	0.826	0.843	0.866	0.686
64	1.478	1.432	1.408	1.347	1.815
63	0.811	0.841	0.843	0.866	0.686
33	0.835	0.769	0.843	0.767	0.686
66	1.204	1.229	1.173	1.210	1.347
65	0.810	0.803	0.843	0.823	0.686
31	0.891	0.659	0.843	0.343	0.686
32	0.895	0.610	0.843	0.264	0.686
34	0.397	-	0.843	0.342	0.686
35	0.225	-	0.843	0.260	0.686
68	0.835	0.769	0.843	0.767	0.686
36	0.830	0.507	0.843	0.556	0.686

TABLE 2.10. RATIO OF MOMENTS FOR ULTIMATE LOAD ANALYSIS TO ELASTIC ANALYSIS FOR FACTORED LOADS - EXAMPLE 3

Section	$\frac{M_{du}^j}{M_u^j}$				
	Case 1	Case 2	Case 3	Case 4	Case 5
1	0.823	0.824	0.772	0.820	0.633
38	1.332	1.368	1.279	1.285	1.554
3	0.843	0.838	0.733	0.666	0.633
40	1.321	1.307	1.274	1.313	1.554
39	0.659	0.699	0.862	0.858	0.633
4	0.786	0.780	-	-	-
5	1.152	1.128	-	-	-
42	0.782	0.866	0.596	0.653	0.633
6	1.063	1.049	1.233	0.821	0.633
7	0.849	0.851	0.813	0.838	0.633
44	1.325	1.364	1.280	1.309	1.562
9	0.881	0.864	0.809	0.721	0.633
46	1.338	1.329	1.282	1.303	1.562
45	0.609	0.658	0.820	0.845	0.633
10	0.985	0.961	-	-	-
11	1.025	0.997	-	-	-
48	0.877	0.909	0.801	0.806	0.633
12	0.891	0.817	0.826	0.675	0.633
13	0.838	0.848	0.816	0.850	0.633
50	1.309	1.338	1.264	1.297	1.528
15	0.878	0.833	0.816	0.664	0.633
52	1.313	1.324	1.264	1.297	1.528
51	0.674	0.712	0.817	0.850	0.633
16	0.998	0.959	-	-	-
17	1.000	0.973	-	-	-
54	0.885	0.931	0.816	0.816	0.633
18	0.886	0.805	0.819	0.612	0.633
19	0.822	0.832	0.817	0.853	0.633
56	1.301	1.341	1.258	1.294	1.515

(contd)

TABLE 2.10. (contd)

Section	$\frac{M^j_{du}}{M^j_u}$				
	Case 1	Case 2	Case 3	Case 4	Case 5
21	0.862	0.808	0.817	0.636	0.633
58	1.307	1.309	1.258	1.294	1.515
57	0.723	0.764	0.817	0.853	0.633
22	1.000	1.025	-	-	-
23	1.000	1.015	-	-	-
60	0.873	0.881	0.817	0.746	0.633
24	0.870	0.698	0.817	0.479	0.633
25	0.804	0.832	0.817	0.865	0.633
62	1.298	1.318	1.257	1.306	1.514
27	0.834	0.716	0.817	0.575	0.633
64	1.310	1.346	1.257	1.306	1.514
63	0.759	0.788	0.817	0.865	0.633
28	1.000	0.783	-	-	-
29	1.000	0.797	-	-	-
66	0.854	0.953	0.817	0.795	0.633
30	0.849	0.724	0.817	0.528	0.633
31	0.789	0.815	0.817	0.834	0.633
68	1.260	1.254	1.221	1.238	1.442
33	0.812	0.725	0.817	0.645	0.633
70	1.262	1.288	1.221	1.238	1.442
69	0.778	0.772	0.817	0.834	0.633
34	1.000	1.610	-	-	-
35	1.000	1.771	-	-	-
72	0.812	0.725	0.817	0.645	0.633
36	0.807	0.388	0.817	0.345	0.633

2.6.4. Discussion

It can be observed from the design examples that the proposed procedure by adjustment of rotation yields rapid convergence of solution. The number of plastic hinges obtained by this procedure is noted to be less than α, the indeterminacy number for the frame, due to assigning of zero rotations for some of the column hinges according to step 3(b) of the procedure. However, practical considerations of symmetry in design and low values of permissible rotations in columns show that the suggested procedure is reasonable. This is also illustrated by the inelastic stage-by-stage analysis of the frames.

The position of plastic hinges as obtained by the ultimate load analysis program for case 2 of the hinge pattern under loading condition I compares well with the plastic hinge pattern at failure by the inelastic analysis as shown in Figs. 2.10 to 2.12. However, it may be important to note some of the differences in the position of plastic hinges as obtained by the two analyses and this aspect is discussed below.

The frames have been designed for the moments obtained by the ultimate load analysis program and in the design of percentage of steel reinforcement practical aspects such as symmetry, minimum steel requirements and detailing practice have been considered as shown in Tables 2.2 to 2.4. The inelastic analysis program used this set of data for reinforcement details, in the calculation of actual moments of resistance of sections at yield and ultimate limits for identifying the position of plastic hinges. Also as the solution proceeds by increments of loading the EI values of members based on the actual moment-curvature relations that correspond to the stress resultants relevant to the load stage have been used in the analysis. But in the simplified limit method the EI values of members have been calculated for the limit L_1 of the critical section based on the moment-rotation characteristics of the members. Hence it has been found that some of the plastic hinges, which have been considered in the ultimate load analysis, have yet to open up according to the inelastic stage-by-stage analysis. However, the actual load

factors at failure of the frames as obtained by the inelastic analysis, are greater than the load factor 1.25 for which they are designed. These results illustrate the adequacy of the proposed program for the design of reinforced concrete frames under ultimate loading conditions.

The results of the analysis for the ratio of moments by ultimate load analysis to elastic analysis for factored loads (Tables 2.8 to 2.10) have been found useful to study the amount of moment redistribution in frames. It has been observed, for the frames worked out here, that the amount of moment redistribution under loading condition I is about 15 per cent in beams and under loading condition II is 30 per cent in beams (and columns as well in symmetrical frames). It has been found difficult to generalise the amount of moment redistribution in columns under loading condition I as can be seen from the variation of the values shown in Tables 2.8 to 2.10.

The running of the ultimate load analysis program is quite economical as can be seen from the time taken on CDC 6400 for the examples presented here. This encourages its use in design offices.

Example	C.P. time (seconds)
1	12.1
2	16.0
3	16.25

2.7 RECOMMENDED PROCEDURE FOR ULTIMATE LOAD DESIGN OF REINFORCED CONCRETE FRAMES

Based on this investigation the following procedure is suggested for the ultimate load design of reinforced concrete frames.

1. Work out a preliminary design using the guide lines given in References (56, 57). As a first step the ultimate load analysis program itself can be used to obtain an elastic solution for factored loads.

2. Design the members for the analysis carried out in the previous step. Computation charts, as those given in Reference (12) may be prepared in the design office that will simplify the design calculations for the percentage of reinforcement and EI values. The permissible inelastic rotations may be calculated using the design curves given in Fig.2.3.

3. Using the ultimate load analysis program analyse the frame and check the values of the parameters used in the analysis and, if necessary, redesign the sections. With experience a close agreement may be achieved within two or three trials.

4. In case of frames subject to large side sway the coefficients suggested by Nahhas and Yu (53, 54), described in section 6.7, may be used to magnify the lateral loads to safeguard against instability.

CHAPTER THREE

A LINEAR PROGRAMMING FORMULATION FOR OPTIMAL LIMIT DESIGN OF REINFORCED CONCRETE FRAMES

3.1 INTRODUCTION

A study of the limit design of reinforced concrete frames through the examples presented in Chapter 2 has shown that the following points require careful consideration in the design based on plastic analysis under ultimate loads:

1. The values of flexural rigidity, EI, of the members which are used in deformation calculations must be consistent with the behaviour of the members corresponding to the relevant load stage.

2. The rotation capacity of reinforced concrete members depends, amongst other factors, on the nature of the force action to be resisted such as moment or moment and axial load and also on the percentage of reinforcement. In the case of beams with heavy reinforcement the permissible rotation may be less than 0.01 and in columns with heavy axial loads such as the case in the intermediate columns of lower storeys of multi-storey frames, the permissible rotation may be as low as 0.001.

Thus if a reinforced concrete frame were designed on the assumption of unlimited ductility, premature failure may occur due to the actual ductility limitations and before the formation of a collapse mechanism.

3. The design must ensure satisfactory behaviour of the members under working loads. This serviceability criterion is not incorporated in the simplified limit method but is recommended to be checked separately.

With the development of mathematical programming techniques and the availability of large computing facilities there has been growing interest to formulate mathematical programs for optimal limit design which would include all the design criteria of interest. The existing methods of optimal design due to Cohn and Grierson are examined in Chapter 1.

In the light of the above discussion the present work is concerned with the development of a linear programming method for optimal limit design which explicitly limits the rotation of plastic hinges for a given scheme of loading and appropriate values of member stiffnesses as well as satisfying serviceability conditions under working loads. In this Chapter the optimal design problem and the constraints associated with the compatibility and limited ductility, equilibrium and serviceability requirements of the frame will be discussed in detail. The objective function will also be described. The optimal limit design problem is formulated as a linear programming problem and is presented in a form suitable for solution by using the standard simplex algorithm.

3.2 THE OPTIMAL LIMIT DESIGN PROBLEM

Consider a reinforced concrete frame of given geometry, pattern of loading and member sizes. The optimal design problem is to determine the value of design bending moment at all the critical sections such that the following conditions are satisfied:

1. Optimality (O): the total volume of reinforcing steel required is a minimum.
2. Compatibility and Limited Ductility (CLD): the bending moment distribution should satisfy all compatibility and parity conditions and the rotation at all plastic hinges should be within the permissible range.
3. Equilibrium (E): the bending moment distribution should satisfy the moment and force equilibrium requirements of the frame.
4. Serviceability (S): the design bending moment M_d^j at any section j should not be less than a specified minimum value which would implicitly ensure satisfactory behaviour of the members under working loads.
5. Mechanism (M): a plastic collapse mechanism cannot form at a load less than the specified ultimate load.

3.2.1. Definition of Design Moment

Cohn (18, 19) introduced the concept of yield load factor and yield safety parameter to define the design bending moment at a section. This

approach, which is explained below, is extremely useful to express the serviceability criterion in the optimal design method.

The ultimate load on a structure, W_u, can be expressed as a linear combination of dead, live and wind loads with the corresponding load factors, thus

$$W_u = \lambda_D W_D + \lambda_L W_L + \lambda_W W_W \qquad (3.1)$$

The load factors of equation (3.1) will, in general be different. Where all three types of loading are applied, attention will be confined to the case of equal load factors in order to simplify the calculations,

$$\lambda_D = \lambda_L = \lambda_W = \lambda_u \qquad (3.2a)$$

In the case where only dead and live loads are applied the simplifying assumption is made that the dead and live loads have a constant ratio but the corresponding partial load factors are of different magnitudes. Thus for this case,

$$\lambda_D = a\,\lambda_L$$

and $$W_D = b^1 W_L$$

where a and b^1 are constants.

Once again,

$$W_u = \lambda_u W \qquad (3.2b)$$

where in this case,

$$\lambda_u = \frac{1 + ab^1}{1 + b^1} \cdot \lambda_L$$

For any critical section j the parameter λ^j will be defined as,

$$\lambda^j = \frac{M_y^j}{M^j} \qquad (3.3)$$

and λ^j will be termed the yield moment factor.

Let critical section q be the location of the first plastic hinge to form. Then the load factor λ_1 corresponding to the initiation of inelastic frame behaviour is given by

$$\lambda_1 = \lambda^q = \frac{M_y^q}{M^q}$$

$$W_1 = \lambda_1 W \tag{3.4}$$

where W_1 will be termed the yield load of the frame.

When the loading is increased beyond this yield load further sections will become plastic hinges and there will be redistribution of moments in the frame. The ultimate load (W_u) is related to the working load (W) by equation (3.2) but $\overline{M}_j$ defined by,

$$\overline{M}_j = \frac{M_d^j}{\lambda_u} \tag{3.5}$$

differs from working load moment M^j because of the previously noted moment redistributions.

Thus,

$$M_d^j \leq M_y^j \tag{3.6}$$

$$M_y^j = \lambda^j M^j$$

$$M_d^j = \lambda_u \overline{M}^j$$

$$\overline{M}^j \leq x^j M^j \tag{3.7}$$

where $$x^j = \frac{\lambda^j}{\lambda_u} \tag{3.8}$$

and x^j is termed the 'yield safety parameter' for the j^{th} section.

Substituting from equation (3.7) into equation (3.5) yields,

$$M_d^j \leq x^j M_u^j \qquad (3.9)$$

where M_u^j is the factored elastic moment.

It can be observed from equation (3.9) that the critical sections, where plastic hinges form, will be designed for the yield moment of the sections and the other sections will be designed for a moment less than the yield moment of the section. For the linear programming formulation, it has been found convenient to express the design moment as,

$$M_d^j = x_d^j M_u^j \qquad (3.10)$$

where x_d^j is termed the design moment parameter for the j^{th} section. Following the criteria of design described above, the values of x^j for plastic hinge sections will be equal to the values of x_d^j. The other sections will be designed such that the yield safety parameters, x^j, of these sections will be greater than the values of x_d^j.

Knowing the values of M_u^j from an elastic analysis for factored loads, the optimal design problem is concerned with determining the values of x_d^j which satisfy the (O), (CLD), (E), (S) and (M) criteria of the frame.

3.3. COMPATIBILITY AND LIMITED DUCTILITY CRITERIA

A frame which is α times indeterminate can be reduced to a determinate form by the suitable insertion of α hinges. Such a reduced structure can be used as the basis of all static and kinematic analyses. Fig.3.1. shows two types of moment releases for a frame which is α times indeterminate. The selected hinges will be termed 'basic' and will be numbered 1 to α. The remaining critical sections will be termed 'non-basic' and will be numbered $(\alpha + 1)$ to c where c is the number of critical sections. It should be emphasised that it is not implied that the basic hinges are the actual plastic hinges at ultimate load. As discussed in Chapter 2, the compatibility equation relating the angular discontinuities at the 'basic' and 'non-basic' hinges is given by,

$$\sum_{j=1}^{\alpha} g_{ij}\, m^j + v_{io} + \sum_{q=\alpha+1}^{c} k_{iq}\, \theta_n^q + \theta_b^i = 0 \quad (i = 1, 2, .., \alpha) \qquad (3.11)$$

where θ_n^q and θ_b^i are as shown in Fig.3.1.

In order that all stress resultants shall correspond to strain resultants the following parity rule can be applied to all plastic hinges,

$$m^r\, \theta^r \geq 0 \qquad (r = 1, 2, \ldots, c) \qquad (3.12)$$

substituting for m^r from equation (3.10) the above rule can be stated as,

$$x_d^r\, M_u^r\, \theta^r \geq 0 \qquad (r = 1, 2, \ldots, c) \qquad (3.13)$$

Noting that x_d^r would be restricted to take only positive values equation (3.13) becomes,

$$M_u^r\, \theta^r \geq 0 \qquad (r = 1, 2, \ldots, c) \qquad (3.14)$$

For the discussion to follow, it was found convenient to express θ^r as

$$\theta^r = \delta_r\, |\theta^r| \qquad (3.15)$$

where δ_r will be termed the "parity delta". According to the parity rule expressed by equation (3.14) the value of δ_r will be as follows:

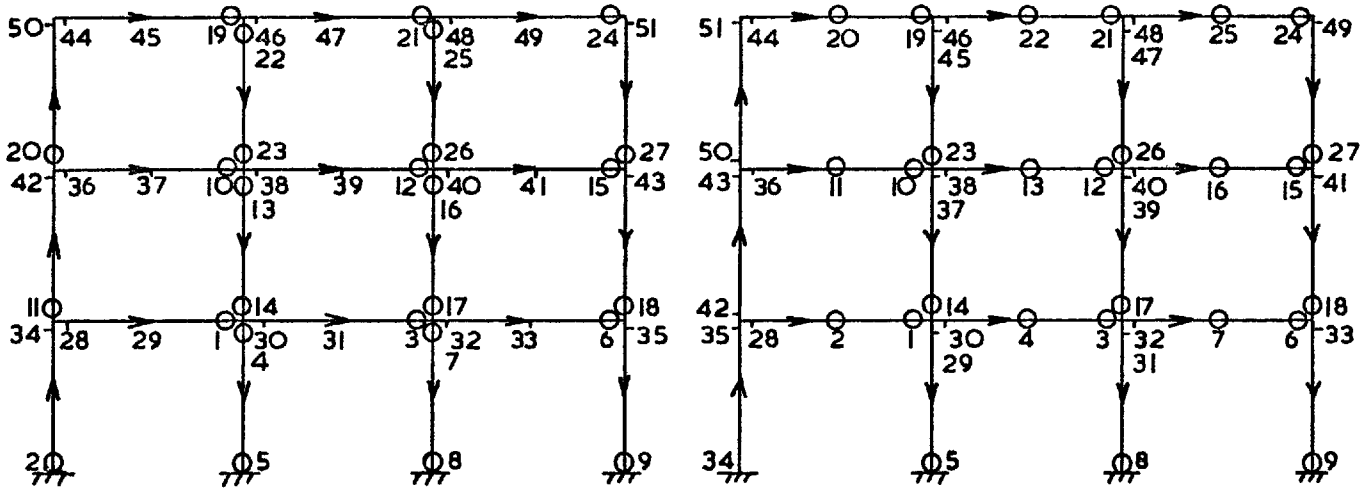
$$\delta_r = +1 \quad \text{for } M_u^r > 0$$

$$\delta_r = -1 \quad \text{for } M_u^r < 0 \qquad (3.16)$$

Substituting equations (3.10) and (3.15) into equation (3.11) yields,

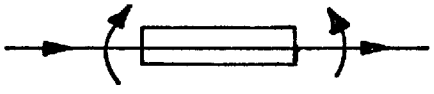
$$\sum_{j=1}^{\alpha} g_{ij}\, M_u^j\, x_d^j + v_{io} + \sum_{q=\alpha+1}^{c} k_{iq}\, \delta_q\, |\theta_n^q| + \delta_i\, |\theta_b^i| = 0$$

$$(i = 1, 2, \ldots, \alpha) \qquad (3.17)$$



(a) System A (b) System B

FIG. 3.1 RELEASE SYSTEMS FOR A FRAME



Positive moment



Positive rotation

FIG. 3.2 SIGN CONVENTIONS

The value of δ_r is determined from the sense of moment M_u^r, known from elastic analysis for factored loads, through equation (3.16).

The inelastic rotation θ^r in equation (3.17) can be expressed in terms of the permissible rotation, θ_p^r, as

$$|\theta^r| = |\theta_p^r| - y_{c+r} \qquad (3.18)$$

where y_{c+r} is a slack variable and is subjected to the following restrictions,

$$\text{(i)} \quad y_{c+r} \geq 0 \qquad (3.19)$$

This condition will ensure satisfaction of the limited ductility criterion i.e., the inelastic rotation at section r shall not exceed the allowable rotation θ_p^r. The lower bound value y_{c+r} will make $|\theta^r| = |\theta_p^r|$. The simplex algorithm (58) used for solving the linear program treats both design and slack variables as non-negative. Hence equation (3.19) need not be stated explicitly.

$$\text{(ii)} \quad y_{c+r} \leq |\theta_p^r| \qquad (3.20)$$

This constraint ensures both the sense invariance of θ^r and the satisfaction of the parity rule. The upper bound value $y_{c+r} = |\theta_p^r|$ indicates zero inelastic rotation and the section, therefore, remains elastic.

Substituting from equation (3.18) into equation (3.17) yields:

$$\sum_{j=1}^{\alpha} g_{ij} M_u^j x_d^j + v_{io} + \sum_{q=\alpha+1}^{c} k_{iq} \delta_q \{|\theta_p^q| - y_{c+q}\} +$$

$$\delta_i \{|\theta_p^i| - y_{c+i}\} = 0 \qquad (i = 1, 2, \ldots, \alpha) \qquad (3.21)$$

Equations (3.20) and (3.21) jointly express the compatibility and limited ductility requirements for the frame.

The rotational capacity of reinforced concrete sections can be expressed as a linear function of moment m^r in the following form:

$$\theta_p^r = B_1^r + B_2^r \, |m^r| \tag{3.22}$$

Noting that $m^r = M_u^r \, x_d^r$ equation (3.22) may be expressed as,

$$\theta_p^r = B_1^r + B_2^r \, |M_u^r| \, x_d^r \tag{3.23}$$

Substituting from equation (3.23) into equations (3.20) and (3.21) and after rearrangement the following constraints are obtained.

$$\sum_{j=1}^{\alpha} g_{ij} \, M_u^j \, x_d^j + v_{io} + \sum_{q=\alpha+1}^{c} k_{iq} \, \delta_q \, \{ (B_1^q + B_2^q \, |M_u^q| \, x_d^q) - y_{c+q} \}$$

$$+ \delta_i \, \{ (B_1^i + B_2^i \, |M_u^i| \, x_d^i) - y_{c+i} \} = 0 \quad (i = 1, 2, \ldots, \alpha) \tag{3.24}$$

$$y_{c+r} \leq B_1^r + B_2^r \, |M_u^r| \, x_d^r \quad (r = 1, 2, \ldots, c) \tag{3.25}$$

Equations (3.24) and (3.25) are the compatibility and limited ductility criteria for the frame.

3.4. EQUILIBRIUM CRITERIA

The moments at the non-basic hinge sections can be determined from the moment and force equilibrium conditions of the frame. The influence diagrams such as those drawn in Fig.2.5 could be used to express the moment distribution in terms of the moments at the α basic hinge sections. For example, the moments at the non-basic hinge sections of the frame of Fig.2.5 are given by,

$$m^4 = k_{14} \, m^1 + k_{24} \, m^2 + k_{34} \, m^3 + m_o^4$$

$$m^5 = k_{15} \, m^1 + k_{25} \, m^2 + k_{35} \, m^3 + m_o^5 \tag{3.26}$$

Noting that by the principle of contragredience (36, 37) the static and kinematic matrices are related as $h_{qj} = k_{jq}$, the above equations become,

$$m^4 = h_{41}\, m^1 + h_{42}\, m^2 + h_{43}\, m^3 + m_o^4$$

$$m^5 = h_{51}\, m^1 + h_{52}\, m^2 + h_{53}\, m^3 + m_o^5 \qquad (3.27)$$

Thus in general the bending moments at the non-basic hinge sections can be expressed by,

$$\sum_{j=1}^{\alpha} h_{qj}\, m^j + m_o^q = m^q \qquad (q = \alpha + 1, \ldots, c) \qquad (3.28)$$

Substituting for m^r from equation (3.10) into equation (3.28),

$$\sum_{j=1}^{\alpha} h_{qj}\, M_u^j\, x_d^j + m_o^q = M_u^q\, x_d^q \qquad (q = \alpha + 1, \ldots, c) \qquad (3.29)$$

Equation (3.29) represents the equilibrium criteria for the frame.

3.5. SERVICEABILITY CRITERIA

3.5.1. Introduction

Any design of reinforced concrete frame based on the behaviour under ultimate load must satisfy the serviceability requirements under working load. These requirements are that,

1. no plastic hinge occurs at working load
2. the deflections are within the allowable limits
3. the width and spacing of cracks are within the desired limits
4. the stresses in steel are less than the permissible values.

Cohn and Grierson (39, 40) have studied the above serviceability requirements with a view to express them as serviceability criteria in optimal design. The following is a summary of the work reported by them.

3.5.2. No Plastic Hinges at Working Load

While limit design recognizes and allows for the plastic behaviour of sections serviceability demands that this behaviour must not occur at service loads. Therefore, restrictions must be placed on all design variables such that no plastic hinges may form in the structure under working load.

If W is the working load for a frame and W_1 is the load corresponding to the yielding of a section j then for no plastic hinge to occur at section j, $W_1 > W$. From equation (3.8) the yield safety parameter x^j is given by

$$x^j = \frac{\lambda^j}{\lambda_u}$$

Therefore the serviceability condition that no plastic hinge occurs under working loads can be expressed as,

$$x^j > \frac{1}{\lambda_u} \qquad (3.30)$$

3.5.3. Control of Deflections

The deflections at various points of a frame under working loads must satisfy the safety requirements of partition walls, finishes etc., and should be such as not to cause discomfort or alarm to the users of the structure. The rigidity of the frame at service load is dependent on the design of the critical sections for ultimate loading conditions. Therefore, restriction must be placed on the design variables such that the lateral and vertical deflections under working loads are within the desired limits.

For a reinforced concrete structure the computation of deflections requires consideration for the inelastic behaviour of sections, the variation of rigidity along the members and the long term effects due to creep. More research is required in this area before stipulating the

necessary conditions on the design variables that would satisfy the deflection requirements. Hence, at this stage it is necessary to check the deflection by separate calculation or to follow the stiffness requirements for beams and columns as recommended by Code of Practice (62) which would implicitly satisfy the deflection conditions.

3.5.4. Control of Cracking

The maximum crack width in structures though significant as an important serviceability requirement can only be described in relatively broad limits. However, it is known that the type of structure and the environment in which it is situated may influence the permissible limit for the crack widths. A number of investigators in recent years have suggested formulae for the maximum crackwidth in reinforced concrete members, w_{max}, as a function of a wide variety of different governing parameters. A comprehensive discussion on the subject can be found in reference (60).

It has been shown that the stress in tensile steel, f_{st}, is a major variable affecting the width of cracks and that w_{max} can be expressed in the following form,

$$w_{max} = \bar{k} f_{st}$$

where $\bar{k}$ is a parameter defining other variables such as diameter of bar, percentage of reinforcement, area of concrete surrounding the bar, concrete cover, depth of section etc.

Assuming f_{st} is the stress in steel under working load and w_a is the allowable crackwidth at the section, serviceability requires,

$$\bar{k} f_{st} \leq w_a$$

But $f_{st} = \frac{f_y}{\lambda^j} = \frac{f_y}{x^j \lambda_u}$ where f_y is the yield stress of steel.

Therefore, the serviceability condition for limiting crack width is,

$$x^j \geq \frac{\bar{k} f_y}{\lambda_u w_a} \qquad (3.31)$$

3.5.5. Control of Steel Stresses

With increasing use of high strength bars for reinforcement it is found desirable to limit the stresses in tensile steel under working load so as to ensure the above controls for cracking and deflections are valid. If f_{sw} is the allowable stress in tensile steel, then the above serviceability requirement can be stated as,

$$x^j \geq \frac{f_y}{\lambda_u f_{sw}} \tag{3.32}$$

3.5.6. Serviceability Criteria

The above discussion in sections 3.5.2. to 3.5.5. shows that the serviceability requirements can be expressed in a form

$$x^j \geq \frac{A}{\lambda_u}$$

where the value of A is defined by a particular serviceability condition.

Since $x^j = \frac{\lambda^j}{\lambda_u}$ and λ_u is a constant, the above equation implies that a lower bound is to be placed on the yield moment factor, λ^j, for each of the critical sections. For any critical section this lower bound is determined by the particular serviceability requirement that places the greatest restriction on the value of its design variable. If λ_*^j is the specified yield moment factor to satisfy the serviceability requirements then the limiting value of the yield safety parameter is given by,

$$x_*^j = \frac{\lambda_*^j}{\lambda_u} = L^j \tag{3.33}$$

Thus the serviceability requirements are said to be satisfied, if

$$x^j \geq L^j \tag{3.34}$$

Following the discussion on the definition of design moment in

section 3.2.1, the above serviceability criteria can be expressed as

$$x_d^j \geq L^j \qquad (3.35)$$

3.6. MECHANISM CRITERIA

It is necessary to ensure that a plastic collapse mechanism does not form at a load less than the selected ultimate load. The linear program can be greatly simplified by restricting plastic hinge formation to $(\alpha + 1)$ selected critical sections of which not more than α plastic hinges may be considered to have opened. These hinges are not necessarily the basic hinges.

This simplification has the extra advantage of eliminating the arbitrary mechanism deformations in the elasto-plastic compatibility equations (3.11) and experience in the design of six frames described in Chapter 6 indicates that the resultant loss of economy is negligible.

The computer program developed for optimal limit design of frames, handles the choice of plastic hinges through the use of plastic hinge indicator for a critical section. The possible position of plastic hinges are selected in a systematic manner depending on the type of hinge pattern considered for analysis and this is discussed in the next Chapter under section 4.5.

3.7. OBJECTIVE FUNCTION AND OPTIMALITY CRITERION

3.7.1. Introduction

The optimality criterion is expressed through either a maximisation or minimisation of an objective function of design variables. The objective function may, for example, represent the area of the moment diagram, cost of concrete and steel or the volume of reinforcement with the variables associated with the design moments, the geometric configuration of the structure or the flexural rigidity, EI, of the members. Theoretically all of the objective functions are non-linear. However, as explained in the previous sections all of the constraints associated with the compatibility, limited ductility, equilibrium and serviceability criteria of the optimal design are linear functions of the design variables x_d^j. Hence in this formulation the selected optimality criterion is the

the minimisation of the total volume of steel reinforcement for the frame, which could be represented by a linear function as explained below.

3.7.2. Area of Reinforcement

For the ultimate strength design of beam and column sections design charts similar to that given in reference (12) are available for different Code specifications. By suitable approximations to these design charts the percentage of reinforcement for beam and column sections can be represented by a linear function, for specified intervals, in the following form:

Beam sections,

$$p_j \frac{\sigma_{al}}{\sigma_b} = \bar{D}_1 \frac{M_d^j}{\sigma_b\, bd^2} + \bar{D}_2 \qquad (3.36)$$

Column sections,

$$p_j \frac{\sigma_{al}}{\sigma_b} = \bar{D}_3 \frac{M_d^j}{\sigma_b\, bd^2} + \bar{D}_4 \frac{P}{\sigma_b\, bd} + \bar{D}_5 \qquad (3.37)$$

where $\bar{D}_1$, $\bar{D}_2$, $\bar{D}_3$, $\bar{D}_4$ and $\bar{D}_5$ are constants.

Substituting in equations (3.36) and (3.37) for the design bending moment M_d^j from equation (3.10) the area of reinforcement for a critical section j can be expressed as follows,

$$A_j = D_6 + D_7\, x_d^j \qquad (3.38)$$

3.7.3. Formulation of the Objective Function

The flexural reinforcement provided at a critical section is bent or terminated at various points depending on the bond, anchorage, shear and moment requirements of the Code of Practice adopted for design. Thus the reinforcement for a frame is such that (1) the number of longitudinal bars is constant over various lengths of the members (2) as one or more bars are terminated at a particular point, a different amount of reinforcement prevails over the adjacent member length and (3) all of the

flexural reinforcement for a critical section j terminates at some distance $\bar{l}_j$ from the section. It has been shown (40) that this detailing practice can be used to define the 'equivalent length', l_j, over which all of the reinforcement for section j can prevail constant before it is terminated. The value of l_j can be calculated by equating the actual volume of reinforcement over distance $\bar{l}_j$ and the volume required assuming a constant reinforcement over the equivalent length l_j.

Thus the volume of reinforcement with respect to a critical section j is given by,

$$V_j = A_j l_j = (D_6 + D_7 x_d^j) l_j$$

$$\text{or} \quad V_j = D_1^j + D_2^j x_d^j \tag{3.39}$$

The objective function, V, representing the total volume of reinforcement for the frame is, therefore, given by,

$$V = \sum_{j=1}^{c} D_1^j + D_2^j x_d^j \tag{3.40}$$

3.8 LINEAR PROGRAMMING FORMULATION

The optimal frame design problem with the compatibility and limited ductility, equilibrium and serviceability criteria discussed above as the governing constraints can be stated as follows:

Minimize:

$$\text{Objective function, } V = \sum_{j=1}^{c} D_1^j + D_2^j x_d^j \tag{3.41}$$

subject to:

Compatibility and limited ductility constraint:

$$\sum_{j=1}^{\alpha} g_{ij} M_u^j x_d^j + v_{io} + \sum_{q=\alpha+1}^{c} k_{iq} \delta_q \{ (B_1^q + B_2^q |M_u^q| x_d^q - y_{c+q} \} +$$

$$\delta_i \{ (B_1^i + B_2^i |M_u^i| x_d^i) - y_{c+i} \} = 0 \quad (i = 1, 2, \ldots, \alpha) \tag{3.42}$$

$$y_{c+r} \leq B_1^r + B_2^r |M_u^r| x_d^r \quad (r = 1, 2, \ldots, c) \tag{3.43}$$

Equilibrium constraint:

$$\sum_{j=1}^{\alpha} h_{qj} M_u^j x_d^j + m^q = M_u^q x_d^q \quad (q = \alpha + 1, \alpha + 2, \ldots, c) \tag{3.44}$$

Serviceability constraint:

$$x_d^j \geq L^j \quad (j = 1, 2, \ldots, c) \tag{3.45}$$

This is a linear programming problem which can be solved by using the standard simplex algorithm (58).

3.8.1. Lower Bound Restrictions

If the following substitution is made for the design variable x_d^j, the lower bound restriction of equation (3.45) can be replaced by the non-negativeness of the transformed variables.

$$x_d^j = L^j + U^j y_j \quad (j = 1, 2, \ldots, c) \tag{3.46}$$

The constant U^j introduced in the above equation will, by suitable stipulation, enable to control the bending moment value at a section with respect to the elastic moment for factored loads.

Substituting for x_d^j into equations (3.41) to (3.44) and introducing slack variables, the problem can be expressed in the standard form of a linear program:

$$\text{Min. } z = \{c\}^T \{y\} \tag{3.47}$$

$$\text{Subject to } [A]\{y\} = \{b\} \tag{3.48}$$

$$\text{and} \quad \{y\} \geq \{0\} \tag{3.49}$$

where the cost coefficients (c_j), structural coefficients (a_{ij}) and the stipulations, b_i are given below:

$$z = V - \sum_{j=1}^{c} D_1^j + D_2^j L^j \tag{3.50}$$

$$c_j = D_2^j U^j \qquad (j = 1, 2, \ldots, c) \tag{3.51}$$

For $i = 1, 2, \ldots, \alpha$

$$a_{ij} = g_{ij} M_u^j U^j \qquad (j = 1, 2, \ldots, \alpha),\ j \neq i \tag{3.52}$$

$$a_{ii} = g_{ii} M_u^i U^i + \delta_i B_2^i |M_u^i| U^i \tag{3.53}$$

$$a_{ij} = k_{ij} \delta_j B_2^j |M_u^j| U^j \quad (j = \alpha+1, \ldots, c) \tag{3.54}$$

$$a_{i(c+i)} = - \delta_i \tag{3.55}$$

$$a_{i(c+j)} = - k_{ij} \delta_j \qquad (j = \alpha+1, \ldots, c) \tag{3.56}$$

$$b_i = - v_{io} - \sum_{j=1}^{\alpha} g_{ij} M_u^j L^j - \delta_i B_1^i - \delta_i B_2^i |M_u^i| L^i - \sum_{j=\alpha+1}^{c} k_{ij} \delta_j \{B_1^j + B_2^j |M_u^j| L^j\} \tag{3.57}$$

For $i = \alpha+1, \alpha+2, \ldots, c$

$$a_{ij} = h_{ij} M_u^j U^j \qquad (j = 1, 2, \ldots, \alpha)\ j \neq i \tag{3.58}$$

$$a_{ii} = h_{ii} M_u^i U^i - M_u^i U^i \tag{3.59}$$

$$b_i = M_u^i L^i - m_o^i - \sum_{j=1}^{\alpha} h_{ij} M_u^j L^j \tag{3.60}$$

For i = c+1, c+2, ..., 2c

$$a_{i\,(i-c)} = -B_2^{(i-c)} \left| M_u^{(i-c)} \right| U^{(i-c)} \tag{3.61}$$

$$a_{ii} = 1 \tag{3.62}$$

$$a_{i(i+c)} = 1 \tag{3.63}$$

$$b_i = B_1^{(i-c)} + B_2^{(i-c)} \left| M_u^{(i-c)} \right| L^{(i-c)} \tag{3.64}$$

The coefficients not defined by the above equations would be zero.

3.8.2 Additional Design Constraints

It may be necessary from practical considerations to introduce additional design constraints as described below.

It may be desirable to restrict the value of the bending moment with respect to the elastic moment value for factored loads. For example, the moments at the ends of the beams may be restricted not to exceed the equivalent elastic value. This may be achieved by assigning $U^j = 1 - L^j$ and introducing a constraint.

$$y_j \leq 1 \tag{3.65}$$

Sometimes it may be found desirable to keep symmetry in design and hence may be necessary to restrict the moment at a section not to exceed the value at a corresponding symmetrical section. This may easily be included by incorporating the necessary symmetry constraint. With this type of constraint the cost coefficient, c_j, may correspondingly be weighted to keep the symmetry in design.

The design constraints, some of them discussed above, must form a consistent set with the governing constraint equations.

3.8.3 Change in Sign of Moment

During the process of calculation of optimal solution for the frame with the inelastic rotations at critical sections, the bending moment at some of the sections may change from positive to negative or vice versa with reference to the elastic solution. This may be treated in a similar

fashion to the non-negative constraint of a linear programming problem (59). The design variable y_j is expressed as a difference of two positive variables noting that in the simplex algorithm the value of the variables are positive, thus

$$y_j = y'_j - y''_j \tag{3.66}$$

It can be shown (59) that no more than one of the complementary variables (y'_j and y''_j) can be non-zero.

It becomes difficult to include an inelastic rotation at the section, where the moment changes in sign, into the compatibility equation satisfying the parity rule as well. However in practical designs, such sections may be treated as having zero rotations, (i.e. remained elastic) without significant error from the practical point of view.

3.9 SOLUTION OF THE OPTIMAL DESIGN PROBLEM

The optimal limit design problem can be formulated as an L.P. problem with the (O), (CLD), (E) and (S) criteria expressed in equations (3.41) to (3.45) as the governing constraints. Having worked out the values of M_u^j from elastic analysis for factored loads and specified the values of L^j and U^j, the cost and structural coefficients, and the stipulations can be computed using the equations (3.50) to (3.64). The L.P. problem can thus be reduced to a standard form as given by equations (3.47) to (3.49) and solved using the standard simplex algorithm. A computer program developed for the formulation and solution of the O.L.D. problem is described in the next Chapter.

CHAPTER FOUR

COMPUTER PROGRAM FOR OPTIMAL LIMIT DESIGN

4.1. INTRODUCTION

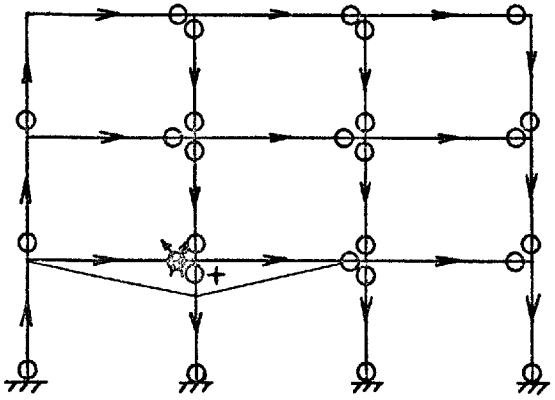
A linear programming model has been proposed, in the previous Chapter, for the optimal limit design of reinforced concrete frames. This formulation has constraints associated with the compatibility, limited ductility, equilibrium and serviceability requirements of the frame. A computer program developed for the formulation and solution of the optimal limit design problem will be explained here with the aid of a flow chart. The computations of flexibility and kinematic matrices used in the program are also discussed. The input and output details of the program are described.

4.2. FLEXIBILITY MATRIX

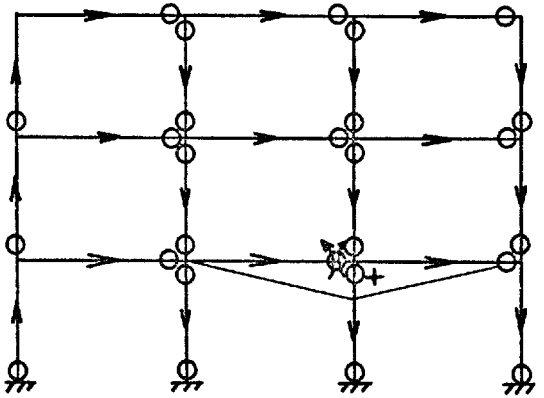
The release system chosen for the computation of flexibility matrix, [G], is shown in Fig.4.1. This release system is advantageous in plotting the moment diagrams (m_o and k_i) for load and for unit actions at the releases as shown in Fig.4.1. The numbering of the influence diagrams correspond to that adopted for releases of Fig.3.1(a). The coefficients g_{ij} of the flexibility matrix, [G], and v_{io} of the displacement vector, $\{v_o\}$ are calculated in the program using the expressions given in Reference (7). However, these coefficients are transformed to the directed graph sign convention as explained below.

Fig.4.2. shows the influence diagrams for a frame due to unit values of moments at the releases according to the simplified limit method of Baker. The moment diagrams are plotted on the tension side of the member and the signs of the diagrams are marked according to the directed graph sign convention. The influence diagrams for positive unit values of moments at the releases according to the directed graph sign convention are given in Fig.4.3. It can be observed that the influence diagrams of Figs. 4.2 and 4.3 differ only in their signs and they are related as,

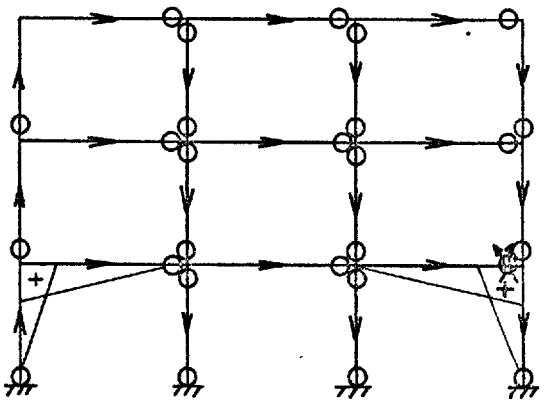
$$k_i^D = \beta_i k_i^S \qquad (4.1)$$



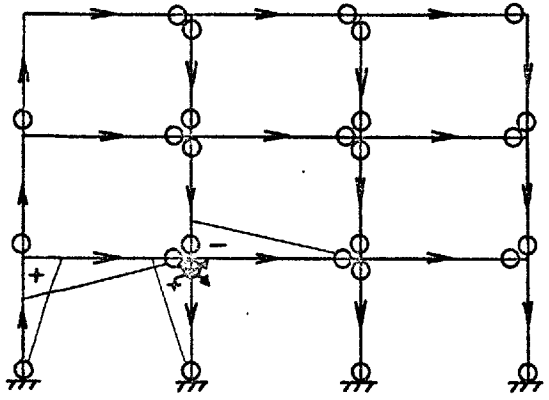
k_1



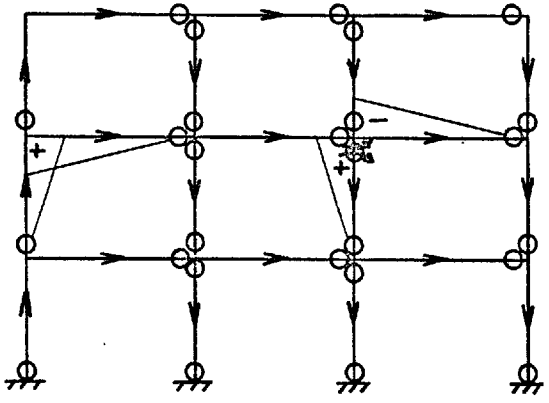
k_3



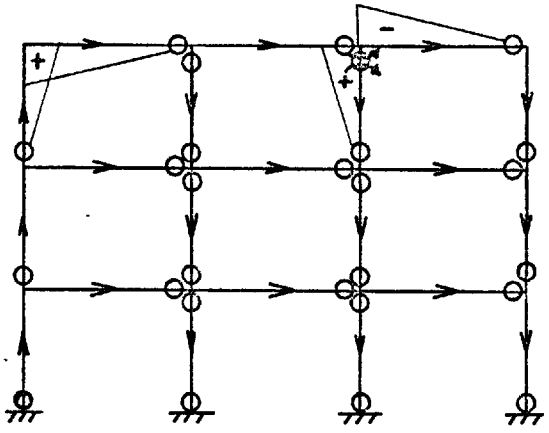
k_6



k_4

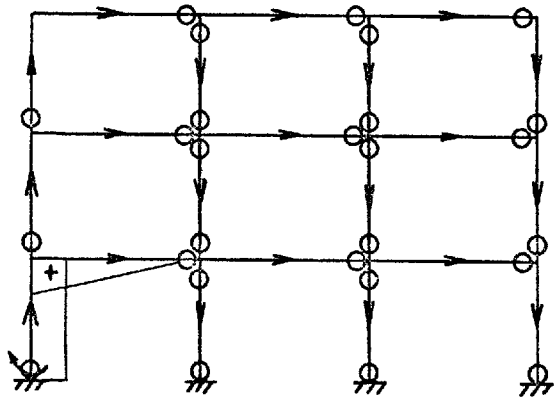


k_{16}

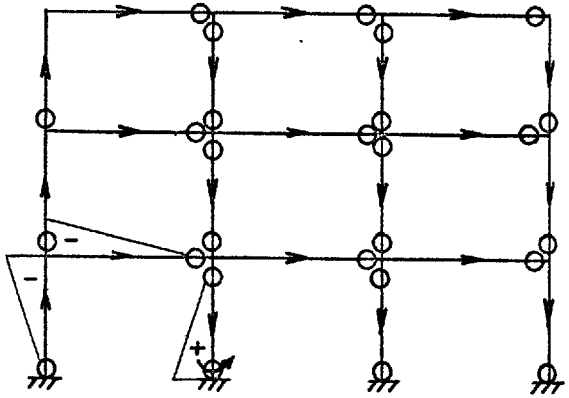


k_{25}

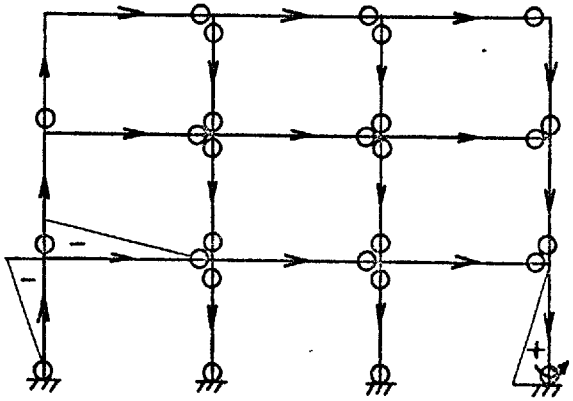
FIG. 4.1 (a)



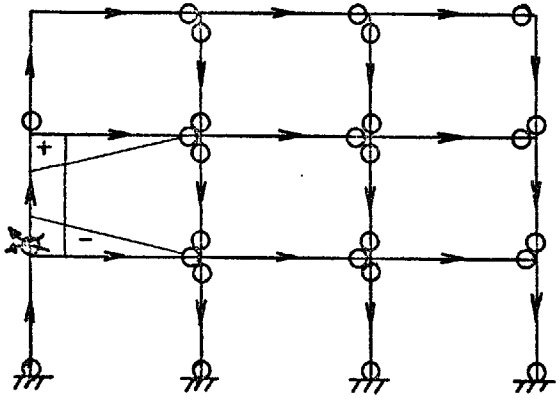
k_2



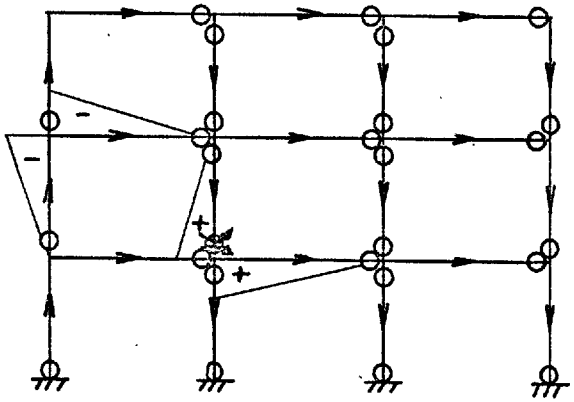
k_5



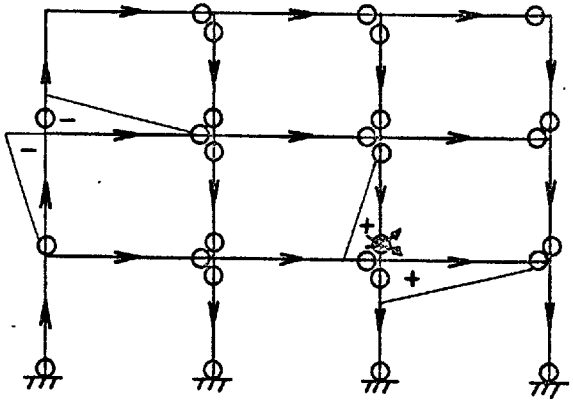
k_9



k_{11}



k_{14}



k_{17}

FIG. 4.1(b)

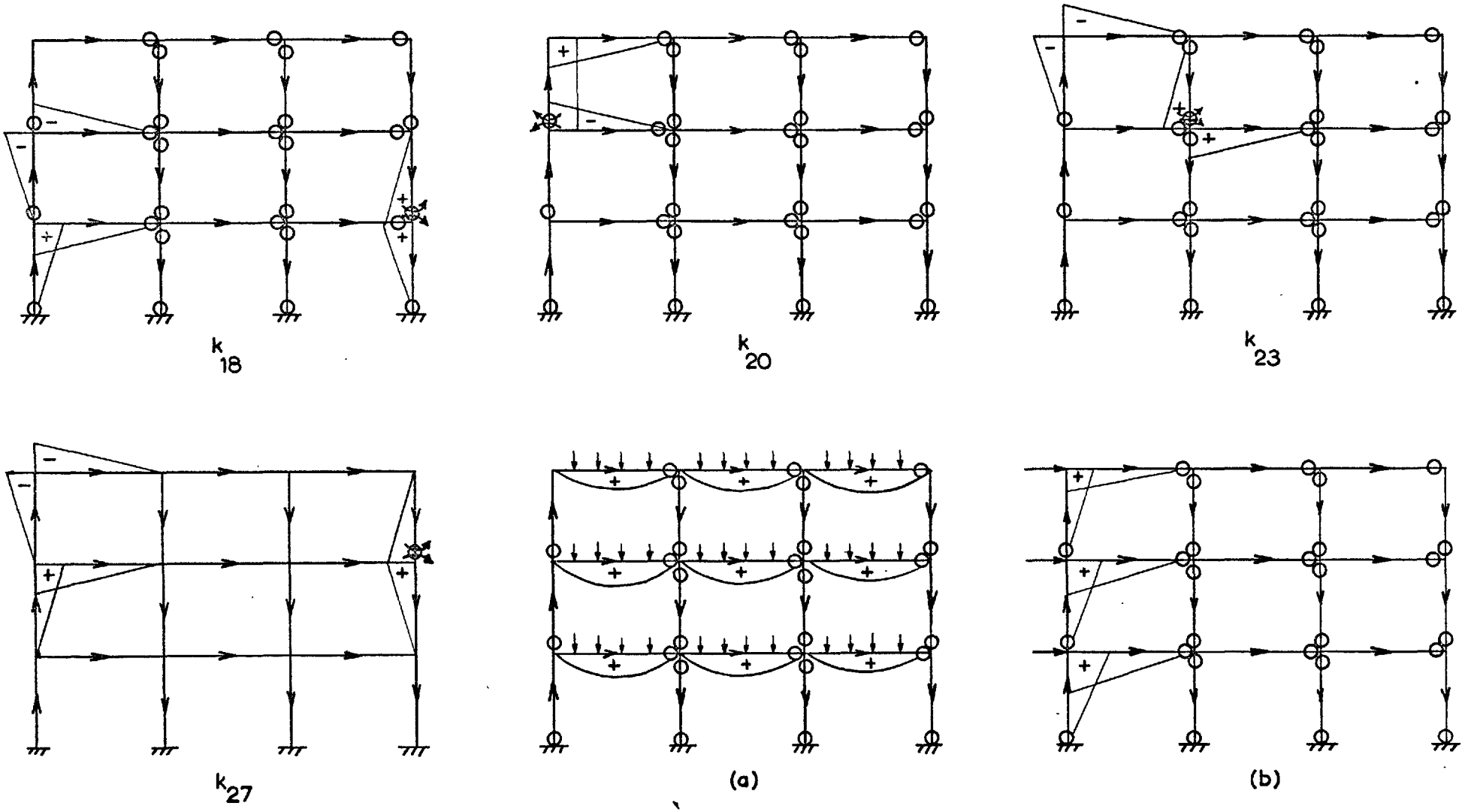


FIG. 4.1(c) TYPICAL MOMENT DIAGRAMS FOR UNIT ACTIONS AT BASIC HINGES AND FOR LOADS

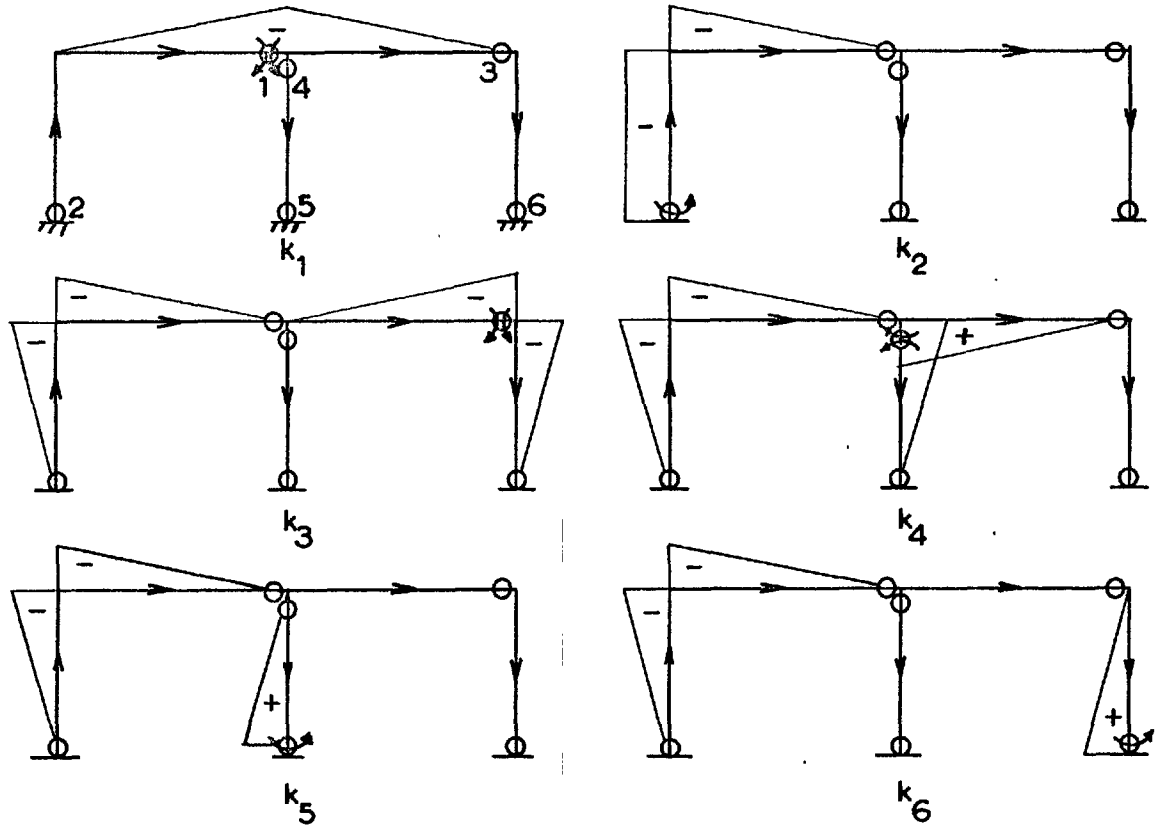


FIG. 4.2 INFLUENCE DIAGRAMS (S)

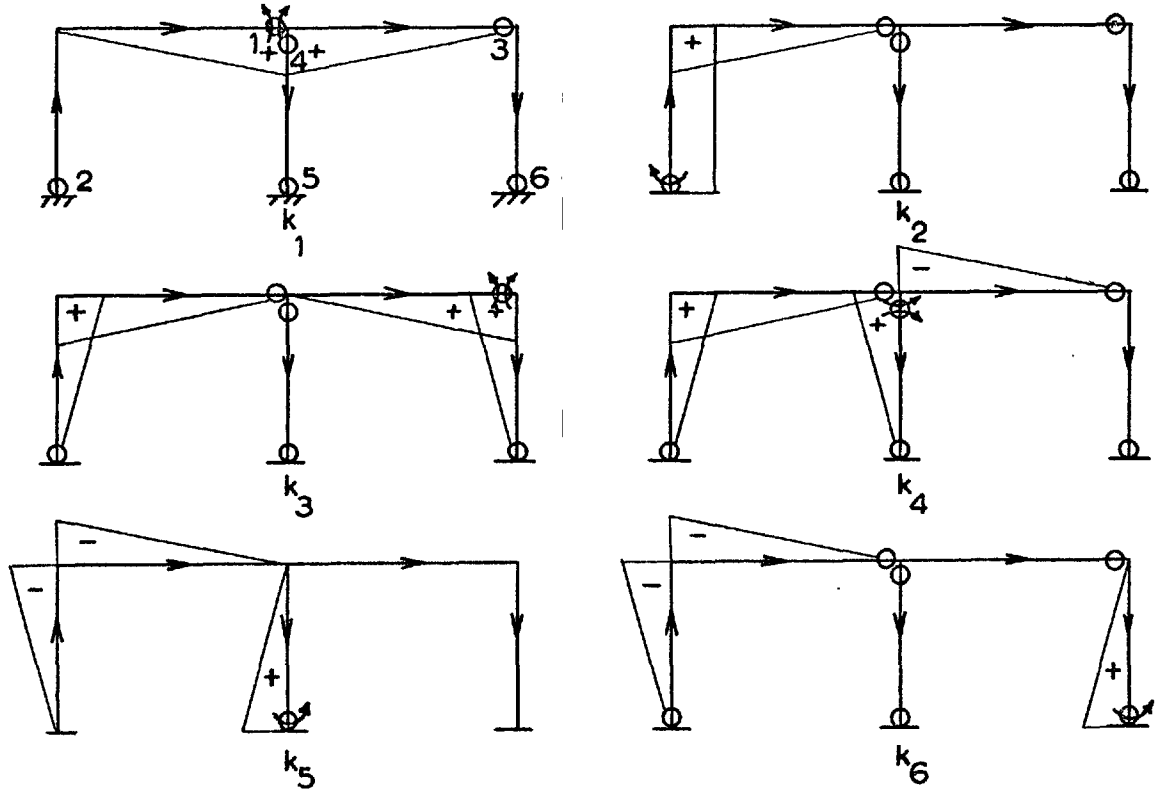


FIG. 4.3 INFLUENCE DIAGRAMS (D)

where the value of β_i is +1 or -1 according as the unit actions applied at the releases of Fig. 4.2. are positive or negative respectively. Thus,

$$\beta_i = -1 \text{ for 'b' and 'a' type of hinges}$$

$$\beta_i = +1 \text{ for 'c' type of hinges} \qquad (4.2)$$

Since $g_{ij} = \int \frac{k_i k_j}{EI} ds$, the flexibility coefficient g_{ij}^D for the directed graph sign convention is given by,

$$g_{ij}^D = \beta_i \beta_j g_{ij}^s \qquad (4.3)$$

where g_{ij}^s is the flexibility coefficient calculated according to the simplified limit method of Baker.

Similarly it can be shown that,

$$v_{io}^D = \beta_i v_{io}^s \qquad (4.4)$$

Thus the coefficients g_{ij}^s and v_{io}^s calculated using the expressions given in Reference (7) are transformed to the directed graph sign convention through equations (4.3) and (4.4).

4.3. STATIC AND KINEMATIC MATRICES

It has been explained in section 2.3 that the value of the element k_{jq} of the kinematic matrix is given by the ordinate at a section q of the influence diagram k_j. Thus the values of k_{jq} can be calculated from the influence diagrams such as shown for a frame in Fig.4.1.

By the principle of contragredience the static and kinematic matrices are related as,

$$h_{qj} = k_{jq}$$

$$\text{i.e. } [H] = [K]^T \qquad (4.5)$$

Thus having worked out the kinematic matrix as above, the static matrix can be computed through equation (4.5).

A subroutine of the program generates these coefficients and assembles these matrices.

4.4. TRANSFORMATION OF BASIS

It may be desired in the analysis for optimal solution to have a different release system. The transformation to another basis (i.e. release system) is done using the procedure explained in Reference (61). The following is a brief summary of the expressions used in connection with the transformation of basis.

The redundant actions $\{m_b^B\}$ at the releases of the system B can be expressed in terms of the actions $\{m_b\}^A$ at the releases of the system A as,

$$\{m_b{}^B\} = [Q]\{m_b{}^A\} \tag{4.6}$$

where [Q] is called the release transformation matrix of the order $\alpha \times \alpha$.

The flexibility matrix $[G^B]$, the displacement vector $\{v_o^B\}$, the static matrix $[H^B]$ and the particular solution due to loads $\{m_o^B\}$ for the release system B are given by the following expressions:

$$[G^B] = [Q^{-1}]^T [G_A^A] [Q^{-1}] \tag{4.7}$$

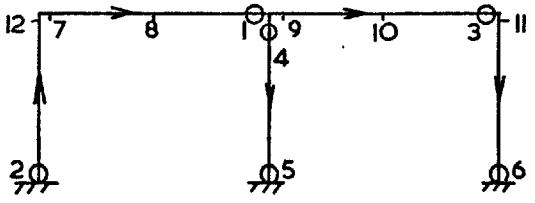
$$\{v_o^B\} = [Q^{-1}]^T \{v_o^A\} - [G^B] \{m_{oB}^A\} \tag{4.8}$$

$$[H^B] = [H^A] [Q]^{-1} \tag{4.9}$$

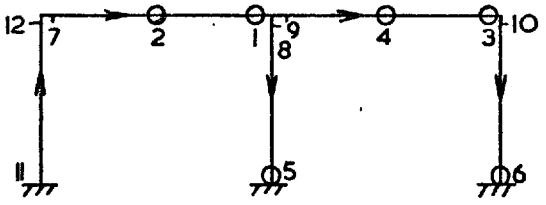
$$\{m_o^B\} = \{m_o^A\} - [H^B] \{m_{oB}^A\} \tag{4.10}$$

where $\{m_{oB}^A\}$ would be the values of $\{m_o^A\}$ at the positions of the redundant actions $\{m_b^B\}$

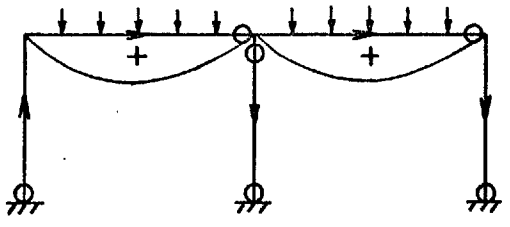
The expressions (4.7) to (4.10) show that for a complete transformation from release system A to system B, only the release transformation matrix [Q] and vector $\{m_{oB}^A\}$ are required to be calculated. The



(a) System A



(b) System B



(c) m_o diagram

FIG. 4.4 RELEASE SYSTEMS AND m_o DIAGRAM FOR A FRAME

coefficients of [Q] and $\{m_{oB}^{A}\}$ are easily calculated from the k_i and m_o^q diagrams of system A as illustrated below.

Fig. 4.4. shows two types of release systems A and B for a frame. The influence diagrams, k_i, for the frame for release system A are shown in Fig.4.3 and the particular solution diagram, m_o, for a loading condition is shown in Fig.4.4. The release transformation matrix [Q] and the vector $\{m_{oB}^{A}\}$ required for the transformation from release system A to B are given below.

$$[Q] = \begin{bmatrix} 1 & 0 & 0 & 0 & 0 & 0 \\ \frac{1}{2} & \frac{1}{2} & \frac{1}{2} & \frac{1}{2} & -\frac{1}{2} & -\frac{1}{2} \\ 0 & 0 & 1 & 0 & 0 & 0 \\ \frac{1}{2} & 0 & \frac{1}{2} & -\frac{1}{2} & 0 & 0 \\ 0 & 0 & 0 & 0 & 1 & 0 \\ 0 & 0 & 0 & 0 & 0 & 1 \end{bmatrix}$$

$$\{m_{oB}^{A}\} = \begin{bmatrix} 0 \\ m_o^{A(8)} \\ 0 \\ m_o^{A(10)} \\ 0 \\ 0 \end{bmatrix}$$

where $m_o^{A(8)}$ and $m_o^{A(10)}$ are the values of m_o diagram for release system A at the sections 8 and 10 respectively (Fig. 4.4.(c)).

4.5. CASES OF HINGE PATTERN FOR THE ANALYSIS OF FRAMES

The following two loading conditions (Fig.4.5) are considered for the analysis of optimal solution:

Loading condition I : $\lambda_C (W_D + W_L + W_W)$

Loading condition II: $\lambda_D W_D + \lambda_L W_L$

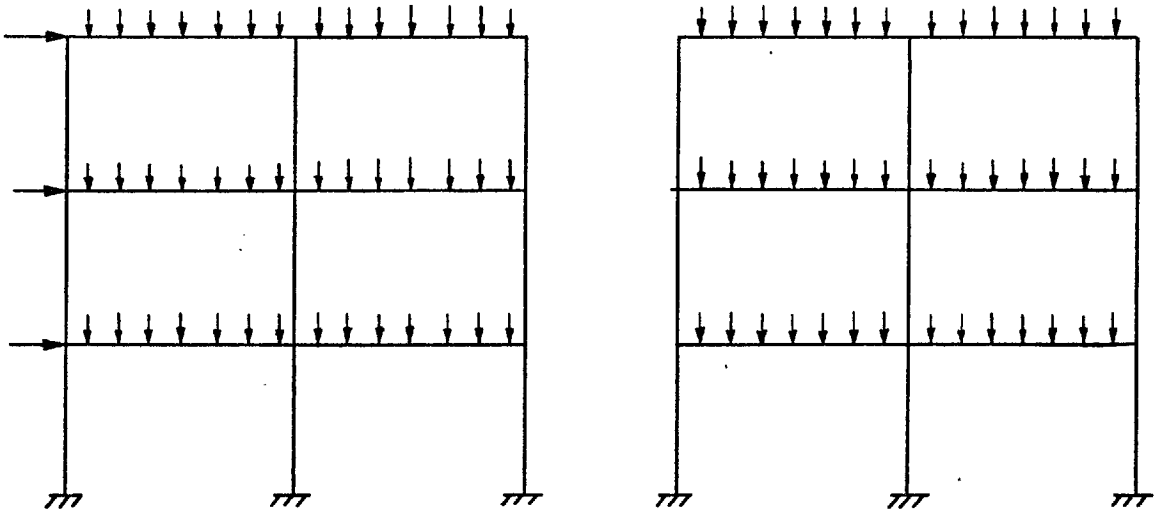


FIG. 4.5 LOADING CONDITIONS

In order to study the merits of economy for certain of the specific design requirements, explained below, the following three cases of hinge pattern have been considered for each of the loading conditions. The choice of the position of plastic hinges is handled in the computer program through the use of Plastic Hinge Indicator (PHI) for each section which will be assigned the value of one for a plastic hinge and zero for no hinge to form at the section.

Case 1. Hinges at ends of beams only.

A recent investigation (53, 54) has shown that for frames which require consideration of instability effects under ultimate load it would be desirable to avoid plastic hinges in columns. Hence in the case of loading condition I the plastic hinges are allowed to form only at the leeward end of the beams and for loading condition II the plastic hinges are allowed to form at both ends of the beams. The hinges at the midspan sections of the beams are avoided due to reasons discussed below.

Case 2. Beam and column hinges but no hinge at mid-span section of beams.

For satisfactory serviceability conditions under working load, especially to avoid excessive deflection, it has been recommended by Baker (7) that hinges at mid-span sections of beams may be avoided. Hence in this case assuming that there are no serious stability problems, beam and column hinges are allowed to form but the hinges at mid-span sections of beams are avoided.

The available choice of plastic hinges in this case may lead to situations involving an overall or local mechanism of the frame. As the linear programming formulation does not include constraints for the mechanism conditions of the frame, the possible positions of plastic hinges are chosen based on practical consideration of designs, such that the number of possible plastic hinges are restricted to a maximum of α and also avoid local mechanisms. This selection of hinge positions is discussed below.

It has been observed from the working of design examples, that for loading condition I plastic hinges may not form at the sections of the windward side column in the first bay of the frame and also at the left end sections of beams, as these sections will be designed for a resisting moment equal to the value at a corresponding symmetrical section, which

in normal cases is greater than the actual moment occurring at these sections. Thus the location of plastic hinges are confined to the other column sections and the right end sections of beams as shown in Fig.4.6. This choice of hinges may lead to joint mechanisms at the joints along the end columns, but their formation is avoided through a trial analysis in the computer program. First an optimal solution is worked out for the position of hinges shown in Fig.4.6 and each end joint is checked to find whether a joint mechanism is present. If a joint mechanism is identified the section, which experiences the least inelastic rotation, would be taken for future analysis as the section where no plastic hinge would form (i.e. the value of PHI for that section will be assigned zero). It may be noted from the above discussion that this hinge pattern yields the number of plastic hinges less than α.

For loading condition II, it has been observed in the case of symmetrical frames that maximum amount of moment redistribution and the resulting economy is achieved under case 1 of the hinge pattern. However, the positions of plastic hinges shown in Fig.4.8 have been tried for case 2 of hinge pattern.

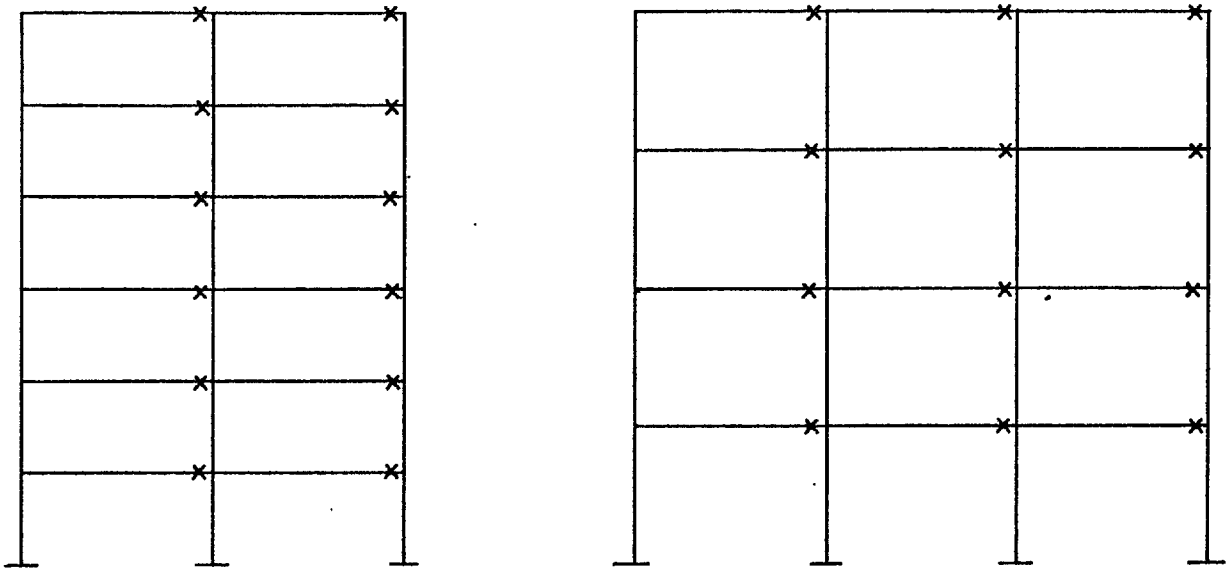
Case 3. No restriction of hinges.

For the cases of frames that satisfy the above two requirements of design, plastic hinges are allowed to form at all the critical sections as described below.

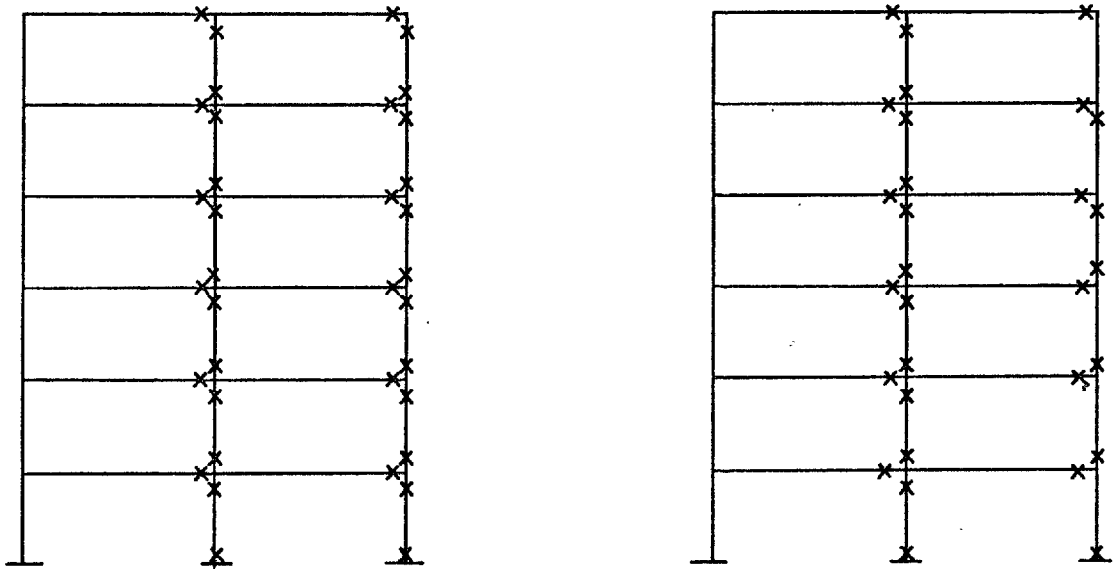
For loading condition I the position of plastic hinges for case 2 of hinge pattern, described above, is taken as the basis for further analysis. As case 3(a) of the analysis the values of moments (obtained for case 2) for the mid-span sections of the first and the last bays are compared and possible hinge positions are chosen at those sections where the bending moments are greater than the corresponding symmetrical sections. In case of frames with more than two bays the position of plastic hinges at mid-span sections of adjacent bays are tried successively for analysis.

Additional trials are made (indicated as cases 3(b) and 3(c) for two examples in Fig.4.7) as described in the following. The program scans all the column hinges and assigns the value of PHI as zero for those column sections which experienced zero inelastic rotation in the previous case of hinge pattern. Depending on the additional number of

LOADING CONDITION I



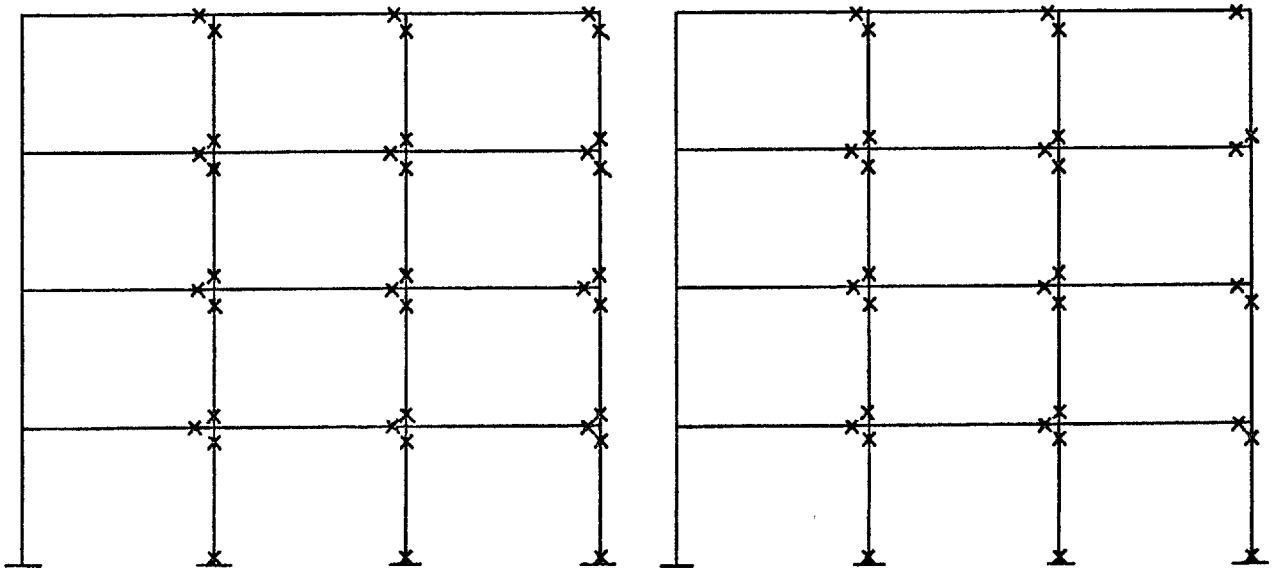
CASE 1



Possible location of hinges

CASE 2

(Joint mechanisms avoided-an example)



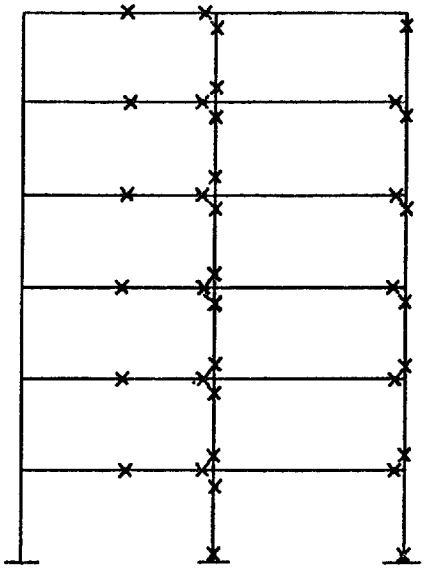
Possible location of hinges

CASE 2

(Joint mechanisms avoided-an example)

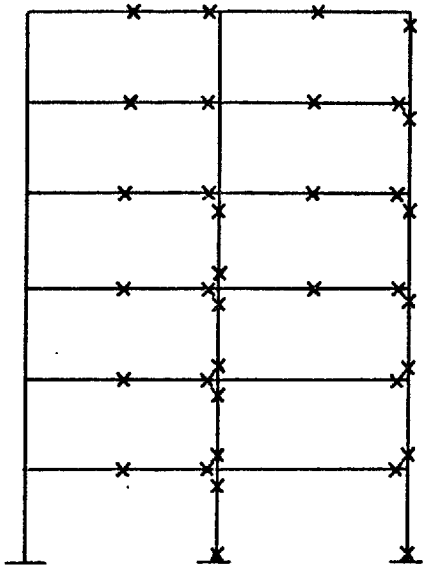
FIG. 4.6 POSITION OF HINGES

LOADING CONDITION I

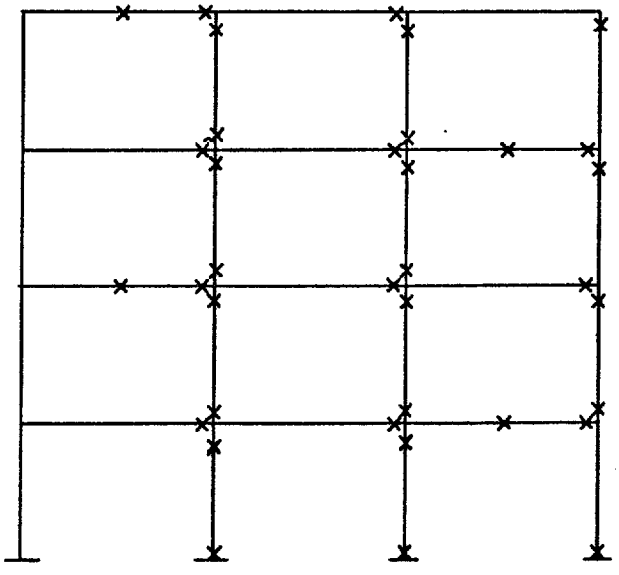


CASE 3 (a)

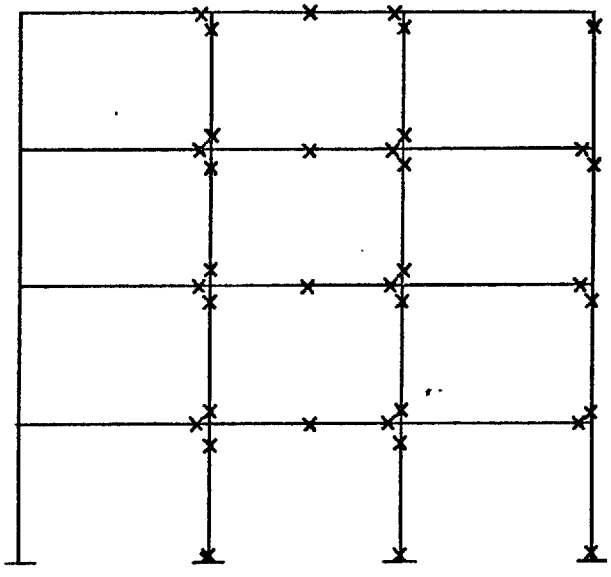
(i)



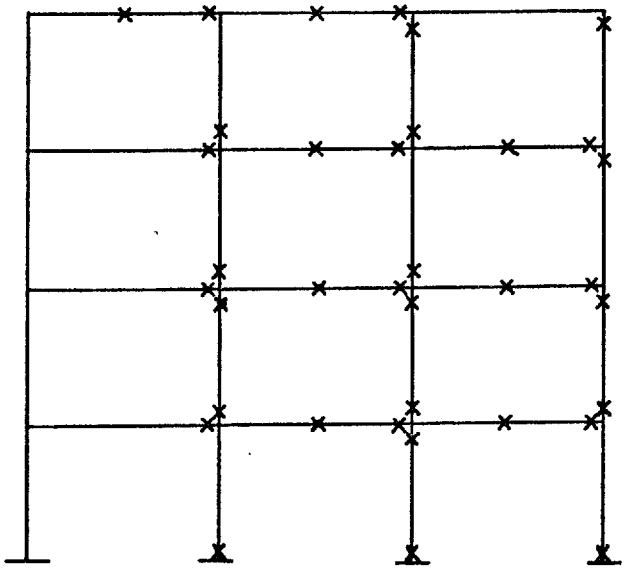
CASE (b)



CASE 3(a)



CASE 3(b)

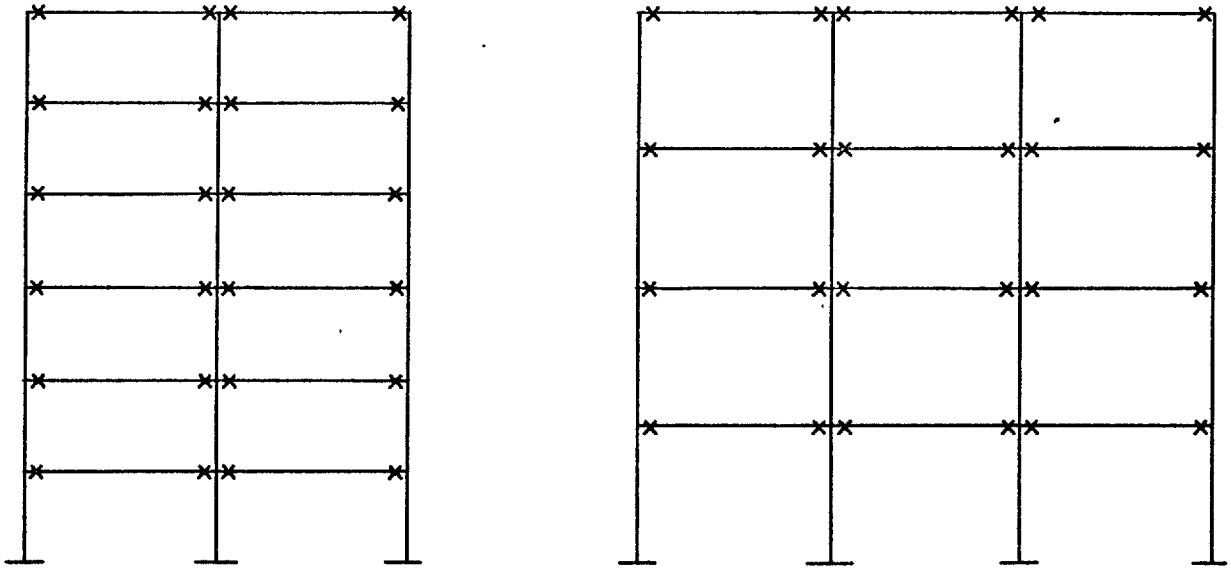


CASE 3(c)

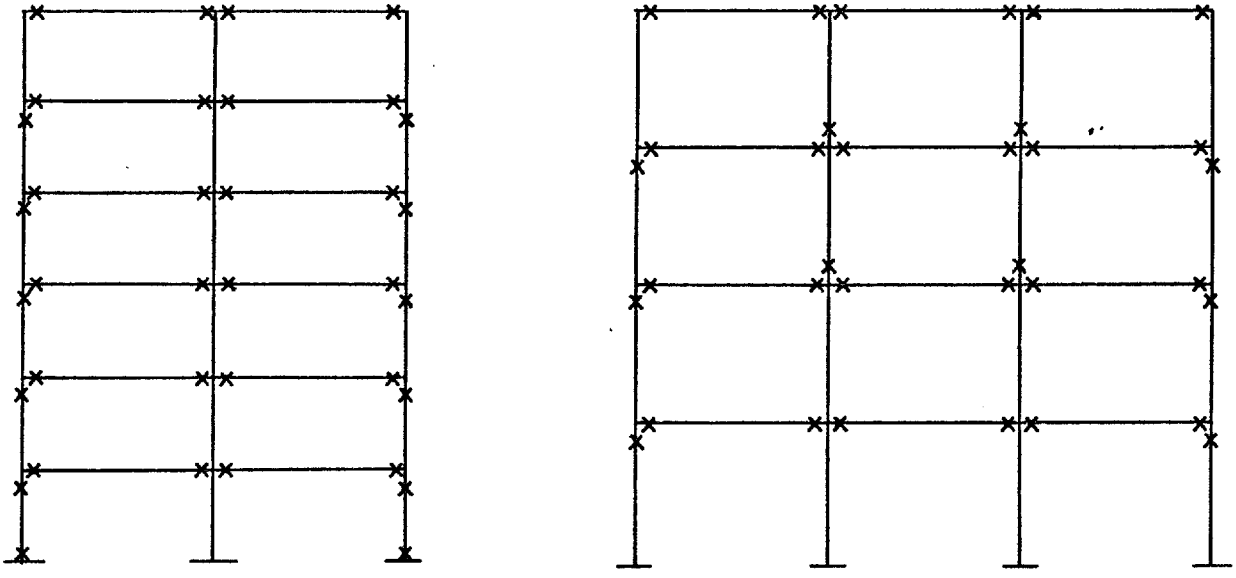
(ii)

FIG. 4.7 EXAMPLE OF POSITION OF HINGES FOR CASE 3

LOADING CONDITION II



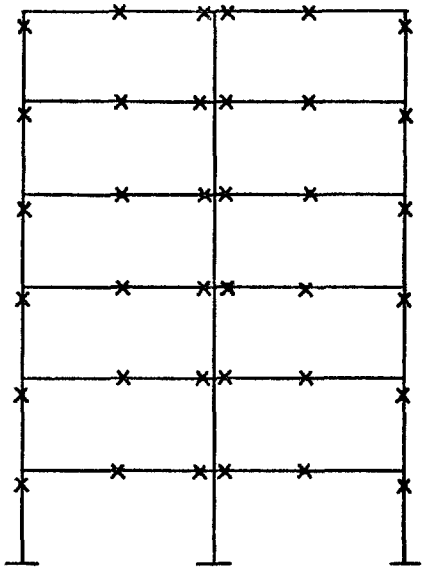
CASE 1



CASE 2

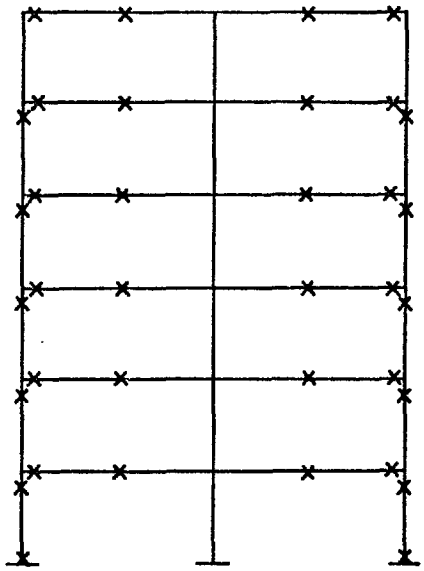
FIG. 4.8 POSITION OF HINGES

LOADING CONDITION II

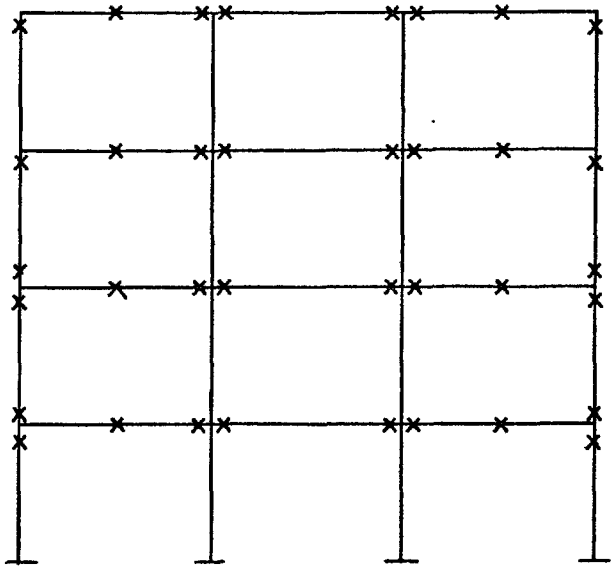


CASE 3(a)

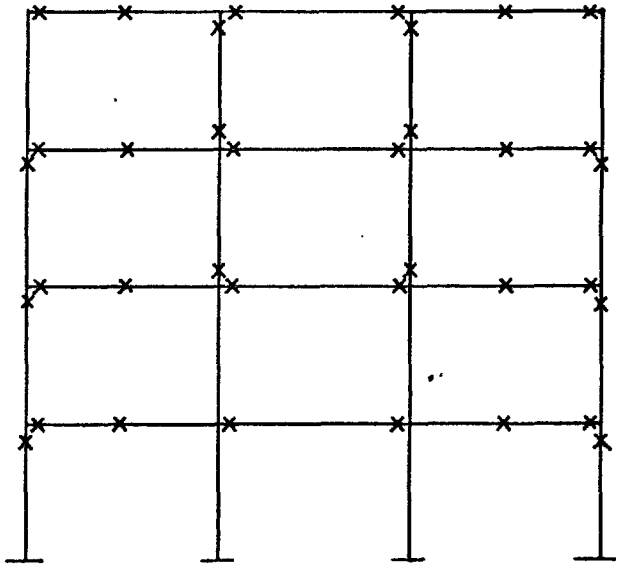
(i)



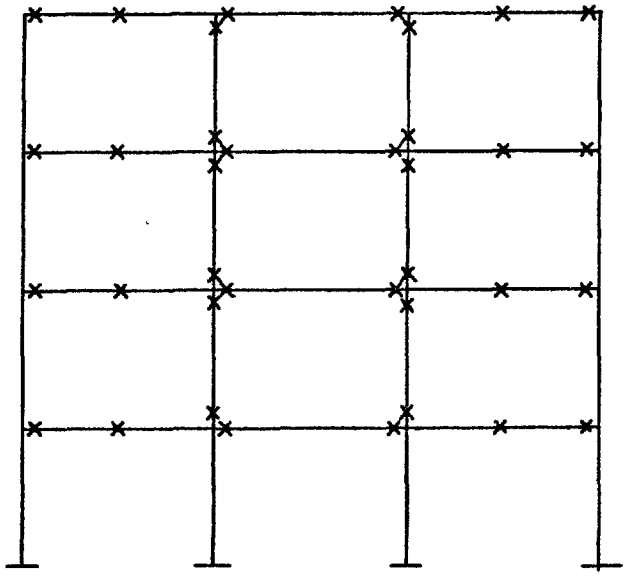
CASE 3(b)



CASE 3(a)



CASE 3(b)



CASE 3 (c)

(ii)

FIG. 4.9 POSITION OF HINGES FOR CASE 3

possible plastic hinges as obtained above, plastic hinges at other critical mid-span sections of beams are chosen for further analysis. Fig. 4.7. illustrate the possible position of plastic hinges obtained in the analysis for two of the design examples discussed in Chapter 6. Fig.4.9. gives the possible position of plastic hinges for case 3 under loading condition II.

4.6. COMPUTER PROGRAM FOR OPTIMAL LIMIT DESIGN

4.6.1. Sequence of Operations

A computer program has been developed for the optimal limit design of reinforced concrete frames based on the linear programming formulation described in Chapter 3. The program analyses a frame for optimal solution for three cases of hinge pattern, explained in section 4.5, under each of the two loading conditions. The logic of the computer program, coded in FORTRAN IV, is outlined in the flow chart shown in Fig.4.10. Following is a step-by-step description of the main operations executed by the program.

1. Read and print input data (Phase I). The input data required for the program is listed separately.

2. For a frame with the hinge release system A shown in Fig.3.1, work out the coefficients g_{ij} of the flexibility matrix [G]. The expressions given in Reference (7) have been used for the calculation of flexibility coefficients and this computation is carried out through a set of subroutines. Each of these subroutines is programmed to calculate the values of g_{ij} due to unit action at a particular type of hinge as described below.

Subroutine	Unit actions at (Ref: Fig.2.4)
ROBN1	'b' type of hinges in bays except the first and the last ones.
ROB1	'b' type of hinges in the first bay.
ROBN	'b' type of hinges in the last bay.
ROA	'a' type of hinges.
ROC1	'c' type of hinges in the first bay.
ROC	'c' type of hinges in all the bays except the first bay.
ROCNN	'c' type of hinges of the last one in the end bay.

3. Workout the displacement vector $\{v_o\}$ for each of the two loading conditions using a subroutine DISL.

4. As the flexibility matrix and displacement vectors are calculated for the sign convention adopted in Reference (7) (Fig.2.4), transform the matrix [G] and $\{v_o\}$ to the directed graph sign convention shown in Fig.3.1 by using equations 4.3 and 4.4.

5. For transformation from release system A to B determine the release transformation matrix [Q] through a subroutine QMAT.

6. Calculate the flexibility matrix [G] for release system B using equation 4.7. $[G^B] = [Q^{-1}]^T \{V_o^A\} - [G^B] \{m_o^A{}_B\}$

7. The influence diagrams shown in Figs. 4.1 are used to compute the values of k_{ij} and a subroutine KVM assembles the kinematic matrix [K]. The static matrix [H] is also computed as $[H] = [K]^T$. The kinematic and static matrices thus calculated for release system A are transformed to release system B through equation 4.9.

8. Calculate the vectors $\{m^A_{oB}\}$ and $\{v_o\}$ for release system B.

9. Elastic analysis for factored loads: The inverse of the flexibility matrix [G] is calculated using the subroutine MINV. This subroutine uses the standard Gauss-Jordon method to invert a matrix. The compatibility equation (3.11) is solved for the values of moments at the basic hinges with zero values of inelastic rotation at all the hinges. The moments at the non-basic hinge sections are calculated through a subroutine CALMAC which uses the equilibrium equation (3.28) for this computation. The axial loads in columns are computed through a subroutine AXIAL. The results of elastic analysis for two loading conditions are printed out.

10. Read input data (Phase II) as listed in section 4.6.2.

11(a) Calculate the area of steel for beam and column sections using equations (3.36) and (3.37). In the present program the design equations (6.1) to (6.7) have been used for this computation with a view to illustrate the design examples described in Chapter 6. However, linear approximations to any other design charts can be used. The cost coefficients c_j are calculated using equation (3.51) and the objective function (equation 3.50) for the problem is formulated.

11(b) Calculate the permissible rotations (equation 3.23) for the basic and non-basic hinge sections. Expressions given in Chapter 6 are used in this program.

12 to 18. The analysis for different cases of hinge pattern, explained in section 4.5, is handled in the program through the use of plastic hinge indicator (PHI) for a critical section. A value of one indicates that a plastic hinge is allowed to form at the section and a value of zero indicates no plastic hinge at the section. In steps 13 to 18 the plastic hinge indicators are assigned proper values for each case of hinge pattern under loading condition I. The possible location of hinges for all the three cases are explained in section 4.5 and illustrated in Figs. 4.6 to 4.9.

19 to 22. Assign proper values of PHI for each of the three cases of hinge pattern under loading condition II as described in the previous section.

23. The subroutine ABMAT formulates the compatibility, limited ductility and equilibrium constraints of the linear programming problem. The cost and structural coefficients and the stipulations are calculated using equations (3.52) to (3.64). Additional design constraints as discussed in section 3.8.2 are included in the program. The constraints are assembled in a standard form of linear program expressed in equation (3.48). The L.P. problem formulated as above is solved for optimal solution using the subroutine SIMPLE. This subroutine SIMPLE is a routine developed by RAND Corporation and uses the revised simplex algorithm for solving an L.P. problem.

24. For case 2 of hinge pattern under loading condition I, the mechanism conditions at the joints along the end column are checked and the procedure explained in section 4.5 is adopted for the choice of position of plastic hinges to avoid joint mechanism.

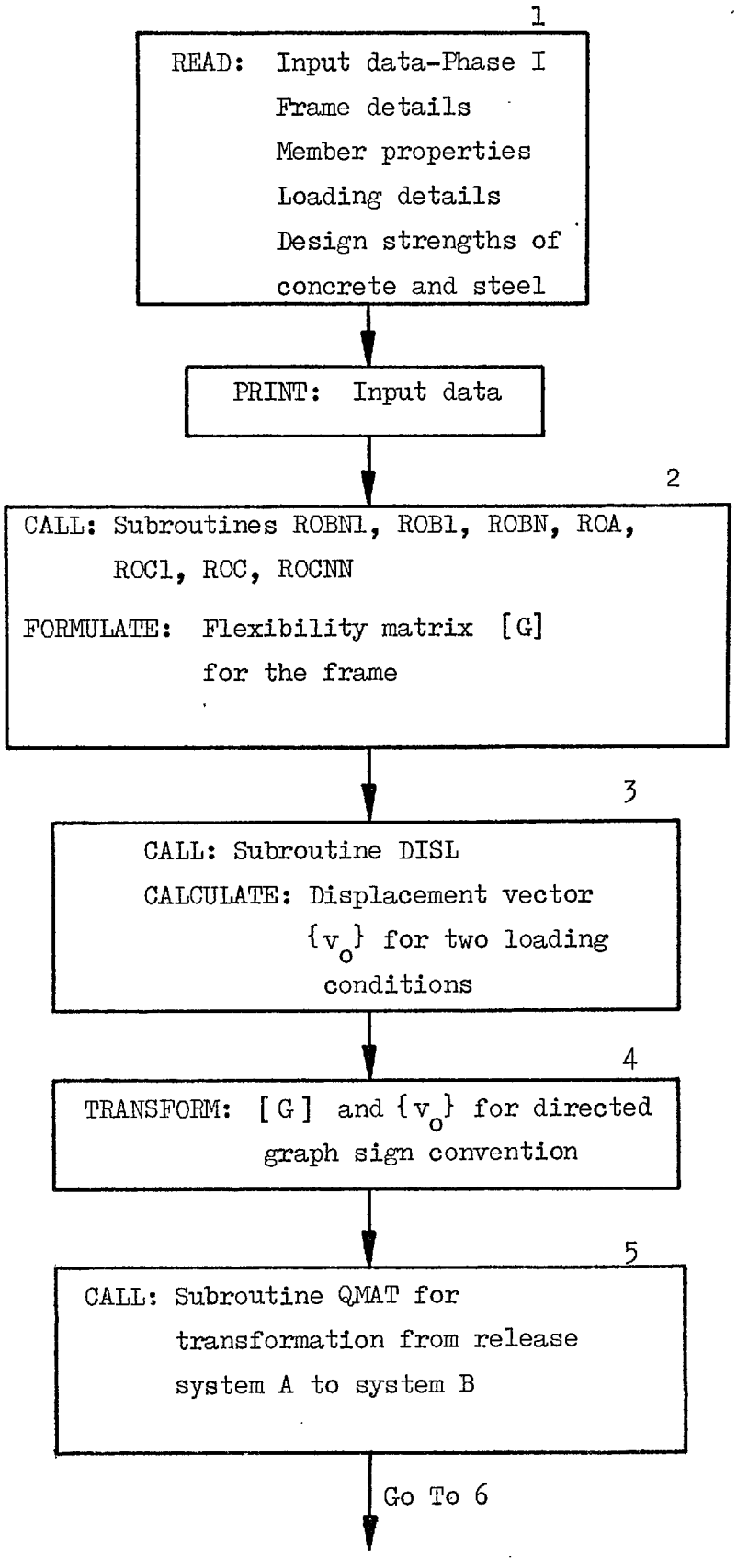
25. Calculate the moments at all the sections using equations (3.46) and (3.10) and axial loads in columns through subroutine AXIAL. The volume of steel required according to elastic analysis for factored loads (U.S.D) and according to optimal limit design (O.L.D) are calculated. The percentage economy for O.L.D. is worked out. The results of O.L.D. are printed out.

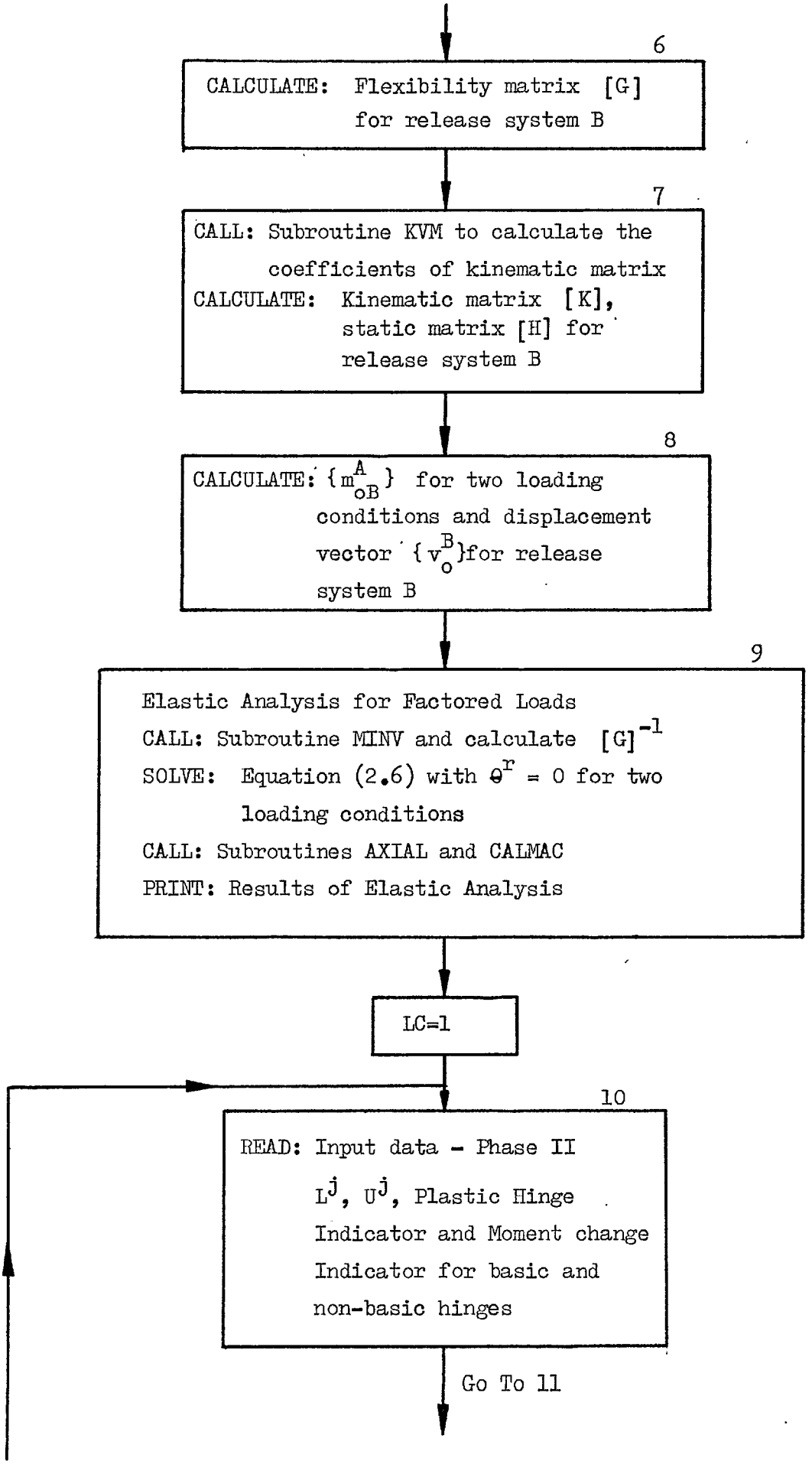
26. Steps 12 to 25 are repeated for each case of hinge pattern.

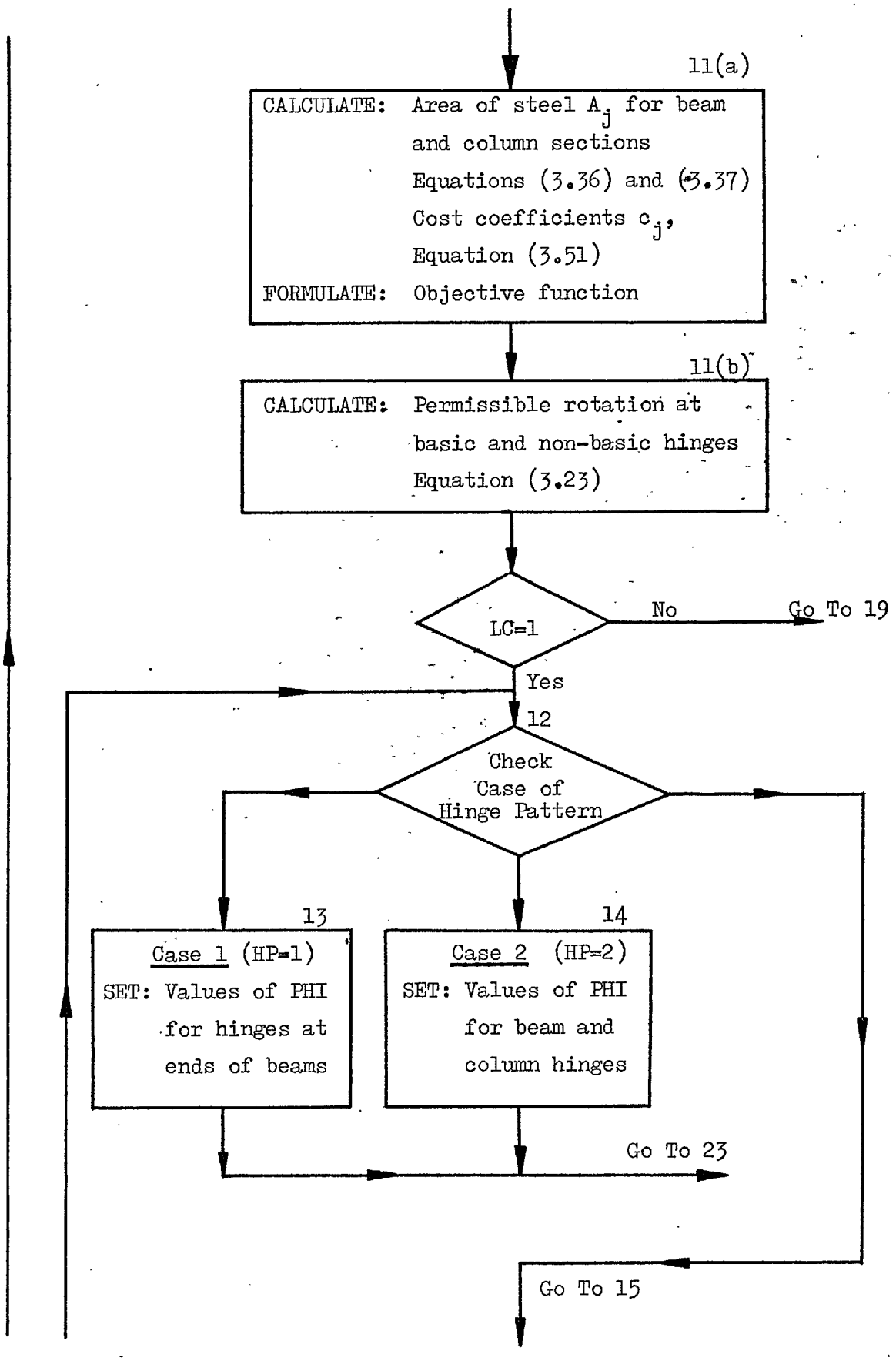
27. The analysis is carried out for loading condition II following the steps 10 to 26.

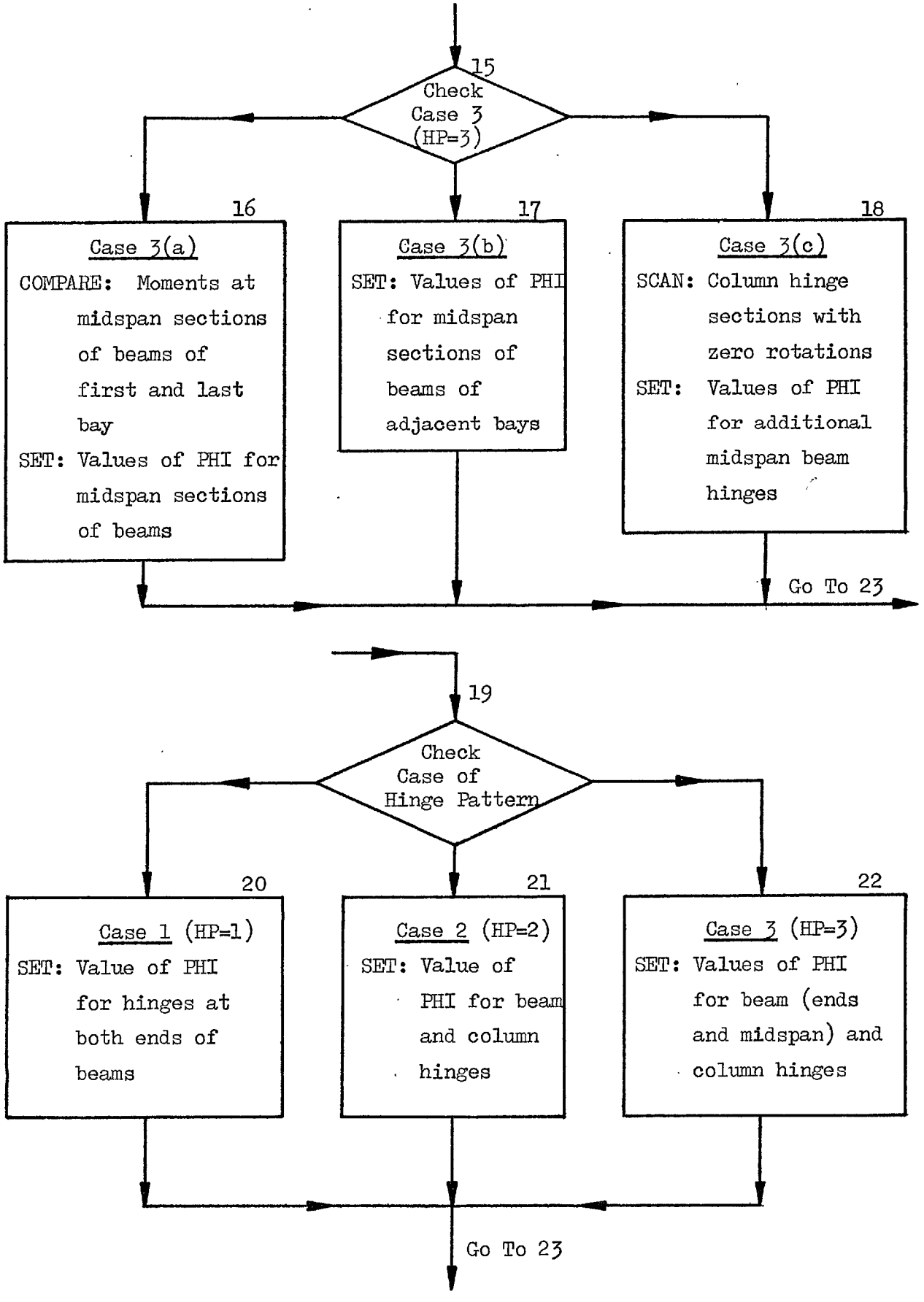
FIG. 4.10. FLOW CHART

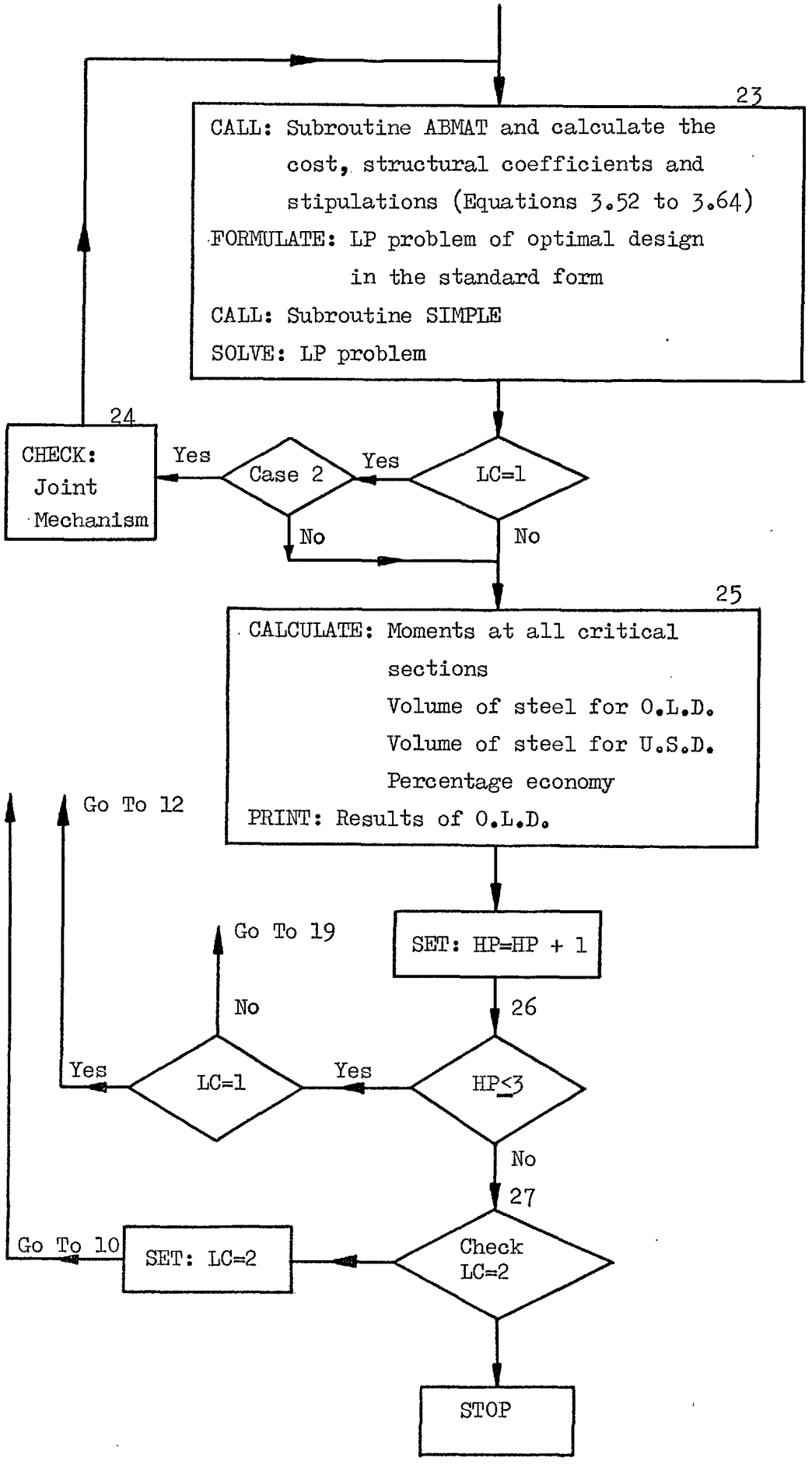
OPTIMAL REINFORCED CONCRETE FRAME DESIGN PROGRAM




6
CALCULATE: Flexibility matrix [G] for release system B
7
CALL: Subroutine KVM to calculate the coefficients of kinematic matrix
CALCULATE: Kinematic matrix [K], static matrix [H] for release system B
8
CALCULATE: $\{m_{oB}^{A}\}$ for two loading conditions and displacement vector $\{v_{o}^{B}\}$ for release system B
9
Elastic Analysis for Factored Loads
CALL: Subroutine MINV and calculate $[G]^{-1}$
SOLVE: Equation (2.6) with $\theta^{r} = 0$ for two loading conditions
CALL: Subroutines AXIAL and CALMAC
PRINT: Results of Elastic Analysis
LC=1
10
READ: Input data - Phase II
L^{j}, U^{j}, Plastic Hinge Indicator and Moment change Indicator for basic and non-basic hinges
Go To 11


11(a)
CALCULATE: Area of steel A_j for beam and column sections
Equations (3.36) and (3.37)
Cost coefficients c_j, Equation (3.51)
FORMULATE: Objective function
11(b)
CALCULATE: Permissible rotation at basic and non-basic hinges
Equation (3.23)
LC=1
No
Go To 19
Yes
12
Check Case of Hinge Pattern
13
Case 1 (HP=1)
SET: Values of PHI for hinges at ends of beams
14
Case 2 (HP=2)
SET: Values of PHI for beam and column hinges
Go To 23
Go To 15


15
Check
Case 3
(HP=3)
16
Case 3(a)
COMPARE: Moments at midspan sections of beams of first and last bay
SET: Values of PHI for midspan sections of beams
17
Case 3(b)
SET: Values of PHI for midspan sections of beams of adjacent bays
18
Case 3(c)
SCAN: Column hinge sections with zero rotations
SET: Values of PHI for additional midspan beam hinges
Go To 23
19
Check
Case of
Hinge Pattern
20
Case 1 (HP=1)
SET: Value of PHI for hinges at both ends of beams
21
Case 2 (HP=2)
SET: Value of PHI for beam and column hinges
22
Case 3 (HP=3)
SET: Values of PHI for beam (ends and midspan) and column hinges
Go To 23


23
CALL: Subroutine ABMAT and calculate the cost, structural coefficients and stipulations (Equations 3.52 to 3.64)
FORMULATE: LP problem of optimal design in the standard form
CALL: Subroutine SIMPLE
SOLVE: LP problem
24
CHECK: Joint Mechanism
Yes
Case 2
Yes
LC=1
No
No
25
CALCULATE: Moments at all critical sections
Volume of steel for O.L.D.
Volume of steel for U.S.D.
Percentage economy
PRINT: Results of O.L.D.
Go To 12
Go To 19
SET: HP=HP + 1
No
26
Yes
LC=1
Yes
HP≤3
No
27
Go To 10
SET: LC=2
Check LC=2
STOP

4.6.2. Input

The input data to be supplied for the program are as follows:

Phase I

1. Number of storeys and number of bays.

2. Type of supports: These are entered as numerical integers whose value indicates whether a particular support is hinged or fixed.

3. Design strengths of concrete and steel.

4. Beam properties and loads:
   (a) Beam number, length, effective depth, width of flange near mid-span, EI value, equivalent length of steel at mid-span and end sections.
   (b) Simply supported moment values ($\frac{WL}{8}$) due to dead and live load.

5. Column properties:
   Column number, height, breadth, effective depth, total depth and EI value.

6. Wind load:
   Total wind load shear at each storey level.

Phase II

The following set of data is required for each of the two loading conditions:

1(a) Lower bound values, L^j, for the basic hinges.
(b) Lower bound values, L^j, for the non-basic hinges.

2(a) Upper bound values, U^j, for the basic hinges.
(b) Upper bound values, U^j, for the non-basic hinges.

3(a) Plastic Hinge Indicator for the basic hinges.
(b) Plastic Hinge Indicator for the non-basic hinges.
(1 for plastic hinge, 0 for no plastic hinge)

4(a) Moment Change Indicator for the basic hinges.
(b) Moment Change Indicator for the non-basic hinges
(1 for possible change in sign of moment, 0 for no such change.)

Fig. 3.1(b) indicates the numbering system required for the preparation of input data.

4.6.3. Output

The output of the program is listed below:

1. Frame and member properties as given in the data.
2. Results of elastic analysis for factored loads under two loading conditions (printed separately):
   For each storey -
   Beams - Moments at the left end, mid-span and right end.
   Columns - Moments at the top and bottom ends, and axial load.
3. Results of optimal solution for two loading conditions (printed separately):
   (a) For each storey -
   Beams - Moments at the left end, mid-span and right end.
   Columns - Moments at the top and bottom ends, and axial load.
   (b) Volume of steel for elastic analysis.
   (c) Volume of steel for optimal design.
   (d) Percentage economy for optimal design compared to ultimate strength design for elastic analysis for factored loads.

4.6.4. Discussion

The optimal limit design program described above was run on CDC 6400 and 6600 at Imperial College and University of London Computing Centre respectively. In order to analyse larger sizes of frames, such as 2 bays and 6 storeys described in Chapter 6, within the working core memory of 49,000 words, it was found necessary to store the matrix [A] of the linear program on a tape during the execution of the subroutine SIMPLE. The actual central core memory required for a problem depends on the size of the frames and hence on the number of constraint equations and variables of the linear program. The following table gives these details for the design examples discussed in Chapter 6.

Example	Case of Hinge Pattern	No. of constraint equations (LC.I)	No. of variables (LC.I)	Central core memory (words)	C.P. Time (for LCs.I & II) in secs.
1	1 2 3	17 20 21	22 28 30	22,272	30.71
2	1 2 3	34 42 42	44 60 60	22,528	44.85
3	1 2 3	46 56 57	59 79 81	29,120	118.53
5	1 2 3	92 112 112	116 156 156	48,960	1302.14
6	1 2 3	102 124 126	126 170 174	48,960	891.78

The computing time required for complete solution depends on the size of the frame. It is difficult to generalize in this respect particularly with problems involving several cases of hinge pattern. However, it is worth mentioning that for frames, shown in Fig. 6.1., the analyses for a given set of PHI for two loading conditions required only 75 to 435 seconds on CDC 6400. The CP time given in the above Table refers to the time taken for completing analyses of all cases of hinge pattern under two loading conditions.

The Optimal limit design program described here offers the following facilities:

1. Any Code specification for the design of reinforced concrete sections, which could be approximated to piece-wise linear relationships may be incorporated in the program.

2. Different choice of plastic hinge pattern to satisfy specific design requirements can be analysed by suitable use of the plastic hinge indicator for critical sections.

CHAPTER FIVE

EXPERIMENTAL INVESTIGATION OF FLEXURAL RIGIDITY OF T-BEAMS FOR FRAME DESIGN

5.1. INTRODUCTION

The limit analysis and design of reinforced concrete frames require relatively precise knowledge of the EI values of the members. The investigations in this respect reported so far were concerned with the study on the rectangular sections of beams and columns (14, 44, 45). This experimental investigation was, therefore, conducted on T-beams subjected to negative moments at the ends which would simulate the conditions that exist in the beams of multi-storey building frames. The aims of the tests were as follows:

(i) To study the moment-curvature characteristics of various sections and the curvature distribution along the beam, which has different sectional behaviour due to varying nature of moments - T sections in the positive moment zone and rectangular section in the negative moment zone.

(ii) To propose a suitable model for the calculation of equivalent EI value for the beam to be used in the computation of end rotations.

5.2. TEST SPECIMENS

In order to simulate the behaviour of beams in frames and continuous structures, the test specimens were overhang beams subjected to loads at the two ends of overhang and at the centre. The simply supported span length and overhang length, on either side, were 12'0" and 3'0" respectively.

One of the cross-sectional dimensions considered important in the effective T-beam action was the width of flange. According to the Draft B.S. Code (62) the effective width of flange should not exceed the smaller of:

(i) the width of the web plus one-fifth of the distance between the points of zero bending moment and

(ii) the actual width of the flange.

For a continuous beam the distance between the points of zero bending moment may be taken as 0.7 times the effective span.

To satisfy the above requirements for various ratios of end to mid-span moments a width of flange of 500 mm was found suitable for this investigation.

Eight beams were tested in all and these were divided into two series; six beams in series A and two beams in series B. The width of flange for beams in series A was 500 mm and that for beams in series B was 700 mm.

All the beams were designed primarily to fail in flexure. The resistance to shear was provided and checked according to the recommendations made in the Draft B.S. Code (62) and in Reference (64).

The percentage of reinforcement at the support and mid-span sections was varied in all the six beams of series A to obtain the different ratios of ends to mid-span moments. The two beams B1 and B2 of series B were designed to have the same reinforcement as for beams A2 and A4 of Series A. Thus it was hoped to study the effect of increased flange width in those beams of series B.

The reinforcement details of all the eight beams are shown in Figs. 5.1 to 5.8 and the properties of the test specimens are given in Table 5.1.

5.3. MATERIALS AND FABRICATION

5.3.1. Concrete Mix

Concrete mix designed to give a cylinder strength of 4000 psi at 28 days was used for all the beams. The maximum size of the aggregates was $\frac{3}{8}$". The mix proportions are given below:

Ordinary Portland cement	112 lb.
Sand (B.S.25 - B.S.100)	100 lb.
Sand ($\frac{3}{16}$" - B.S.25)	233 lb.
Coarse aggregates ($\frac{3}{8}$" - $\frac{3}{16}$")	367 lb.
Water	89 lb.

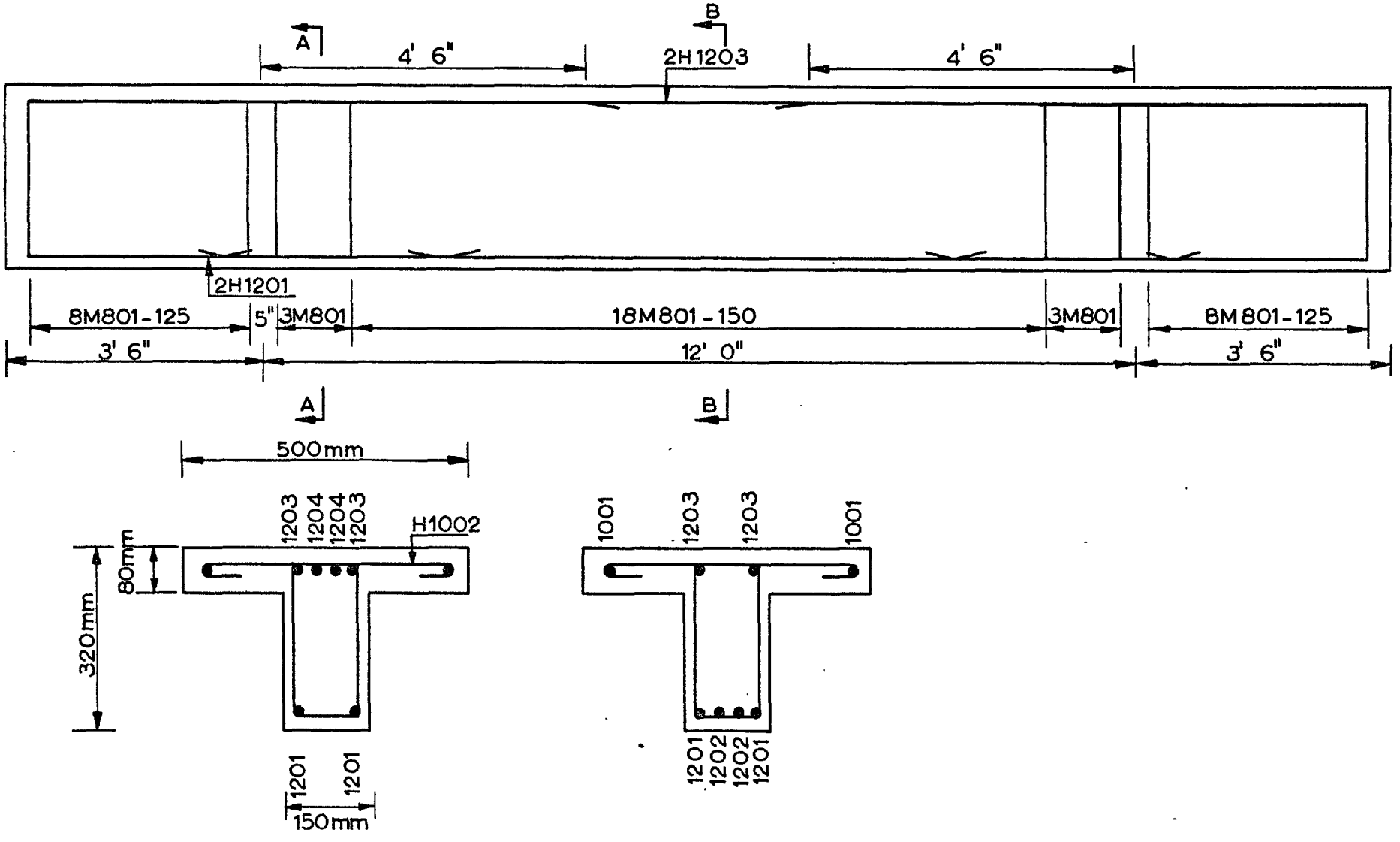


FIG. 5.1 REINFORCEMENT DETAILS FOR BEAM A1

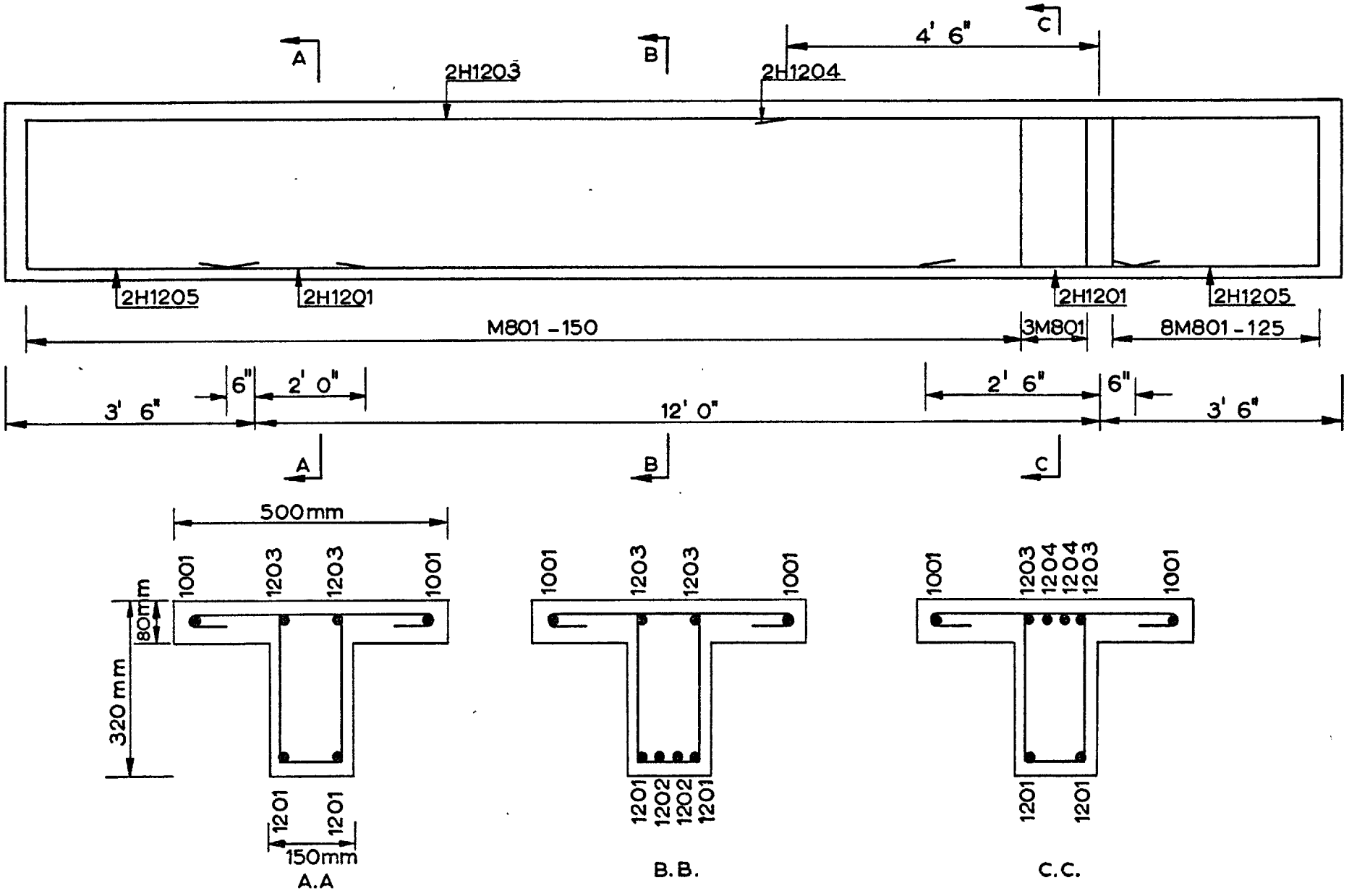
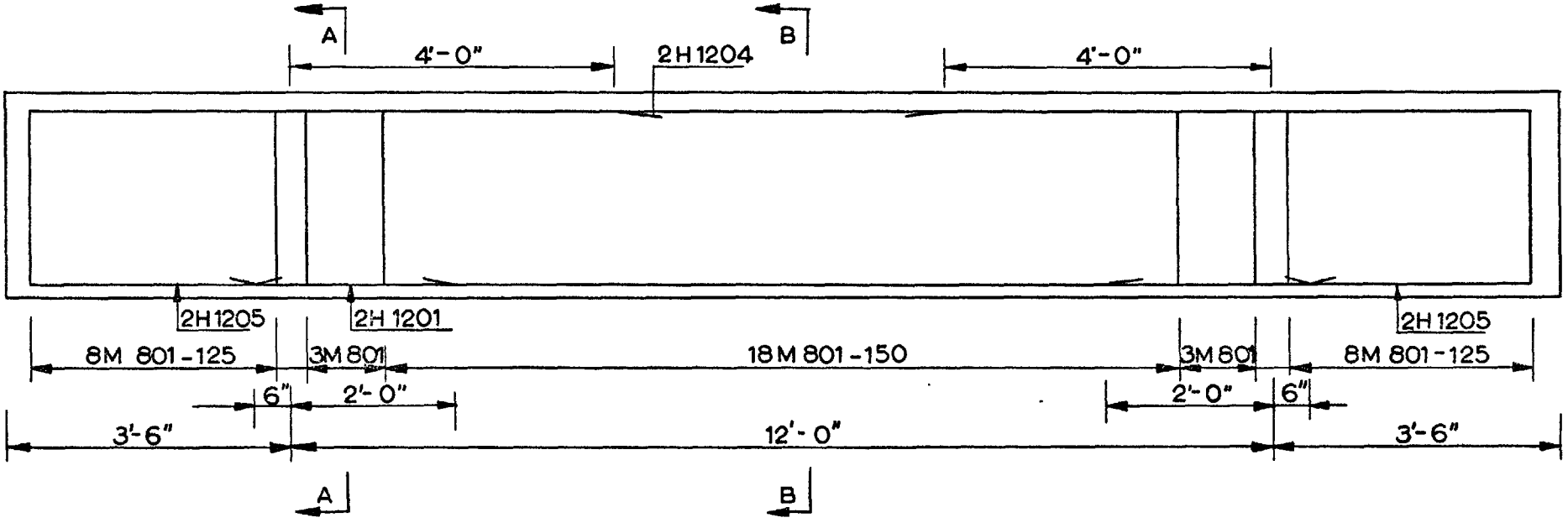


FIG. 5.2 REINFORCEMENT DETAILS FOR BEAM A2



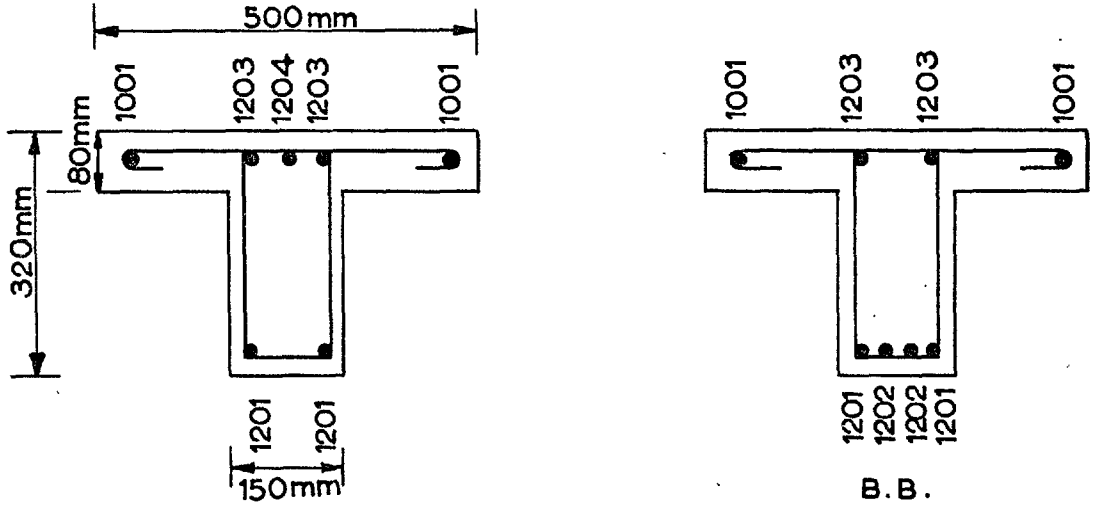


FIG. 5.3 REINFORCEMENT DETAILS FOR BEAM A3

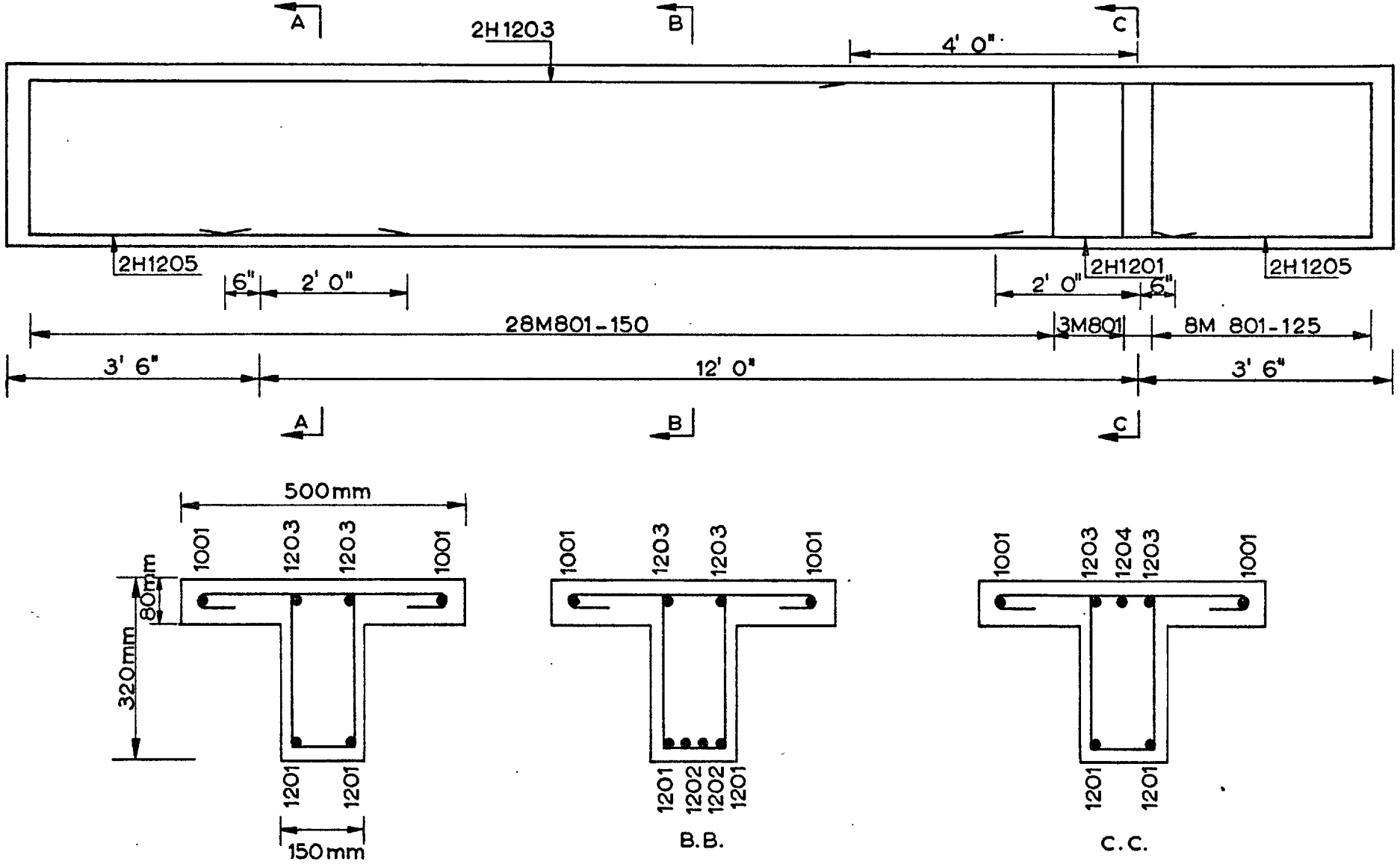


FIG. 5.4 REINFORCEMENT DETAILS FOR BEAM A4

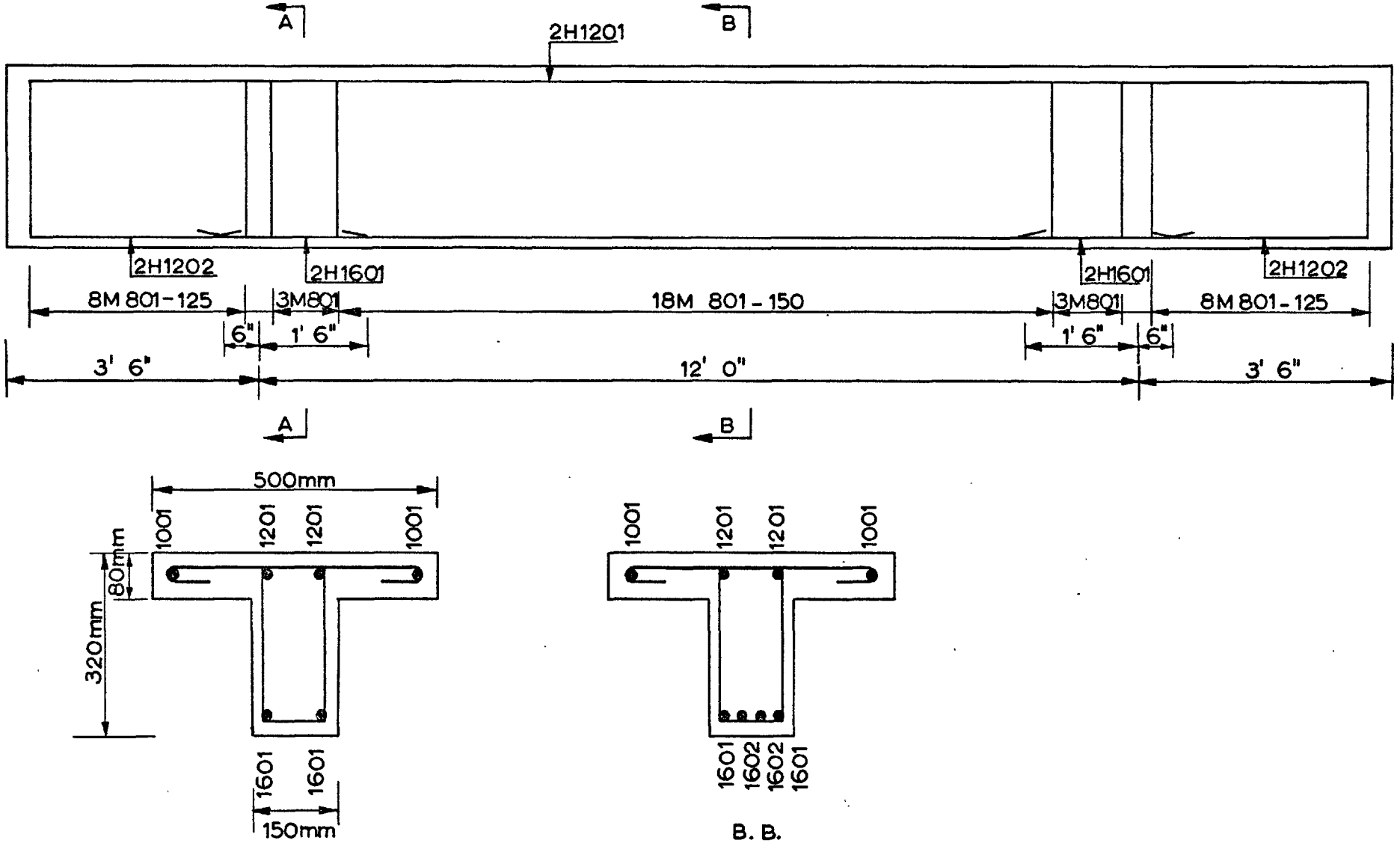


FIG. 5.5 REINFORCEMENT DETAILS FOR BEAM A5

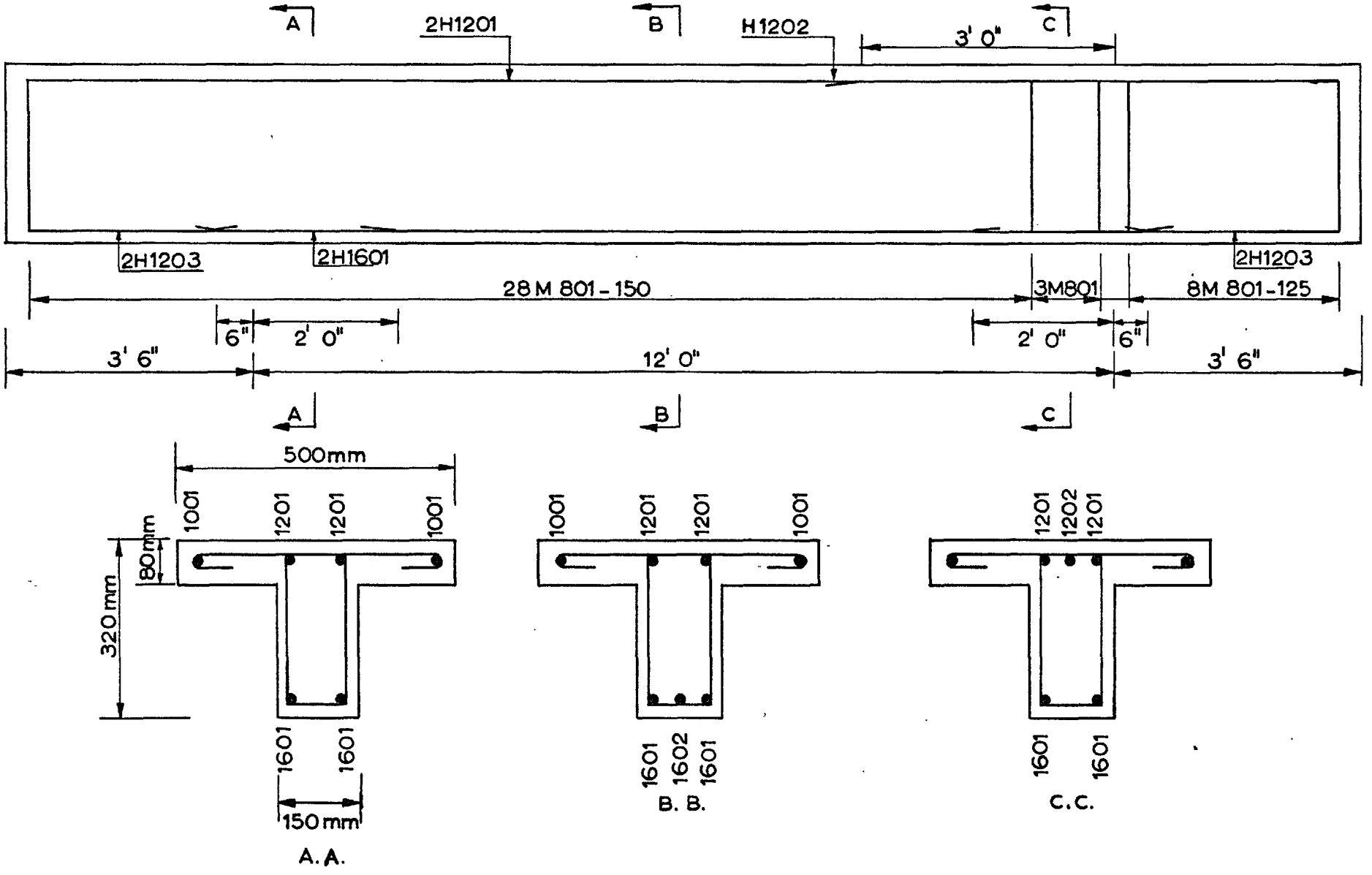


FIG. 5.6 REINFORCEMENT DETAILS FOR BEAM A6

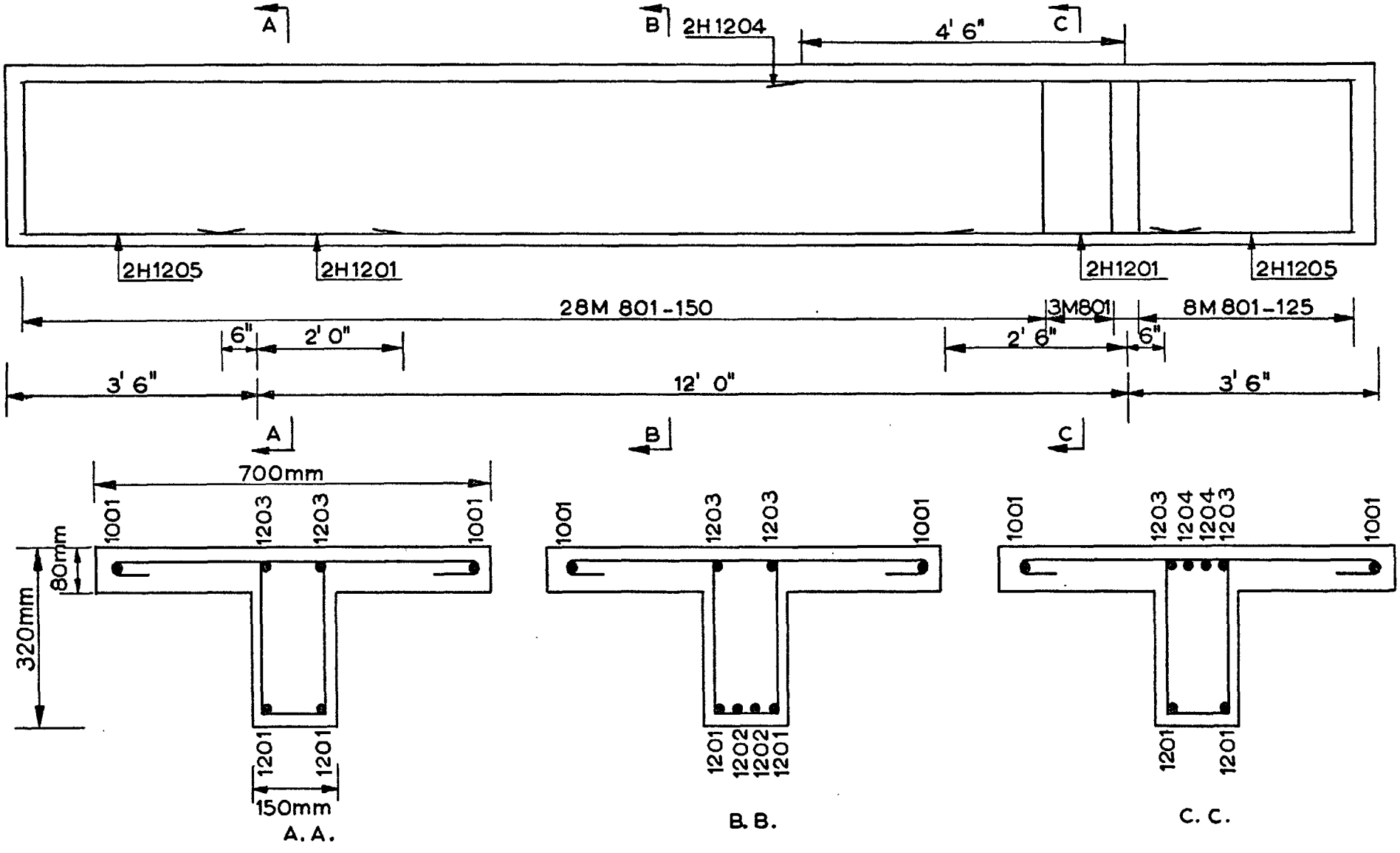


FIG. 5.7 REINFORCEMENT DETAILS FOR BEAM B1

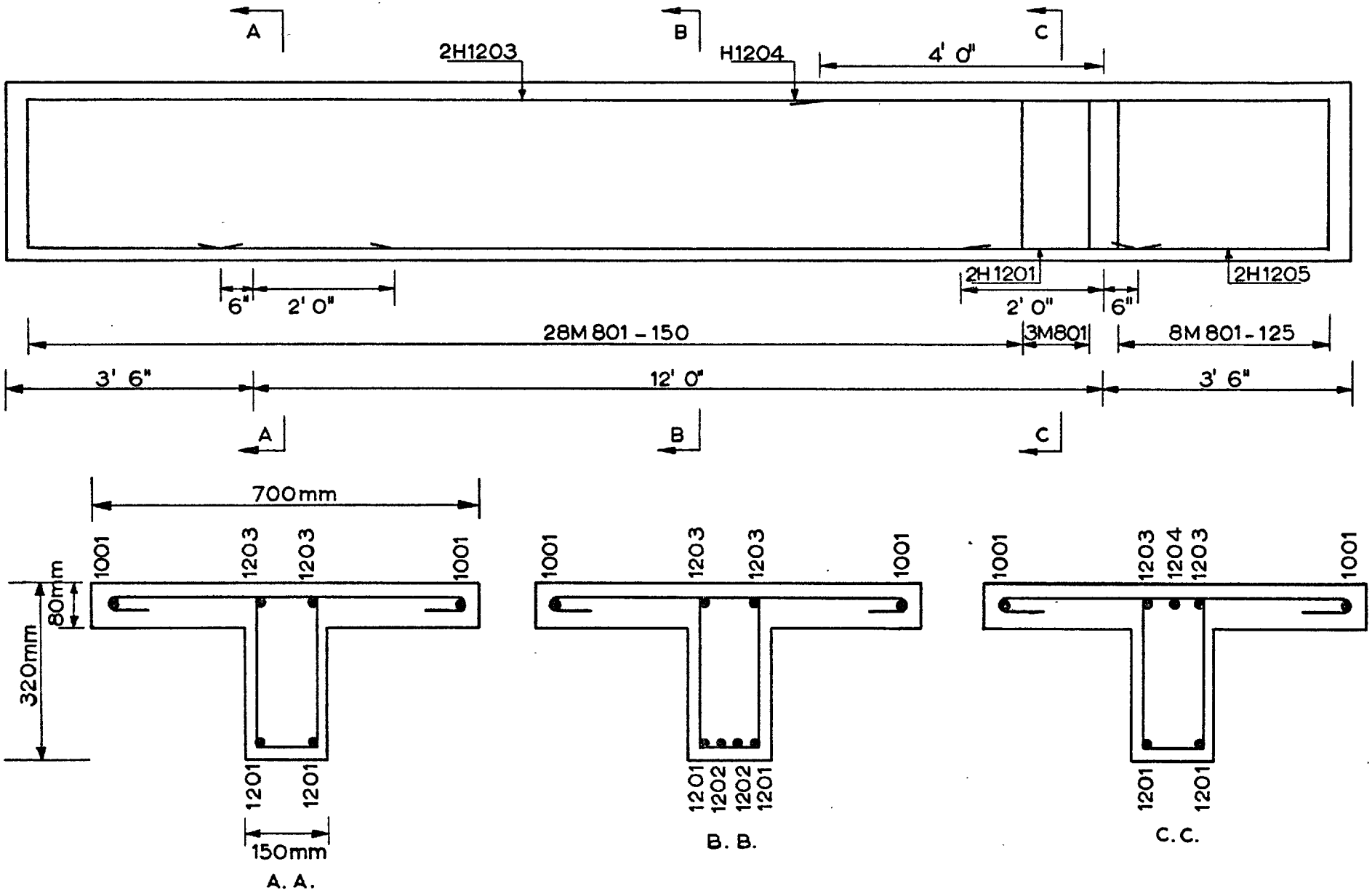


FIG. 5.8 REINFORCEMENT DETAILS FOR BEAM B2

TABLE 5.1 PROPERTIES OF TEST BEAMS

Beam No.	Section	Tension Reinforcement p%	Compression Reinforcement p^1%	Modulus of Elasticity E_s kN/mm^2	Yield Strength of Reinforcement N/mm^2	Concrete Cylinder Strength N/mm^2
A1	2	1.420	-	199.1	450.0	27.45
	16	1.420				
	9	0.303	0.270	199.1	450.0	
A2	2	0.867	-	199.1	450.0	25.22
	16	1.400				
	9	1.303	0.270	199.1	450.0	
A3	2	1.130	-	199.1	450.0	26.72
	16	1.130				
	9	0.303	0.270	199.1	450.0	
A4	2	0.867	-	199.1	450.0	25.73
	16	1.130				
	9	0.303	0.270	199.1	450.0	
A5	2	0.867	-	199.1	450.0	25.38
	16	0.867				
	9	0.550	0.270	194.8	395.0	
A6	2	0.867		199.1	450.0	24.0
	16	1.130				
	9	0.410	0.270	194.8	395.0	
B1	2	0.867		199.1	450.0	22.67
	16	1.400				
	9	0.220	0.193	199.1	450.0	
B2	2	0.867		199.1	450.0	24.01
	16	1.130				
	9	0.220	0.193	199.1	450.0	

5.3.2. Reinforcing Steel

The main reinforcement for the beams consisted of 12 and 16 mm diameter hot rolled deformed bars. The stress-strain characteristics of the bars were determined by conducting tension tests on three sample specimens for each type. Fig. 5.9. shows the stress-strain curves for 12 and 16 mm diameter bars. The average values of the yield and ultimate strength of the bars are marked in Fig. 5.9. It can be observed that the stress-strain curves are similar to that of mild steel bars with a definite yield range upto a strain of 0.01.

In all the beams mild steel bars of 6 mm diameter and of yield strength 250 N/mm^2 were used for vertical stirrups.

5.3.3. Casting and Curing

The beams were cast in wooden forms made of plywood stiffened with battens to maintain the beam shape. The casting of the beams involved using six to seven batches of concrete and necessary care was exercised to get uniformity along the whole length. The concrete was compacted by using needle vibrator.

The moulds were covered with polythene sheets for 24 hours after casting and then the moulds were stripped. The specimens were then laid horizontally on the floor with the control specimens placed along-side and were subject to moist curing under polythene sheets for seven days. Subsequently the specimens were allowed to cure under standard open laboratory conditions. The beams were tested at an approximate age of 28 days.

5.3.4. Control Specimens

Two cylinders (6" x 9") and one cube (6" x 6" x 6") for each batch of concrete were cast along with the beam. These control specimens were cured along with the beam as described above. The control specimens were tested for the crushing strength a day before the test of the corresponding beam. The average values of the strengths are given in Table 5.1.

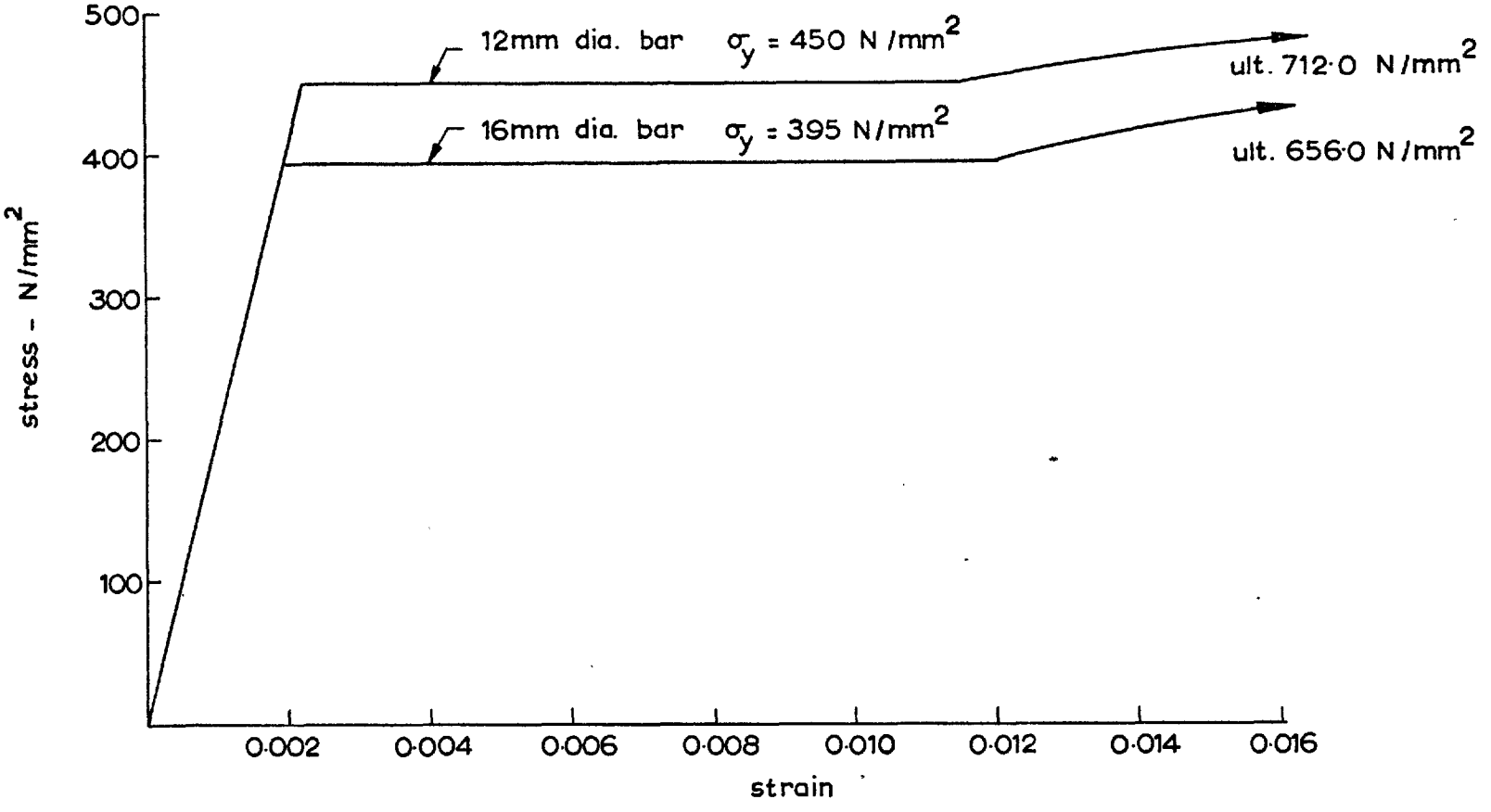


FIG. 5.9 TYPICAL STRESS - STRAIN CURVES FOR REINFORCEMENT

5.4. DESCRIPTION OF TESTS

5.4.1. Test Set-up

The test arrangement for a typical beam is shown in Fig.5.10 and Plate 1. The loads on the beams were applied by Amsler jacks of 10 tons capacity at the ends and of 20 tons capacity at the centre. The jacks were mounted on loading frames reacting against the test floor and were operated through independent cabinets. The loading and support platens consisted of steel plates of 6" x 4" x 2" as shown in Fig. 5.10.

5.4.2. Instrumentation

Concrete strains at various sections were measured using 2" 'demec' strain gauges. Fig. 5.11(a) shows the layout of the strain measurements. The sections across which strain measurements were made were numbered from 1 to 17. The main object of this scheme was to obtain information which would enable to plot the moment-curvature relation at various critical sections and also the curvature distribution along the length of the beam. Besides, electrical strain gauges were used to measure the maximum concrete strain at the two support sections. Steel strains at the support and mid-span sections were measured by means of electrical strain gauges embedded in slots cut in the bars at these sections.

The rotation of the beam was measured at seven sections of the beam using clinometers. Fig. 5.11(b) shows the positions of the clinometer readings.

The deflections of the beam at sections 5, 7, 9, 11 and 13 were measured using mechanical deflection gauges reading to 0.001".

5.4.3. Test Procedure

All the beams were tested under incremental loading where the loads were increased in nine to ten stages. The first four load increments were each made equal to 15% of the calculated ultimate load, the next three increments, were each made equal to 10% and each of the subsequent increments was 5% of the ultimate load. Attempts were made to maintain the ratios of the ends to mid-span moments constant at all load stages.

Strain readings (demec gauge) for sections 1, 2, 3; 7, 8, 9; and 15, 16, 17 (shown in Fig. 5.11) were taken for all the load stages while



PLATE 1(a) TEST SET-UP : A GENERAL VIEW

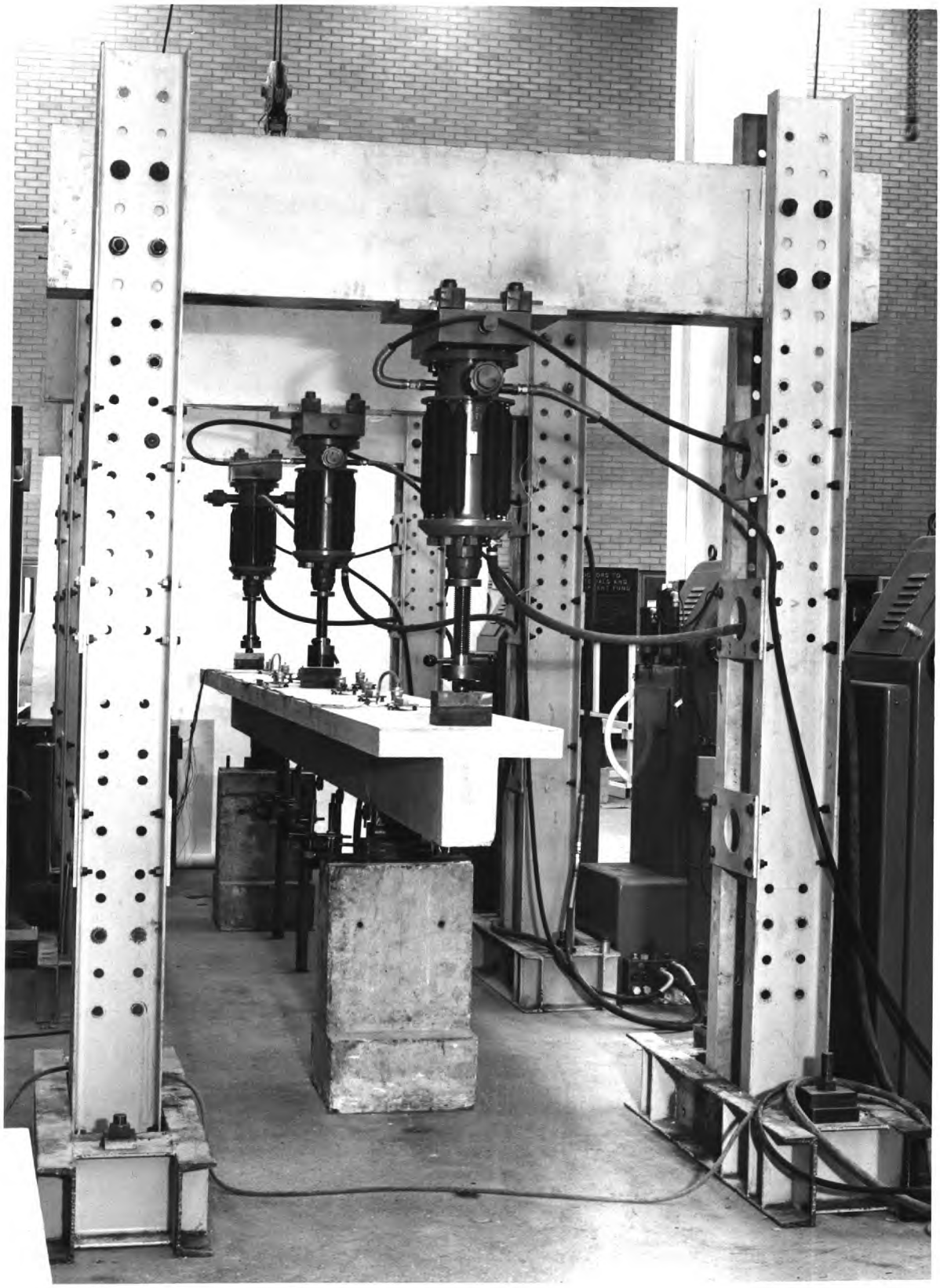


PLATE 1(b) TEST SET - UP : LOADING AND SUPPORT ARRANGEMENT

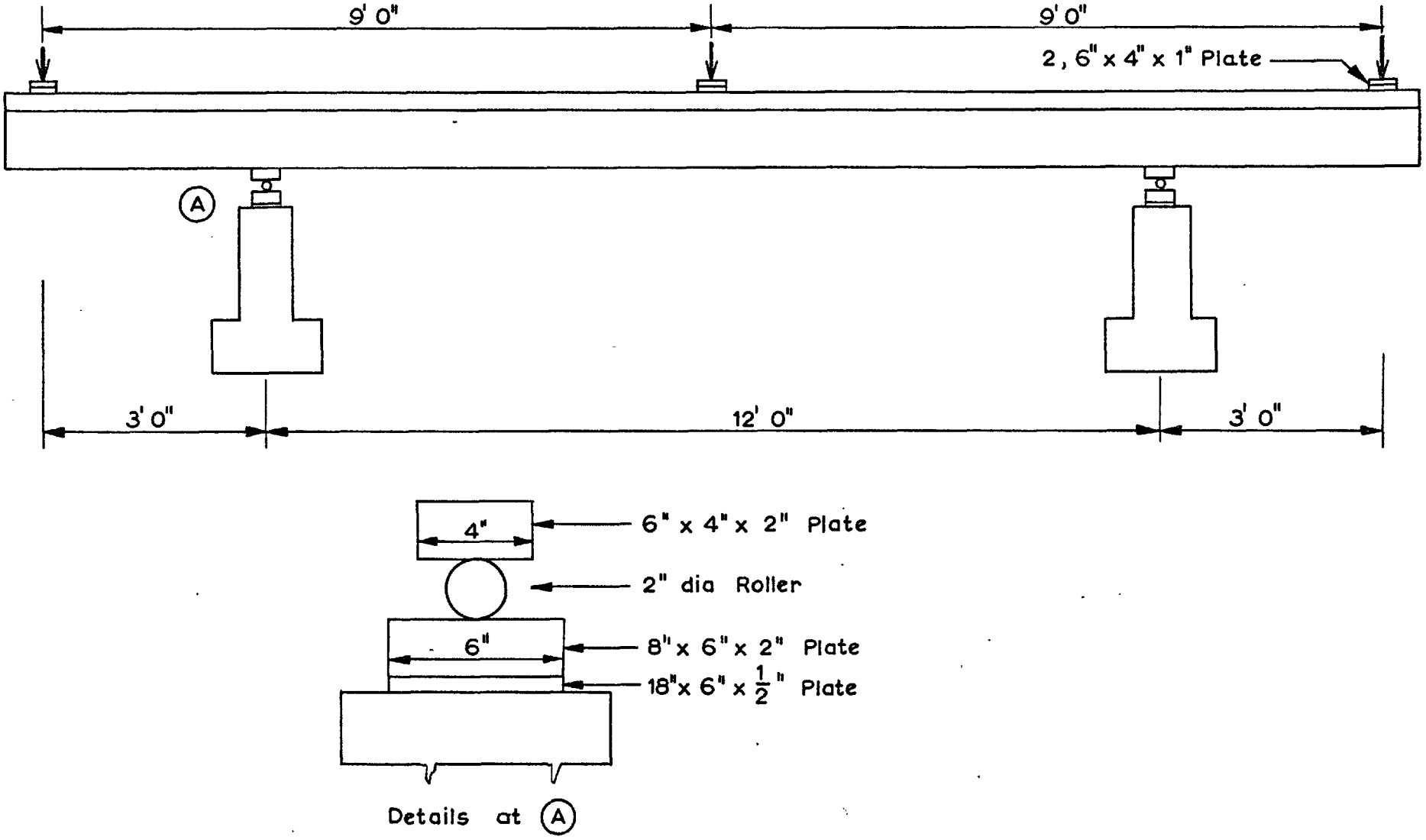
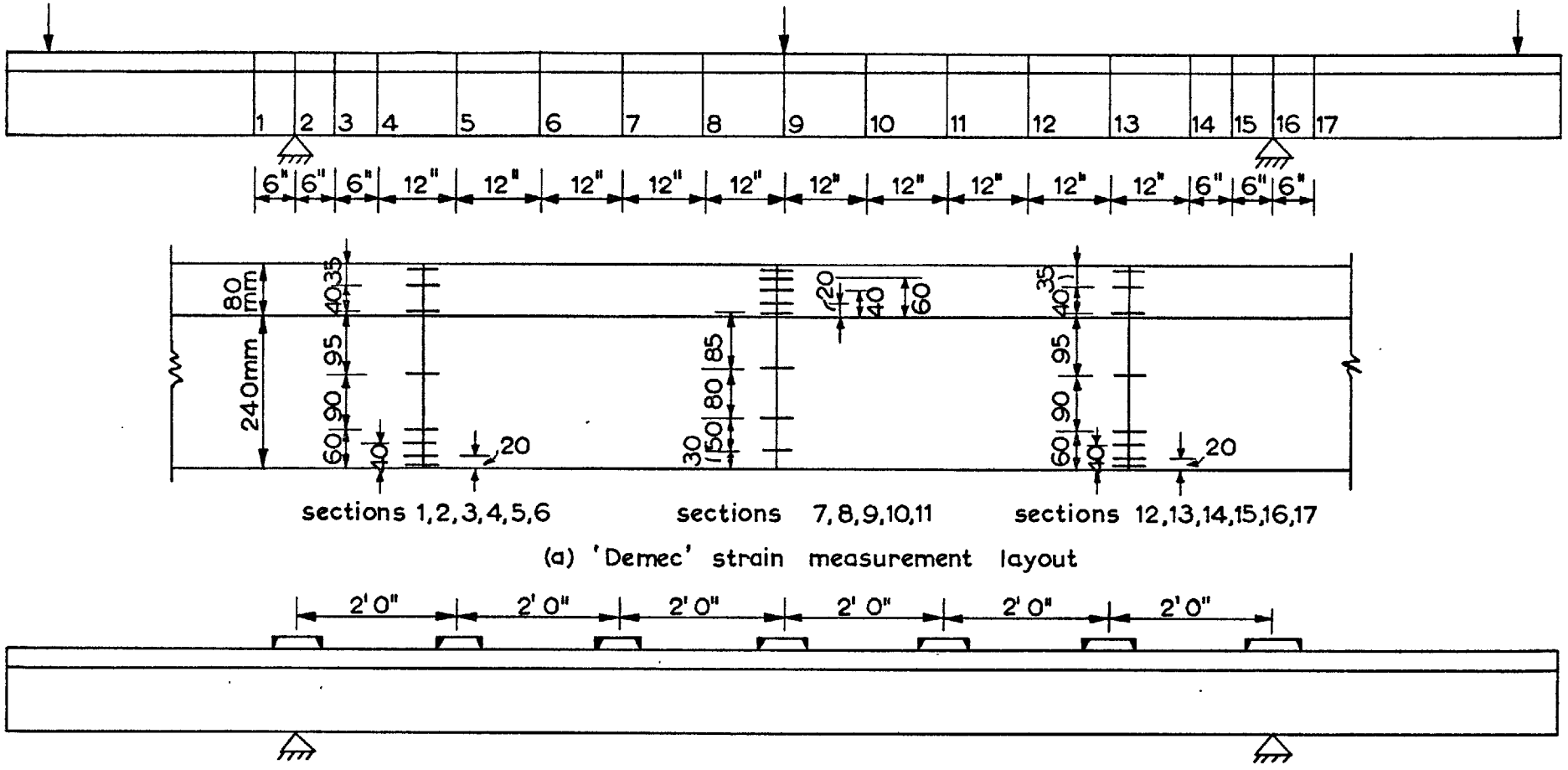


FIG. 5.10 GENERAL LAYOUT FOR BEAM TESTS



(a) 'Demec' strain measurement layout

(b) clinometer layout

FIG. 5.11 INSTRUMENTATION

that of other sections were taken only for alternate load stages. Electrical strain gauge, clinometer and deflection measurements were made for all load stages. On the average each load stage required about 30 minutes for taking all the readings. The applied loads were kept approximately constant while the instrument readings were taken.

5.4.4. Behaviour of Test Beams

The behaviour of all the test beams was essentially similar, since all the beams were under-reinforced and failed by concrete crushing after the tensile reinforcement had yielded by varying amounts.

Flexural cracks were first visible at between 20 and 30 percent of ultimate load. These cracks widened and extended toward the compression zone slowly as the load was increased. Towards the final stages of loading shear cracks were also formed but the provision of adequate shear reinforcement prevented the failure predominantly due to shear. After yield of the tensile reinforcement the cracks widened rapidly and the first visible signs of distress in compression zone occurred when the maximum concrete compressive strain was about 0.003. As the load was further increased the cracking and surface spalling in the concrete compression zone increased in severity and the final failure occurred when the maximum concrete strain was in excess of 0.0035. Plate 2 shows the crack pattern of all the beams tested in this programme.

5.5. MOMENT-CURVATURE RELATIONS

A knowledge of moment-curvature relations for reinforced concrete member sections is essential to study the EI values to be used in the deformation calculation. In this section expressions will be derived for the moment-curvature relations for the rectangular and T sections of beam members. Based on L_1 and L_2 limit concepts of Baker, typical design charts will be presented for the calculation of EI values to be used in the limit design of reinforced concrete frames. The experimental results of moment-curvature relations will be compared with the theoretical curves.

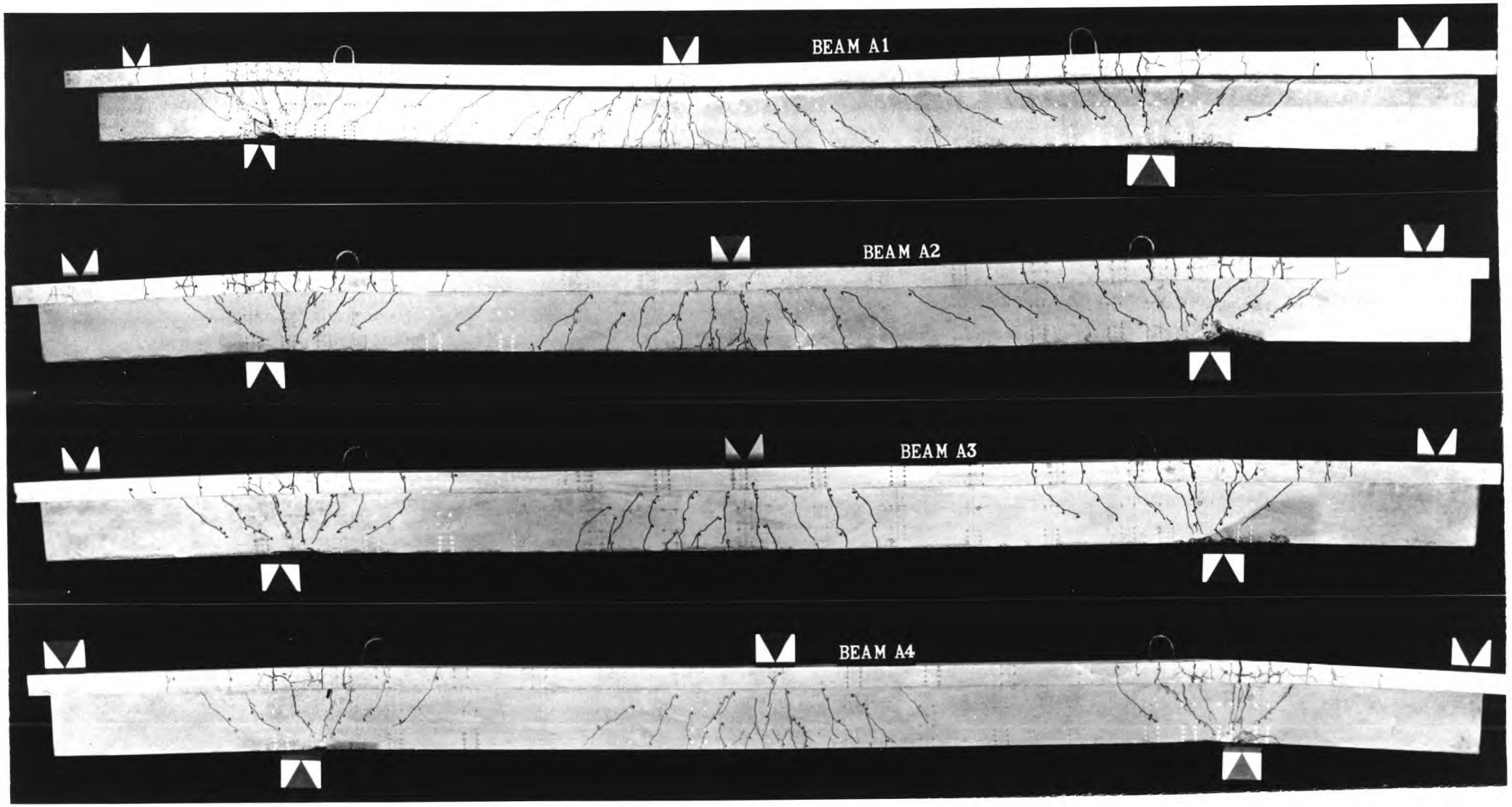


PLATE 2(a) CRACK PATTERN OF BEAMS AFTER FAILURE

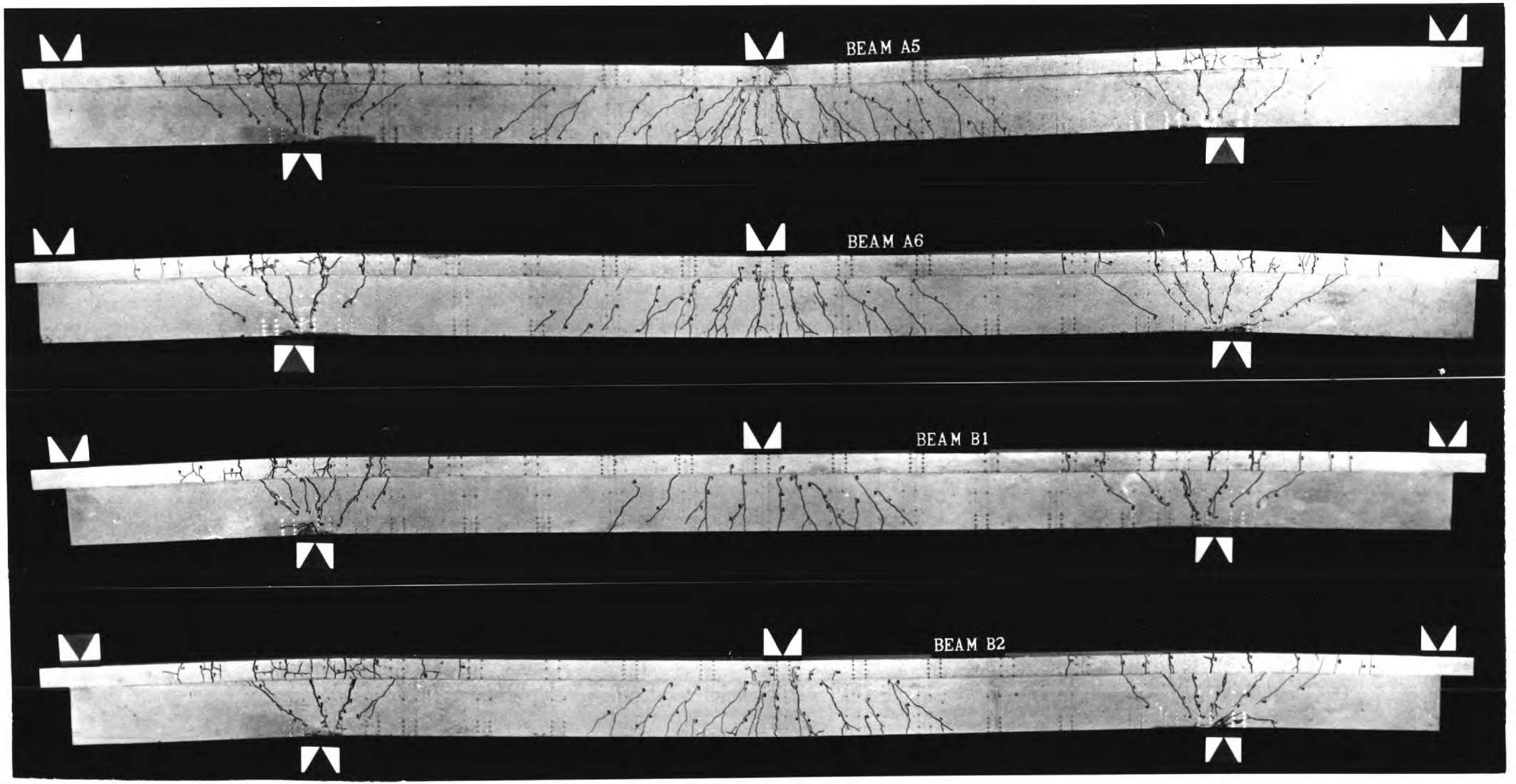


PLATE 2(b) CRACK PATTERN OF BEAMS AFTER FAILURE

5.5.1. Basic Assumptions

The following assumptions are made in the derivation of moment-curvature relations:

1. The stress-strain relations of the materials are known.
2. Concrete has no strength in tension.
3. The strain variation across the section is linear.
4. Flexural deformations only are considered. Deformations due to shear is neglected.
5. Strain reversal, unloading and time dependent effects are neglected.

5.5.2. Stress-Strain Relations

In the derivation of expressions the stress-strain relation for steel in tension and compression are assumed to be of the bilinear type, shown in Fig.5.12(a). For hot rolled deformed bars, used in this investigation, the actual stress-strain relations shown in Fig. 5.9 exhibit this characteristic upto a strain of 0.01.

The stress-strain relation for concrete in uniaxial compression and its application to the analysis of reinforced concrete sections have been studied by various research workers in the last two decades (65, 66, 10, 51, 67). A comprehensive review of these investigations has recently been reported by Sargin (67) who conducted an extensive investigation to suggest a unified stress-strain relation for concrete.

The following are the major factors that influence the stress-strain relation for concrete:

(a) concrete strength

(b) amount, spacing and grade of lateral reinforcement

(c) creep

(d) strain gradient

(e) size of specimen and type of loading

(f) relative areas of core and cover.

Based on his investigation Sargin proposed the following expression for stress-strain relation for concrete,

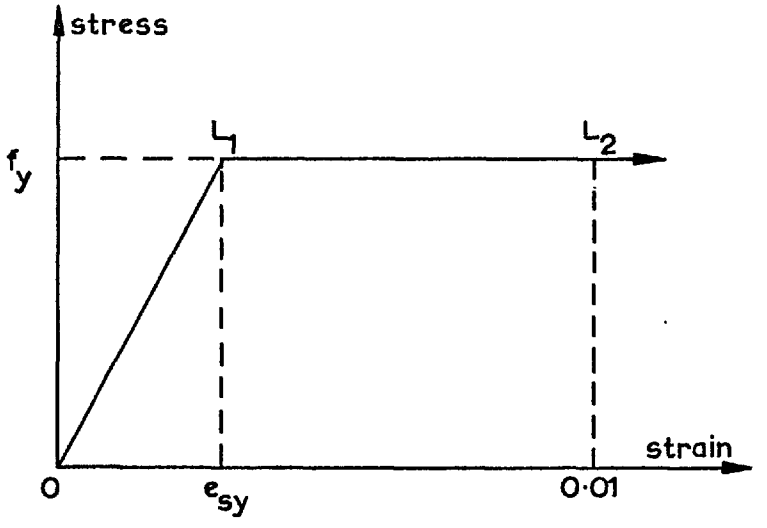


FIG. 5.12 (a) STRESS STRAIN CURVE FOR STEEL IN COMPRESSION AND TENSION

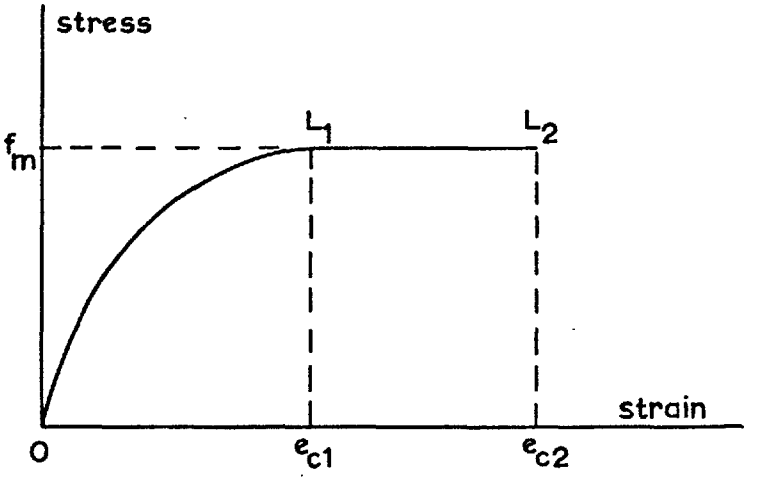


FIG. 5.12 (b) STRESS STRAIN CURVE FOR CONCRETE IN COMPRESSION

$$f_c = K_3 f_c \frac{AK_6 + (D-1) K_6^2}{1 + (A-2) K_6 + DK_6^2} \qquad (5.1)$$

where $K_6 = \frac{e_c}{e_{c1}}$ and $A = \frac{E_c e_{c1}}{K_3 \sigma_b}$

The main variables in equation (5.1) are f_c, K_3, E_c, e_{c1} and D. The effect of the major factors (a to e, listed above) that affect the stress strain relation was analysed by studying their influence on the five parameters of the proposed equation (5.1). Sargin derived the necessary expressions, based on his theoretical and experimental investigation, for the calculation of these parameters. It has been shown that the stress-strain relation proposed by earlier investigators are special cases of the equation (5.1).

The aims of the present investigation on T-beams were to study the moment-curvature relation of different critical sections along the beam and to propose a suitable design equation for the calculation of equivalent EI value to be used in connection with the calculation of end rotations in frame analysis. The limit states L_1 and L_2 defined by Baker (explained in Chapter 2) would be used for the calculation of equivalent EI values. With these objects in view the stress-strain relation for concrete is assumed to be of the parabolic-rectangular type (Fig.5.12(b)) defined by the limiting strains e_{c1} and e_{c2} and a maximum stress f_m which is considered a certain fraction of cylinder strength ($f_m = K_3 f_c$). This relation is generally in agreement with many of the proposals put forward in recent years by various authors and Codes of Practice (10, 51, 62, 63).

5.5.3. Derivation of Expressions

RECTANGULAR BEAM

Fig. 5.13 shows the stress, strain and force distribution across a typical rectangular section. The parabolic-rectangular stress-strain relation can be defined by the following equations,

$$f_x = f_m \left[2\left(\frac{e_x}{e_{c1}}\right) - \left(\frac{e_x}{e_{c1}}\right)^2\right] \quad , \quad (e_x \leq e_{c1}) \qquad (5.2a)$$

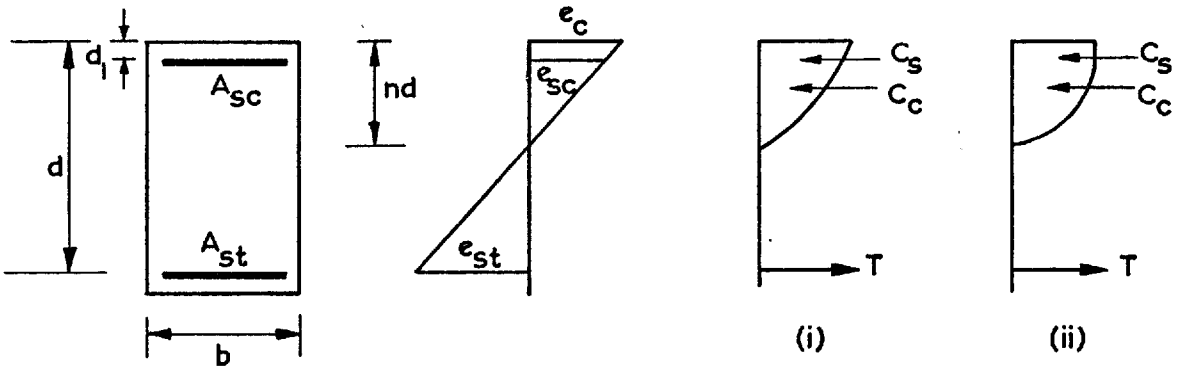


FIG. 5.13 RECTANGULAR BEAM : DISTRIBUTION OF STRAIN AND STRESS

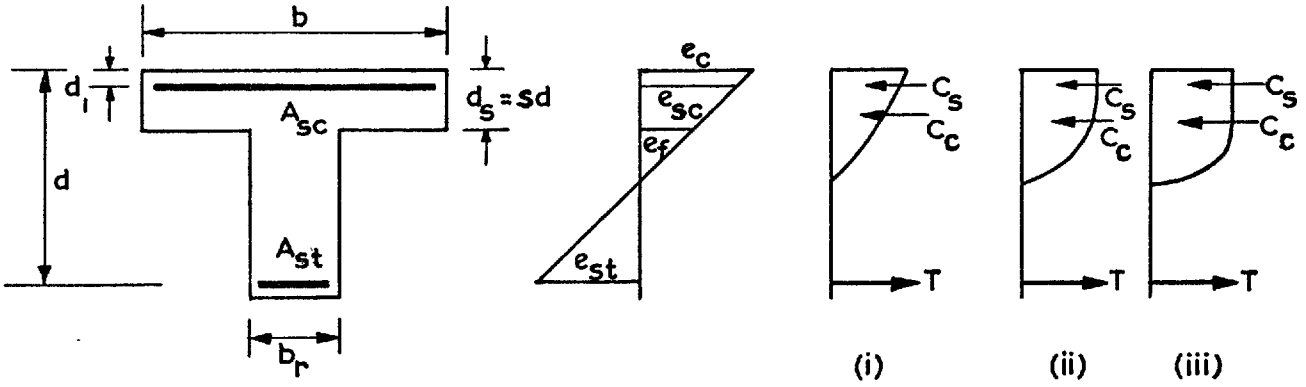


FIG. 5.14 T - BEAM : DISTRIBUTION OF STRAIN AND STRESS

$$f_x = f_m \qquad (e_{c1} \leq e_x \leq e_{c2}) \qquad (5.2b)$$

Case 1 $\qquad e_c \leq e_{c1} \quad (K_6 \leq 1)$

The stress, f_x, at any distance x above the neutral axis is given by,

$$f_x = f_m \left[\frac{2}{e_{c1}} \cdot \frac{e_c}{nd} \cdot x - \left(\frac{e_c}{nd}\right)^2 \cdot \frac{1}{e_{c1}^2} \cdot x^2 \right]$$

Compression C_c in concrete,

$$C_c = \int_o^{nd} f_x \, b \, d \, x$$

$$= f_m b \int_o^{nd} \left[\frac{2}{e_{c1}} \cdot \frac{e_c}{nd} \cdot x - \left(\frac{e_c}{nd}\right)^2 \cdot \frac{1}{e_{c1}^2} \cdot x^2 \right] dx$$

$$= f_m \, b \, n \, d \left[\frac{e_c}{e_{c1}} - \frac{1}{3} \left(\frac{e_c}{e_{c1}}\right)^2 \right]$$

$$= f_m \, b \, n \, d \; K_6 \left(1 - \frac{1}{3} K_6\right)$$

hence $C_c = K_1 f_m \, b \, n \, d$

where $K_1 = K_6 \left(1 - \frac{1}{3} K_6\right)$ $\qquad (5.3)$

Taking moments about the top edge,

$$C_c \cdot K_2 \cdot nd = \int_o^{nd} f_x \, b \, (nd - x) \, dx$$

$$= f_m b \int_o^{nd} \left[\frac{2}{e_{c1}} \cdot \frac{e_c}{nd} \cdot x - \left(\frac{e_c}{nd}\right)^2 \cdot \left(\frac{1}{e_{c1}}\right)^2 x^2 \right] (nd - x) \, dx$$

$$= f_m\, b\, n\, d^2\, K_6\, (\tfrac{1}{3} - \tfrac{1}{12} K_6) \qquad (5.4)$$

Substituting for C_c from equation (5.3) into equation (5.4) and simplifying,

$$K_2 = \frac{4 - K_6}{12 - 4K_6} \qquad (5.5)$$

Case 2. $\qquad e_{c1} \leq e_c \leq e_{c2} \quad (1 \leq K_6 \leq \frac{e_{c2}}{e_{c1}})$

Compression C_c in concrete,

$$C_c = \tfrac{2}{3} f_m\, b\, \frac{nd}{e_c} \cdot e_{c1} + f_m\, b\, (nd - \frac{nd}{e_c} \cdot e_{c1})$$

$$= f_m\, b\, n\, d\, (1 - \frac{1}{3 K_6})$$

Hence, $K_1 = 1 - \frac{1}{3 K_6}$ (5.6a)

Taking moments about the top edge,

$$C_c \cdot K_2 nd = \tfrac{2}{3} f_m\, b\, \frac{nd}{e_c} \cdot e_{c1}\, (nd - \tfrac{5}{8} \frac{nd}{e_c} \cdot e_{c1}) + f_m \cdot \frac{b}{2} \cdot (nd - \frac{nd}{e_c} \cdot e_{c1})^2 \qquad (5.6b)$$

Substituting equation (5.6a) into equation (5.6b) and simplifying,

$$K_2 = \frac{\frac{1}{2} - \frac{1}{3}(\frac{1}{K_6}) + \frac{1}{12}(\frac{1}{K_6})^2}{K_1} \qquad (5.7)$$

The stresses in compression and tension steel are given by,

$$f_{sc} = \frac{e_c\, (n - \frac{d_1}{d})}{n} E_s \qquad (\leq f_y) \qquad (5.8)$$

$$f_{st} = \frac{e_c (1-n)}{n} E_s \qquad (\leq f_y) \qquad (5.9)$$

The force equilibrium of the section requires,

$$K_1 f_m b n d + A_{sc} f_{sc} = A_{st} f_{st} \qquad (5.10)$$

$$\text{or} \quad K_1 n + q_{sc} \frac{f_{sc}}{f_y} = q_{st} \cdot \frac{f_{st}}{f_y} \qquad (5.11)$$

$$\text{where} \quad q_{sc} = \frac{A_{sc}}{bd} \frac{f_y}{f_m}$$

$$q_{st} = \frac{A_{st}}{bd} \frac{f_y}{f_m} \qquad (5.12)$$

Considering the moment equilibrium of the section,

$$M_r = K_1 f_m b n d (d - K_2 nd) + A_{sc} f_{sc} (d - d_1) \qquad (5.13)$$

$$\text{or} \quad \frac{M_r}{f_m bd^2} = K_1 n (1 - K_2 n) + q_{sc} \frac{f_{sc}}{f_y} (1 - \frac{d_1}{d}) \qquad (5.14)$$

T-BEAM

The force and moment equilibrium of T-section, shown in Fig.5.14, can be derived using the equations got for the analysis of rectangular sections. The results are summarized in the following:

Case 1(a). $K_6 \leq 1.0$

$$K_1 = K_6 (1 - \tfrac{1}{3} K_6)$$

$$K_1^1 = K_8 (1 - \tfrac{1}{3} K_8)$$

$$K_2 = \frac{4 - K_6}{12 - 4K_6}$$

$$K_2^1 = \frac{4 - K_8}{12 - 4K_8} \qquad (5.15)$$

Case 1(b) $\qquad 1.0 < K_6 \leq 1.75 \; ; \; K_8 \leq 1.0$

$$K_1 = 1 - \frac{1}{3K_6}$$

$$K_1^1 = K_8 \left(1 - \tfrac{1}{3} K_8\right)$$

$$K_2 = \frac{\frac{1}{2} - \frac{1}{3}\left(\frac{1}{K_6}\right) + \frac{1}{12}\left(\frac{1}{K_6}\right)^2}{K_1}$$

$$K_2^1 = \frac{4 - K_8}{12 - 4K_8} \tag{5.16}$$

The force equilibrium for case 1(a) and case 1(b) is given by,

$$K_1 n - K_1^1 \left(1 - \frac{b_r}{b}\right)(n - s) + q_{sc} \frac{f_{sc}}{f_y} = q_{st} \frac{f_{st}}{f_y} \tag{5.17}$$

The moment equilibrium for case 1(a) and case 1(b) is given by,

$$\frac{M_r}{f_m b d^2} = K_1 n \left(1 - K_2 n\right) - K_1^1 (n - s)\left(1 - \frac{b_r}{b}\right) x$$

$$\left[\left(1 - K_2^1 n\right) - s\left(1 - K_2^1\right)\right] + q_{sc} \frac{f_{sc}}{f_y} \left(1 - \frac{d_1}{d}\right) \tag{5.18}$$

Case 2 $\qquad 1.0 < K_6 \leq 1.75 \; ; \; 1.0 < K_8 \leq 1.75$

$$K_1 = 1 - \frac{1}{3K_6}$$

$$K_2 = \frac{\frac{1}{2} - \frac{1}{3}\left(\frac{1}{K_6}\right) + \frac{1}{12}\left(\frac{1}{K_6}\right)^2}{K_1} \tag{5.19}$$

The force equilibrium is given by,

$$K_1 n \cdot \frac{b_r}{b} + \left(1 - \frac{b_r}{b}\right) s + q_{sc} \frac{f_{sc}}{f_y} = q_{st} \frac{f_{st}}{f_y} \tag{5.20}$$

The moment equilibrium is given by,

$$\frac{M_r}{f_m b d^2} = K_1 \frac{b_r}{b} n (1 - K_2 n) + s (1 - \frac{b_r}{b})(1 - \frac{s}{2}) + q_{sc} \frac{f_{sc}}{f_y} (1 - \frac{d_1}{d}) \quad (5.21)$$

If the neutral axis falls within the flange the force and moment equilibrium of the section are expressed by equations (5.11) to (5.14).

Curvature and EI value

The curvature at any strain level is given by,

$$\phi = \frac{1}{R} = \frac{e_c}{nd} = \frac{M}{EI} \quad (5.22)$$

$$\text{or} \quad EI = \frac{Mnd}{e_c} \quad (5.23)$$

As discussed in Chapter 2 the flexural rigidity, EI, for a member is calculated corresponding to the moment, M_{ry} at limit L_1. Thus,

$$EI = \frac{M_{ry} n_1 d}{e_{c1}} = \frac{M_{ry}(1 - n_1)d}{e_{s1}} \quad (5.24)$$

5.5.4. Computer Program for Moment-Curvature Calculations

An iterative process is employed to calculate the moment curvature relation at any strain level e_c. The basic steps of the method are described below:

1. Starting from a specified initial strain, increase the concrete strain e_c at some prescribed intervals upto a maximum value of e_{c2}.
2. At any strain level e_c find by successive iteration a suitable value of n that satisfies the force equilibrium within a specified tolerance Δ , i.e.,
$$|C - T| \leq \Delta$$
3. Using the values of e_c and n solve the moment equilibrium equation for M and calculate the corresponding curvature.

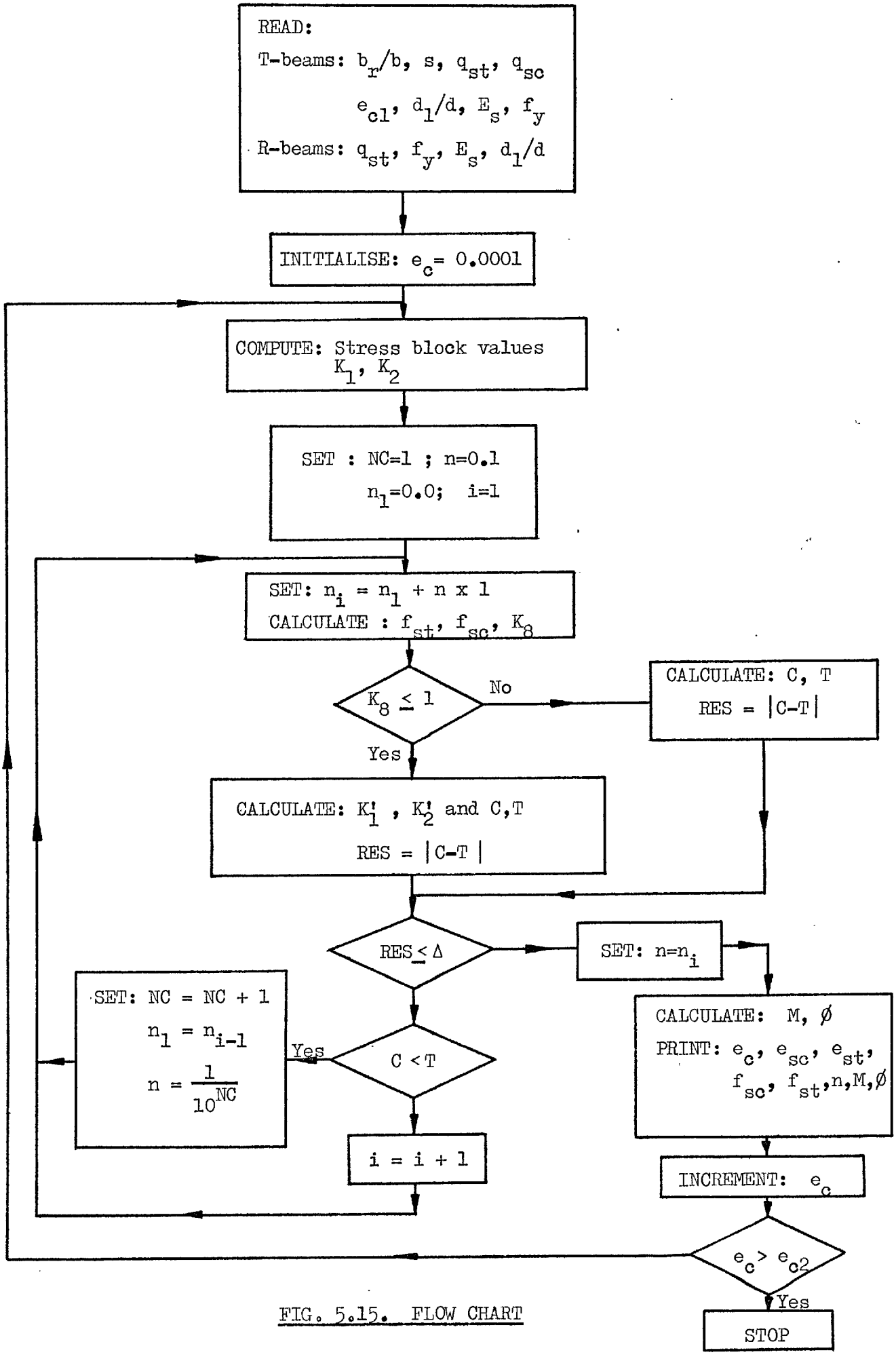


FIG. 5.15. FLOW CHART

COMPUTER PROGRAM FOR MOMENT-CURVATURE CALCULATIONS

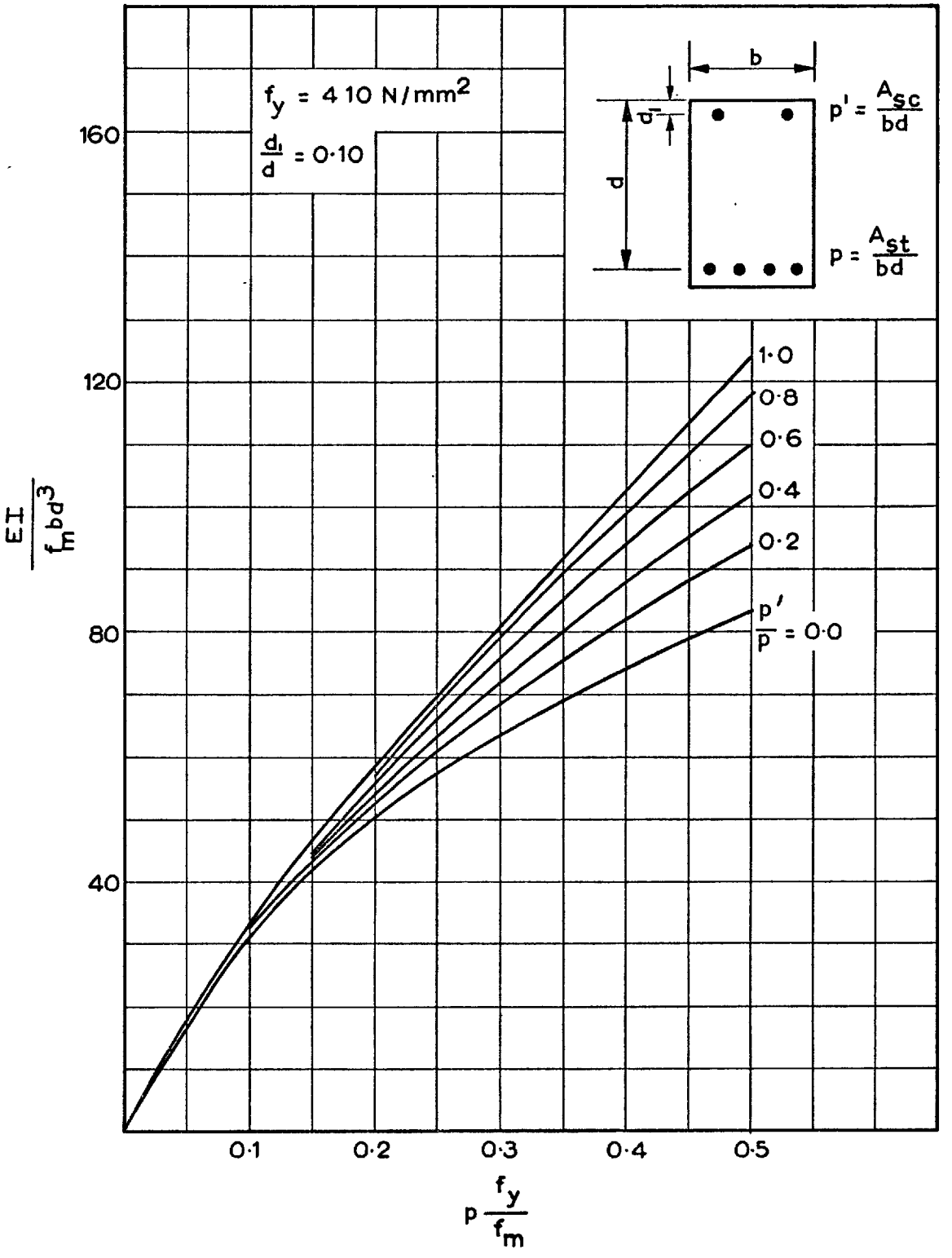


FIG. 5.16 DESIGN CHART FOR VALUES OF EI
(RECTANGULAR SECTIONS)

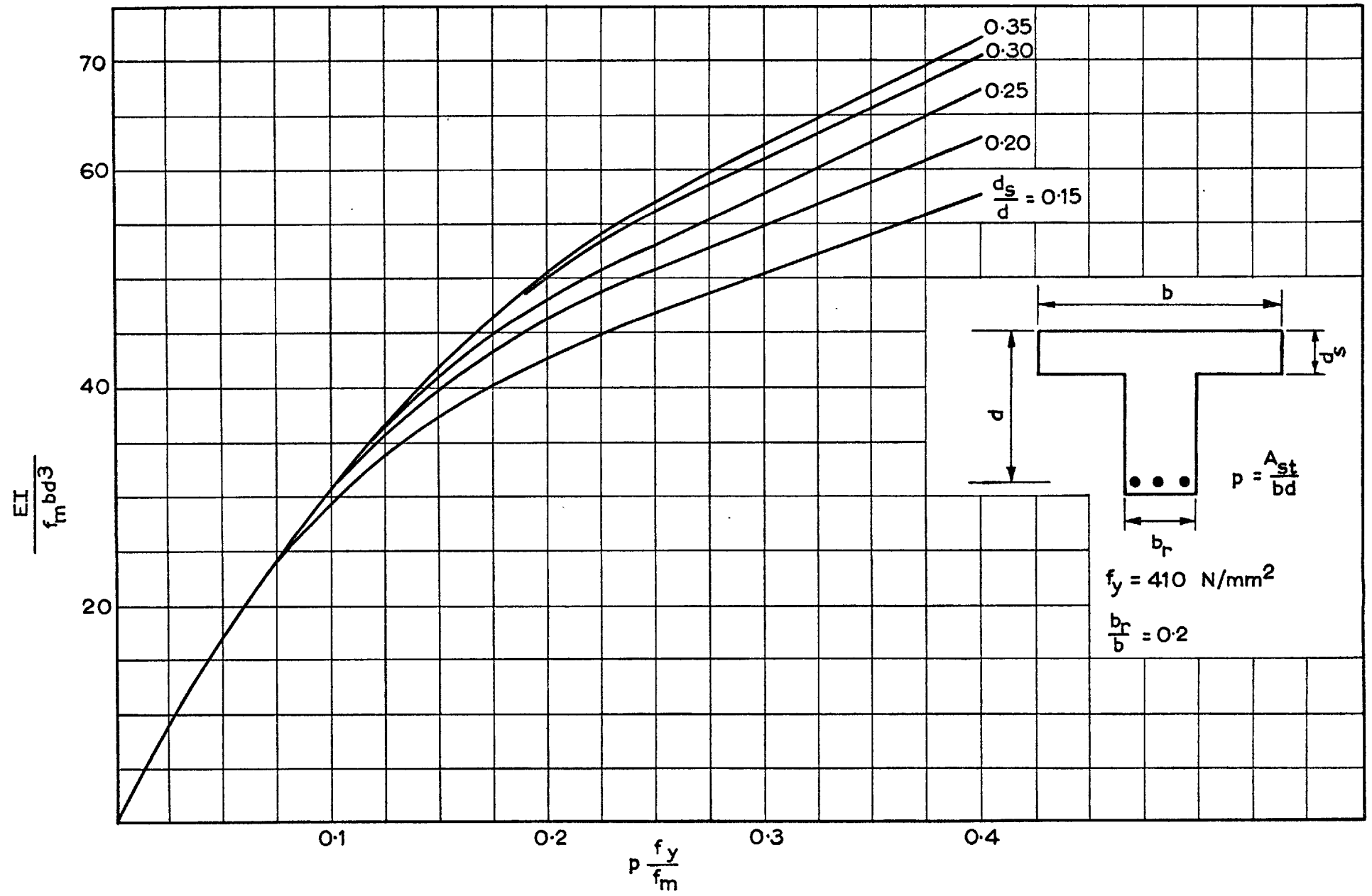


FIG. 5.17 DESIGN CHART FOR VALUES OF EI. (T - SECTIONS)

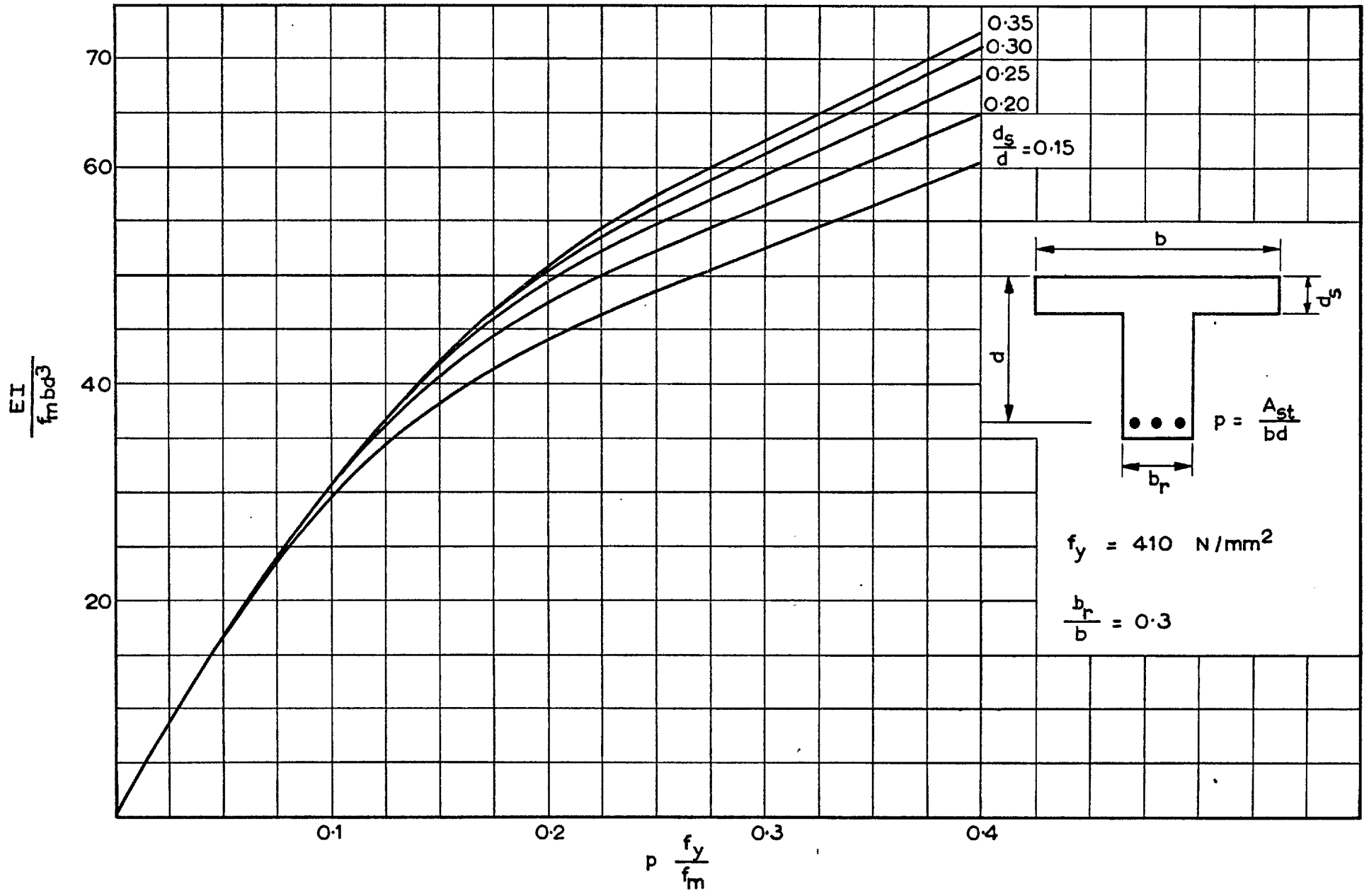


FIG. 5.18 DESIGN CHART FOR VALUES OF EI (T - SECTIONS)

Fig. 5.15 shows the flow chart of the computer program developed for moment-curvature calculations.

5.5.5. Design Charts for Values of EI

The values of EI for rectangular and T-beam sections can be calculated using the equation (5.24). The computer program described in the previous section has been used to prepare a set of design charts. Typical charts for rectangular and T sections are given in Figs. 5.16 to 5.18, for steel of yield strength of 410 N/mm^2. Knowing the values of percentage of reinforcement and the material strengths, f_c and f_y, these charts can be used to calculate the value of EI at limit L_1, which would be required for frame analysis and for the computation of equivalent EI_e to be discussed later.

5.5.6. Comparison of Experimental and Theoretical Moment-Curvature Relations

The moment-curvature relations for various sections of test specimens were calculated using the strain readings recorded at different load stages. Figs.5.19 to 5.26 show the experimental results of moment-curvature relations for sections in the positive and negative moment regions of all the beams and the theoretical curves for the support sections and mid-span section in the corresponding region.

The theoretical moment-curvature relation was calculated using the theory and computer program described in the earlier sections. The ordinate f_m of the stress-strain curve for concrete was assumed as f_c. This followed the recommendation by Baker and Amarakone (10) for stress-strain curve for concrete which was found satisfactory for the analysis of beam sections when the coefficient of depth of neutral axis was less than 0.5.

It has generally been found that the moment-curvature relation for critical sections follows closely with the theoretical curve. The moment-curvature relation for the sections away from the critical section deviate from the theoretical curve and the difference is more marked as the distance of the section is increased from the critical section of that region. The difference between theoretical and experimental curves may briefly be explained in the following way. In the

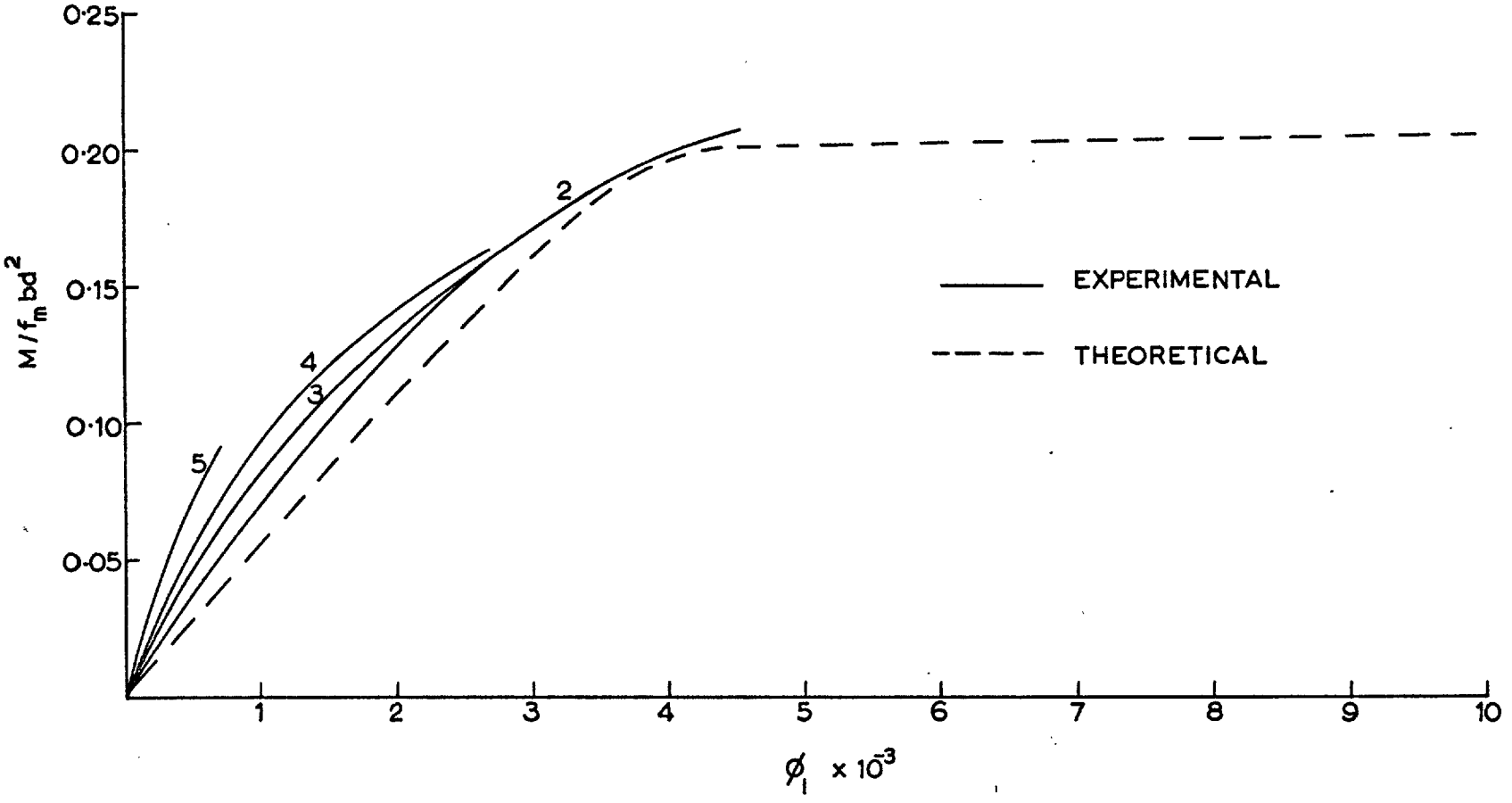


FIG. 5.19 (a) MOMENT - CURVATURE DIAGRAMS. BEAM A1. - SECTIONS 2, 3, 4, 5

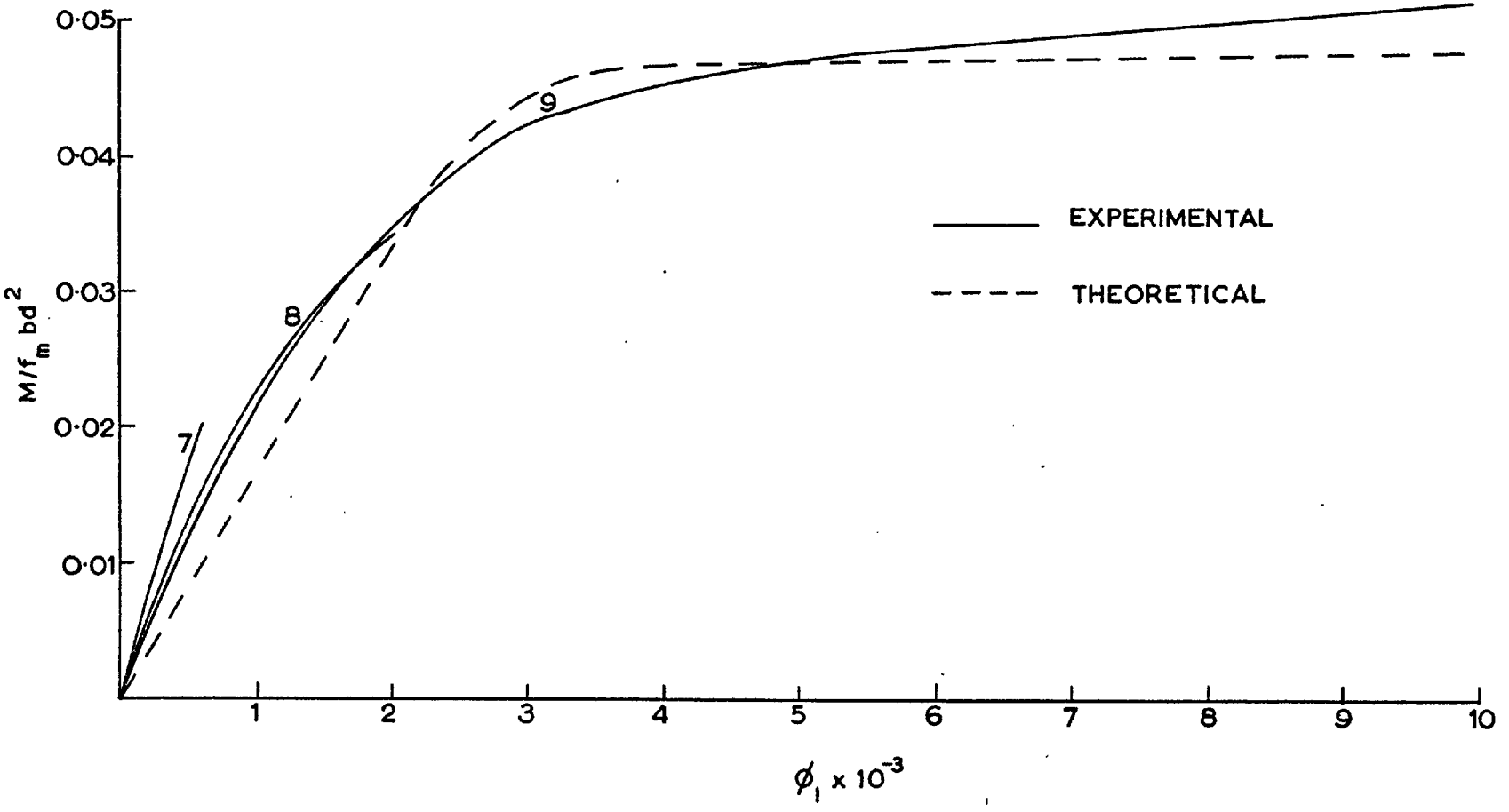


FIG. 5.19 (b) MOMENT - CURVATURE DIAGRAMS. BEAM A1 - SECTIONS 7, 8, 9

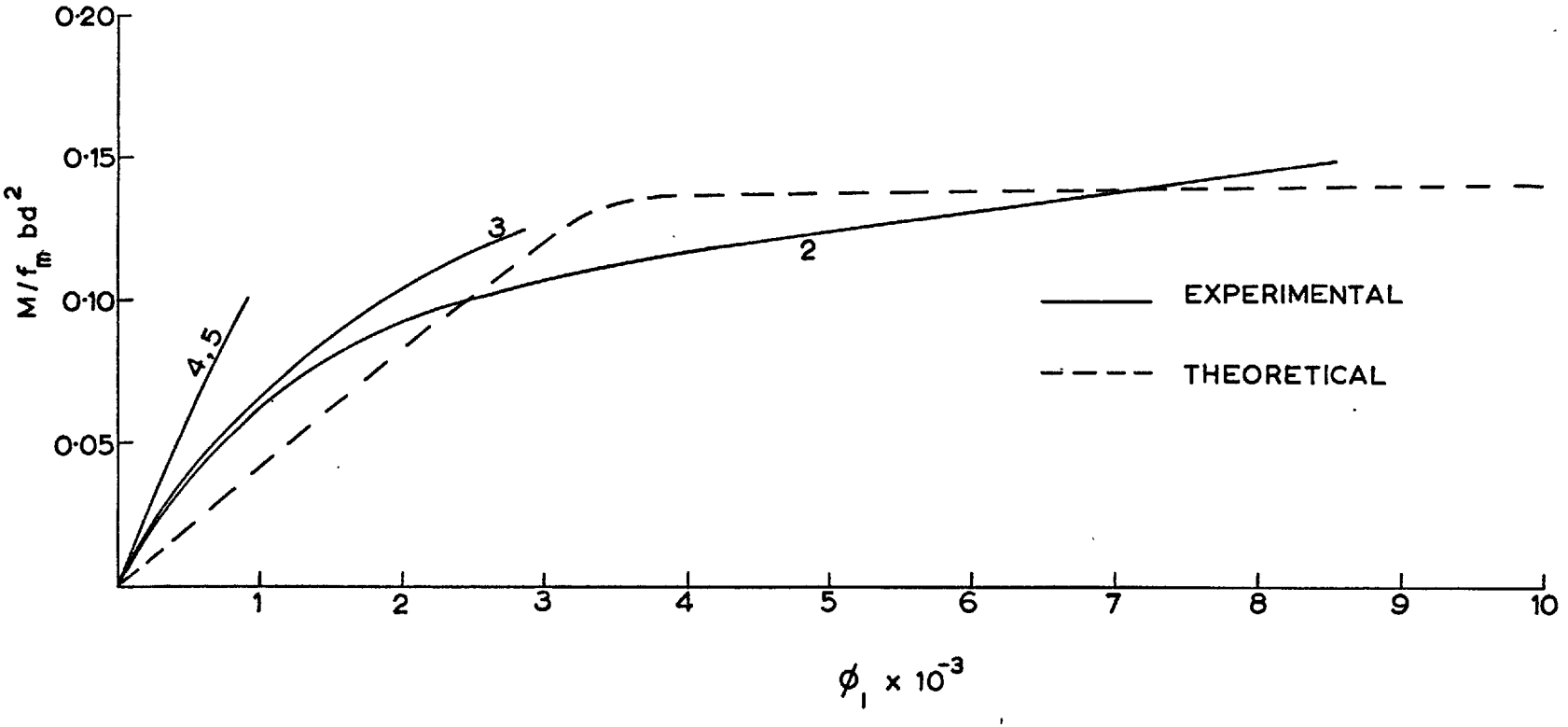


FIG. 5.20 (a) MOMENT - CURVATURE DIAGRAMS. BEAM A2 - SECTIONS 2,3,4,5

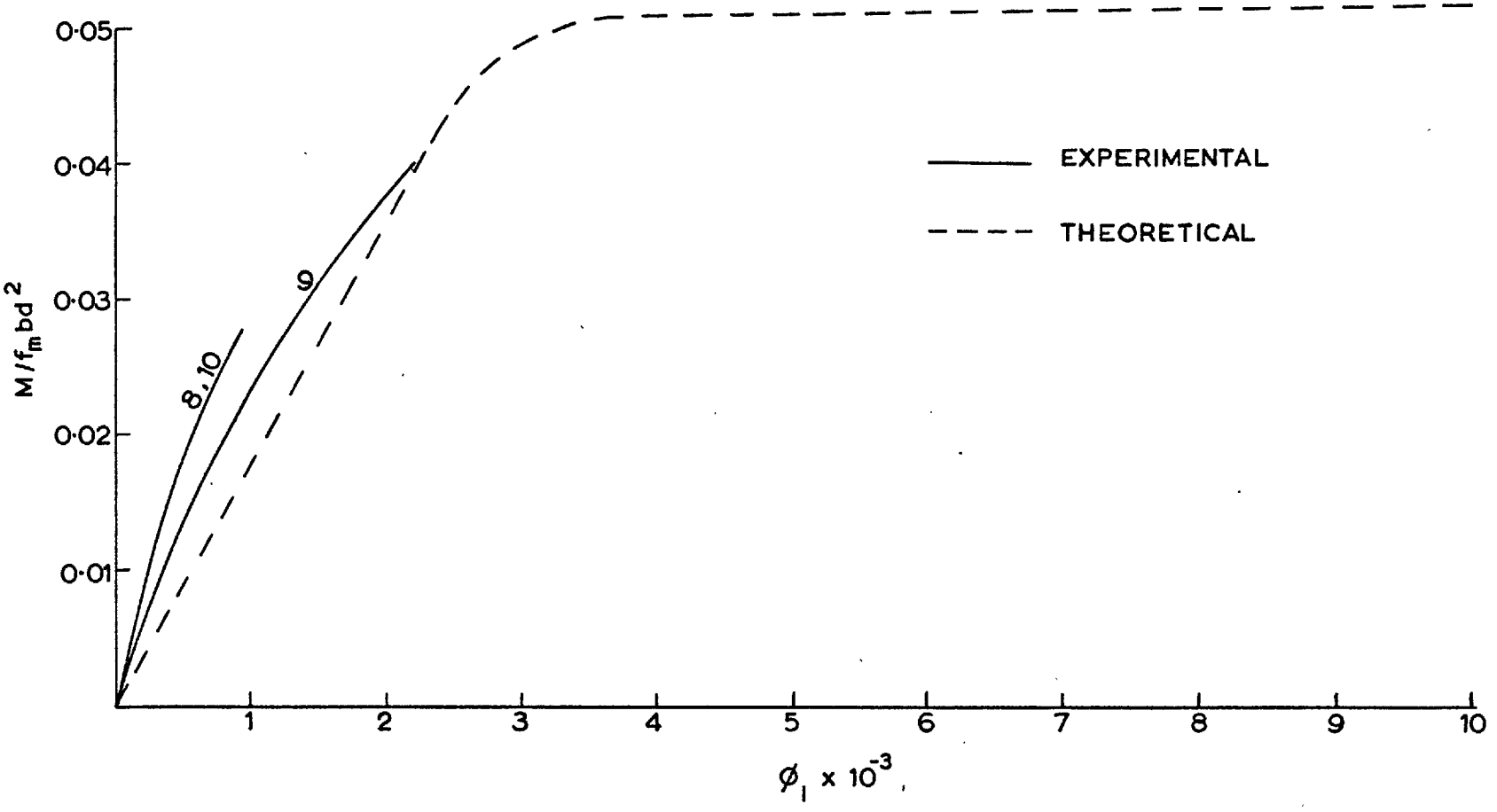


FIG. 5.20 (b) MOMENT - CURVATURE DIAGRAMS. BEAM A2 - SECTIONS 8, 9, 10

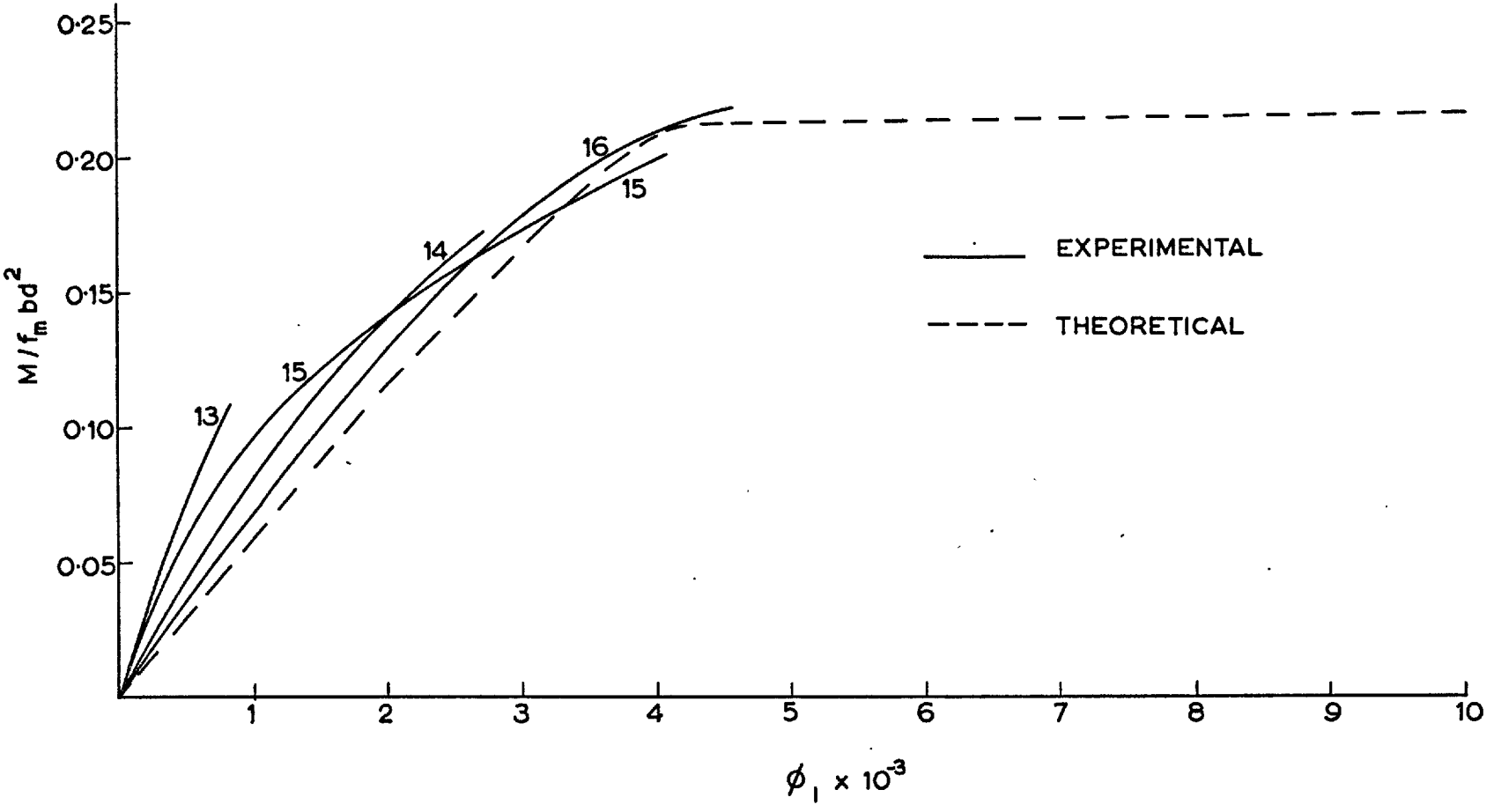


FIG. 5.20 (c) MOMENT - CURVATURE DIAGRAMS. BEAM A2 - SECTIONS 13, 14, 15, 16

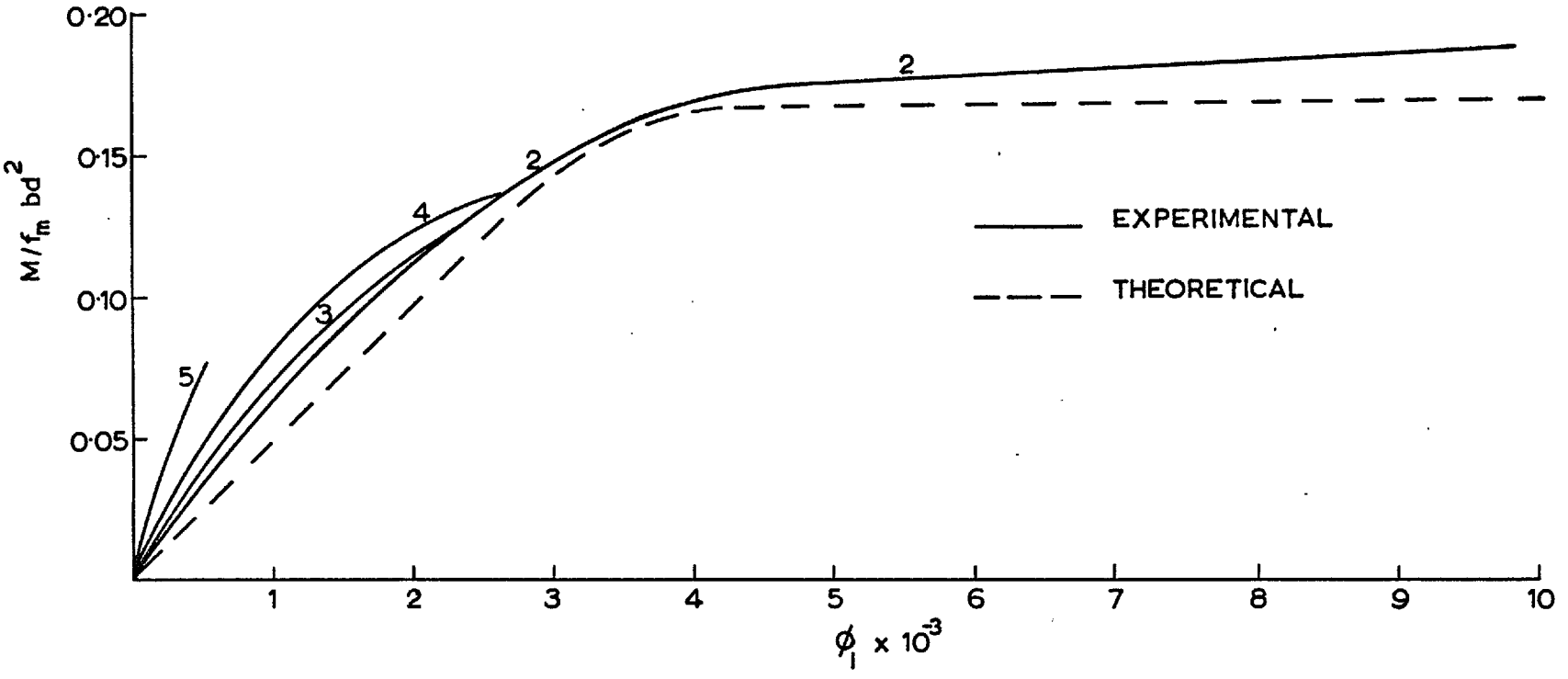


FIG. 5.21 (a) MOMENT - CURVATURE DIAGRAMS. BEAM A3 - SECTIONS 2, 3, 4, 5

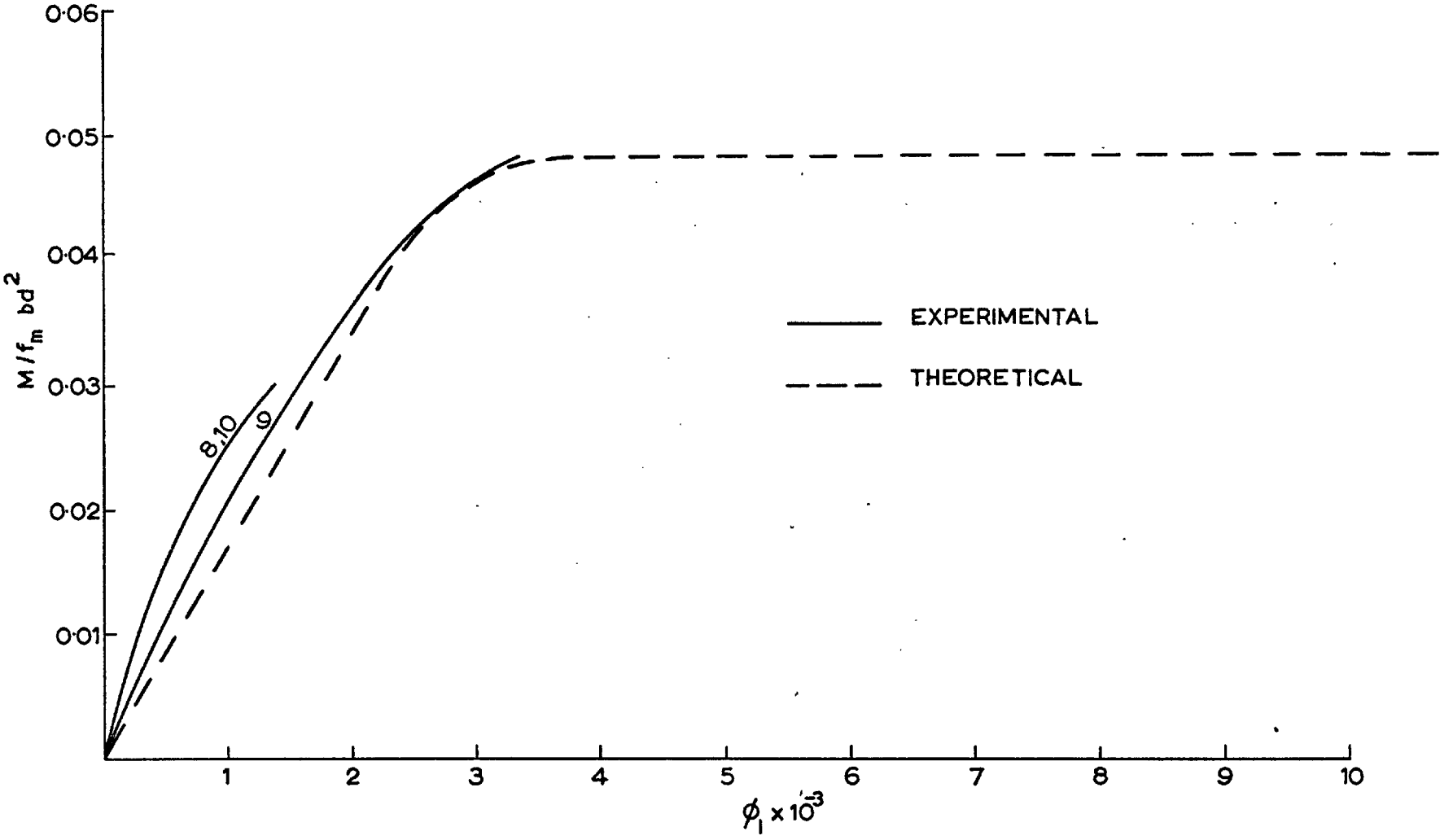


FIG. 5.21 (b) MOMENT - CURVATURE DIAGRAMS. BEAM A3 - SECTIONS 8, 9, 10

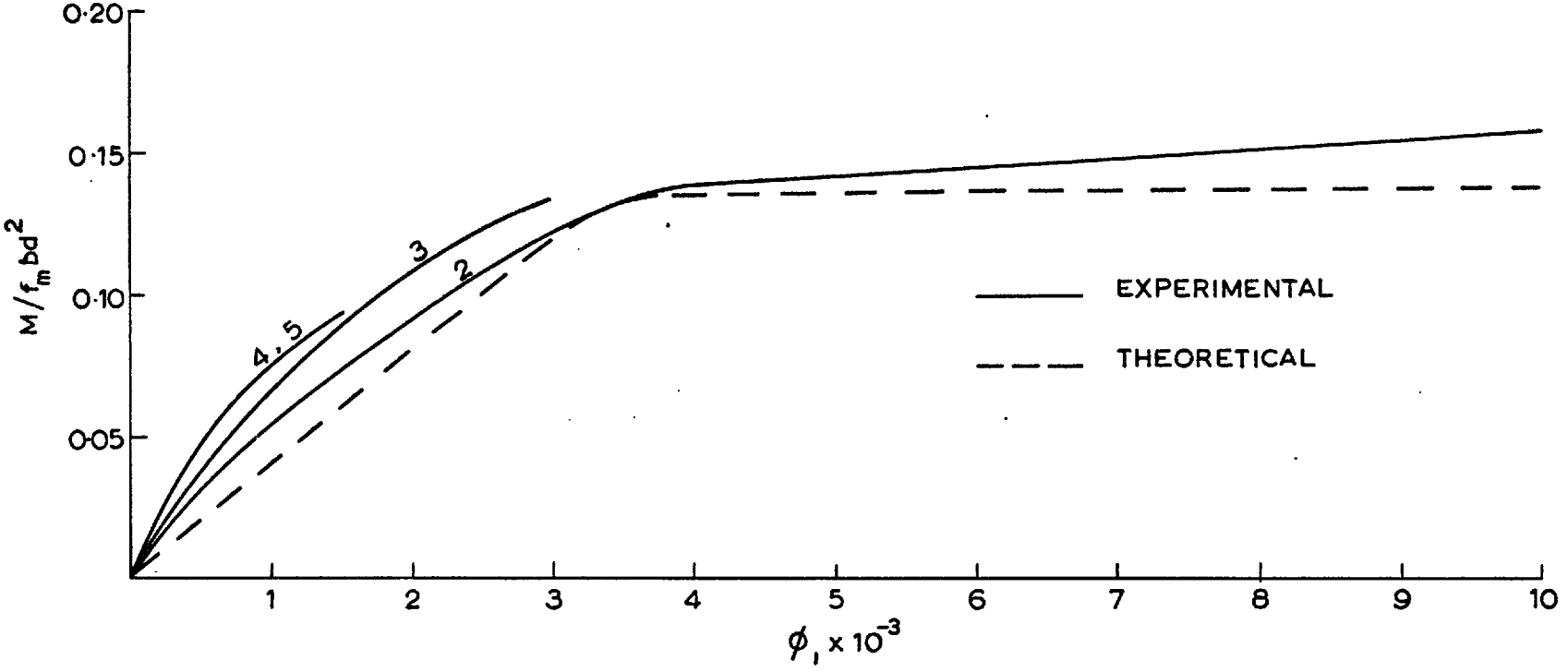


FIG. 5.22 (a) MOMENT - CURVATURE DIAGRAMS. BEAM A4 - SECTIONS 2, 3, 4, 5

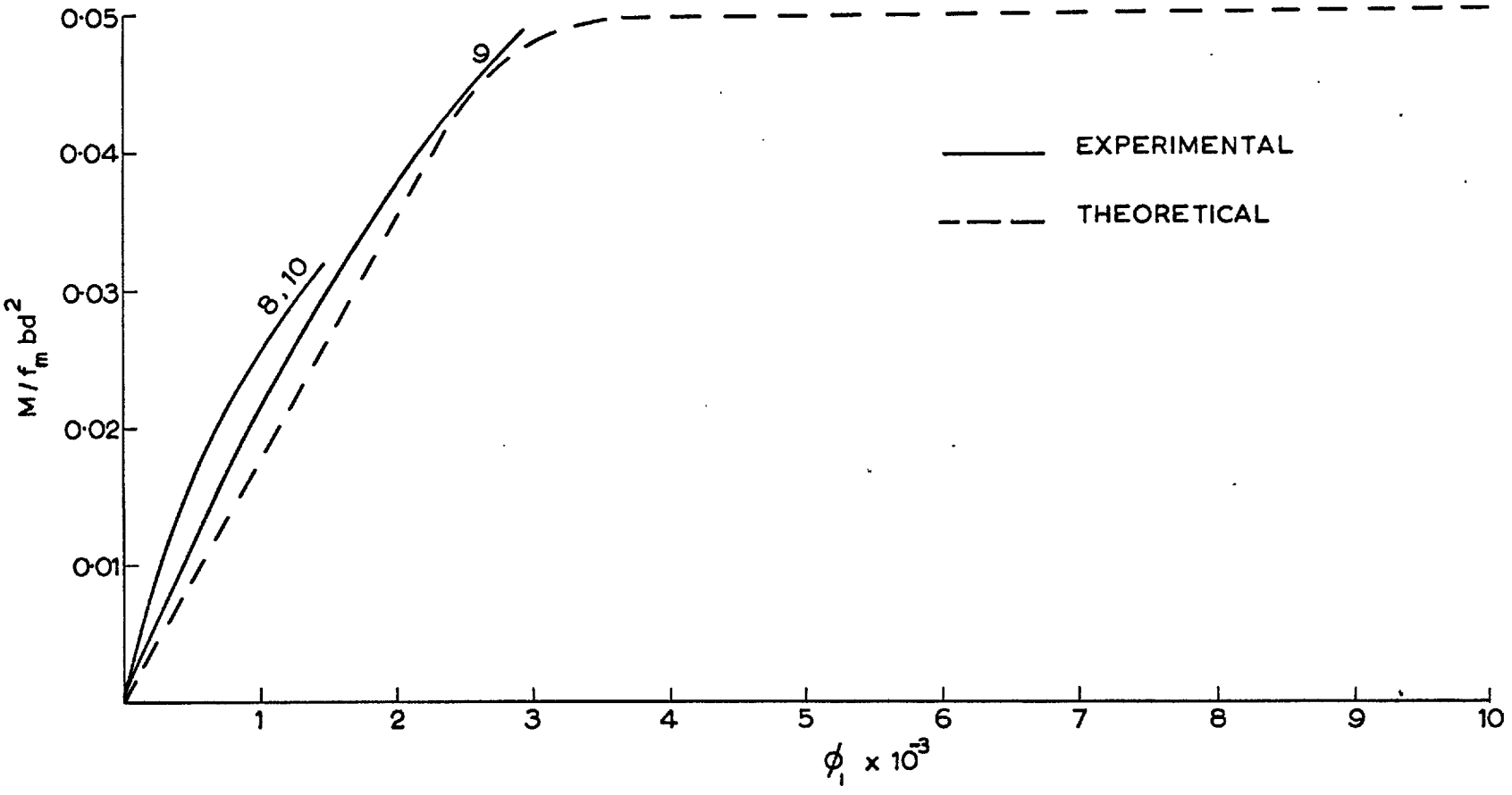


FIG. 5.22 (b) MOMENT - CURVATURE DIAGRAMS. BEAM A4 - SECTIONS 8,9,10

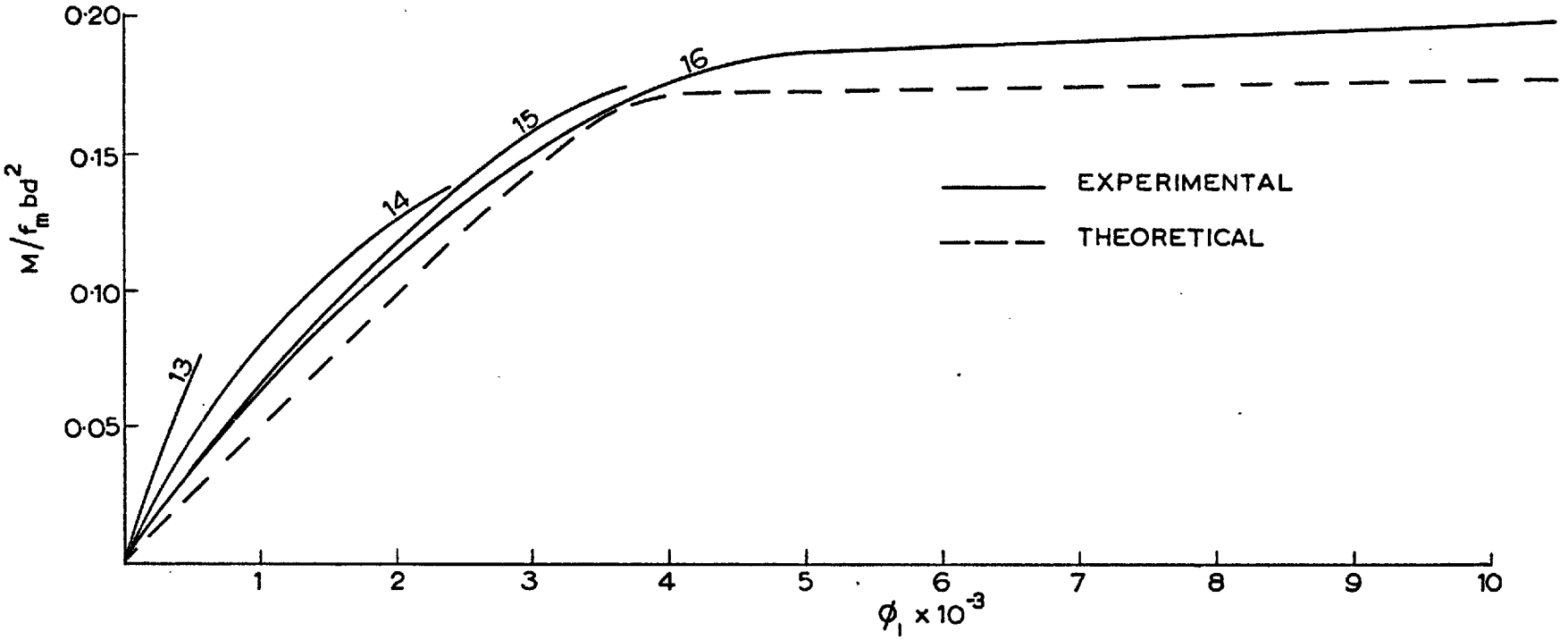


FIG. 5.22 (c) MOMENT - CURVATURE DIAGRAMS. BEAM A4 - SECTIONS 13, 14, 15, 16

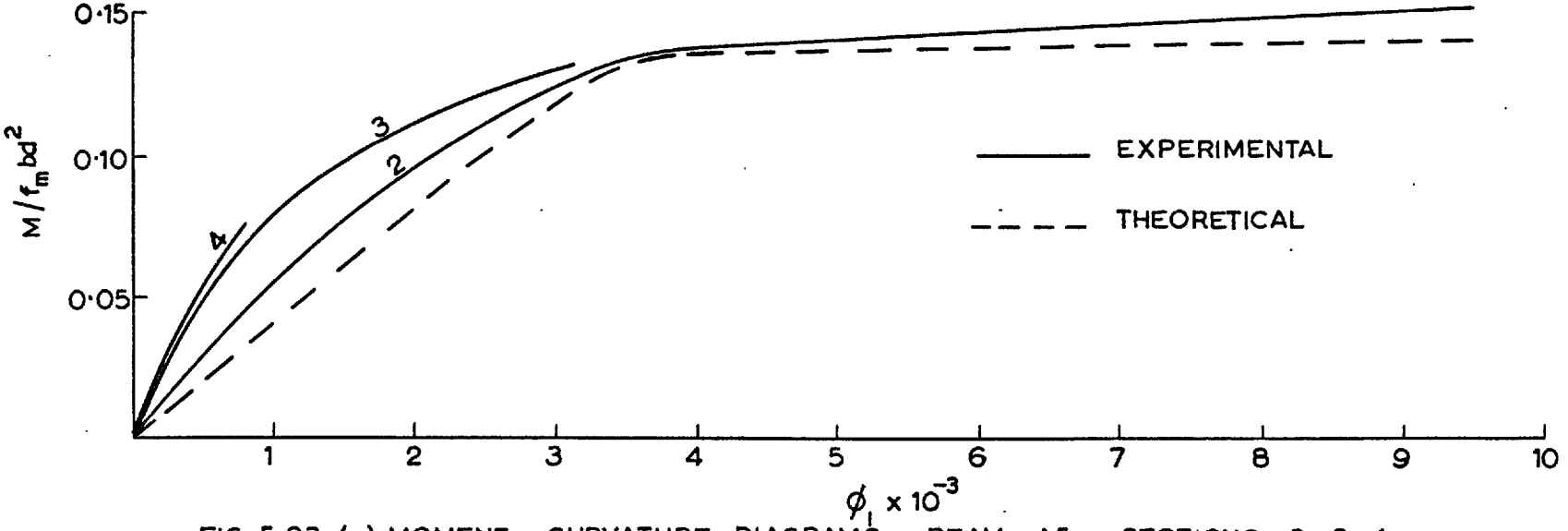


FIG. 5.23 (a) MOMENT - CURVATURE DIAGRAMS. BEAM A5 - SECTIONS 2, 3, 4

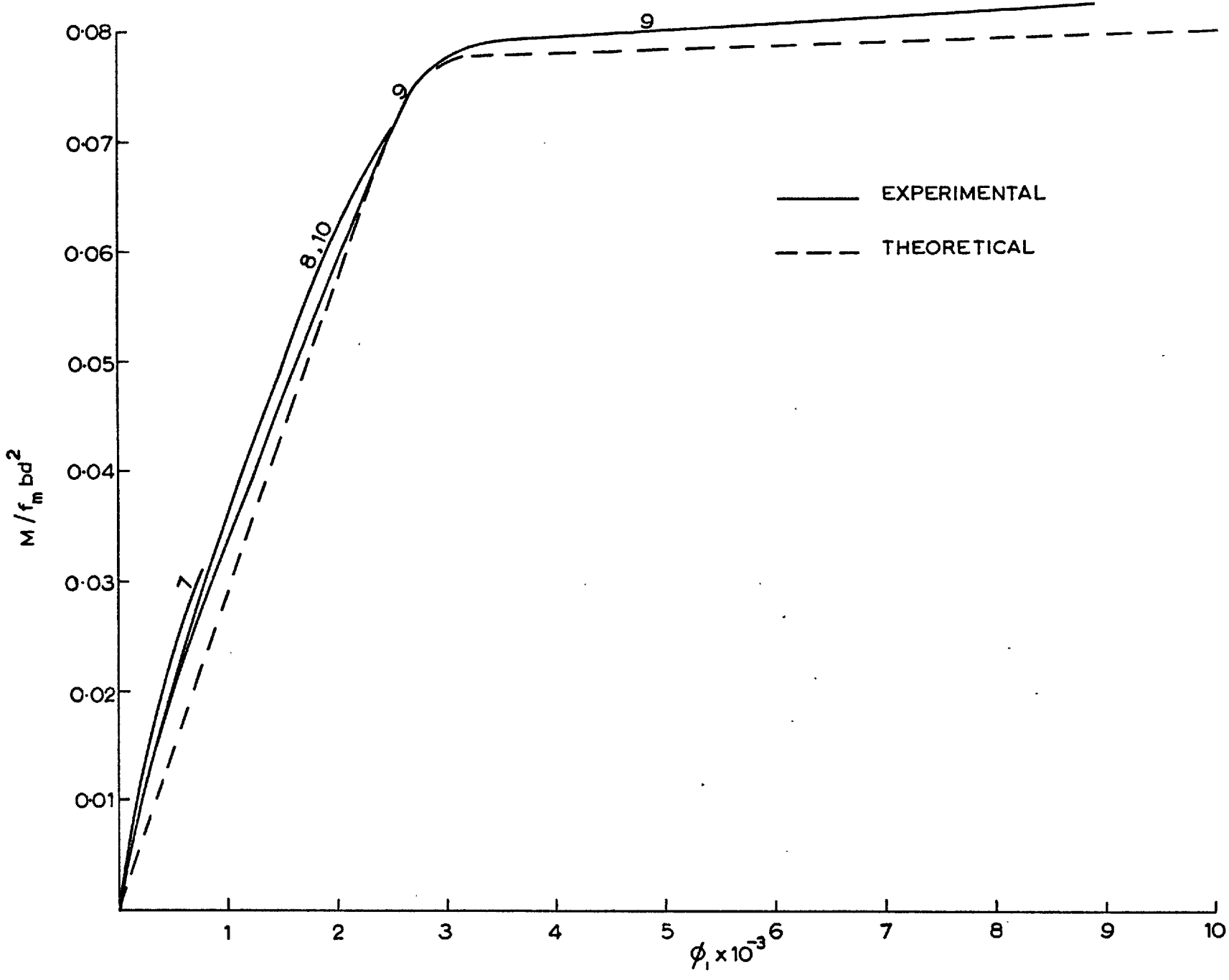


FIG. 5.23 (b) MOMENT - CURVATURE DIAGRAMS. BEAM A5 - SECTIONS 7, 8, 9, 10

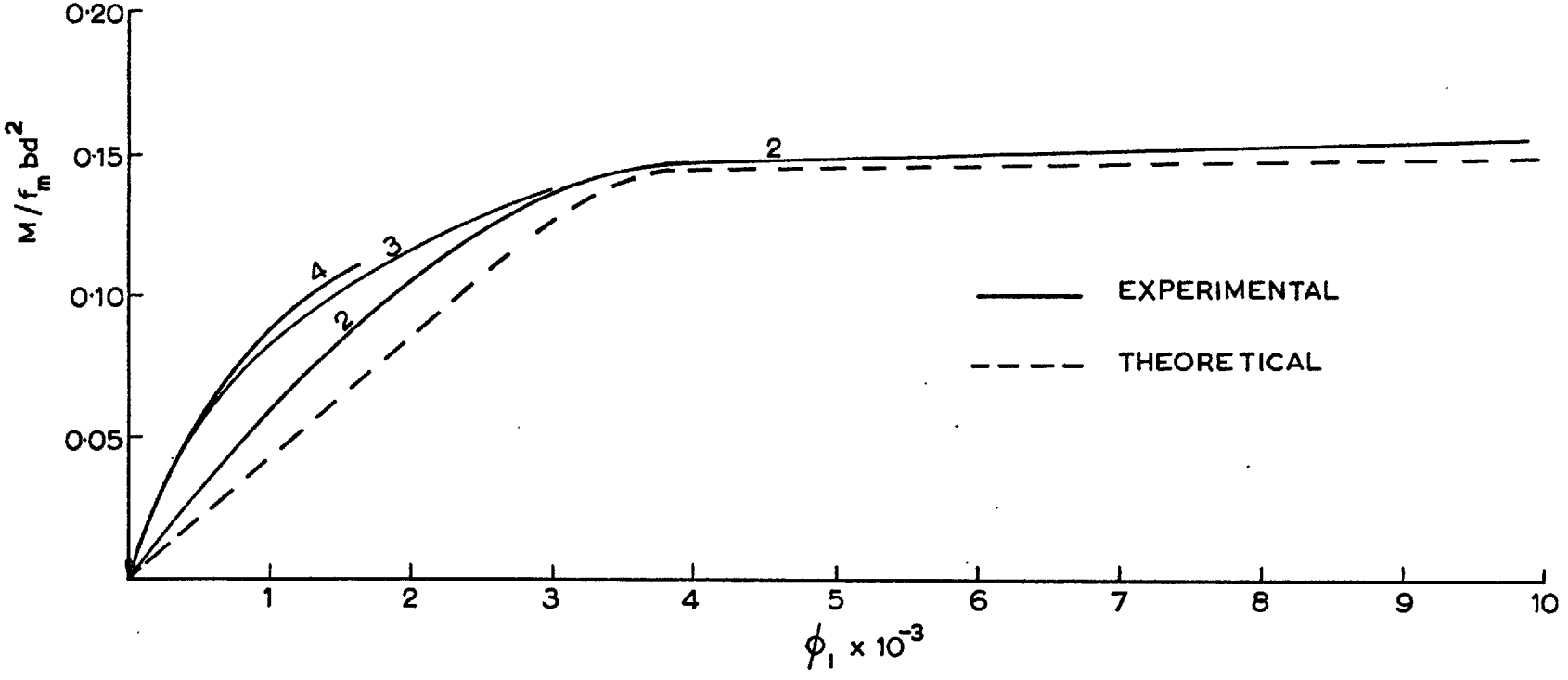


FIG.5.24 (a) MOMENT - CURVATURE DIAGRAMS. BEAM A6 - SECTIONS 2, 3, 4

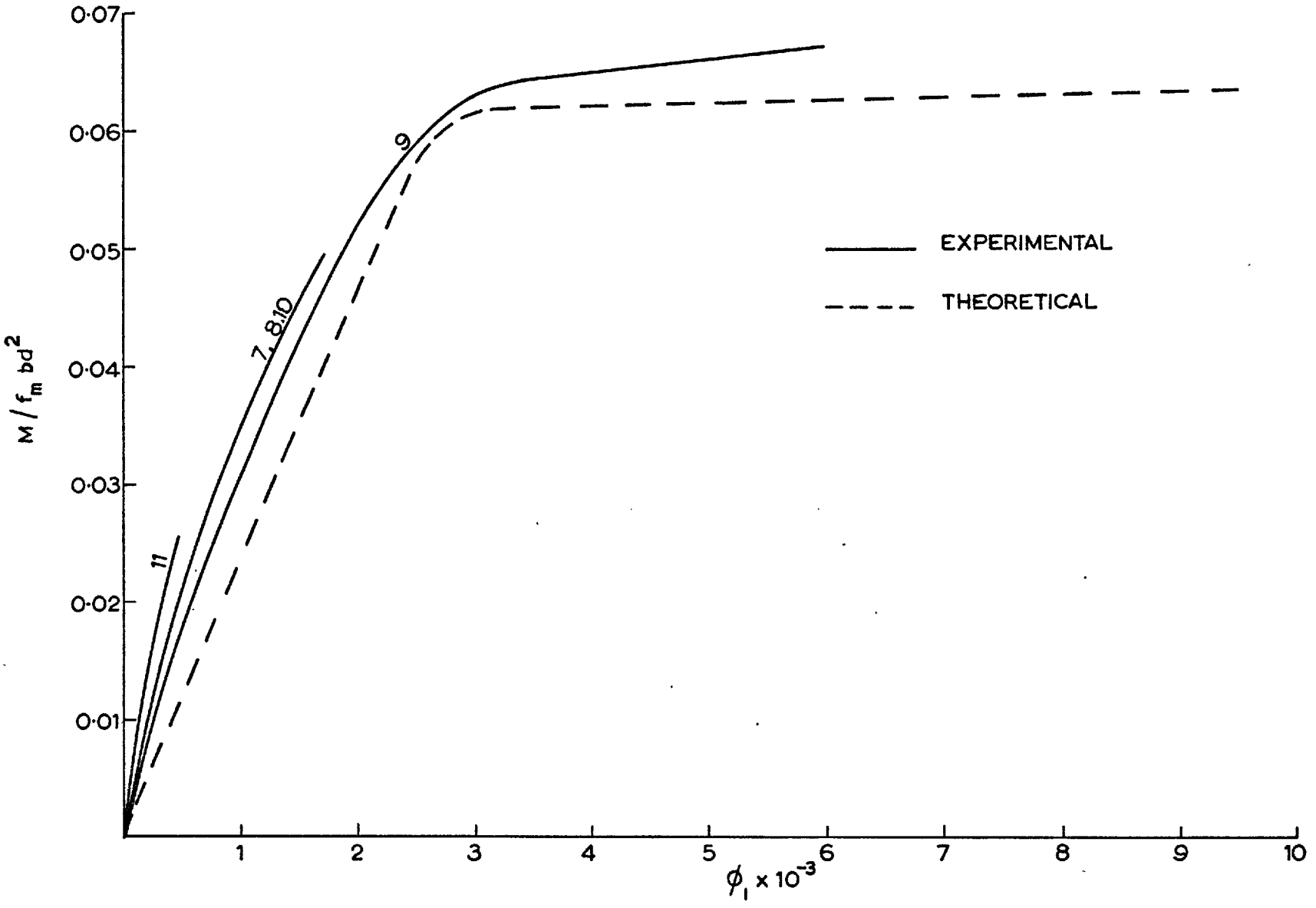


FIG. 5.24 (b) MOMENT - CURVATURE DIAGRAMS. BEAM A6 – SECTIONS 7, 8, 9, 10, 11

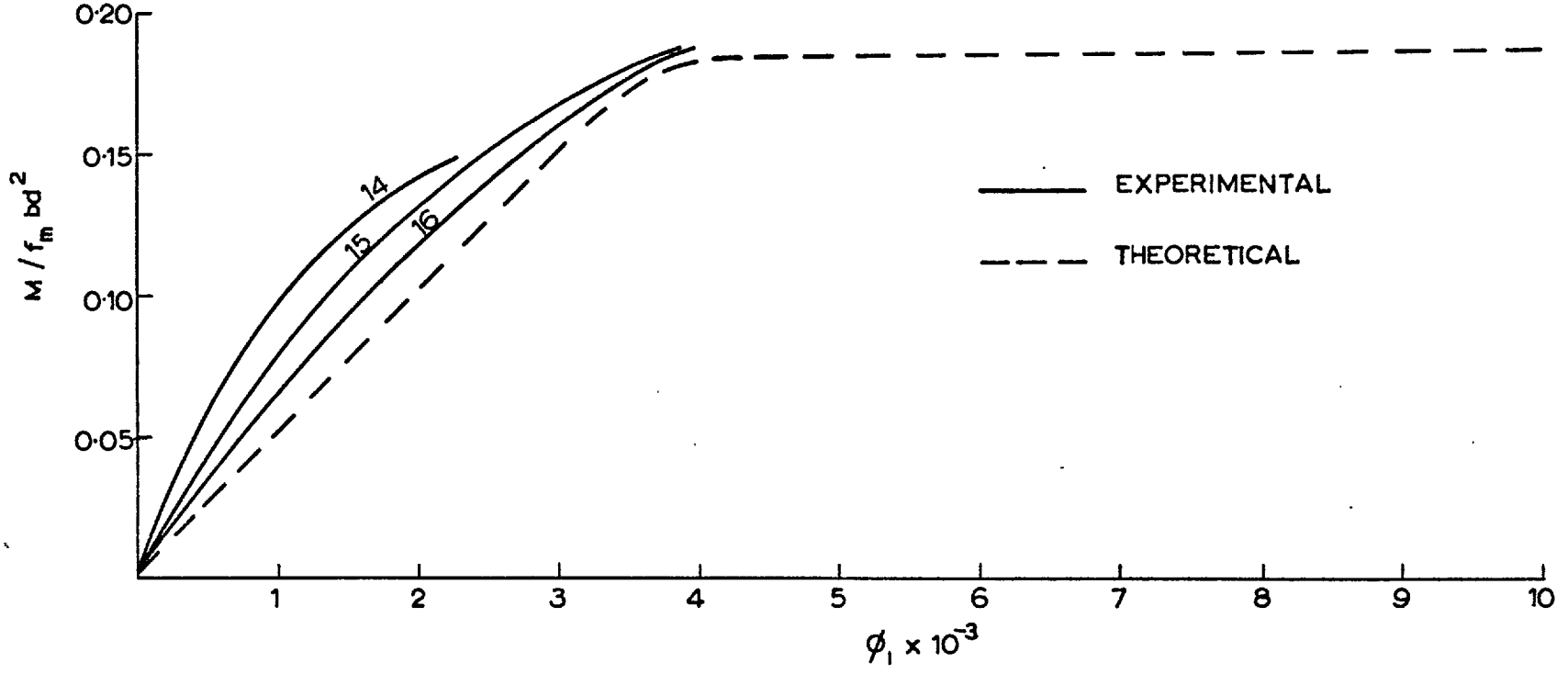


FIG. 5.24 (c) MOMENT - CURVATURE DIAGRAMS. BEAM A6 - SECTIONS 14, 15, 16

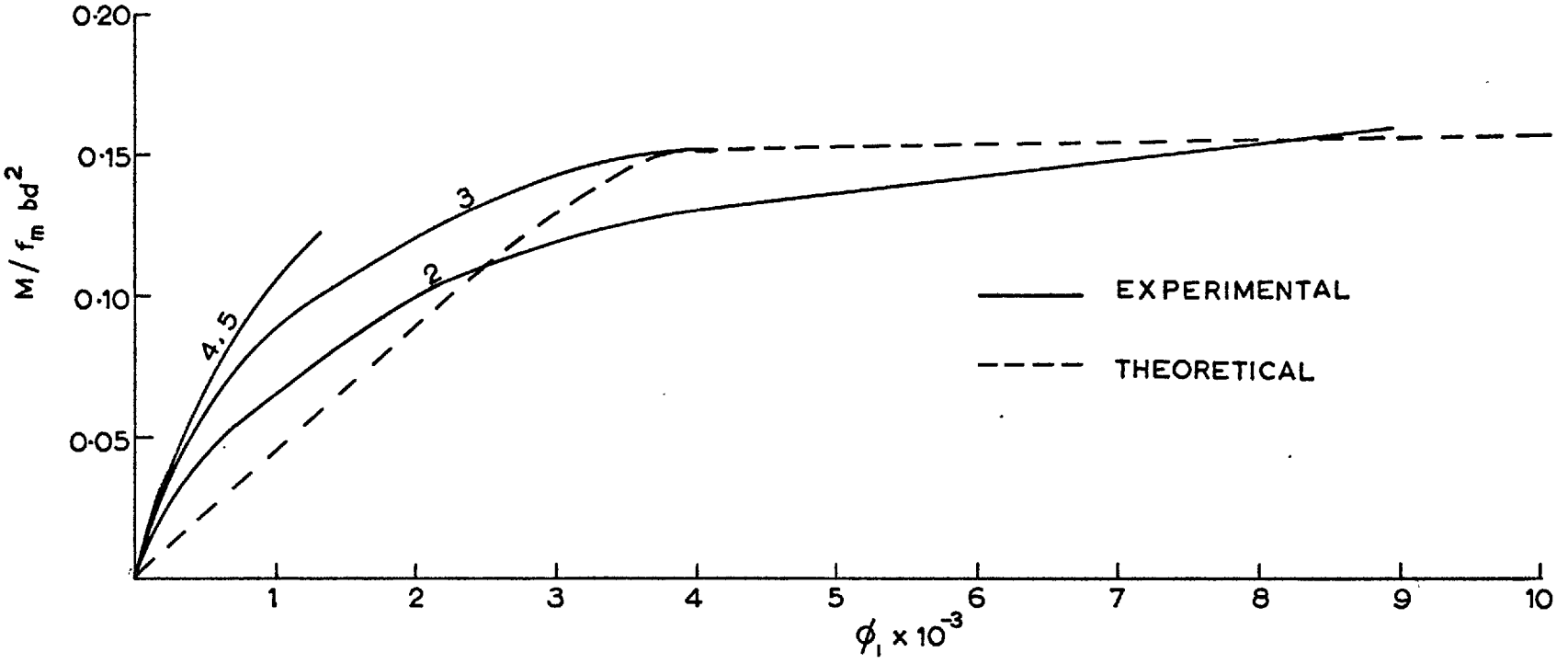


FIG. 5.25 (a) MOMENT - CURVATURE DIAGRAMS. BEAM B1 - SECTIONS 2,3,4,5

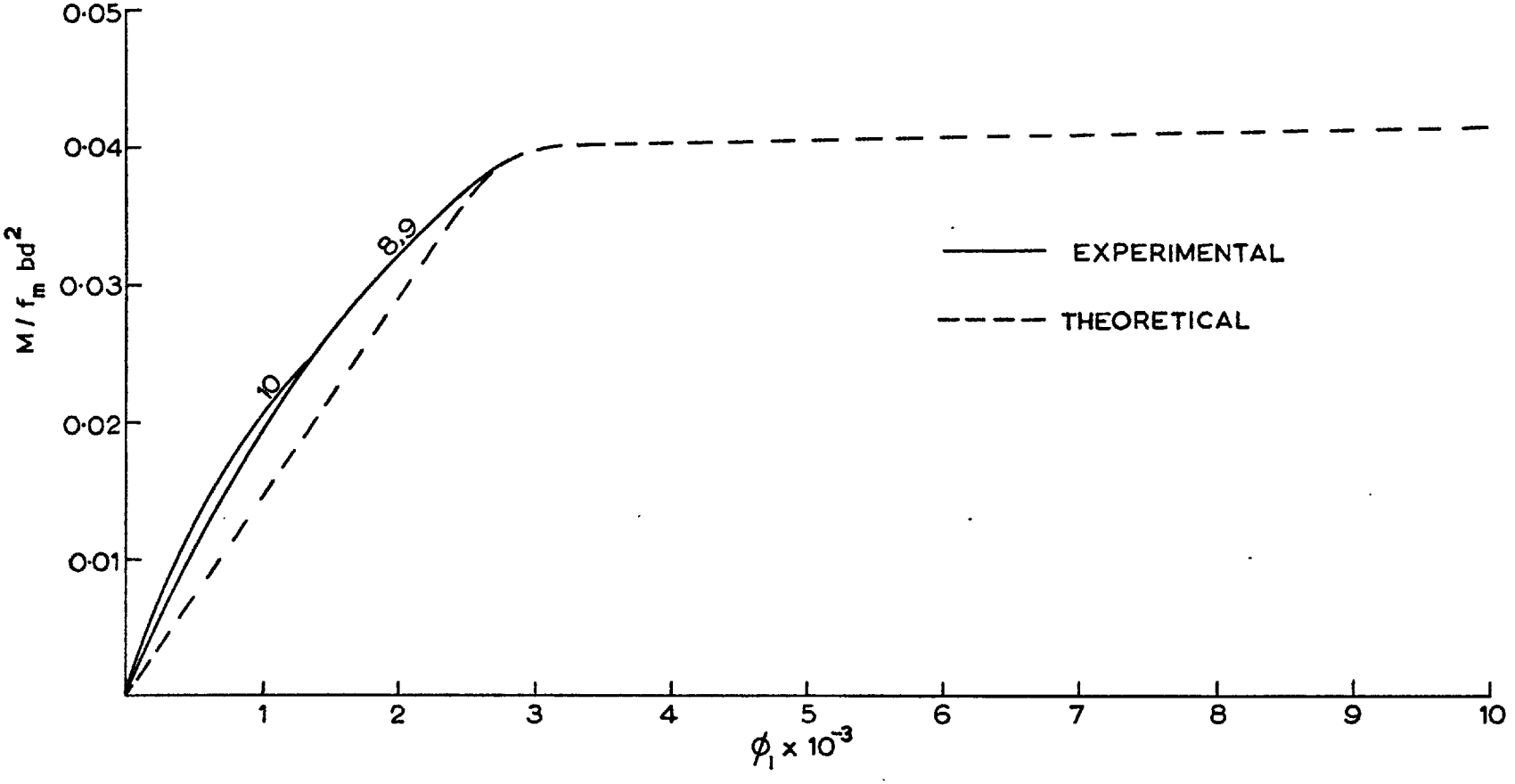


FIG. 5.25 (b) MOMENT – CURVATURE DIAGRAMS. BEAM B1 - SECTIONS 8,9,10

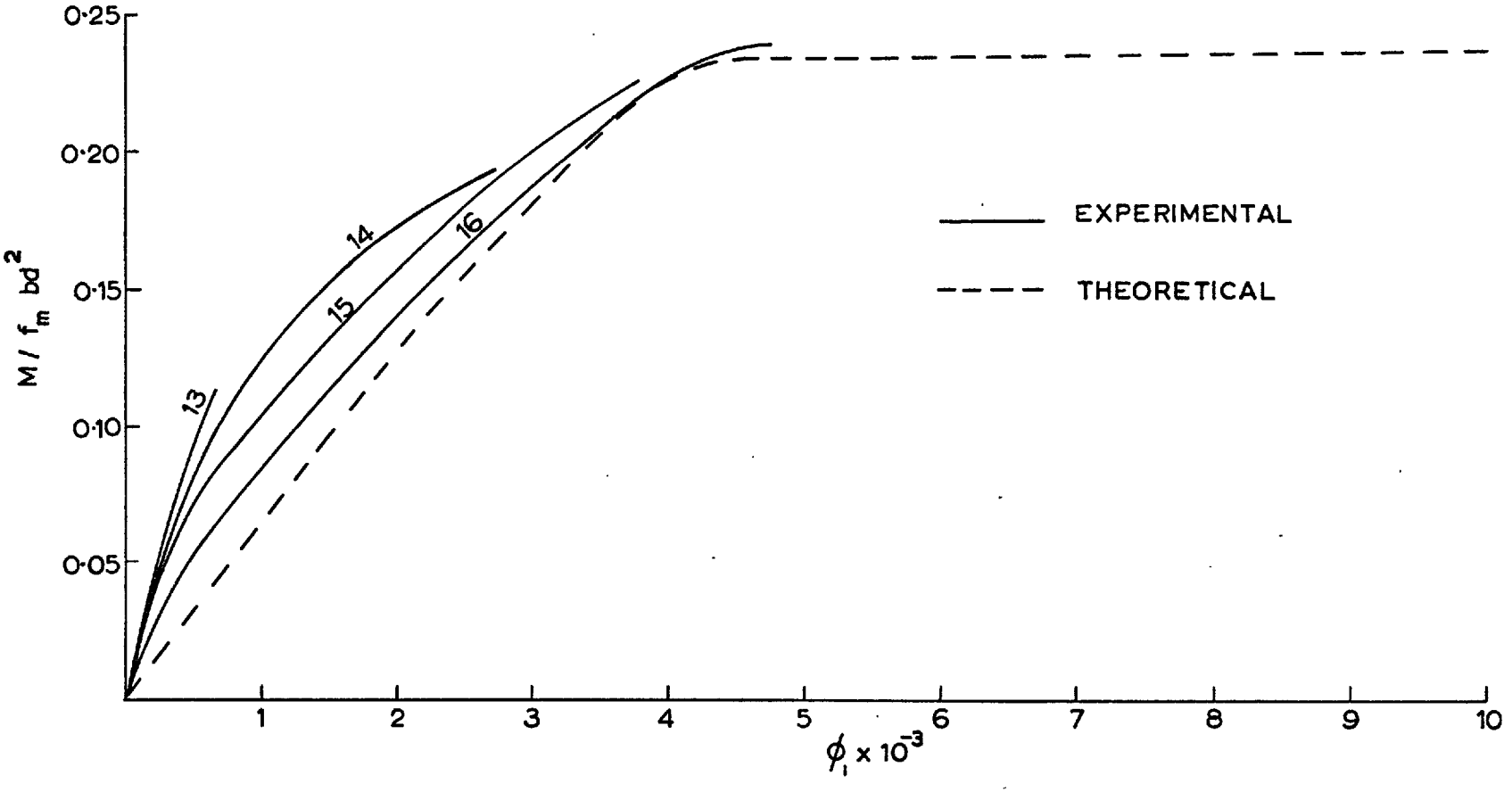


FIG. 5.25 (c) MOMENT - CURVATURE DIAGRAMS. BEAM B1 - SECTIONS 13, 14, 15, 16

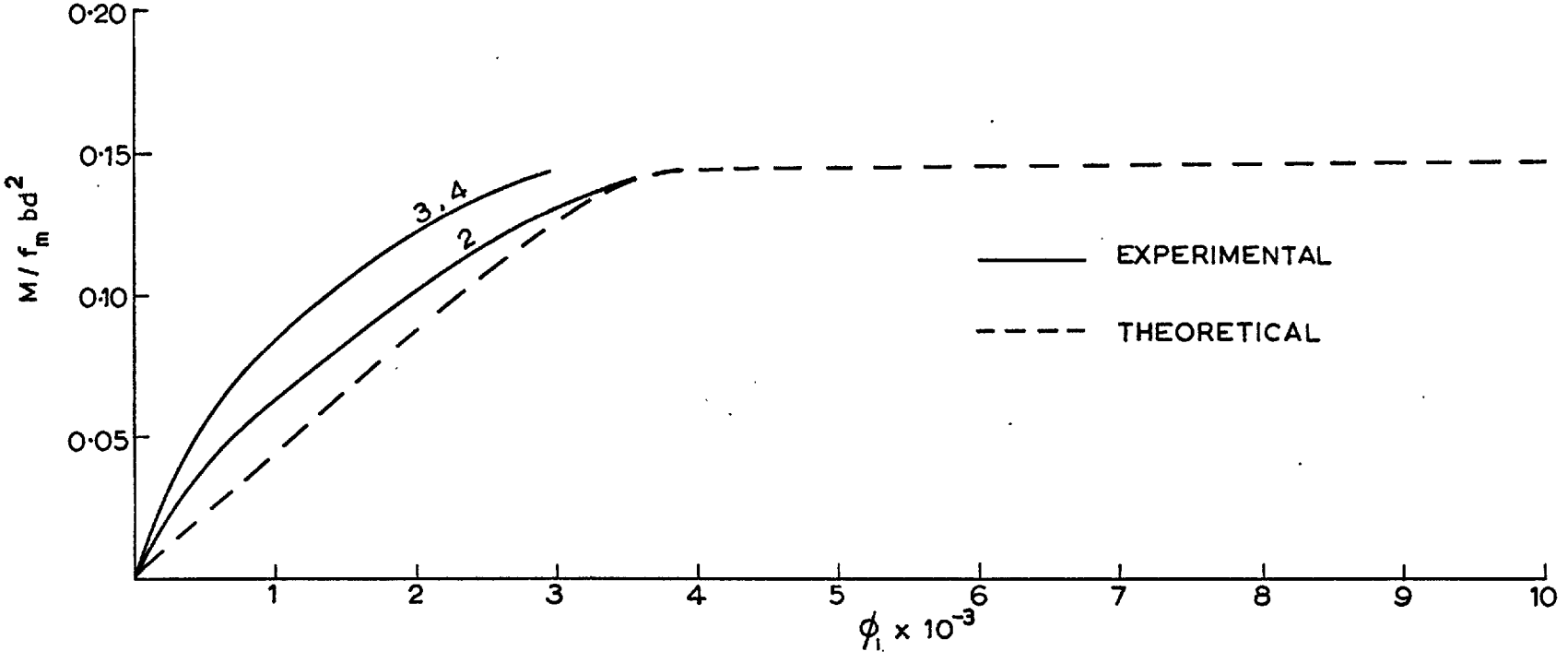


FIG. 5.26 (a) MOMENT - CURVATURE DIAGRAMS. BEAM B2 - SECTIONS 2, 3, 4

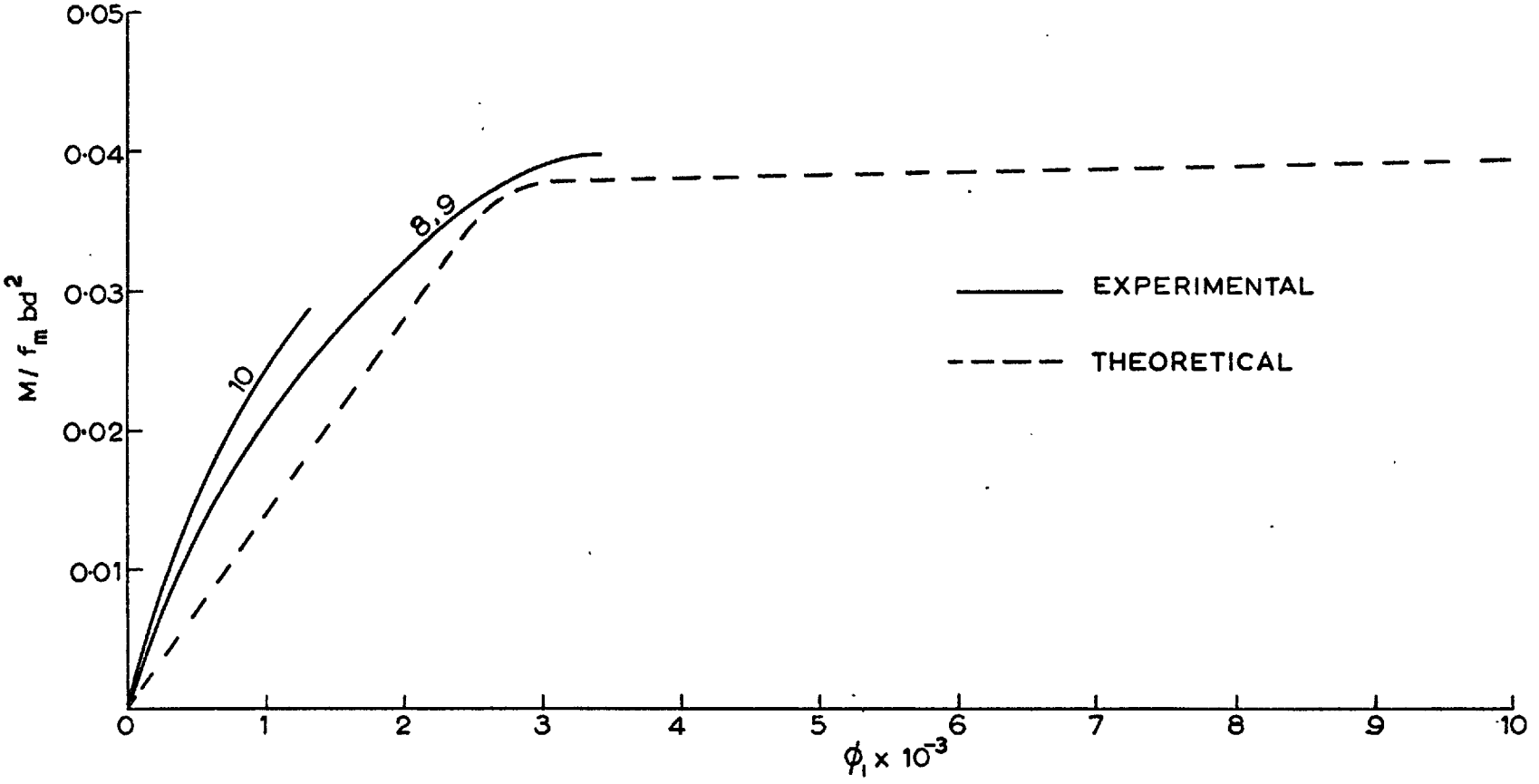


FIG. 5.26 (b) MOMENT - CURVATURE DIAGRAMS. BEAM B2 – SECTIONS 8, 9, 10

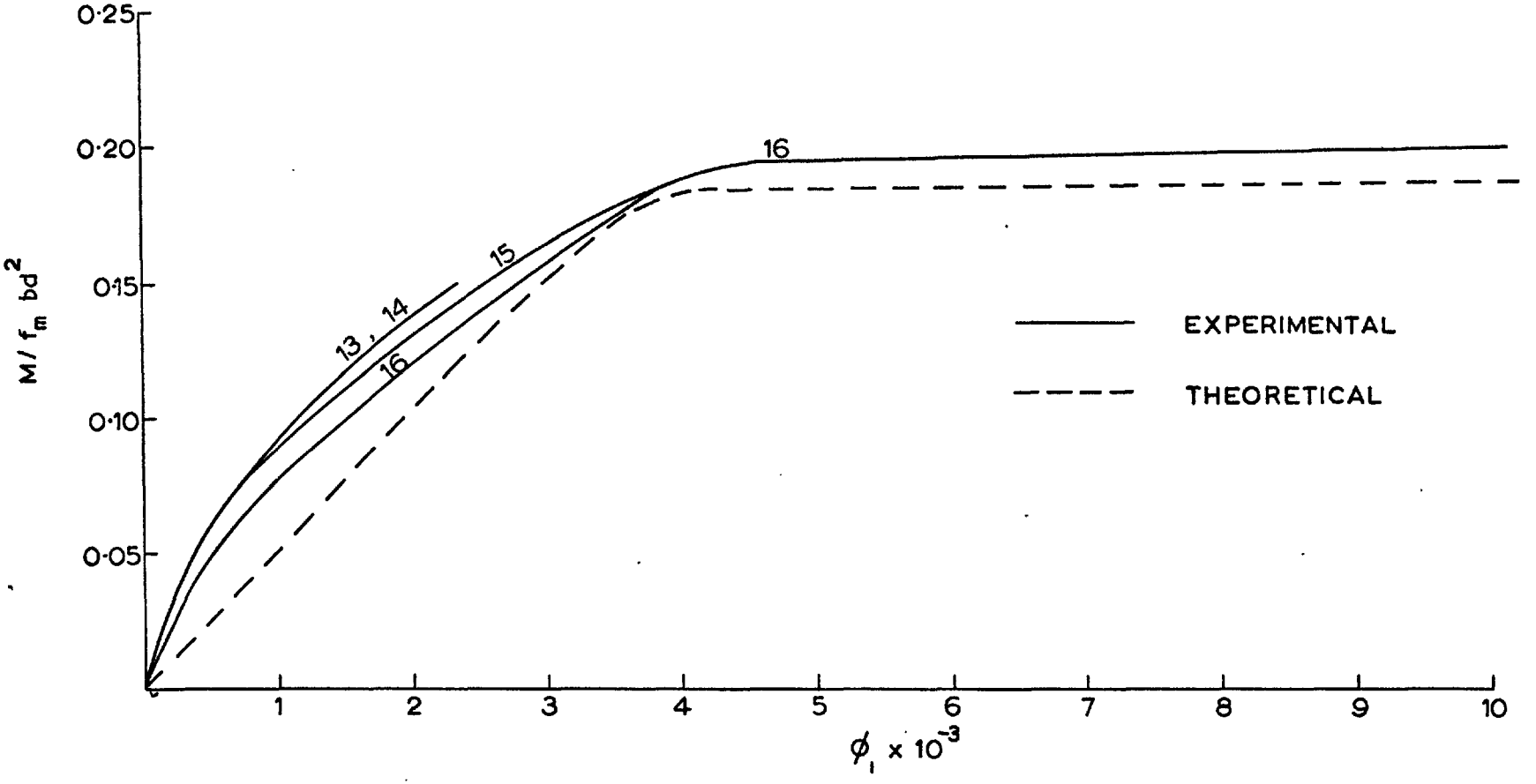


FIG. 5.26 (c) MOMENT - CURVATURE DIAGRAMS. BEAM B2 - SECTIONS 13, 14, 15, 16

derivation of expressions for moment-curvature relations it has been assumed that the section is cracked and concrete does not carry any tensile stress. This assumption is largely true for a critical section where there is heavy cracking at or around the section. But at sections away from the critical section where the strain readings were taken, either the cracks were not developed at those sections or they were wider apart about these sections. (Plate 2 shows the crack pattern for all the eight beams tested in this programme.) Thus the strain distribution at sections in between the cracks are modified due to the stiffness of concrete in between the cracks.

5.6 CURVATURE AND EI DISTRIBUTION

The distribution of curvature along the length of the beams for three load stages are shown in Figs. 5.27 to 5.34. The values of the curvatures were taken from the experimental moment-curvature relations for the corresponding sections, as described in the previous section. The three load stages, marked in Figs. 5.27 to 5.34, were chosen such as to represent a stage below, at or near, and beyond the yielding of tensile steel of one of the critical sections. The value of strain of the tensile steel at the three critical sections for the three load stages are given in Table 5.2. Fig. 5.35 shows the bending moment distribution for the beams at the corresponding load stages marked in the diagrams.

In order to study the variation of flexural rigidity, EI at different sections along the beam at the three load stages, described above, the EI values were calculated using the experimental moment-curvature diagrams and the results were plotted in Figs. 5.36 to 5.43. As the measurements were made at 6" and 12" intervals the variation between two sections was assumed to be linear.

It can be observed from Figs. 5.36 to 5.43 that the EI distribution along the beam is not uniform and that due to inelastic behaviour of the three critical sections, the support and mid-span sections, the curvatures at these sections are markedly increased with a consequent reduction in their flexural rigidities. It is also noted that this significant reduction in flexural rigidity is concentrated over a distance on either side of the critical sections depending on the spread of 'plasticity' to

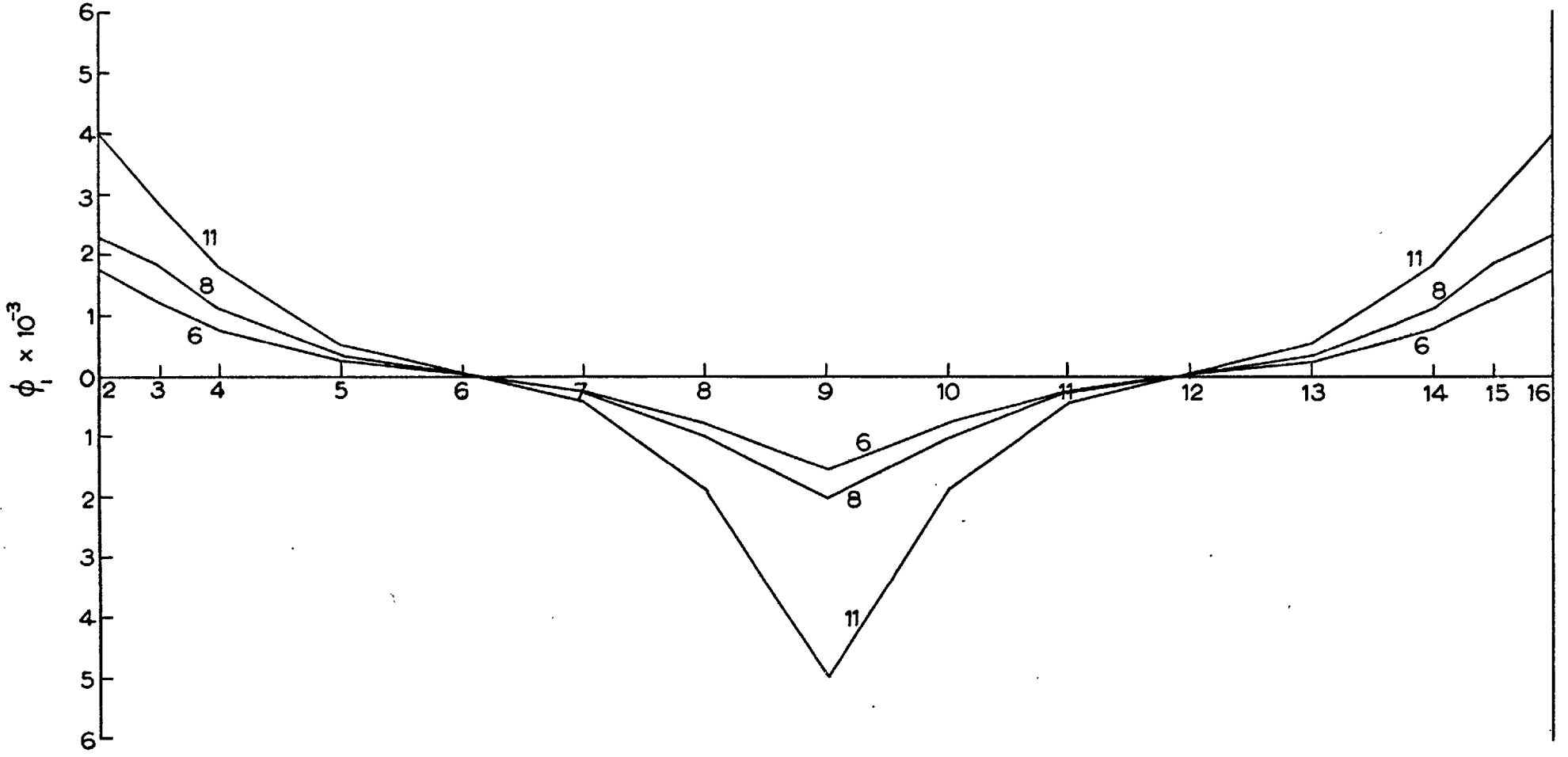


FIG. 5.27 CURVATURE DISTRIBUTION. BEAM A1 - LOAD STAGES 6, 8, 11

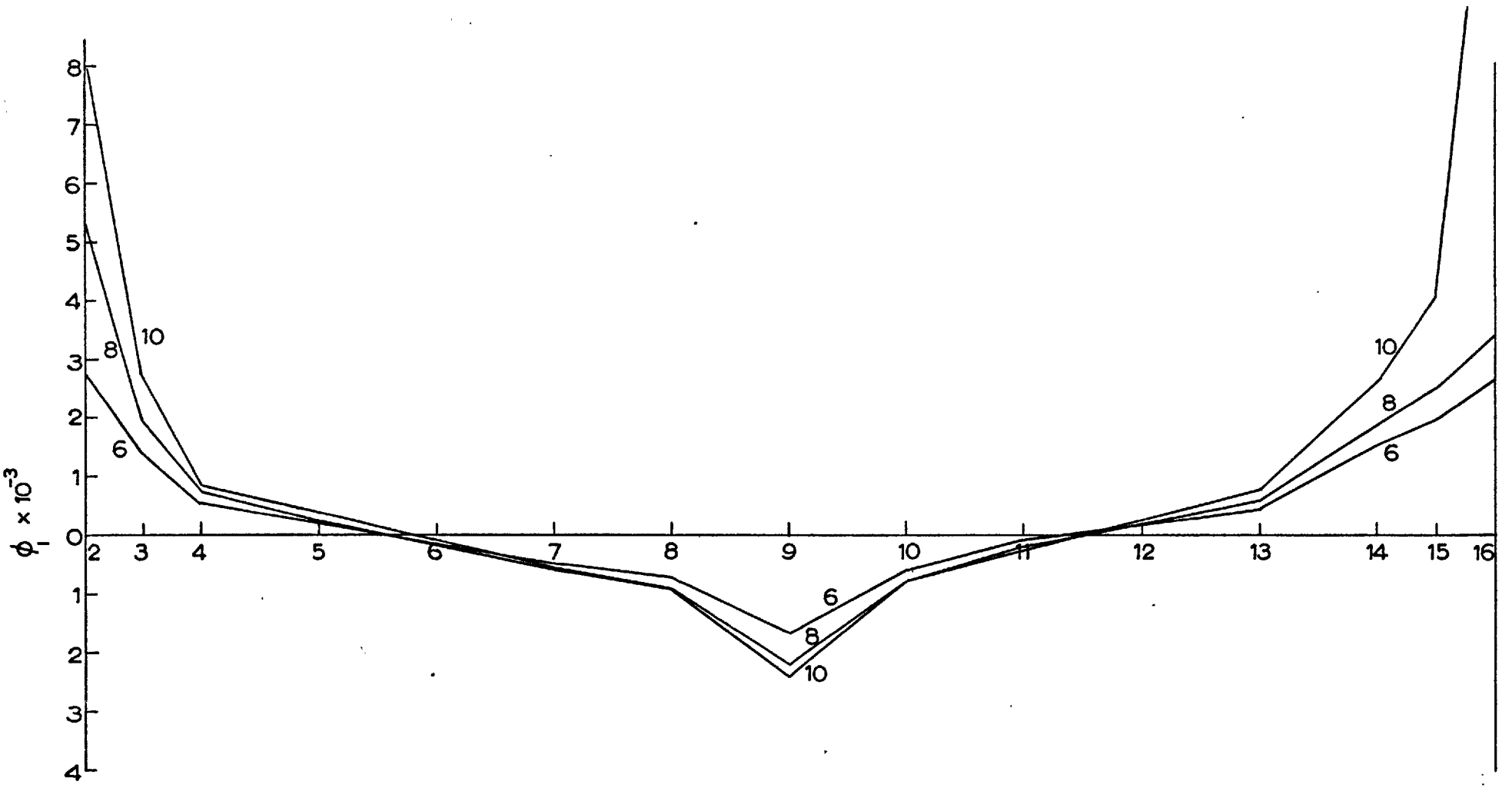


FIG. 5.28 CURVATURE DISTRIBUTION. BEAM A2. LOAD STAGES 6,8,10

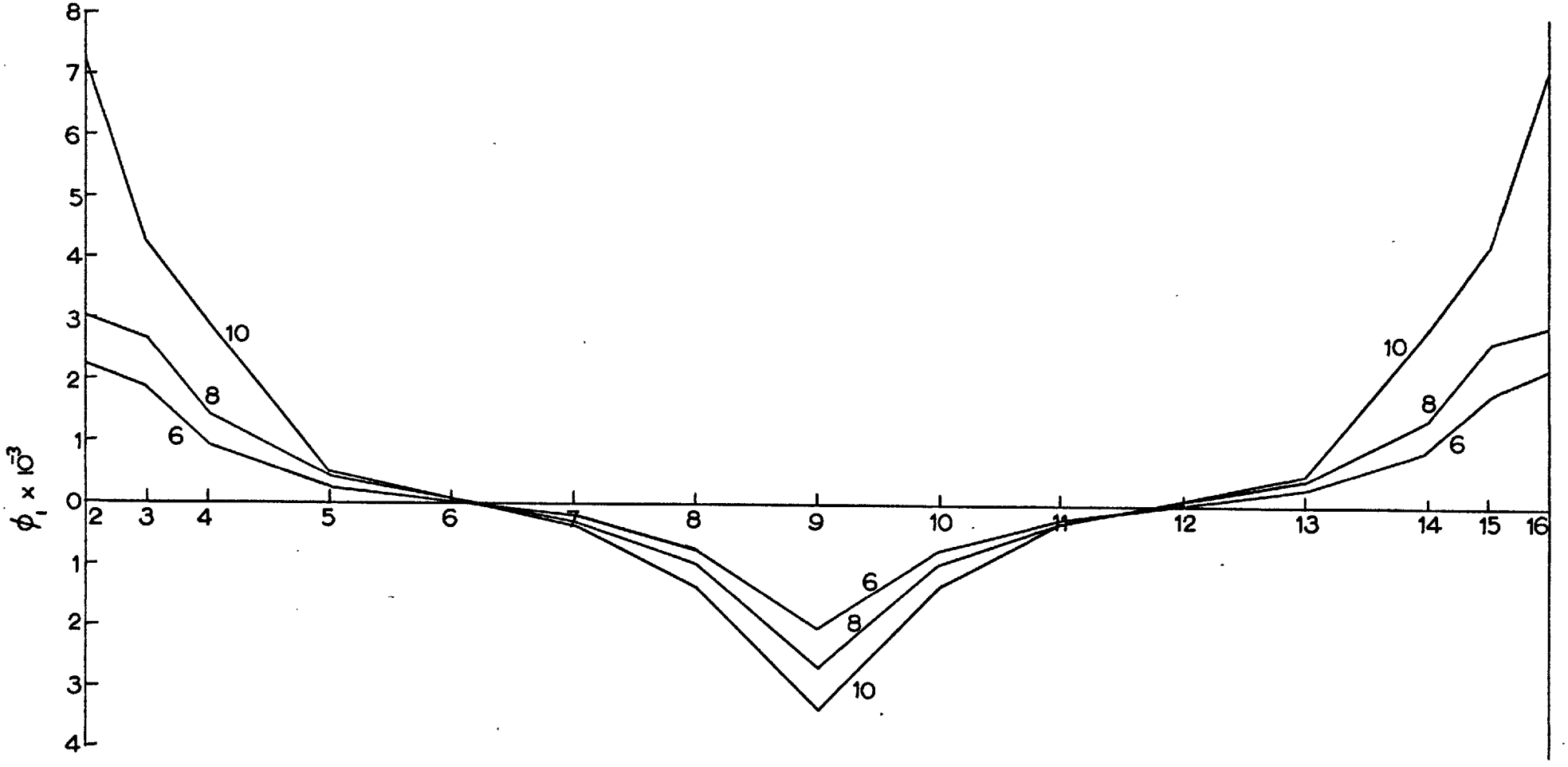


FIG. 5.29 CURVATURE DISTRIBUTION. BEAM A3 - LOAD STAGES 6, 8, 10

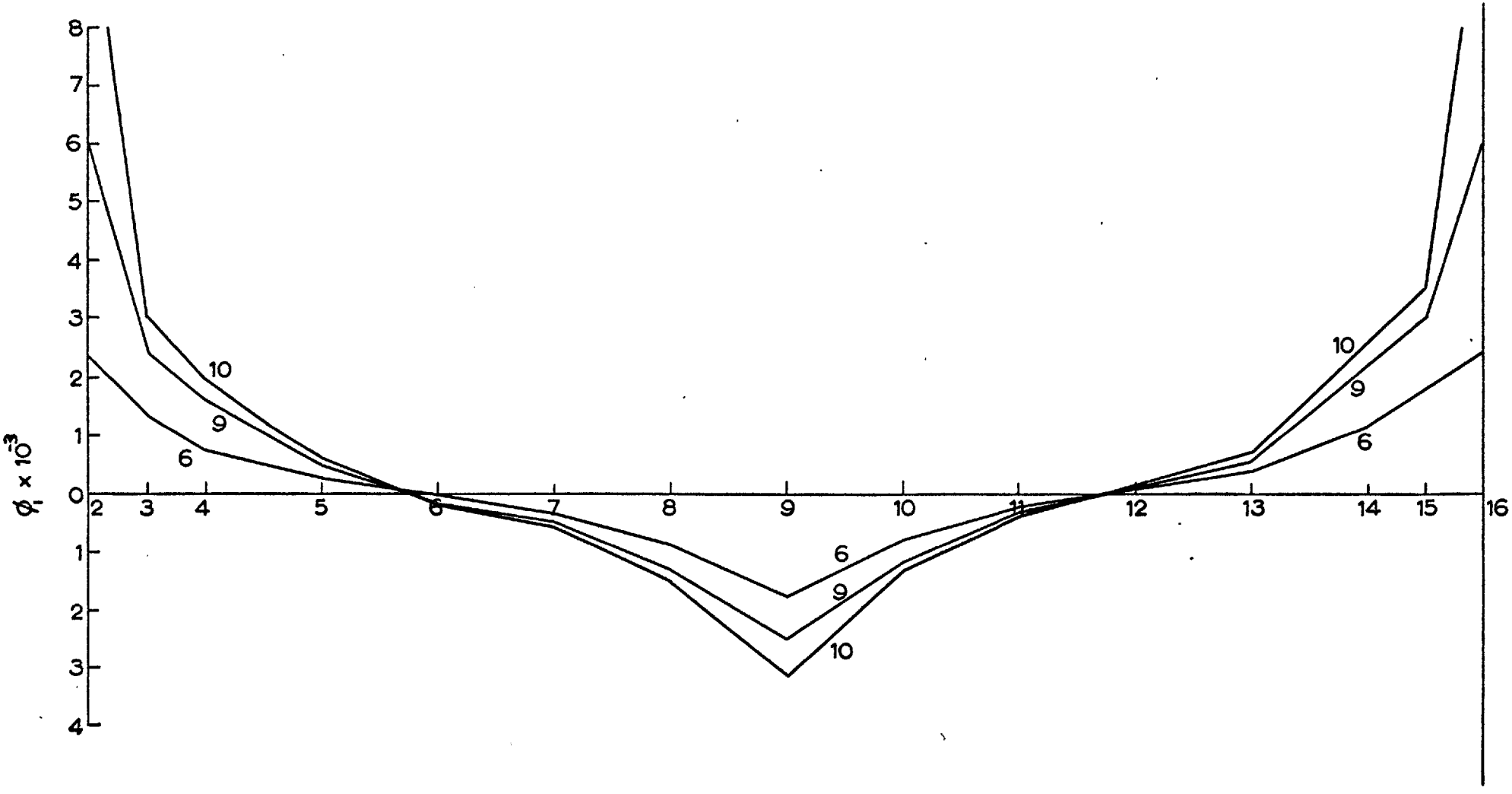


FIG. 5.30 CURVATURE DISTRIBUTION. BEAM A4-LOAD STAGES 6, 9, 10

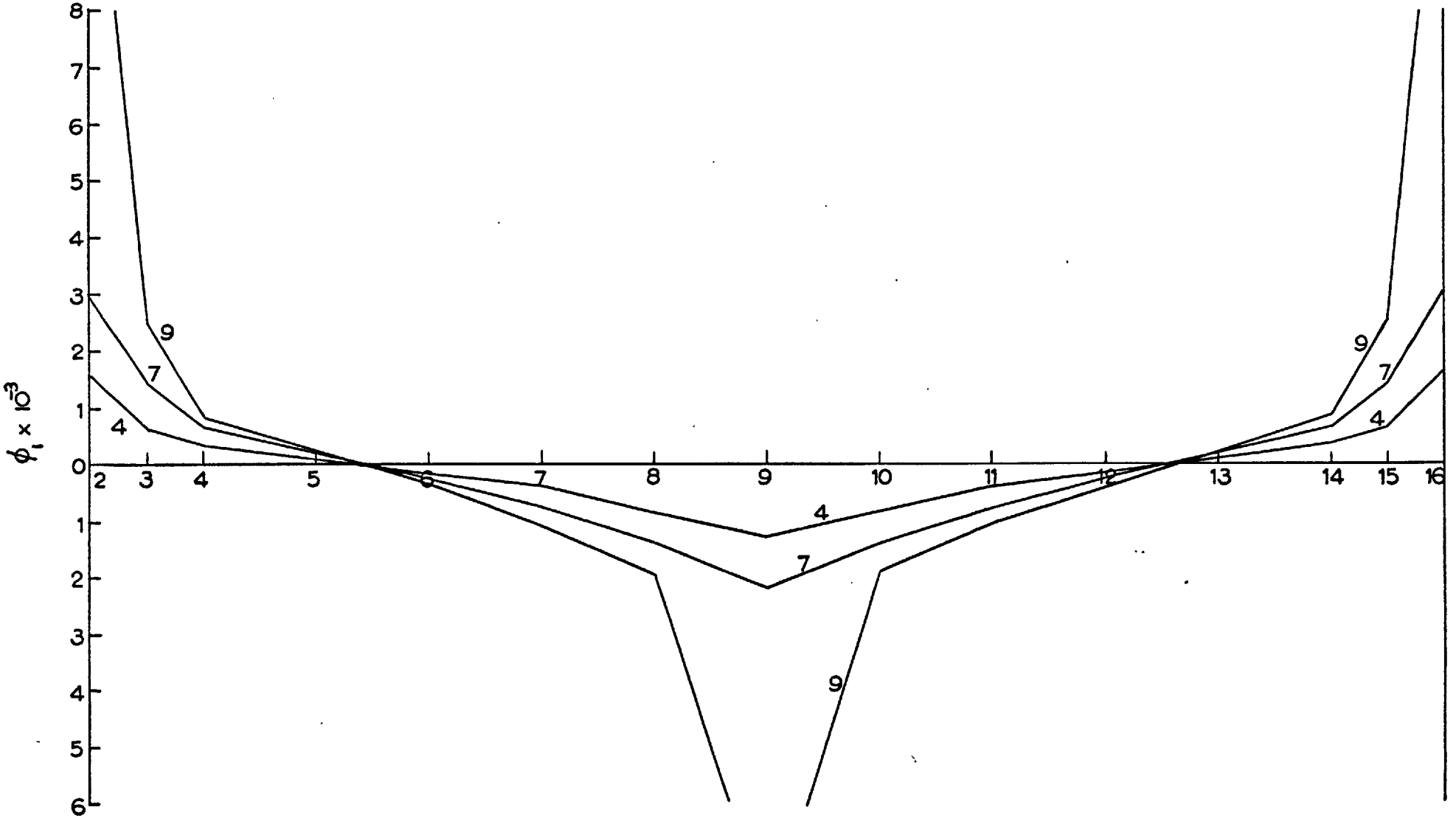


FIG. 5.31 CURVATURE DISTRIBUTION. BEAM A5 - LOAD STAGES 4, 7, 9

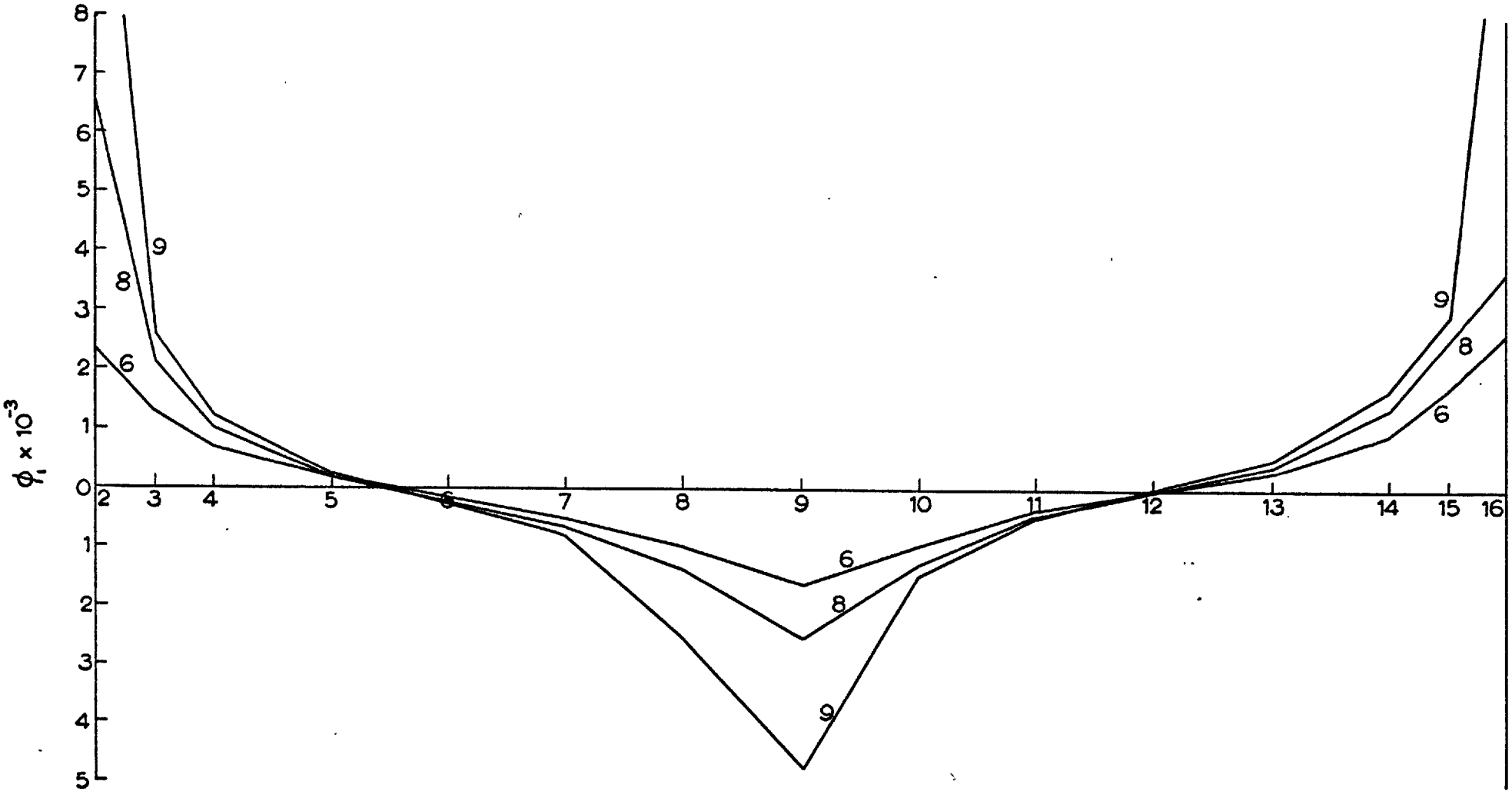


FIG. 5.32 CURVATURE DISTRIBUTION. BEAM A6 - LOAD STAGES 6,8,9

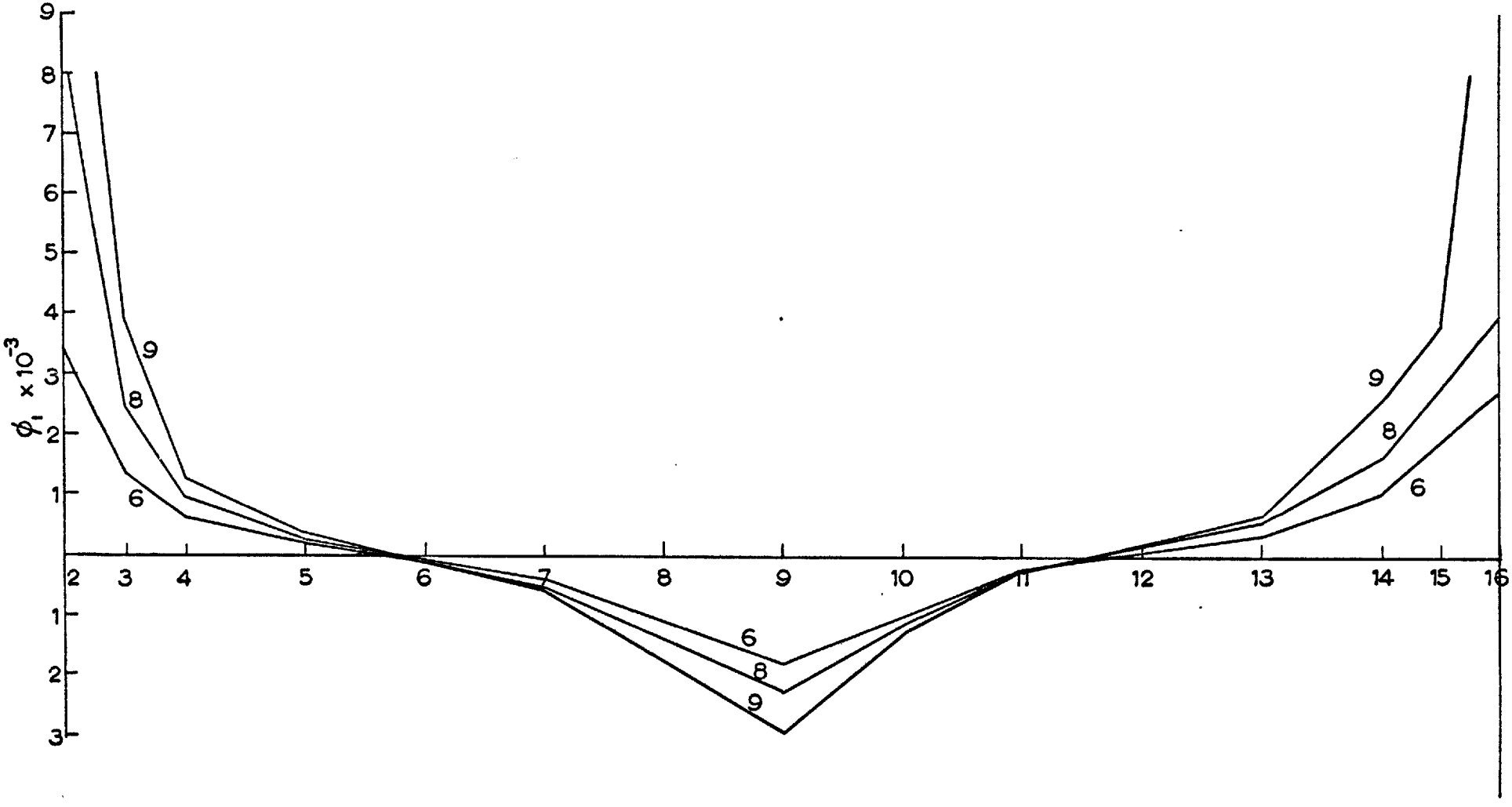


FIG. 5.33 CURVATURE DISTRIBUTION, BEAM B1 - LOAD STAGES 6, 8, 9

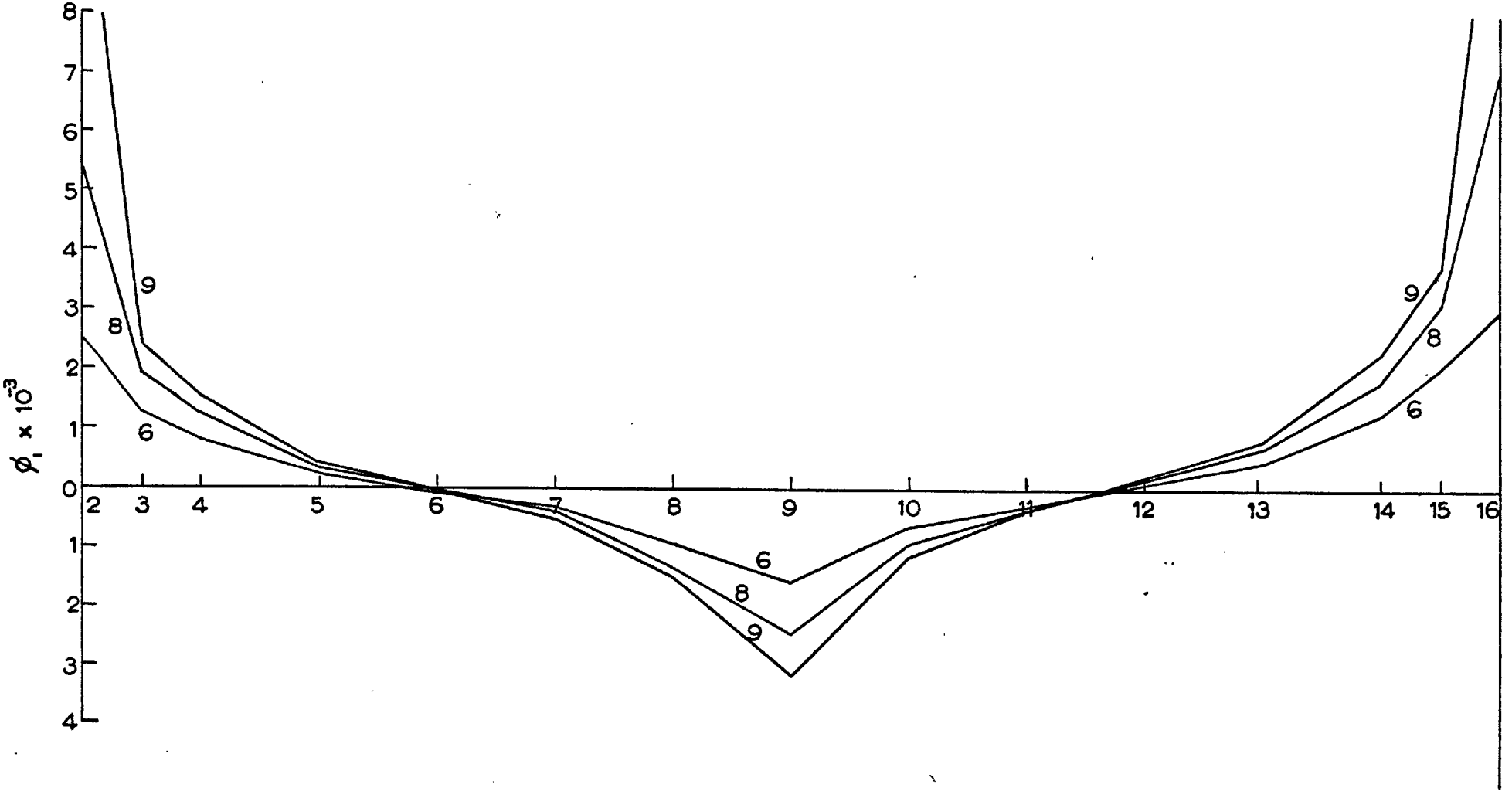


FIG. 5.34 CURVATURE DISTRIBUTION. BEAM B2 - LOAD STAGES 6, 8, 9

TABLE 5.2. VALUES OF TENSILE STEEL STRAINS

Beam	Load Stage	Value of steel strain		
		Section 2	Section 9	Section 16
A1	6	0.0010	0.0013	0.0010
	8	0.0015	0.0016	0.0015
	11	0.0023	0.0025	0.0023
A2	6	0.0012	0.0011	0.0012
	8	0.0019	0.0017	0.0018
	10	0.0025	0.0019	0.0025
A3	6	0.0018	0.0014	0.0018
	8	0.0020	0.0017	0.0020
	10	$> e_{sl}$	0.0020	$> e_{sl}$
A4	6	0.0011	0.0013	0.0012
	9	0.0020	0.0018	0.0024
	10	0.0025	0.0021	$> e_{sl}$
A5	4	0.0010	0.0010	0.0010
	7	0.0019	0.0017	0.0019
	9	$> e_{sl}$	0.0022	$> e_{sl}$
A6	6	0.0015	0.0014	0.0015
	8	0.0021	0.0018	0.0020
	9	0.0026	0.0020	0.0025
B1	6	0.0015	0.0014	0.0015
	8	0.0023	0.0017	0.0016
	9	$> e_{sl}$	0.0020	0.0022
B2	6	-	0.0013	0.0013
	8	-	0.0017	0.0019
	9	-	0.0021	$> e_{sl}$

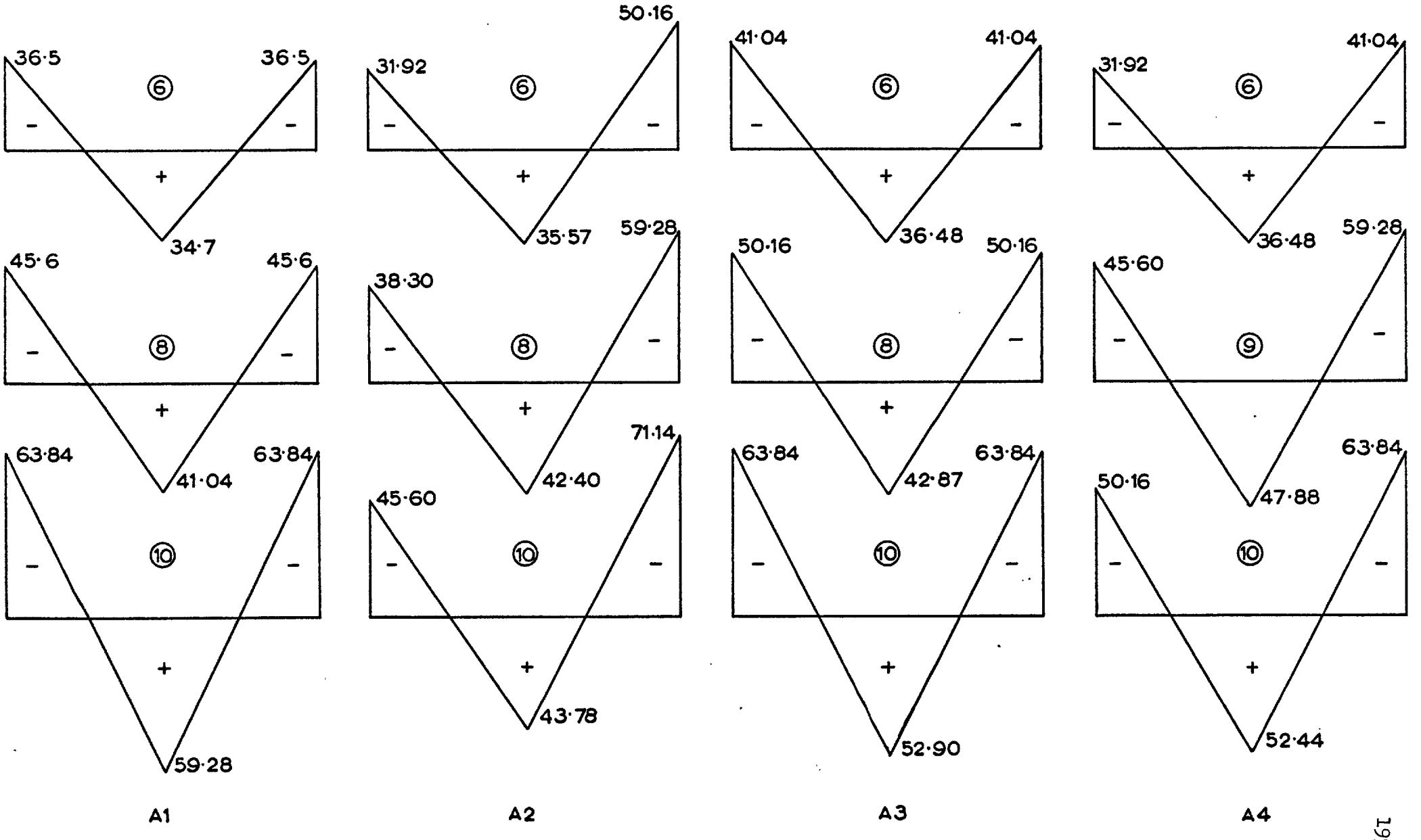


FIG. 5.35(a) BENDING MOMENT DISTRIBUTION FOR TEST BEAMS. (Units in kNm)

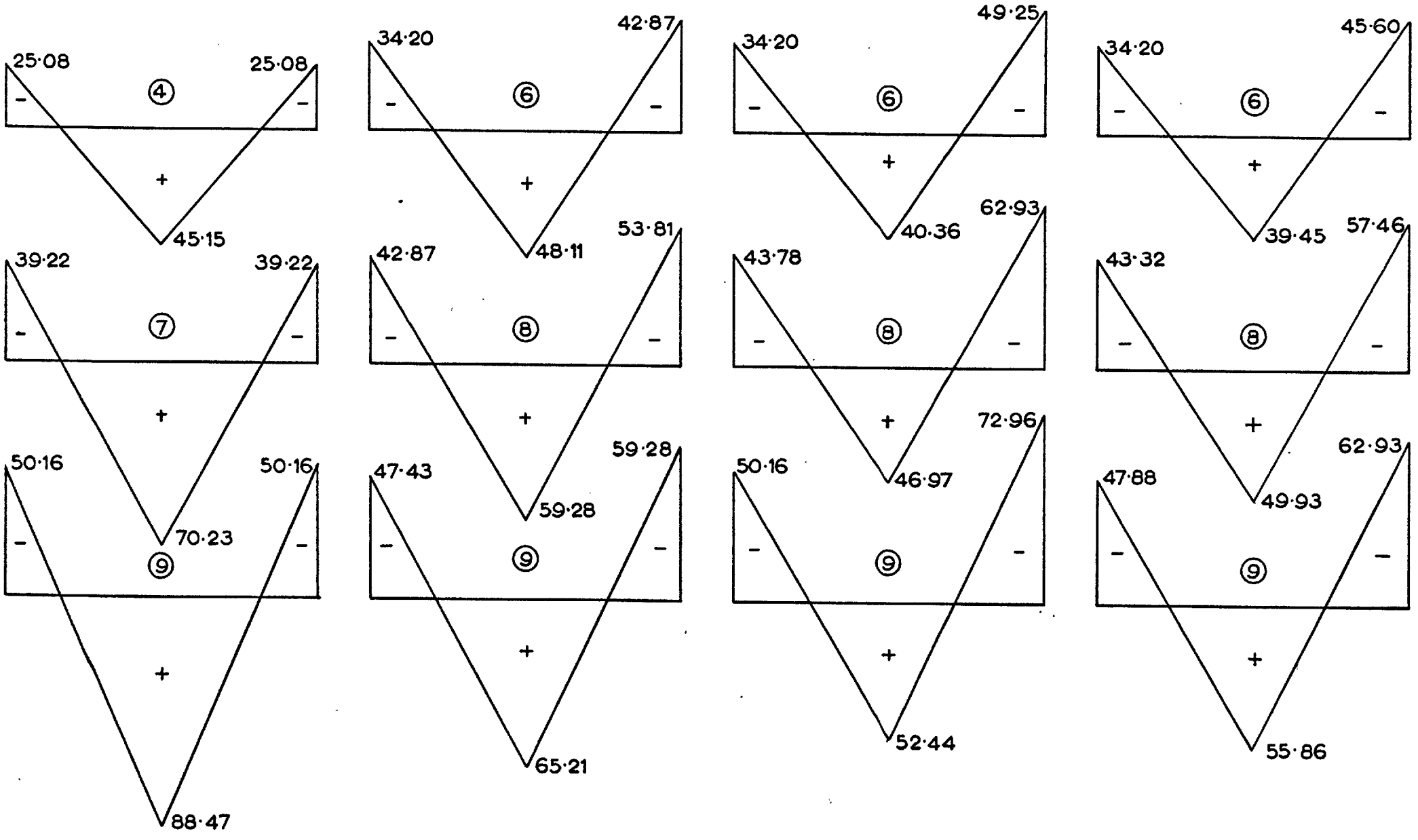


FIG. 5.35(b) BENDING MOMENT DISTRIBUTION FOR TEST BEAMS. (Units in kNm)

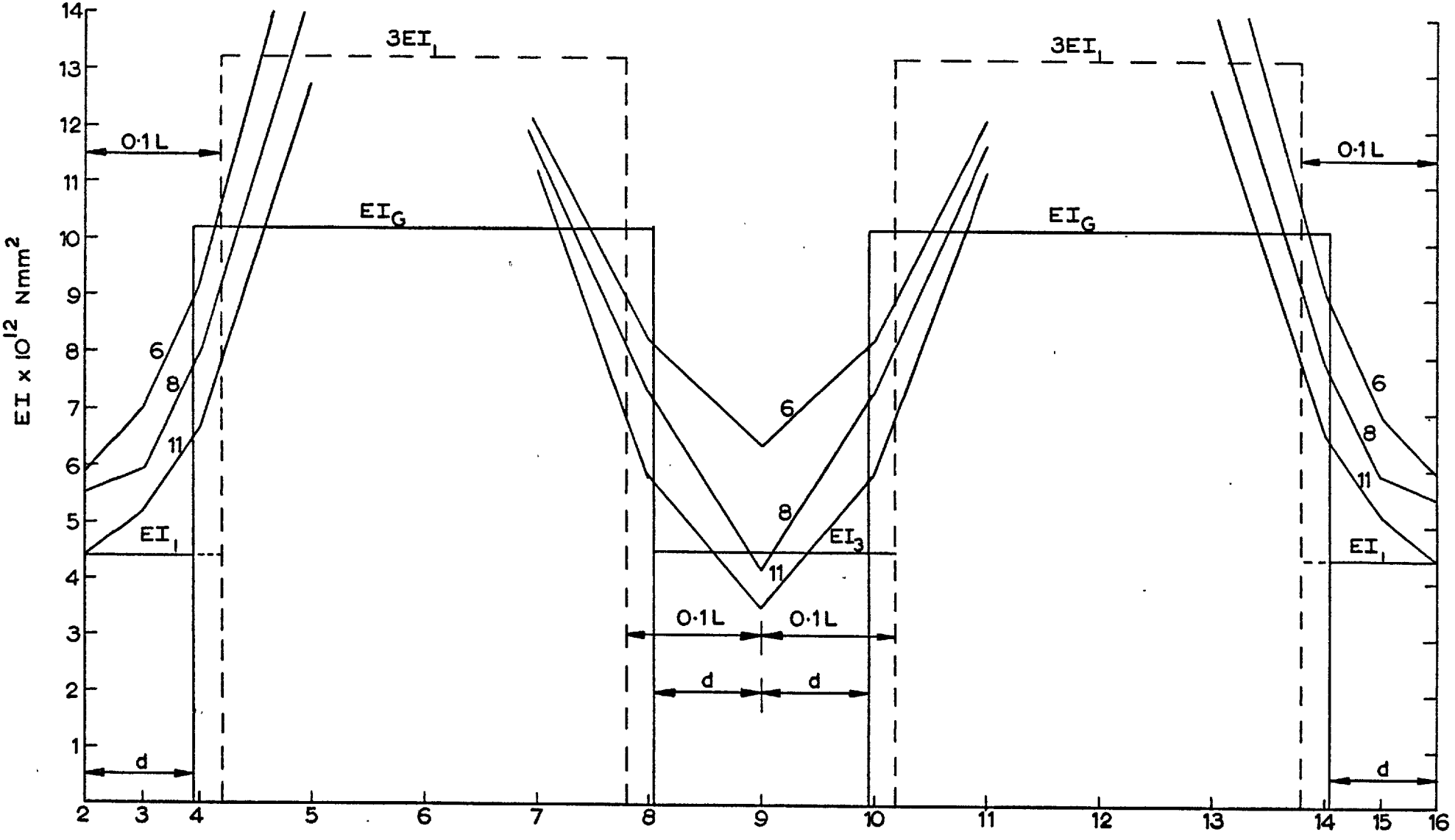


FIG. 5.36 EI DISTRIBUTION. BEAM A1 - LOAD STAGES 6, 8, 11

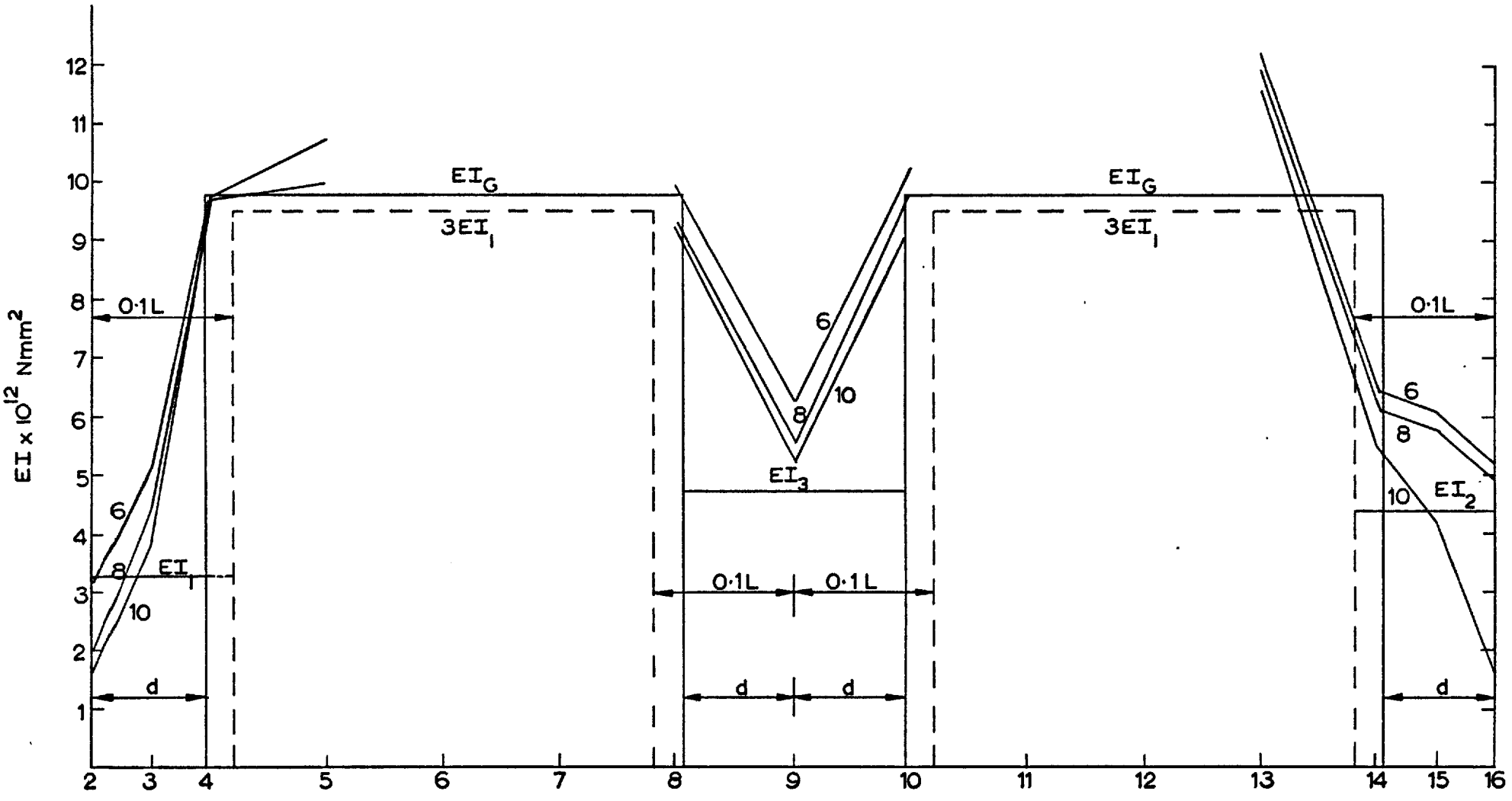


FIG. 5.37 EI DISTRIBUTION. BEAM A2 - LOAD STAGES 6, 8, 10

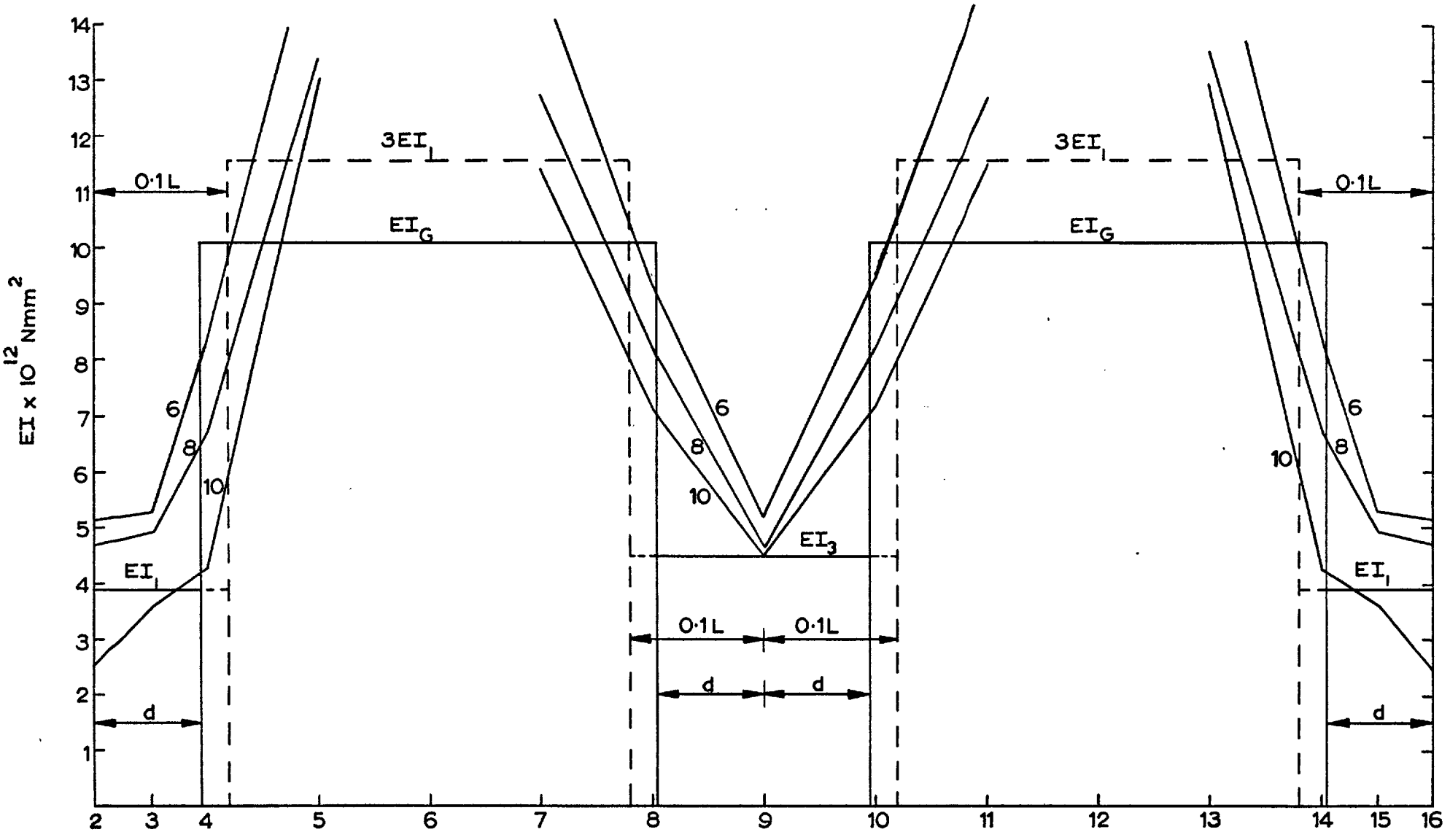


FIG. 5.38 EI DISTRIBUTION. BEAM A3 - LOAD STAGES 6, 8, 10

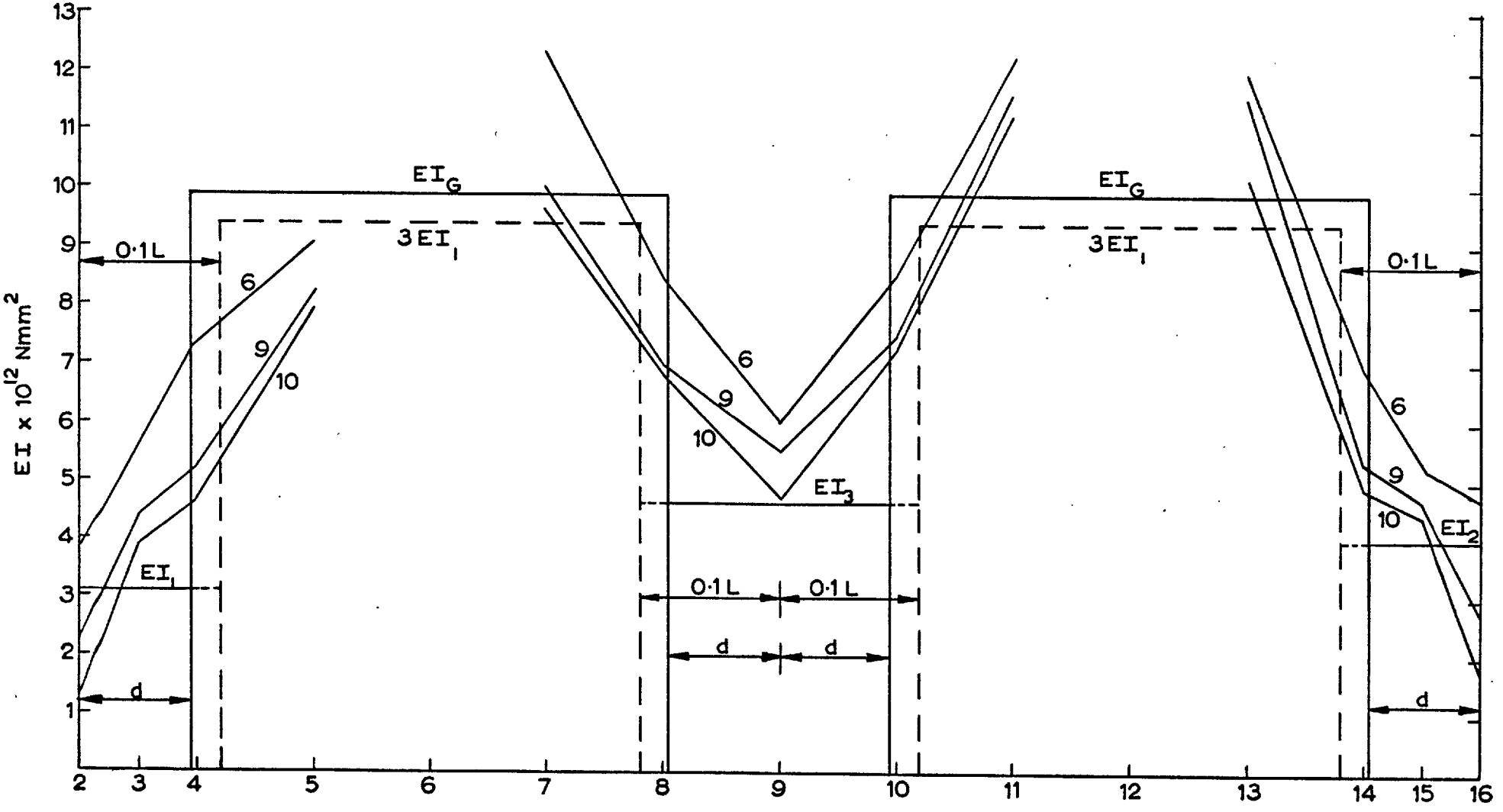


FIG. 5.39 EI DISTRIBUTION. BEAM A4 - LOAD STAGES 6, 9, 10

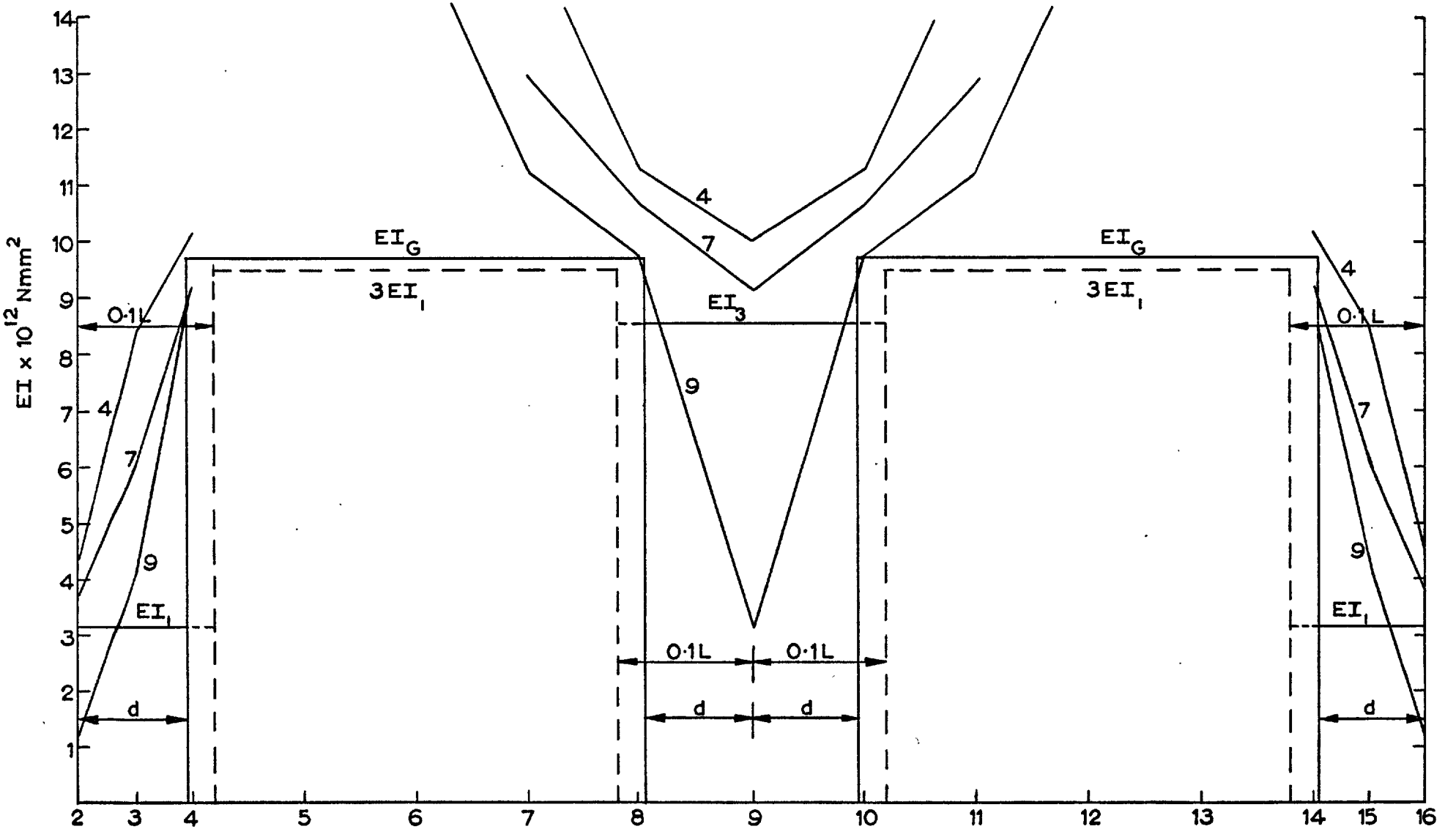


FIG. 5.40 EI DISTRIBUTION. BEAM A5 - LOAD STAGES 4,7,9

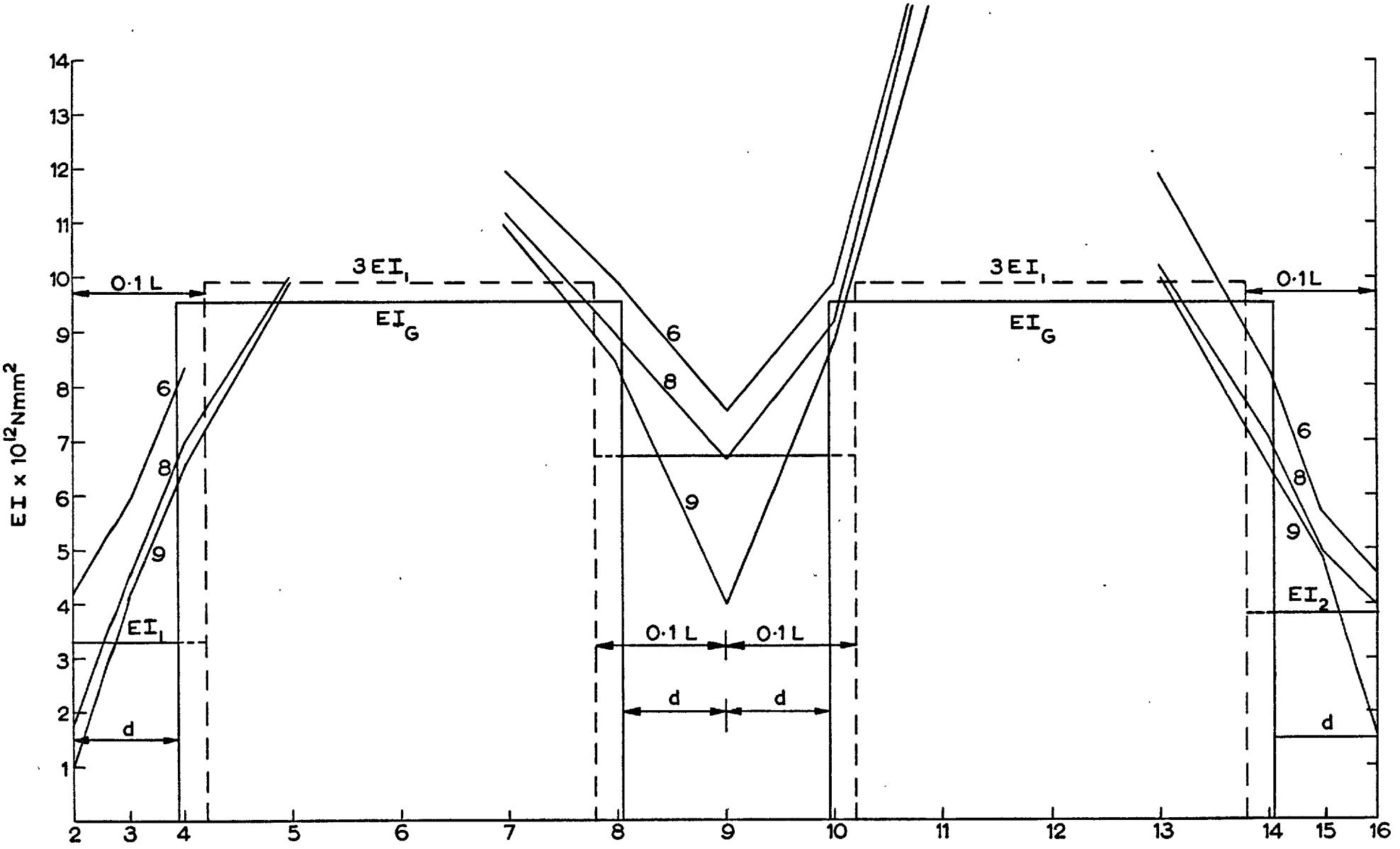


FIG. 5.41 EI DISTRIBUTION. BEAM A6 - LOAD STAGES 6,8,9

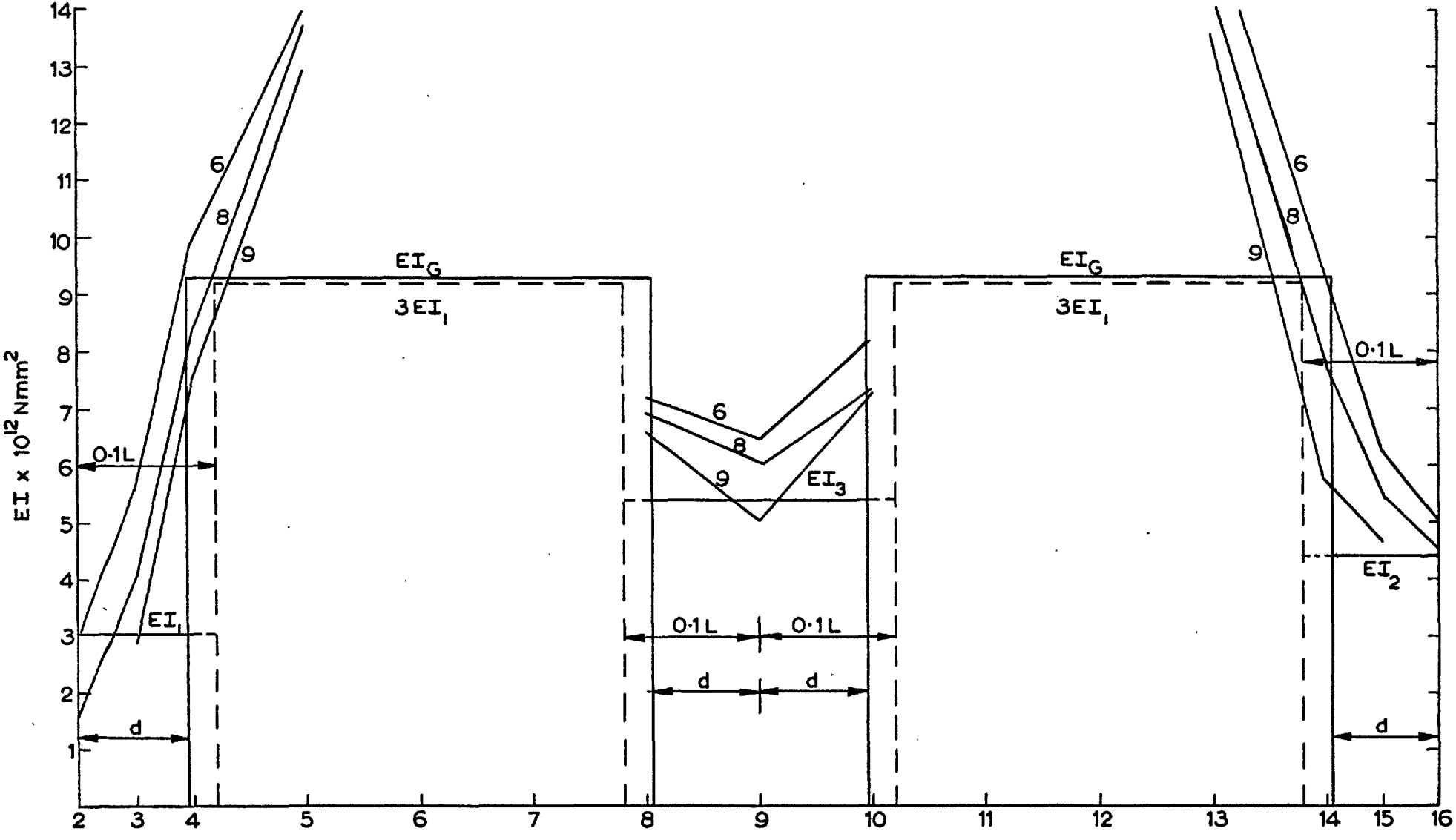


FIG. 5.42 EI DISTRIBUTION. BEAM B1 - LOAD STAGES 6, 8, 9

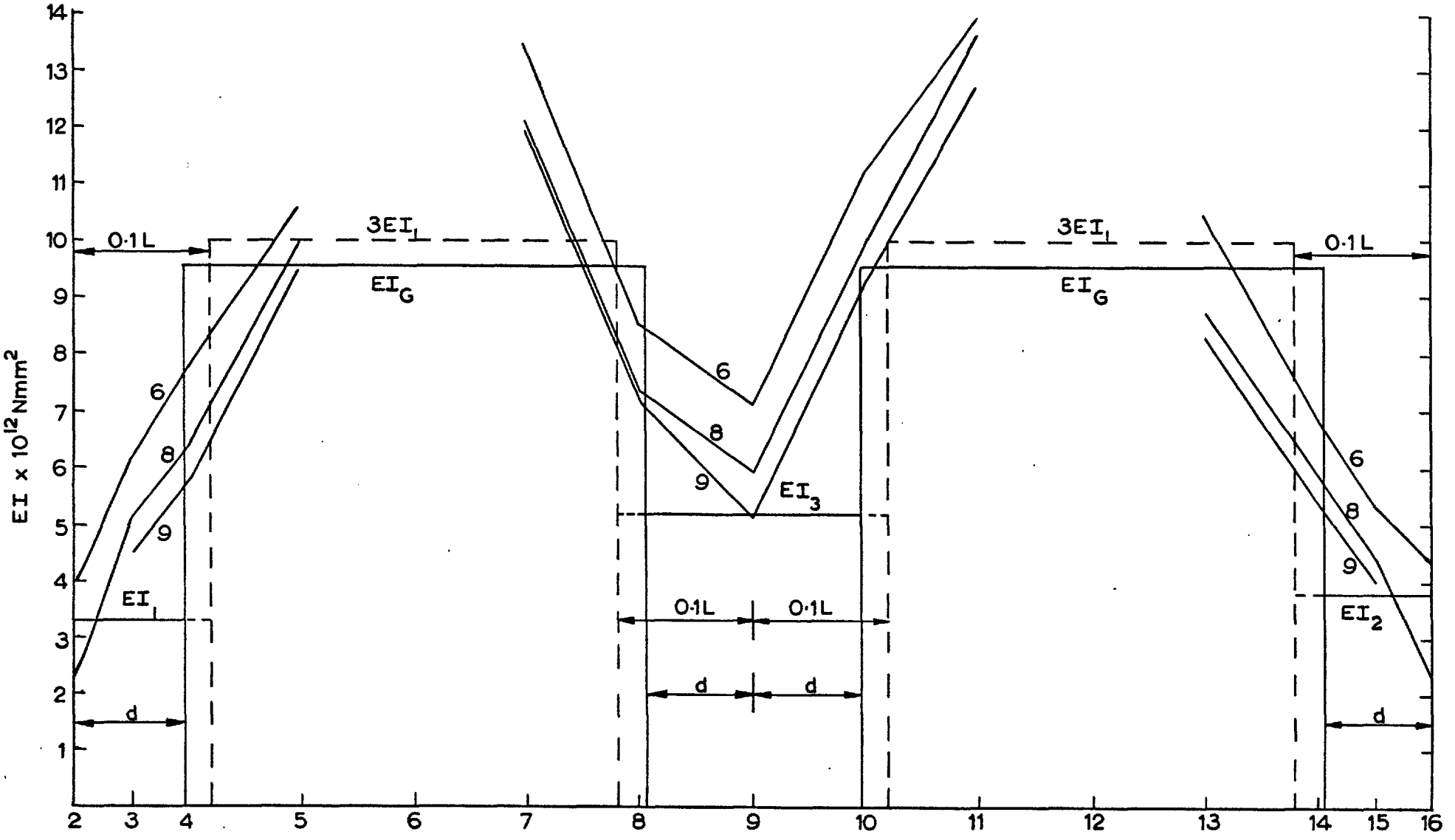


FIG. 5.43 EI DISTRIBUTION BEAM B2 - LOAD STAGES 6, 8, 9

the adjacent sections. (The 'plasticity' mentioned here refers to the attainment of the conditions at limit L_1 discussed in Chapter 2).

5.7. EQUIVALENT EI VALUE

5.7.1. Proposed Models

A study of the EI distribution for the test specimens led to the following two important conclusions:

1. There is a considerable reduction in the value of flexural rigidity at the support and mid-span sections due to inelastic behaviour of these sections near ultimate load.

2. The reduction in flexural rigidity is concentrated over a distance which depends on the spread of plasticity.

Based on the above observations of experimental data a simplified model, shown in Fig. 5.44, is proposed for the EI distribution of T-beams subjected to negative moments at the ends and positive moment at mid-span. It will be shown later that this model is useful for the calculation of equivalent EI to be used in the computation of end rotations of beams in the limit analysis of frames. As illustrated in Fig. 5.44 it is assumed that the EI values are of constant magnitude of EI_1, EI_2 and EI_3 over distances of L_1, L_2 and $2L_3$ and of EI_4 over the remaining length. Thus the EI distribution can be described once the values of these seven parameters are specified.

In the limit design of reinforced concrete frames, as discussed in Chapter 2, the end sections (1) and (2) of beams will be designed for L_2 limit and the section (3) will be designed for L_1 limit. The three sections for all the beams in this test program were also designed for the above conditions. It may be noted that there is a reduction in the EI values at these sections due to inelastic behaviour of these sections at the ultimate load stages. Thus the values of EI_1, EI_2 and EI_3 could be assumed as the corresponding values at the limit L_1 of these sections. Figs. 5.36 to 5.43 show that such an assumption is satisfactory and reasonable.

The values of L_1, L_2 and L_3 depend on the spread of plasticity which in turn depends on the moment gradient, on the effective depth of section and on the percentage of flexural reinforcement for the section. As it

becomes quite complex to take into account all these effects, it has been found desirable to use the experimental evidence to specify the values for L_1, L_2 and L_3. Accordingly the following two sets of values are suggested and these values are plotted in Figs. 5.36 to 5.43.

(i) $L_1 = L_2 = L_3 = d$

(ii) $L_1 = L_2 = L_3 = 0.1L$

The value of EI_4 depends primarily on the effectiveness of T-section in the region $\frac{L}{2} - (L_1 + L_2)$ wherein the nature of moment changes from positive to negative or vice versa. There is a zone in this region in which the moment is less than the cracking moment of the section and hence the entire concrete section is effective in contributing to the overall stiffness of the beam. The detailing of the reinforcement in this region which depends on the flexural shear and bond requirements has considerable influence on the spacing and width of cracks and hence on the rigidity of the beam. Based on this experimental investigation the following two values are proposed.

Case 1. $EI_4 = EI_G$

It is assumed that the value of EI_4 is equal to that of the gross concrete rectangular section of the T-beam as,

$$EI_4 = E_c \times \frac{1}{12} b_r t^3$$

where the modulus of elasticity E_c for concrete can be calculated using the expression given in Codes of Practice.

The values of EI_G for the test specimens are plotted in the EI distribution diagrams, Figs. 5.36 to 5.43, and this assumption is found to be reasonable. It will also be shown later that this assumption gives good agreement between the experimental results and the calculated values for end rotations.

With the above assumption for EI_4, the following values are specified for the seven parameters that define the EI distribution. This model will be referred to as Model Type 1.

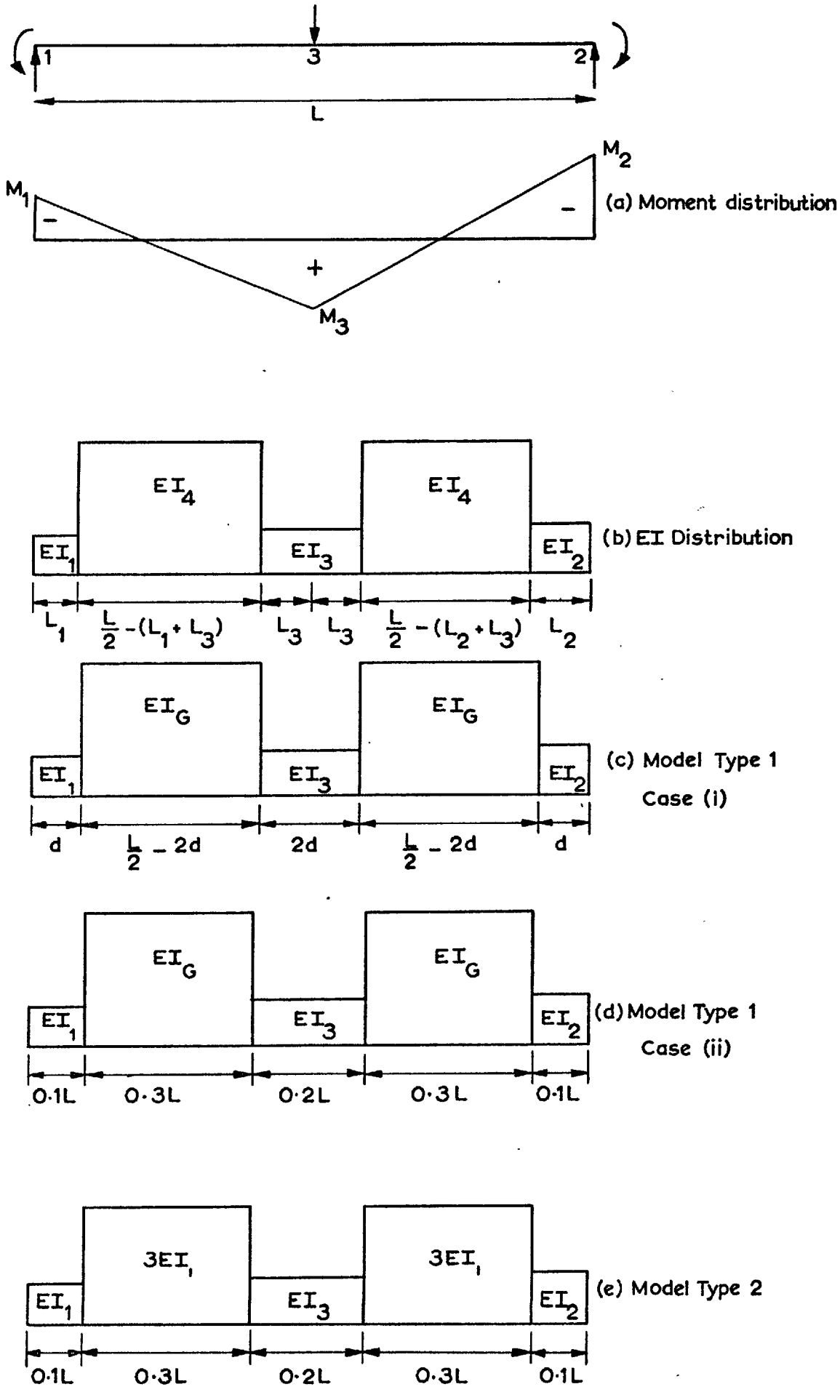


FIG. 5.44 PROPOSED MODELS FOR EI DISTRIBUTION

1. EI_1 = Value of EI at limit L_1 of section 1

   EI_2 = Value of EI at limit L_1 of section 2

   EI_3 = Value of EI at limit L_1 of section 3

2. $EI_4 = E_c \times \frac{1}{12} b_r t^3$

3. (i) $L_1 = L_2 = L_3 = d$

   (ii) $L_1 = L_2 = L_3 = 0.1L$

Case 2 $EI_4 = 3\ EI_1$

$L_1 = L_2 = L_3 = 0.1L$

While the Model Type 1 is satisfactory for analysis it is found desirable to specify the value of EI_4 in terms of one of the critical values of the two support sections 1 and 2. This assumption will aid in the derivation of simplified design expressions for the equivalent EI value. Considering the factors that influence EI_4, discussed above, and also from the experimental data it is found suitable to assume that EI_4 is equal to three times EI_1 (EI_1 corresponds to the end where the value is less than the other end section) along with the condition that $L_1 = L_2 = L_3 = 0.1L$. Thus the simplified design model referred to as Model Type 2 for EI distribution will be specified by the following values:

1. EI_1 = Value of EI at limit L_1 of section 1

   EI_2 = Value of EI at limit L_1 of section 2

   EI_3 = Value of EI at limit L_1 of section 3

2. $EI_4 = 3\ EI_1$ (EI_1 refers to section where $EI_1 < EI_2$)

3. $L_1 = L_2 = L_3 = 0.1L$

Figs. 5.36 to 5.43 with the above values plotted show that this idealisation is a good approximation to the actual EI distribution.

5.7.2. Derivation of Expressions

Fig. 5.44 shows the EI distribution according to the assumptions of Model Type 2. For convenience in the derivation of expressions the moments at sections 2 and 3 and the values of EI_2, EI_3 and EI_4 are expressed

as the ratios of the corresponding values at section 1. Thus,

$$R_1 = 1 \; ; \; R_2 = \frac{M_2}{M_1} \; ; \; R_3 = \frac{M_3}{M_1}$$

$$F_1 = 1 \; ; \; F_2 = \frac{EI_2}{EI_1} \; ; \; F_3 = \frac{EI_3}{EI_1} \; ; \; F_4 = \frac{EI_4}{EI_1} \qquad (5.25)$$

For a beam with uniform EI the rotations θ_1 and θ_2 at the ends 1 and 2 are given by,

$$\theta_1 = \frac{L}{24EI} (6M_3 - M_2 - 5M_1)$$

$$= \frac{M_1 L}{24EI} (6R_3 - R_2 - 5) \qquad (5.26)$$

$$\theta_2 = \frac{L}{24EI} (6M_3 - 5M_2 - M_1)$$

$$= \frac{M_1 L}{24EI} (6R_3 - 5R_2 - 1) \qquad (5.27)$$

Case 1 $\qquad R_1 = R_2 = 1 \quad (M_1 = M_2)$

For a beam with the EI distribution shown in Fig.5.44 the end rotation θ_1 $(= \theta_2)$ can be calculated using the Simpson's rule of integration. Thus,

$$\theta_1 = \frac{M_1 L}{6EI_1} \left[- 0.540 + 0.06 R_3 + \frac{-0.90 + 0.90 R_3}{F_4} + \frac{-0.06 + 0.54 R_3}{F_3} \right] \qquad (5.28)$$

Assuming $F_4 = 3$, (Model Type 2) the above expression becomes,

$$\theta_1 = \frac{M_1 L}{6EI_1} \left[- 0.84 + 0.36 R_3 + \frac{-0.06 + 0.54 R_3}{F_3} \right]$$

$$= \frac{M_1 L}{6EI_1} \left[(-0.84 - \frac{0.06}{F_3}) + (\frac{0.54}{F_3} + 0.36)\, R_3\right] \qquad (5.29)$$

The above expression can be simplified without significant error (confirmed with experimental results) as,

$$\theta_1 = \frac{M_1 L}{6EI_1} \left[-0.9 + (0.4 + \frac{0.5}{F_3})\ R_3\right] \qquad (5.30)$$

From equation (5.26) the rotation θ_1 for the case of uniform EI (EI_e) is given by,

$$\theta_1 = \frac{M_1 L}{4EI_e} (R_3 - 1) \qquad (5.31)$$

Equating the expressions (5.30) and (5.31) the equivalent EI is given by,

$$EI_e = EI_1 \frac{1.5\ (R_3 - 1)}{(0.4 + \frac{0.5}{F_3})\ R_3 - 0.9} \qquad (5.32)$$

Dividing the numerator and denominator by $(R_3 - 1)$ and simplifying,

$$EI_e = \frac{1.5}{(0.4 + \frac{0.5}{F_3}) - \frac{(0.5 - \frac{0.5}{F_3})}{(R_3 - 1)}} \qquad (5.33)$$

In order to reduce the asymptotic nature of the above equation the expression in the denominator is expanded as a binomial series and the following two equations are suggested for the calculation of equivalent EI.

$R_3 < 1$

$$EI_e = EI_1 \frac{1.5}{(0.4 + \frac{0.5}{F_3}) + (0.5 - \frac{0.5}{F_3})(1 + R_3 + R_3^2 + R_3^3 + R_3^4)} \qquad (5.34)$$

$R_3 > 1$

$$EI_e = EI_1 \frac{1.5}{(0.4 + \frac{0.5}{F_3}) - \frac{(0.5 - \frac{0.5}{F_3})}{R_3}(1 + \frac{1}{R_3} + \frac{1}{R_3^2} + \frac{1}{R_3^3} + \frac{1}{R_3^4})} \qquad (5.35)$$

Case 2 $R_2 > 1 \quad (M_2 > M_1)$

The end rotation θ_2 can be calculated as before and is given by,

$$\theta_2 = \frac{M_1 L}{6EI_1} \left[(-0.026 + 0.004 R_3) + \frac{(-0.198 + 0.90 R_3 - 0.702 R_2)}{F_4} \right.$$

$$+ \frac{(-0.026 - 0.034 R_2 + 0.54 R_3)}{F_3}$$

$$\left. + \frac{(-0.514 R_2 + 0.056 R_3)}{F_2} \right] \qquad (5.36)$$

Assuming $F_4 = 3$ the above equation becomes,

$$\theta_2 = \frac{M_1 L}{6EI_1} \left[\left(0.304 + \frac{0.056}{F_2} + \frac{0.54}{F_3}\right) R_3 - \right.$$

$$\left. \left(0.234 + \frac{0.514}{F_2} + \frac{0.034}{F_3}\right) R_2 - \left(0.092 + \frac{0.026}{F_3}\right) \right] \qquad (5.37)$$

The above expression can be approximated to the following equation without significant error, which is confirmed by experimental results.

$$\theta_2 = \frac{M_1 L}{6EI_1} \left[\left(0.4 + \frac{0.5}{F_3}\right) R_3 - \left(\frac{0.6}{F_2} + 0.3\right) R_2 \right] \qquad (5.38)$$

For $R_2 = 1$ and $F_2 = 1$ (i.e. case 1) the above equation reduces to,

$$\theta_2 = \theta_1 = \frac{M_1 L}{6EI_1} \left[\left(0.4 + \frac{0.5}{F_3}\right) - 0.9 \right] \qquad (5.39)$$

The equation (5.39) is exactly the same as the one derived for case 1. (Equation (5.32)).

From equation (5.27) the rotation θ_2 for a beam with uniform EI (EI_e) is given by,

$$\theta_2 = \frac{M_1 L}{24EI_e} (6R_3 - 5R_2 - 1)$$

$$= \frac{M_1 L}{4EI_e} (R_3 - \frac{5}{6} R_2 - \frac{1}{6})$$

$$= \frac{M_1 L}{4EI_e} [R_3 - \frac{5}{6} (R_2 - 1) - 1]$$

$$\theta_2 = \frac{M_1 L}{4EI_e} (R_{3e} - 1) \qquad (5.40)$$

where $R_{3e} = R_3 - \frac{5}{6} (R_2 - 1)$ (5.41)

Equating the expressions (5.38) and (5.40) the equivalent EI is given by,

$$EI_e = EI_1 \frac{1.5(R_{3e} - 1)}{(0.4 + \frac{0.5}{R_3}) R_3 - (\frac{0.6}{F_2} + 0.3) R_2} \qquad (5.42)$$

Substituting for R_3 from equation (5.41) the above equation becomes,

$$EI_e = EI_1 \frac{1.5(R_{3e} - 1)}{[(0.4 + \frac{0.5}{F_3}) R_{3e} + \frac{5}{6} (R_2 - 1)(0.4 + \frac{0.5}{F_3}) - (\frac{0.6}{F_2} + 0.3) R_2]} \qquad (5.43)$$

Assuming $\frac{R_2}{F_2} = 1$, the following equation is suggested for the calculation of equivalent EI. This result will be verified with the experimental data.

$$EI_e = EI_1 \frac{1.5 (R_{3e} - 1)}{(0.4 + \frac{0.5}{R_3}) R_{3e} - 0.9 + \frac{2.5}{6F_3} (R_2 - 1)} \qquad (5.44)$$

Dividing the numerator and denominator by $(R_{3e} - 1)$ and adopting the procedure similar to case 1 the following equations are suggested for the calculation of equivalent EI.

Case 1 $\quad R_{3e} < 1$

$$EI_e = \frac{1.5}{(0.4 + \frac{0.5}{F_3}) - [\frac{2.5}{6F_3}(R_2 - 1) - (0.5 - \frac{0.5}{F_3})]} \times [1 + R_{3e} + R_{3e}^2 + R_{3e}^3 + R_{3e}^4] \qquad (5.45)$$

Case 2 $\quad R_{3e} > 1$

$$EI_e = \frac{1.5}{(0.4 + \frac{0.5}{F_3}) + \frac{[\frac{2.5}{6F_3}(R_2 - 1) - (0.5 - \frac{0.5}{F_3})]}{R_{3e}}} \times [1 + \frac{1}{R_{3e}} + \frac{1}{R_{3e}^2} + \frac{1}{R_{3e}^3} + \frac{1}{R_{3e}^4}] \qquad (5.46)$$

5.7.3. Comparison of Experimental Results

Table 5.3 gives the details of the ratios of EI values and the ratios of moments that correspond to the load stage just prior to the yielding of one of the critical sections.

In order to verify the adequacy of the proposed model for the EI distribution which could be used for a rigorous analysis, the theoretical end rotations are calculated using the Model Type 1 proposed in section 5.7.1. The following two cases are considered:

Case (i) $\quad L_1 = L_2 = L_3 = d$

Case (ii) $\quad L_1 = L_2 = L_3 = 0.1L$

The calculated and experimental values of rotations are compared in Table 5.4 for all the eight beams. The value of rotations calculated assuming a constant value of EI_1 are also given therein.

TABLE 5.3 RATIOS OF EI VALUES AND MOMENTS

Beam	EI_1 $\times 10^{12}$ Nmm^2	EI_4 $\times 10^{12}$ Nmm^2	F_2	F_3	F_4	Load Stage	R_1	R_2	R_3
A1	4.42	10.25	1.0	1.017	2.312	10	1.0	1.0	0.917
A2	3.18	9.8	1.387	1.487	3.08	8	1.0	1.55	1.11
A3	3.87	10.1	1.0	1.164	2.607	8	1.0	1.0	0.855
A4	3.13	9.9	1.276	1.487	3.163	8	1.0	1.27	1.09
A5	3.17	9.7	1.0	2.706	3.063	8	1.0	1.0	1.813
A6	3.33	9.55	1.14	2.01	2.868	8	1.0	1.255	1.383
B1	3.06	9.28	1.44	1.79	3.035	8	1.0	1.44	1.07
B2	3.32	9.55	1.14	1.56	2.876	8	1.0	1.32	1.15

TABLE 5.4. RESULTS OF OBSERVED AND CALCULATED ROTATIONS

Beam	Section	$\theta_{obs.}$ radians	θ_{UEI_1} radians	Model Type 1	
				Case (i) θ_{cal} radians	Case (ii) θ_{cal} radians
A1	2	-0.00040	-0.00094	-0.00062	-0.00067
	16	-0.00040	-0.00094	-0.00062	-0.00067
A2	2	-0.00022	+0.00018	-0.00078	-0.00095
	16	-0.00210	-0.00385	-0.00200	-0.00220
A3	2	-0.00120	-0.00170	-0.00140	-0.00153
	16	-0.00120	-0.00170	-0.00140	-0.00153
A4	2	-0.00043	+0.00053	-0.00075	-0.00093
	16	-0.00100	-0.00160	-0.00120	-0.00130
A5	2	+0.00180	+0.01030	+0.00150	+0.00120
	16	+0.00180	+0.01030	+0.00150	+0.00120
A6	2	+0.00040	0.00400	+0.00010	-0.00010
	16	-0.00030	+0.00200	-0.00070	-0.00090
B1	2	-0.00020	0.0	-0.00100	-0.00150
	16	-0.00222	-0.00380	-0.00230	-0.00250
B2	2	-0.00032	+0.00117	-0.00057	-0.00070
	16	-0.00122	-0.00143	-0.00168	-0.00190

TABLE 5.5. COMPARISON OF OBSERVED AND CALCULATED ROTATIONS USING EQUIVALENT EI

Beam	Critical Section	θ_{obs} radians	$\frac{EI_e}{EI_1}$	$\theta_{cal} = \frac{\theta_{UEI_1}}{(\frac{EI_e}{EI_1})}$ radians	$\frac{\theta_{obs}}{\theta_{cal}}$
A1	2 & 16	-0.00040	1.64	-0.00057	0.70
A2	16	-0.00210	1.85	-0.00208	1.01
A3	2 & 16	-0.00120	1.40	-0.00122	0.98
A4	16	-0.00100	1.38	-0.00116	0.86
A5	2 & 16	0.00180	3.0	+0.00343	0.53 *
A6	16	-0.00030	3.0	+0.00067	- **
B1	16	-0.00220	1.55	-0.00245	0.90
B2	16	-0.00120	1.30	-0.00110	1.09

* Beam A5 - Maximum value of $\frac{EI_e}{EI_1} = 3$ is used.

** Beam A6 - Maximum value of $\frac{EI_e}{EI_1} = 3$ is used. The signs of rotations θ_{obs} and θ_{cal} are different.

It can be observed from Table 5.4 that the assumption of uniform EI, may lead to erroneous results depending on the gradient of the moment diagram. In the case of beams (A2, A4, B2) with unequal end moments ($M_2 > M_1$) the nature of rotations are also found to be different from that calculated based on the assumption of constant EI. This confirms the earlier discussion in section 5.7.1 that uniform EI distribution cannot be assumed in the case of beams with varying nature of moment distribution.

The values of end rotations calculated on the basis of Model Type 1 compares reasonably well with the observed values given in Table 5.4. As discussed earlier the values of L_1, L_2 and L_3 depend, amongst other factors, on the spread of plasticity and on the gradient of the moment diagram. This explains the reason for the difference in agreement between the observed and calculated values of rotations for cases 1 and 2. Based on the above observations of this test programme it can be concluded that Model Type 1 with proper choice of L_1, L_2 and L_3 depending on the moment gradient is a good approximation to the actual EI distribution. Further this model can be used for a rigorous frame analysis which treats the members with non-uniform EI distribution.

It is also found desirable to compare the experimental results with the calculated values based on the design Model Type 2 suggested in section 5.7.1. Thus the equivalent EI_e values are calculated using the equations (5.45 and 5.46). These values and the rotations θ_{cal} calculated on the assumption of constant value of EI_e along the beam are given in Table 5.5. A reasonable agreement between the calculated and the observed values show that in the absence of a rigorous analysis using Model Type 1 the equivalent EI_e could be used for the calculation of end rotations.

5.7.4. Proposed Design Procedure

In the last section it has been concluded that for the calculation of end rotations the actual non-uniform EI distribution can be replaced by an equivalent EI_e assumed to be constant along the beam and that the value of EI_e can be calculated using the following equations derived in section 5.7.2.

$R_{3e} < 1$

$$EI_e = \frac{1.5}{(0.4 + \frac{0.5}{F_3}) - [\frac{2.5}{6F_3}(R_2 - 1) - (0.5 - \frac{0.5}{F_3})]\,[1 + R_{3e} + R_{3e}^2 + R_{3e}^3 + R_{3e}^4]} \qquad (5.45)$$

$R_{3e} > 1$

$$EI_e = \frac{1.5}{(0.4 + \frac{0.5}{F_3}) + \frac{[\frac{2.5}{6F_3}(R_2 - 1) - (0.5 - \frac{0.5}{F_3})]}{R_{3e}}} \times$$

$$[1 + \frac{1}{R_{3e}} + \frac{1}{R_{3e}^2} + \frac{1}{R_{3e}^3} + \frac{1}{R_{3e}^4}] \qquad (5.46)$$

where $R_{3e} = R_3 - \frac{5}{6}(R_2 - 1)$

Figs. 5.45 to 5.49 show the graphical plot of the above equations for values of R_2 ranging from 1.0 to 2.0. Based on this investigation a maximum value of $\frac{EI_e}{EI_1} = 3$ is suggested for use in designs even though larger values are possible for certain values of R_3, F_3 and R_2.

For the case of $R_{3e} < 1$ in the region above the line 'CC' there is an increase in the value of $\frac{EI_e}{EI_1}$ with an increase in the value of R_3. This is due to the rotation calculated on the basis of non-uniform EI distribution is less than the value calculated on the basis of constant EI_1. But for the same value of R_3 an increase in the value of F_3 makes the mid-span region of the beam stiffer resulting in an increased end rotation and a consequent reduction in the value of $\frac{EI_e}{EI_1}$. This explains the decrease in the value of $\frac{EI_e}{EI_1}$ with increase in the value of R_3 in the region below the line 'CC'.

The above trends are reversed for the case of $R_{3e} > 1$. In this case practical considerations of design of sections and detailing of reinforcement may be such that it may not be required to use the theoretical curves below the line 'CC' and hence are shown in dotted lines in the Figs. 5.45 to 5.49.

For $R_{3e} = 1$ there are two values of $\frac{EI_e}{EI_1}$ for a particular value of F_3. This is due to the approximation involved in the equations (5.45) and (5.46) defined for $R_{3e} < 1$ and $R_{3e} > 1$. Though it may seem contradictory, it can be observed that for $R_{3e} = 1$ the rotation corresponding to a constant EI is zero. Hence either one of the value could be used without any error.

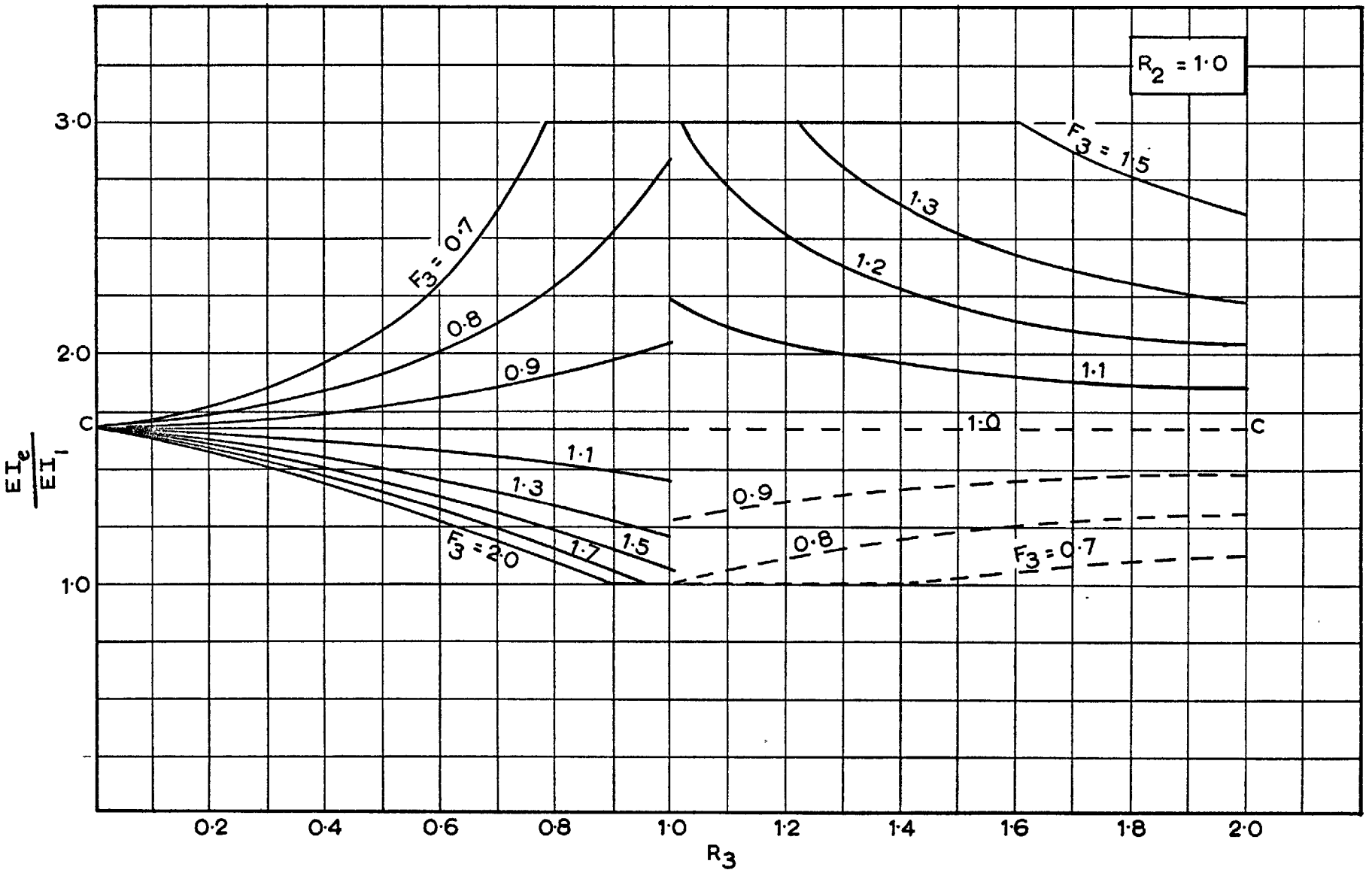


FIG. 5.45 DESIGN CHART FOR EQUIVALENT EI

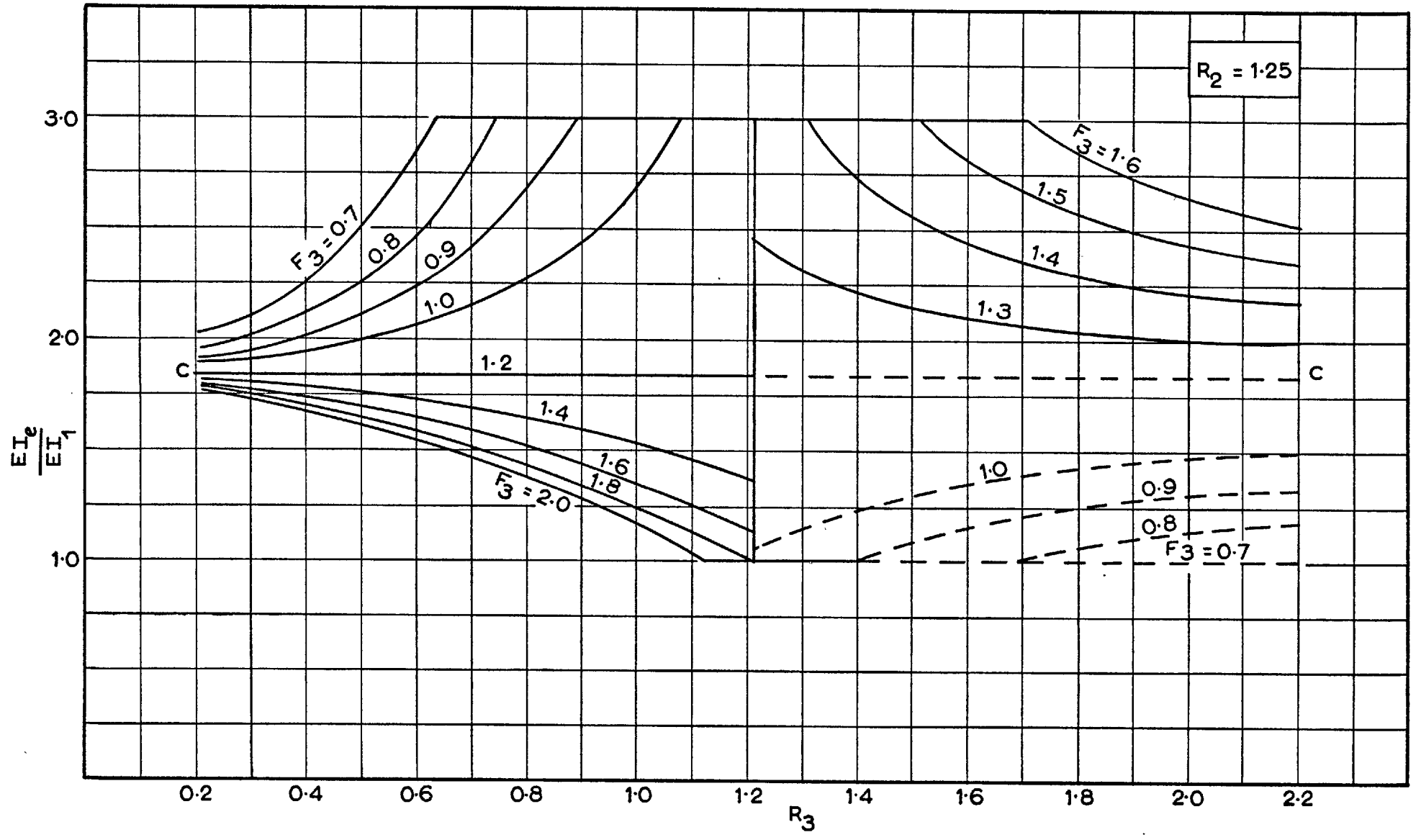


FIG. 5.46 DESIGN CHART FOR EQUIVALENT EI

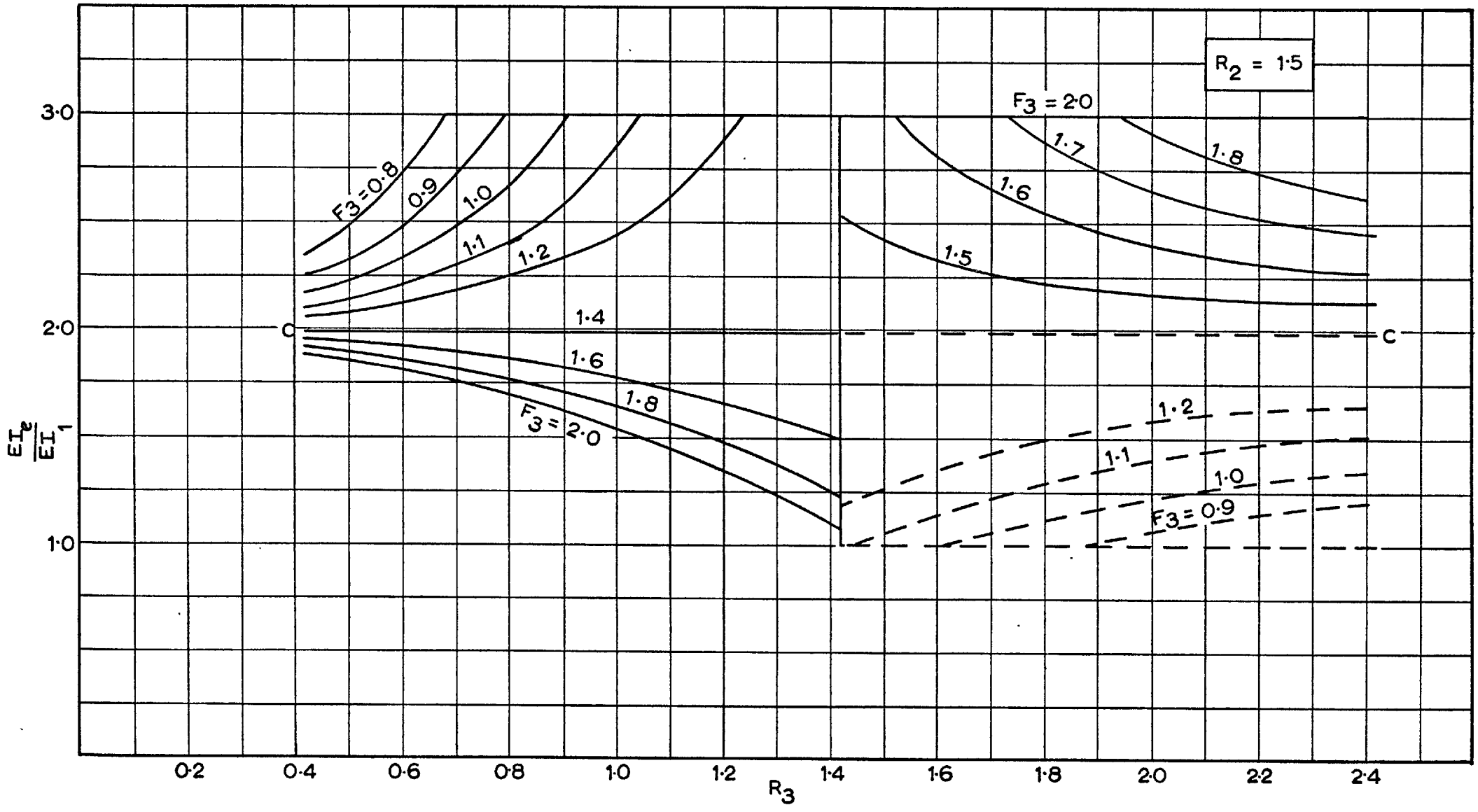


FIG. 5.47 DESIGN CHART FOR EQUIVALENT EI

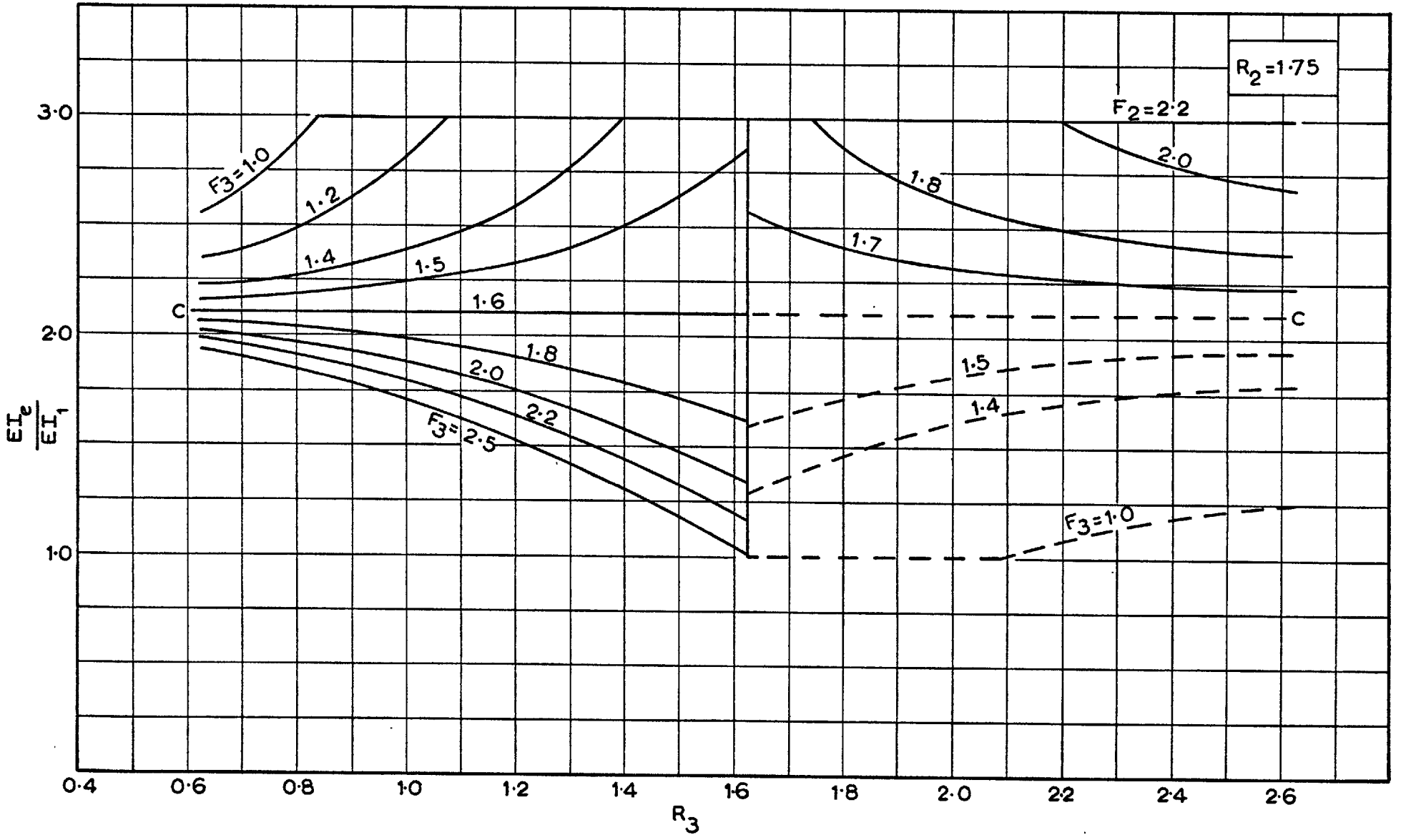


FIG. 5.48 DESIGN CHART FOR EQUIVALENT EI

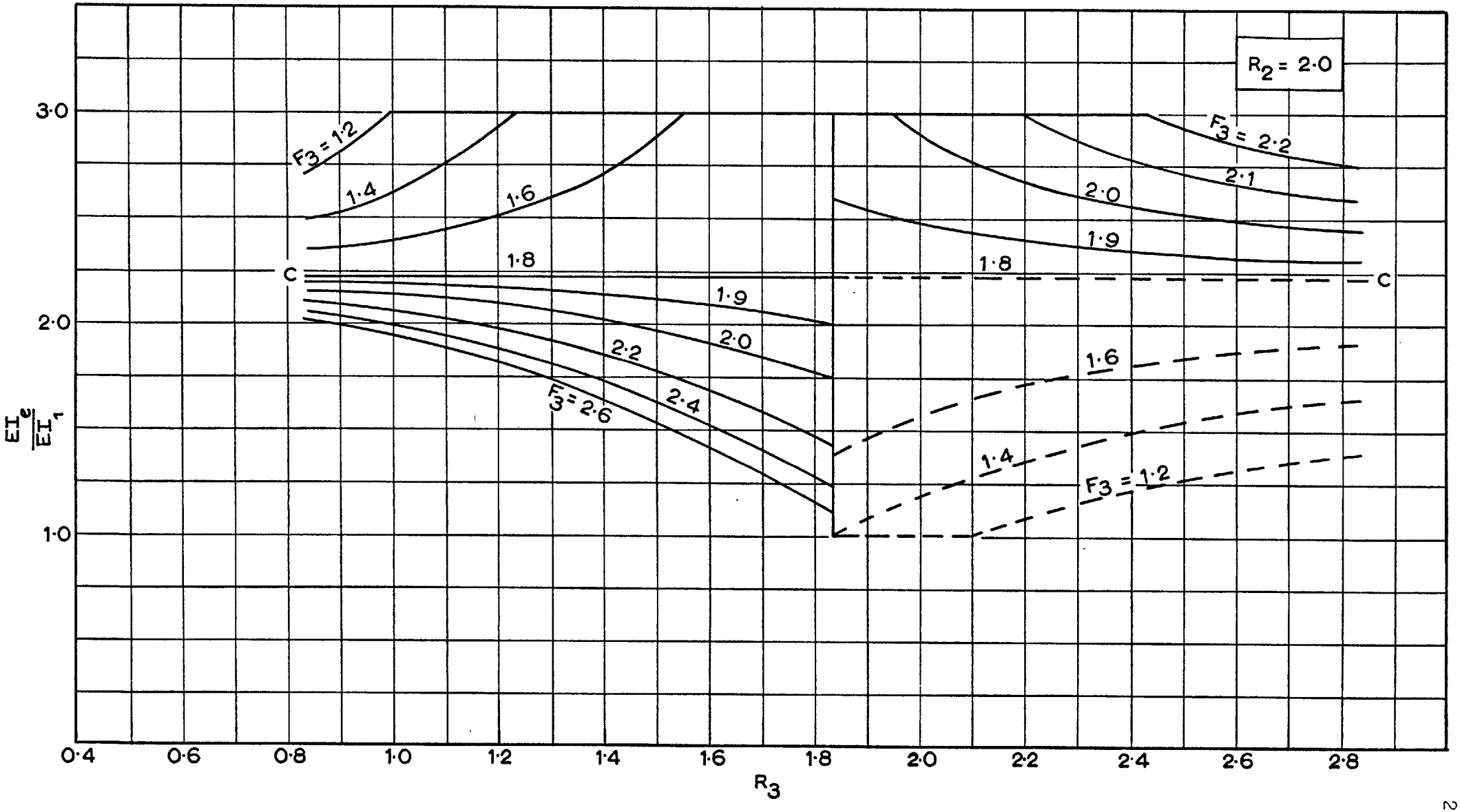


FIG. 5.49 DESIGN CHART FOR EQUIVALENT EI

The following procedure is suggested for the calculation of equivalent EI using the design charts described above:

1. Calculate the values of EI at Limit L_1 for the end (1 and 2) and mid-span (3) sections using the design charts such as those given in Figs. 5.16 to 5.18.

2. Compute (i) the ratio of moments at the ends (R_2) and the ratio of moments at mid-span (R_3) to one of the critical end section.

   (ii) the ratio of EI values at mid-span to one of the critical end section (F_3).

3. Knowing the values of R_2, R_3 and F_3 from above, use the appropriate design charts given in Figs. 5.45 to 5.49 to find the value of $\frac{EI_e}{EI_1}$ and hence determine the value of equivalent EI (EI_e).

The value of equivalent EI computed as above can be used in frame analysis for the calculation of end rotations of T-beams subjected to negative moments at the ends and positive moment at mid-span.

CHAPTER SIX

OPTIMAL LIMIT DESIGN EXAMPLES

6.1. INTRODUCTION

In this Chapter the application of the proposed optimal limit design method to practical cases of design will be described. Six design examples of reinforced concrete frames of different geometry and loading conditions are presented. The optimal limit design program explained in Chapter 4 has been used for the analysis of these frames. The salient details of design and the expressions used in the program for the calculation of percentage of reinforcement and inelastic rotation capacity of sections, are described.

The frames have been analysed for optimal solution for three cases of hinge pattern under two loading conditions. The results of analysis for the distribution of bending moment and plastic hinge pattern are discussed. The economical merits of optimal limit design compared to ultimate strength design based on elastic analysis for factored loads is discussed for different cases of hinge pattern.

In order to study the effect of variation of flexural rigidity of beams due to T-beam action two of the examples have been reworked using the equivalent EI_e values for beams. The results of analysis and the saving of steel reinforcement are compared with the analysis based on uniform EI values for beams.

For the cases of sway frames susceptible to instability effects the mangification to lateral loads suggested by a recent investigation can be used in optimal limit design. This is illustrated by two of the design examples.

6.2. OBJECTIVE FUNCTION

In the optimal design of reinforced concrete frames as discussed in Chapter 3 the objective function represents the total volume of steel reinforcement for the frame. The formulation of objective function involves in determining the area of steel reinforcement for critical

sections using linear functions of the type given by equations (3.36) and (3.37). The steel reinforcement for a critical section is assumed to be extended over an 'equivalent length'. The piecewise linear approximations to the design charts given in Reference (12) which are used in the optimal design examples are described below.

6.2.1. Area of Reinforcement

The computation charts given in Reference (12) are based on the stress-strain curves for concrete and steel given in Fig. 2.2. These design charts are in general non-linear. For the case of beams, since the variables are only $\frac{M_d^j}{\sigma_b bd^2}$ and $p\frac{\sigma_{al}}{\sigma_b}$, linear approximation to the design curves can be made directly. But for columns the calculation of area of reinforcement involves additional variable $\frac{P}{\sigma_b bd}$ due to the axial load. Hence in this case the design charts are replotted with $\frac{M}{\sigma_b bd^2}$ and $p\frac{\sigma_{al}}{\sigma_b}$ as variables for constant values of $\frac{P}{\sigma_b bd}$, and the resulting curves are used to arrive at design expressions which are close and safe approximation to the actual design charts. Based on this study the following equations have been found suitable for use in the optimal design program.

Grade of steel: $\sigma_{al} = 415\ N/mm^2$

Beams:

Rectangular sections

$$\frac{M_d^j}{\sigma_b bd^2} \leq 0.15 \quad \ldots \quad p\frac{\sigma_{al}}{\sigma_b} = \frac{M_d^j}{\sigma_b bd^2} \qquad (6.1)$$

$$\frac{M_d^j}{\sigma_b bd^2} \geq 0.15 \quad \ldots \quad p\frac{\sigma_{al}}{\sigma_b} = 1.4\,\frac{M_d^j}{\sigma_b bd^2} - 0.06 \qquad (6.2)$$

T-sections

$$\frac{M_d^j}{\sigma_b bd^2} \leq 0.15 \quad \ldots \quad p\frac{\sigma_{al}}{\sigma_b} = 1.1\,\frac{M_d^j}{\sigma_b bd^2} \qquad (6.3)$$

Columns:

Tension developed

$$0.1 < \frac{P}{\sigma_b bd} \leq 0.4 \quad \ldots \quad p\frac{\sigma_{al}}{\sigma_b} = 1.25\left(\frac{M_d^j}{\sigma_b bd^2} - 0.08\right) \qquad (6.4)$$

$$0.4 < \frac{P}{\sigma_b bd} \leq 0.8 \quad \ldots \quad p\frac{\sigma_{al}}{\sigma_b} = 1.5\left(\frac{M_d^j}{\sigma_b bd^2} - 0.226 + 0.2\frac{P}{\sigma_b bd}\right) \qquad (6.5)$$

$$0.8 < \frac{P}{\sigma_b bd} \leq 1.0 \quad \ldots \quad p\frac{\sigma_{al}}{\sigma_b} = 1.5\left(\frac{M_d^j}{\sigma_b bd^2} - 0.257 + 0.25\frac{P}{\sigma_b bd}\right) \qquad (6.6)$$

No tension developed

$$1.0 < \frac{P}{\sigma_b bd} \leq 1.8 \quad \ldots \quad p\frac{\sigma_{al}}{\sigma_b} = \frac{2M_d^j}{\sigma_b bt^2} + 0.55\left(\frac{P}{\sigma_b bd} - 1.0\right) \qquad (6.7)$$

6.3. INELASTIC ROTATION CAPACITY OF R.C. MEMBERS

It has been observed in Chapter 2 that the design curves of Fig.2.3 due to Baker and Amarakone (10) could be used for the calculation of rotation capacity of reinforced concrete members. In the linear programming formulation of optimal design of reinforced concrete frames it is required to express the rotation capacity of sections in the following form:

$$\theta_p^r = B_1^r + B_2^r M_d^r$$

Hence before linear approximations can be made directly to the curves of Fig. 2.3 suitable linear equations for the depth of neutral axis have to be obtained through a graphical plot of $\frac{M_d^j}{\sigma_b bd^2}$ vs n_2 for various values of $\frac{P}{\sigma_b bd}$ using the design curves given in Reference (12). These results are combined with Fig.2.3 and the following equations have been found to give satisfactory results for the inelastic rotation capacity on one side of critical section for members with no binders (p" = 0).

Beams

$$\theta_p^r = 0.2 - \frac{10}{231}\,\frac{M_d^j}{\sigma_b bd^2} \qquad (6.8)$$

Columns

$$\frac{P}{\sigma_b bd} \leq 0.2 \quad \ldots \quad \theta_p^r = 0.01 - \frac{M_d^j}{1000\ Pd} \tag{6.9}$$

$$0.2 < \frac{P}{\sigma_b bd} \leq 0.4 \quad \ldots \quad \theta_p^r = 0.003 + \frac{M_d^j}{1000\ Pd} \tag{6.10}$$

$$\frac{P}{\sigma_b bd} > 0.4 \quad \ldots \quad \theta_p^r = 0.002 + \frac{M_d^j}{1000\ Pd} \tag{6.11}$$

6.4. NOTES ON DESIGN AND ANALYSIS

Six reinforced concrete frames have been designed using the optimal limit design method proposed in Chapter 3 and the computer program described in Chapter 4. Fig. 6.1 shows the geometry, member sizes and the numbering of the critical sections of the frames.

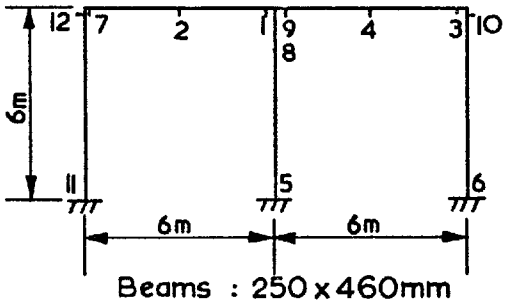
The optimal limit design program requires as input data, the sizes and EI values of the members of the frame. Hence it will be necessary to carry out a preliminary design of the frame. The recommendations made for the ultimate load design of reinforced concrete frames have been followed and found to be useful and efficient for such preliminary designs as well. The EI values of the members have been calculated for the conditions at limit L_1 of the critical sections according to the simplified limit method explained in Chapter 2. The EI values of the members of all the six frames are marked in Fig. 6.2.

The frames have been designed for the working loads given in Table 6.1. The overload factors recommended by Draft British Standard Code of Practice (62) have been used in general for the analysis of optimal designs. But for loading condition I an overload factor of 1.25 has been adopted instead of 1.2 for wind load to simplify the calculations for serviceability factors as explained in Chapter 3. Thus the following two loading conditions have been considered:

Loading Condition I : $1.25\ (W_D + W_L + W_W)$

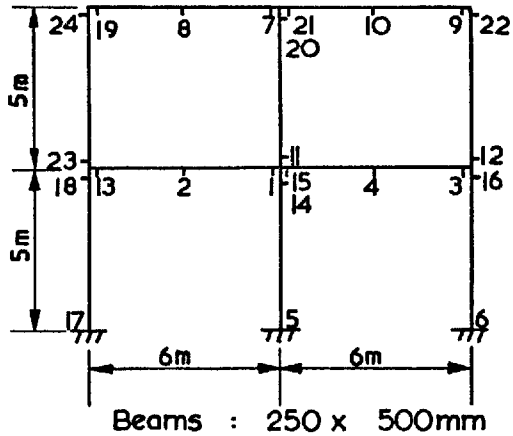
Loading condition II : $1.4\ W_D + 1.6\ W_L$

In addition to the overload factors, material strength factors have also been considered in the designs. Following the CEB Recommendations (63)



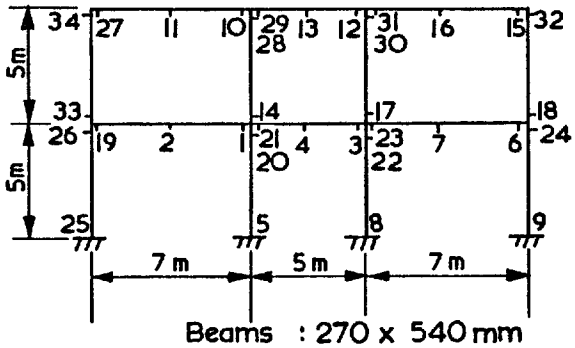
Beams : 250 x 460mm
Columns : 250 x 250mm

EXAMPLE 1



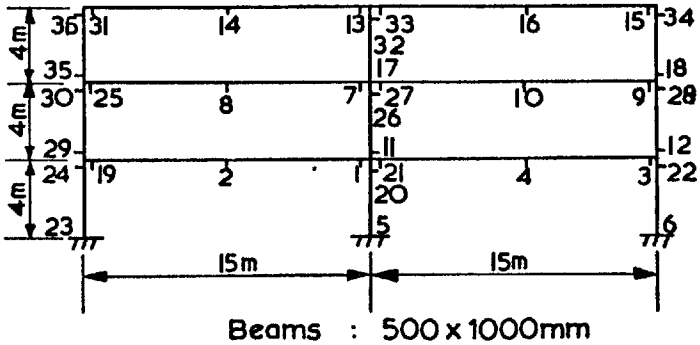
Beams : 250 x 500mm
Columns : 250 x 250 mm

EXAMPLE 2



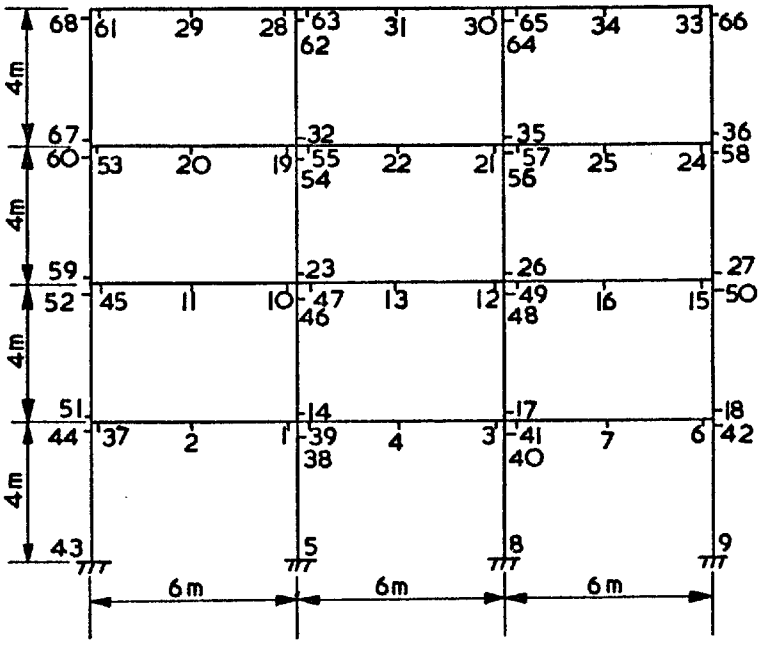
Beams : 270 x 540 mm
Columns : 270 x 270 mm

EXAMPLE 3



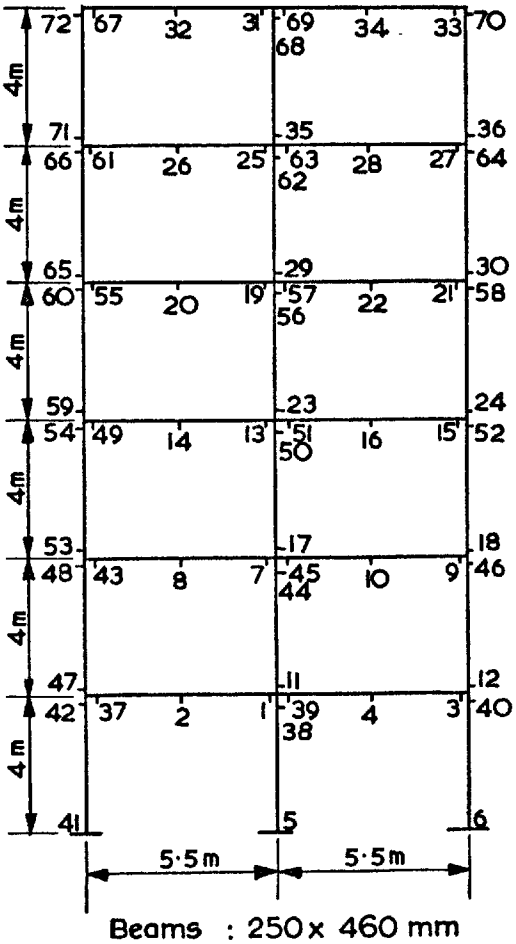
Beams : 500 x 1000mm
Columns : 500 x 700 mm

EXAMPLE 4



Beams : 250 x 450 mm
Columns : 250 x 250 mm

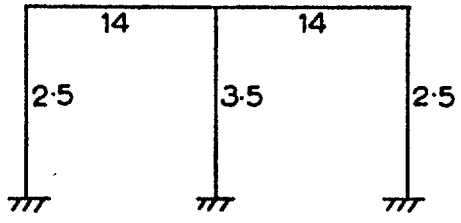
EXAMPLE 5



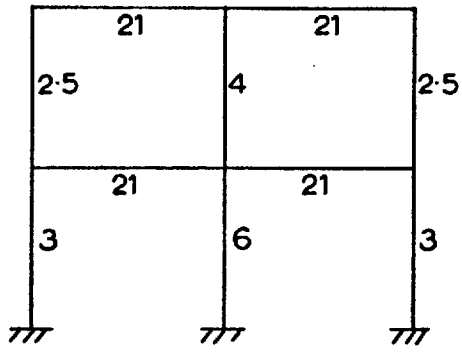
Beams : 250 x 460 mm
Columns : 250 x 250 mm

EXAMPLE 6

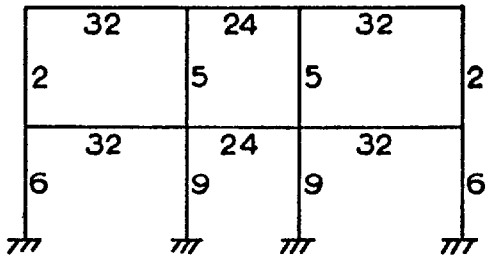
FIG. 6.1 OPTIMAL DESIGN EXAMPLES



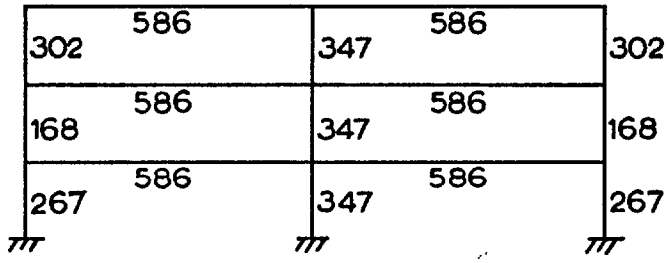
EXAMPLE 1



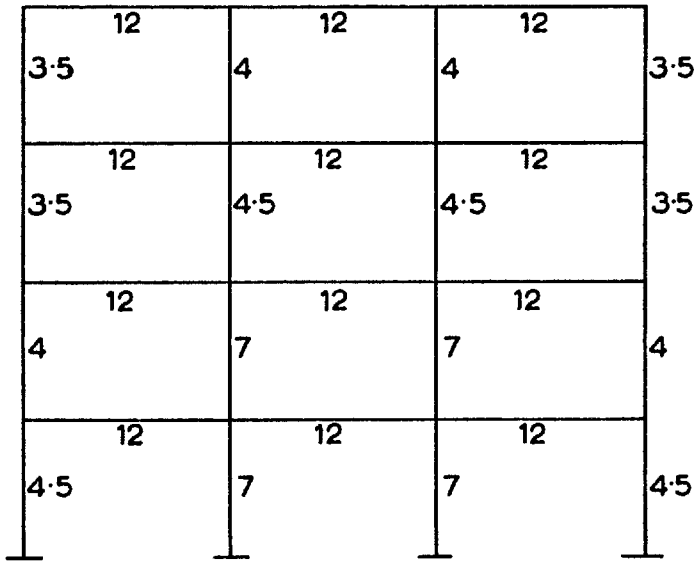
EXAMPLE 2



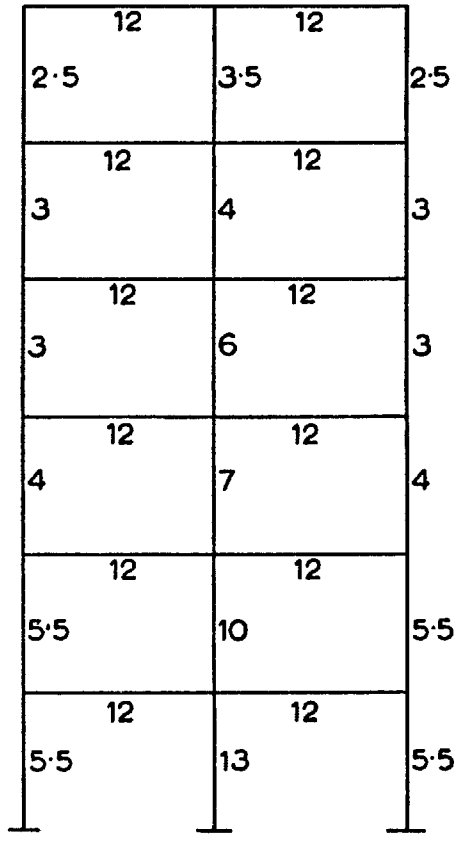
EXAMPLE 3



EXAMPLE 4



EXAMPLE 5



EXAMPLE 6

Units : $(N\,mm^2) \times 10^{12}$

FIG. 6.2 EI VALUES FOR MEMBERS OF THE FRAMES

TABLE 6.1. LOADING, SERVICEABILITY AND STRENGTH DETAILS OF FRAMES

	Optimal Design Example					
	1	2	3	4	5	6
Loadings:						
Live load, kN/m^2	3.75	5.0	5.0	6.0	2.5	3.0
Dead load, kN/m^2	5.0	6.25	6.0	11.0	4.5	5.0
Wind load, kN/m^2	1.0	1.0	1.2	-	0.7	0.7
Beams:						
Live load per metre run, kN/m	15.0	20.0	25.0	36.0	9.4	12.0
Dead load per metre run, kN/m	20.0	25.0	30.0	66.0	19.5	20.0
Wind force:						
Top floor level, kN	20.0	10.0	15.0	-	8.4	5.6
Other floor levels, kN	-	20.0	30.0	-	16.8	11.2
Load factors:						
λ_D	1.4	1.4	1.4	1.4	1.4	1.4
λ_L	1.6	1.6	1.6	1.6	1.6	1.6
λ_C	1.25	1.25	1.25	1.25	1.25	1.25
Serviceability factor: λ_*^j						
Loading condition I	1.06	1.06	1.06	-	1.06	1.06
Loading condition II	1.10	1.10	1.10	1.10	1.10	1.10
Design strengths:						
Concrete, σ_b, N/mm^2	16.0	16.0	16.0	24.0	17.0	16.0
Steel, σ_{al}, N/mm^2	415.0	415.0	415.0	415.0	415.0	415.0

and the Draft British Standard Code of Practice (62) the ratio of design strength to the specified characteristic strength used are $\frac{1}{1.5}$ for concrete and $\frac{1}{1.15}$ for steel. The design strengths of concrete and steel used for the examples are given in Table 6.1. The design strength is used in estimating the resistance of the critical sections while the characteristic strength is used for member rigidity calculations.

The steel reinforcement for a critical section is assumed to be extended over an 'equivalent length' for the calculation of volume of reinforcement for the frame as explained in Chapter 3. For the design examples, the 'equivalent length' of steel reinforcement in beams and columns are assumed as shown in Fig.6.3.

It has been shown earlier that the serviceability requirements of the frame are said to be satisfied if,

$$x^j \geq L^j$$

$$\text{i.e. } \frac{\lambda^j}{\lambda_u} \geq L^j$$

The above requirement needs to specify a lower bound value for x^j or λ^j, the yield moment factor, which will ensure satisfactory behaviour of the members under working loads. With the introduction of limit-state concepts in design and the new overload factors and material strength factors it has been found that more experimental and theoretical research is required in this area to study the behaviour of members under working loads and the effect of yield moment factor of the critical sections on the serviceability requirements regarding crackwidth, deflections etc. As the present work is mainly concerned with the development of the optimal limit design method which includes the serviceability restrictions as one of the constraints, no detailed investigation has been carried out in this direction. Based on the study by Cohn and Grierson (39, 40) it has been found reasonable to assume the lower bound values of x^j as 0.85 and 0.74 for loading conditions I and II respectively. This assumption results in a redistribution of moments of 15 and 26 percent under loading conditions I and II respectively.

The following additional design constraints, as explained in section 3.8.2, have been considered in the optimal limit design of the frames. The moments at the leeward ends of beams for loading condition I and the

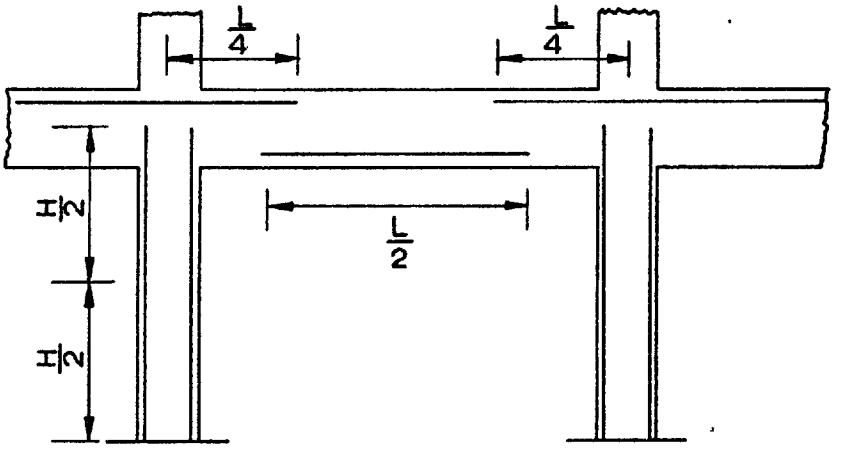


FIG. 6.3 EQUIVALENT LENGTHS OF REINFORCEMENT

moments at both ends of beams for loading condition II, were restricted not to exceed the values of the elastic moment for factored loads. Symmetry in designs for the end columns of a storey and for the ends of beams meeting at a joint were also considered through the necessary constraint equations and the cost coefficients for the objective function.

6.5 RESULTS OF ANALYSIS AND DISCUSSION

The frames have been analysed for three cases of hinge pattern under two loading conditions using the optimal limit design program described in Chapter 4. The results of analysis for the values of bending moment at all the critical sections are given in Tables 6.2 to 6.7. The bending moment diagrams for one of the cases of hinge pattern of optimal limit design (O.L.D) and for the ultimate strength design (U.S.D) based on elastic analysis for factored loads, are plotted in Figs. 6.4 to 6.9.

Figs. 6.10 to 6.15 show the position of plastic hinges as obtained for optimal design for the three cases of hinge pattern for all the six frames. The plastic hinges which have attained their rotation capacities are indicated in the above figures. The sections where critical serviceability conditions have been reached, as noted by the lower bound values L^j for the design variables x_d^j are also shown in Figs. 6.10 to 6.15.

A study of the bending moment distribution for O.L.D. for different cases of hinge pattern show that there is a redistribution of moments resulting in a reduction of the values of moment, compared to U.S.D., at some of the critical sections of beams and columns. The amount of reduction in the values of moment and the relevant position of critical sections depend on the loading condition, type of hinge pattern and the specified lower bound values, L^j, for the design variables x_d^j. For the design examples worked out here, the maximum reduction in the values of bending moment for loading condition I has been observed to be 15 percent. This occurs at sections where the lower bound values L^j for x_d^j have been reached, as marked in Figs 6.10 to 6.15. In the case of loading condition II, for symmetrical frames, a reduction in the value of bending moment by 26 percent has been observed for critical sections at the ends of beams and columns.

The results of O.L.D. for the examples of six frames illustrate that the procedure suggested in Chapter 4 for the possible location of plastic hinges for different cases of hinge pattern is practical and satisfactory.

TABLE 6.2. DESIGN SOLUTIONS: EXAMPLE 1

Section	Loading Condition I				Loading Condition II	
	U.S.D. M_u^j (kNm)	O.L.D. M_d^j (kNm)			U.S.D. M_u^j (kNm)	O.L.D. cases 1 & 2 M_d^j (kNm)
		case 1	case 2	case 3		
7	0.86	2.63	7.41	7.41	-23.64	-17.49
2	95.96	112.00	106.19	106.19	111.09	143.05
1	-202.70	-172.38	-188.78	-188.78	-222.18	-164.42
9	-171.17	-143.10	-160.27	-160.27	-222.18	-164.42
4	90.98	108.06	99.47	99.47	111.09	143.05
3	-40.63	-34.54	-34.54	-34.54	23.64	-17.49
12	0.86	2.63	7.41	7.41	-23.64	-17.49
11	-12.33	-16.12	-20.49	-20.49	11.82	8.75
8	-31.53	-29.28	-28.51	-28.51	0.0	0.0
5	32.43	35.37	31.67	31.67	0.0	0.0
10	-40.63	-34.54	-34.54	-34.54	-23.64	-17.49
6	32.22	32.07	27.39	27.39	11.82	8.75

TABLE 6.3. DESIGN SOLUTIONS: EXAMPLE 2

Section	Loading Condition I				Loading Condition II	
	U.S.D. M_u^j (kN m)	O.L.D. M_d^j (kN m)			U.S.D. M_u^j (kN m)	O.L.D. Cases 1&2 M_d^j (kN m)
		case 1	case 2	case 3		
13	-17.58	-11.47	-7.19	-4.61	-57.14	-42.28
2	115.03	137.48	137.01	121.51	136.47	179.38
1	-258.62	-219.82	-225.04	-258.62	-272.93	-201.97
15	-199.67	-164.76	-171.25	-203.62	-272.93	-201.97
4	114.11	137.39	134.20	118.01	136.47	179.38
3	-78.36	-66.71	-66.60	-66.60	-57.14	-42.28
18	1.72	3.00	8.04	9.88	-24.66	-18.25
17	13.86	-18.06	-23.28	-23.50	12.33	9.13
14	-45.48	-41.08	-38.66	-38.66	0.0	0.0
5	48.74	53.66	49.60	48.23	0.0	0.0
16	-43.13	-36.76	-36.66	-36.66	-24.66	-18.25
6	34.57	34.94	31.26	30.57	12.33	9.13
19	-19.68	-14.66	-15.21	-17.39	-34.12	-25.25
8	120.09	141.08	140.80	139.71	142.22	183.63
7	-246.39	-209.43	-209.43	-209.43	-284.44	-210.49
21	-231.22	-193.69	-193.54	-193.30	-284.44	-210.49
10	118.72	140.30	140.38	140.49	142.22	183.63
9	-37.60	-31.96	-31.96	-31.96	-34.12	-25.25
24	-19.68	-14.66	-15.21	-17.39	-34.12	-25.25
23	19.30	14.47	15.23	14.49	32.47	24.03
20	-15.18	-15.75	-15.90	-16.13	0.0	0.0
11	13.47	13.99	15.14	16.34	0.0	0.0
22	-37.60	31.96	-31.96	-31.96	-34.12	-25.25
12	35.23	29.94	29.94	29.94	32.47	24.03

TABLE 6.4. DESIGN SOLUTIONS: EXAMPLE 3

Section	Loading Condition I				Loading Condition II	
	U.S.D. M_u^j (kN m)	O.L.D. M_d^j (kN m)			U.S.D. M_u^j (kN m)	O.L.D. Cases 1&2 M_d^j (kN m)
		case 1	case 2	case 3		
19	-65.61	-60.93	-48.14	-45.21	-116.52	-86.22
2	229.17	246.01	237.90	239.37	271.71	331.55
1	-317.56	-288.55	-317.56	-317.56	-343.74	-254.37
21	-173.85	-147.77	-179.97	-195.41	-240.72	-178.14
4	13.02	32.70	27.20	19.48	15.53	78.11
3	-229.80	-216.51	-195.33	-195.33	-240.72	-178.14
23	-258.83	-242.15	-220.00	-220.01	-343.74	-254.37
7	226.45	244.44	255.59	255.59	271.71	331.55
6	-129.77	-110.47	-110.31	-110.31	-116.52	-86.22
26	-36.68	-34.53	-25.47	-23.24	-74.71	-55.28
25	2.31	-3.19	-11.95	-14.69	37.35	27.64
20	-85.03	-81.95	-79.87	-72.27	-52.42	-38.79
5	66.55	71.66	64.44	63.13	26.21	19.39
22	2.87	3.41	2.44	2.44	52.42	38.79
8	22.60	28.98	24.37	26.75	-26.21	-19.39
24	-88.60	-75.31	-75.31	-75.31	-74.71	-55.28
9	60.32	58.11	53.21	54.78	37.35	27.64
27	-31.83	-29.31	-26.04	-24.12	-46.27	-34.24
11	261.89	280.08	284.59	265.74	312.99	362.09
10	-285.90	-252.03	-246.29	-285.90	-331.44	-245.26
29	-220.14	-187.12	-187.12	-221.50	-273.92	-202.70
13	-14.82	8.52	19.63	2.44	-17.67	53.55
12	-239.18	-225.53	-203.31	-203.31	-273.92	-202.70
31	-269.87	-251.61	-229.39	-229.39	-331.44	-245.26
16	262.94	275.50	286.61	286.61	312.99	362.09
15	-45.75	-38.89	-38.89	-38.89	-46.27	-34.24
34	-31.83	-29.31	-26.04	-24.12	-46.27	-34.24
33	28.94	26.40	22.67	21.97	41.81	30.94
28	-65.76	-64.91	-59.17	-64.40	-57.51	-42.56
14	58.68	58.82	57.72	49.88	50.60	37.44
30	30.68	26.08	26.08	26.08	57.51	42.56
17	-26.17	-22.24	-22.24	-22.24	-50.60	-37.44
32	-45.75	-38.89	-38.89	-38.89	-46.27	-34.24
18	41.17	35.16	35.00	35.00	41.81	30.94

TABLE 6.5. DESIGN SOLUTIONS: EXAMPLE 4

Section	Loading condition II	
	U.S.D. M_u^j (kN m)	O.L.D. Cases 1 & 2 M_d^j (kN m)
19	-2127.62	-1595.72
2	1577.47	2237.79
1	-3154.94	-2366.20
21	-3154.94	-2366.20
4	1577.47	2237.79
3	-2127.62	-1595.72
24	-1170.20	-877.65
23	585.10	438.82
20	0.0	0.0
5	0.0	0.0
22	-1170.20	-877.65
6	585.10	438.82
25	-2401.14	-1800.86
8	1509.09	2186.50
7	-3018.18	-2263.63
27	-3018.18	-2263.63
10	1509.09	2186.50
9	-2401.14	1800.86
30	-810.40	-607.80
29	957.43	718.07
26	0.0	0.0
11	0.0	0.0
28	-810.40	-607.80
12	957.43	718.07
31	-1989.00	-1491.75
14	1612.13	2263.78
13	-3224.25	-2418.19
33	-3224.25	-2418.19
16	1612.13	2263.78
15	-1989.00	-1491.75
36	-1989.00	-1491.75
35	1590.74	1193.06
32	0.0	0.0
17	0.0	0.0
34	-1989.00	-1491.75
18	1590.74	1193.06

TABLE 6.6. DESIGN SOLUTIONS: EXAMPLE 5

Section	Loading Condition I				Loading Condition II	
	U.S.D. M_u^j (kN m)	O.L.D. M_d^j (kN m)			U.S.D. M_u^j (kN m)	O.L.D. Cases 1&2 M_d^j (kNm)
		case 1	case 2	case 3		
37	-23.05	-15.47	-5.00	-1.13	-74.12	-54.85
2	69.10	75.37	78.13	80.06	79.81	108.68
1	-164.37	-159.41	-164.37	-164.37	-147.96	-109.49
39	-75.74	-69.38	-76.59	-88.22	-131.12	-97.03
4	50.95	61.74	61.63	55.00	59.73	93.82
3	-147.98	-132.76	-125.78	-127.41	-131.12	-97.03
41	-88.07	-79.08	-74.86	-74.86	-147.96	-109.49
7	67.07	78.53	81.43	81.43	79.81	108.68
6	-103.41	-89.47	-87.90	-87.90	-74.12	-54.85
44	-3.6	-2.52	2.63	1.48	-32.07	-23.73
43	-18.0	-22.85	-30.99	-31.29	16.03	11.86
38	-46.32	-43.44	-41.14	-39.38	-6.81	-5.04
5	53.95	59.21	54.47	54.93	3.40	2.52
40	-34.71	-29.50	-29.50	-29.50	6.81	5.04
8	48.15	52.25	48.82	50.13	-3.40	-2.52
42	-51.11	-43.45	-43.45	-43.45	-32.07	-23.73
9	45.35	45.83	43.00	43.84	16.03	11.86
45	-35.76	-23.74	-21.60	-14.05	-76.72	-56.77
11	68.23	74.24	82.30	79.08	79.00	108.08
10	-153.41	-153.41	-139.42	-153.41	-146.99	-108.77
47	-85.32	-79.19	-72.52	-94.11	-130.90	-96.87
13	51.14	64.40	67.89	56.70	59.95	93.98
12	-138.03	-117.64	-117.32	-118.10	-130.90	-96.87
49	-97.38	-83.05	-82.77	-82.77	-146.99	-108.77
16	66.56	80.86	81.00	81.00	79.00	108.08
15	-95.13	-80.86	-80.86	-80.86	-76.72	-56.77
52	-17.04	-11.20	-6.26	-0.13	-41.35	-30.60
51	19.45	12.96	7.63	2.61	42.05	31.12
46	-44.98	-47.90	-41.92	-38.23	-9.83	-7.27
14	42.30	46.59	46.64	36.77	10.02	7.42
48	-28.21	-23.98	-23.98	-24.76	9.83	7.27
17	25.20	24.18	21.42	23.05	-10.02	-7.42
50	-53.50	-45.48	-45.48	-45.48	-41.35	-30.60

(contd)

TABLE 6.6 (Contd)

Section	Loading Condition I				Loading Condition II	
	U.S.D. M_u^j (kN m)	O.L.D. M_d^j (kN m)			U.S.D. M_u^j (kN m)	O.L.D. Cases 1&2 M_d^j (kN m)
		case 1	case 2	case 3		
18	52.29	46.03	44.45	44.45	42.05	31.12
53	-50.00	-38.34	-37.16	-36.32	-77.69	-57.49
20	68.30	77.66	74.71	75.53	78.83	107.96
19	-139.05	131.96	-139.05	-138.24	-146.34	-108.29
55	-99.66	-89.46	-93.01	-92.23	-131.01	-96.95
22	51.05	65.21	63.15	62.40	59.84	93.90
21	-123.87	-105.74	-106.31	-108.59	-131.01	-96.95
57	-110.64	-94.42	-94.04	-94.64	-146.34	-108.29
25	66.20	80.51	80.70	80.40	78.83	107.96
24	-82.58	-70.19	-70.19	-70.19	-77.69	-57.49
60	-16.67	-11.41	-10.86	-9.64	-35.18	-26.03
59	18.73	12.54	15.34	13.92	35.37	26.17
54	-25.83	-27.93	-30.60	-30.20	6.31	-4.67
23	23.11	26.31	24.98	21.06	6.25	4.63
56	-15.06	-12.87	-13.82	-15.50	6.31	4.67
26	12.44	10.61	10.57	10.57	-6.25	-4.63
58	-43.35	-36.85	-36.85	-36.85	-35.18	-26.03
27	41.62	35.38	35.38	35.38	35.37	26.17
61	-37.85	-31.57	-31.78	-31.79	-50.03	-37.02
29	77.83	90.19	90.78	90.77	90.79	116.80
28	-132.11	-113.67	-112.29	-112.29	-150.10	-111.07
63	-114.21	-97.08	-97.08	-97.08	-137.72	-101.92
31	45.32	62.95	62.95	62.65	53.13	88.93
30	-120.77	-102.66	-102.66	-103.25	-137.72	-101.92
65	-123.99	-105.49	-105.39	-105.99	-150.10	-111.07
34	77.06	89.88	89.92	89.63	90.79	116.80
33	-47.51	-40.38	-40.38	-40.38	-50.03	-37.02
68	-37.85	-31.57	-31.78	-31.79	-50.03	-37.02
67	33.30	26.93	26.31	26.68	42.51	31.46
62	-17.90	-16.59	-15.21	-15.21	-12.38	-9.16
32	13.56	14.57	15.44	15.82	9.02	6.68
64	3.22	2.83	2.74	2.74	12.38	9.16
35	-1.83	-1.55	-1.55	-1.55	-9.02	-6.68
66	-47.51	-40.38	-40.38	-40.38	-50.03	-37.02
36	39.23	33.34	33.34	33.34	42.51	31.46

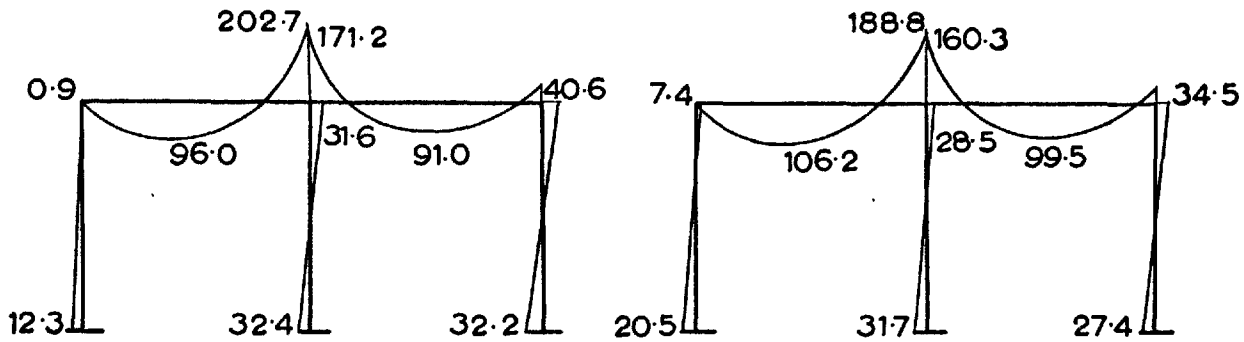
TABLE 6.7. DESIGN SOLUTIONS: EXAMPLE 6

Section	Loading Condition I				Loading Condition II	
	U.S.D. M_u^j (kN m)	O.L.D. M_d^j (kN m)			U.S.D. M_u^j (kN m)	O.L.D. Cases 1 & 2 M_d^j (kN m)
		case 1	case 2	case 3		
37	0.31	6.96	15.04	16.01	-72.46	-53.62
2	59.77	73.14	80.89	79.49	71.11	99.02
1	-183.26	-163.19	-155.77	-159.54	-142.23	-105.25
39	-57.82	-44.25	-39.45	-43.28	-142.23	-105.25
4	60.77	74.60	79.20	77.28	71.11	99.02
3	-123.14	-109.05	-104.67	-104.67	-72.46	-53.62
42	4.58	3.66	6.19	6.94	-29.31	-21.69
41	-29.76	-35.85	-43.33	-43.70	14.66	10.84
38	-66.58	-56.59	-57.32	-56.59	0.0	0.0
5	98.21	108.70	101.59	101.21	0.0	0.0
40	-54.27	-46.13	-46.13	-46.13	-29.31	-21.69
6	54.60	57.08	53.44	53.44	14.66	10.84
43	-6.88	5.67	13.47	14.75	-75.04	-55.53
8	60.78	75.07	84.01	84.65	70.47	98.55
7	-174.06	-158.02	-147.95	-147.95	-140.94	-104.30
45	-64.85	-47.67	-44.37	-43.95	-140.94	-104.30
10	58.67	76.28	77.93	78.14	70.47	98.55
9	-120.32	-102.27	-102.26	-102.27	-75.04	-55.53
48	-3.19	2.76	7.87	7.16	-42.34	-31.33
47	4.28	-3.31	-8.86	-9.07	43.15	31.93
44	-63.15	-62.37	-59.43	-59.27	0.0	0.0
11	58.86	62.34	58.99	59.66	0.0	0.0
46	-68.58	-58.30	-58.30	-58.30	-42.34	-31.33
12	68.87	62.92	58.54	58.54	43.15	31.93
49	-11.80	0.03	6.46	11.08	-64.16	-47.48
14	62.43	77.41	84.00	84.05	73.19	100.56
13	-165.84	-147.72	-140.96	-145.48	-146.38	-108.32
51	-82.29	-61.95	-61.36	-72.63	-146.38	-108.32
16	61.63	79.07	79.37	73.73	73.19	100.56
15	-96.95	-82.41	-82.41	-82.41	-64.16	-47.48
54	-3.45	3.05	6.67	8.33	-35.19	-26.04
53	3.69	-2.90	-5.60	-7.59	32.70	24.20
50	-49.14	-50.31	-47.84	-43.61	0.0	0.0
17	46.06	47.99	44.14	44.72	0.0	0.0
52	-56.21	-47.78	-47.78	-47.78	-35.19	-26.04

(Contd)

TABLE 6.7 (Contd)

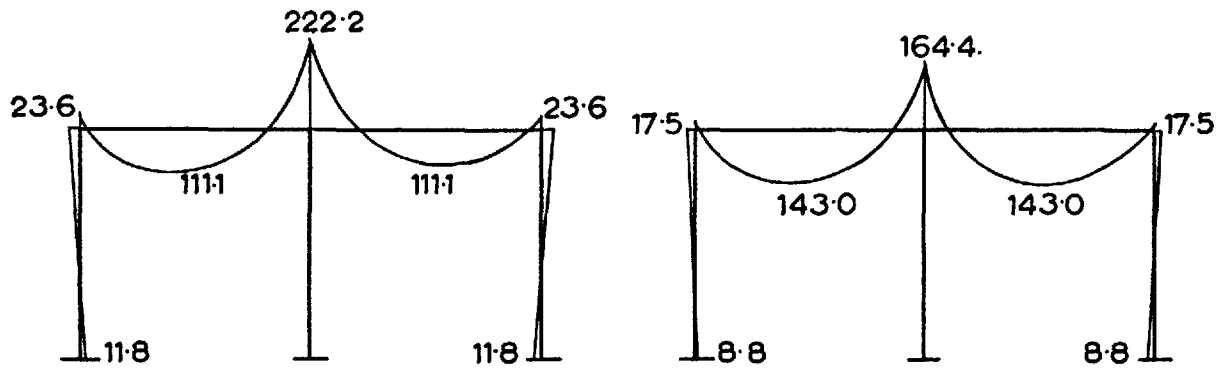
Section	Loading Condition I				Loading Condition II	
	U.S.D. M_u^j (kN m)	O.L.D. M_d^j (kN m)			U.S.D. M_u^j (kN m)	O.L.D. Cases 1 & 2 M_d^j (kN m)
		case 1	case 2	case 3		
18	51.73	43.97	43.97	43.97	32.70	24.20
55	-22.10	-12.33	-8.87	-5.64	-60.09	44.46
20	63.56	79.94	81.67	83.29	74.21	101.31
19	-153.28	-130.29	-130.29	-130.29	-148.42	-109.83
57	-98.30	-75.26	-76.63	-79.89	-148.42	-109.83
22	62.23	79.52	79.05	77.41	74.21	101.31
21	-79.74	-68.19	-67.78	-67.78	-60.09	-44.46
60	-7.43	-2.19	2.07	4.83	-29.66	-21.95
59	8.36	3.02	21.62	-2.74	28.96	21.43
56	-37.80	-38.29	-35.33	-32.13	0.0	0.0
23	34.40	35.45	31.76	29.24	0.0	0.0
58	-42.85	-36.83	-36.42	-36.42	-29.66	-21.95
24	40.74	34.63	34.63	34.63	28.96	21.43
61	-35.18	-26.26	-25.89	-31.49	-59.75	-44.21
26	64.21	79.09	79.27	76.48	74.29	101.38
25	-138.89	-118.06	-118.06	-118.06	-148.59	-109.95
63	-112.97	-91.61	-91.55	-87.75	-148.59	-109.95
28	61.72	76.51	77.38	79.28	74.29	101.38
27	-66.10	-57.87	-56.18	-56.18	-59.75	-44.21
66	-13.32	-8.36	-8.44	-10.66	-30.48	-22.56
65	14.67	10.15	10.94	10.48	30.42	22.51
62	-19.58	-20.14	-21.11	-22.92	0.0	0.0
29	17.18	16.73	18.32	18.26	0.0	0.0
64	-38.34	-34.28	-32.59	-32.59	-30.48	-22.56
30	36.90	31.36	31.36	31.36	30.42	22.51
67	-23.83	-19.10	-18.67	-19.11	-33.09	-24.48
32	68.89	81.82	82.04	81.82	80.96	106.31
31	-140.90	-119.76	-119.76	-119.76	-161.92	-119.82
69	-133.56	-112.06	-112.05	-110.22	-161.92	-119.82
34	68.34	81.51	81.52	82.43	80.96	106.31
33	-32.25	-27.41	-27.41	-27.41	-33.09	-24.48
72	-23.83	-19.10	-18.67	-19.11	-33.09	-24.48
71	21.86	17.90	17.45	20.83	29.27	21.66
68	-7.33	-7.70	-7.71	-9.54	0.0	0.0
35	6.35	6.30	5.40	7.38	0.0	0.0
70	-32.25	-27.41	-27.41	-27.41	-33.09	-24.48
36	27.75	23.59	23.59	23.59	29.27	21.66



U. S. D.

O. L. D
(CASE 2)

LOADING CONDITION I



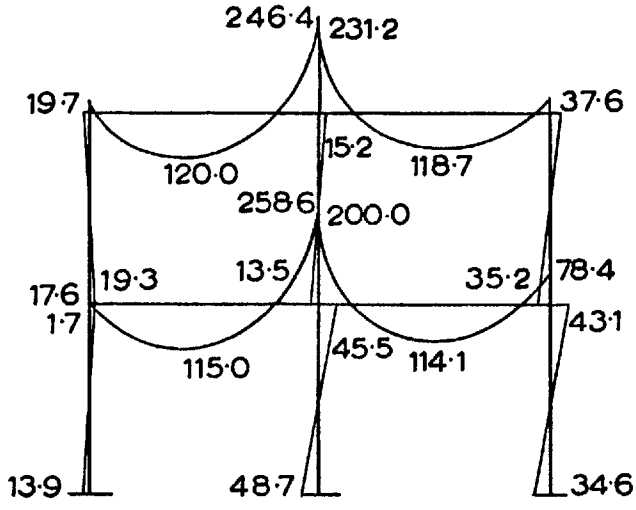
U. S. D.

O. L. D.
(CASES 1 & 2)

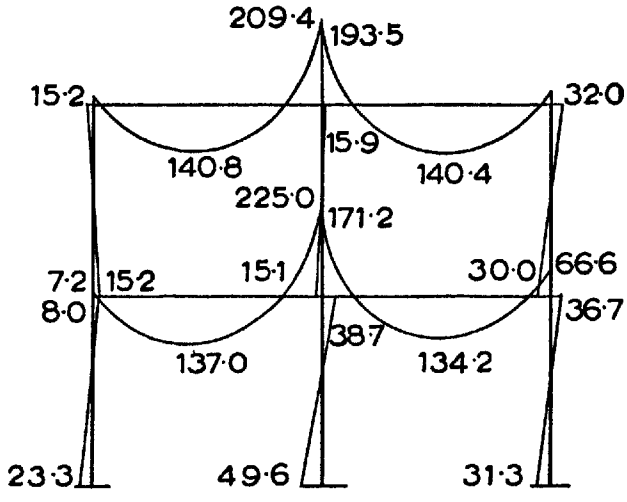
LOADING CONDITION II

FIG. 6.4 B. M. DIAGRAMS. EXAMPLE 1

(units kNm)

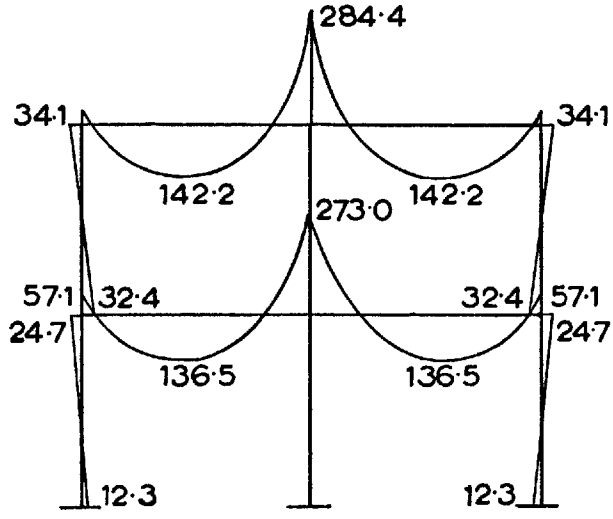


U. S. D

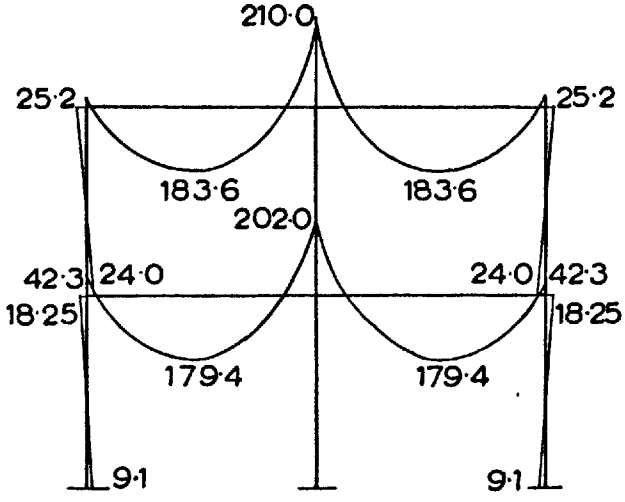


O. L. D.
(CASE 2)

LOADING CONDITION I



U. S. D.

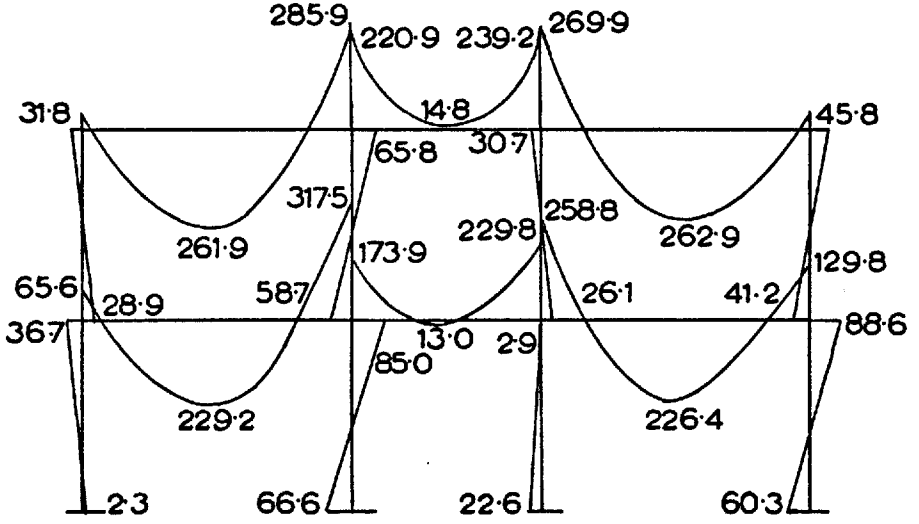


O. L. D.
(CASE 1 & 2)

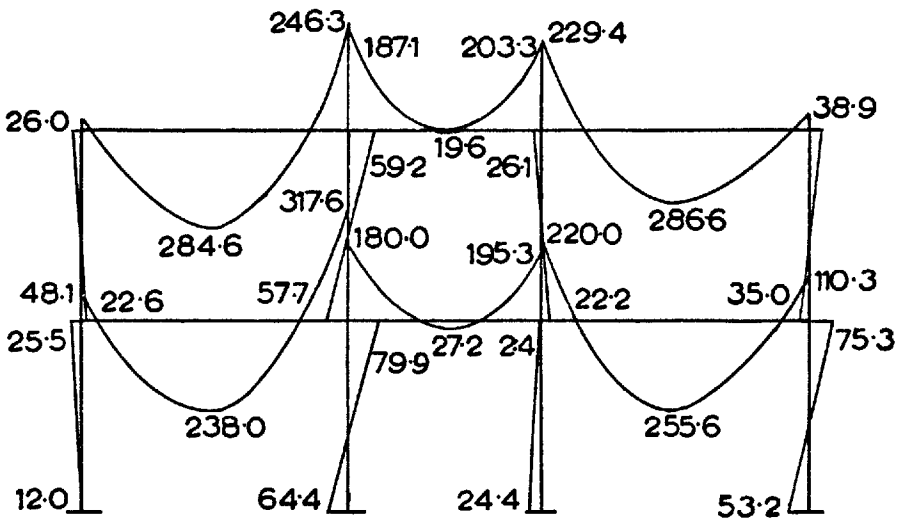
LOADING CONDITION II

FIG. 6.5 B. M. DIAGRAMS. EXAMPLE 2

(units kNm)

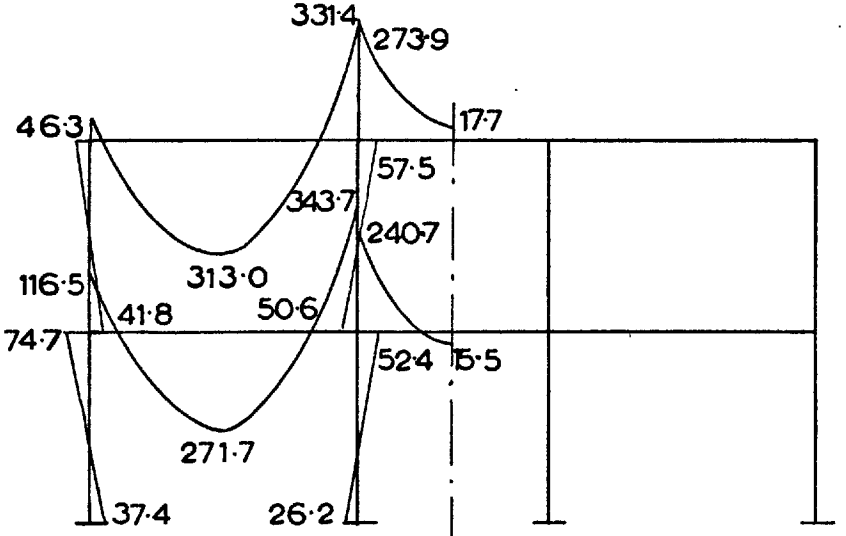


U. S. D.

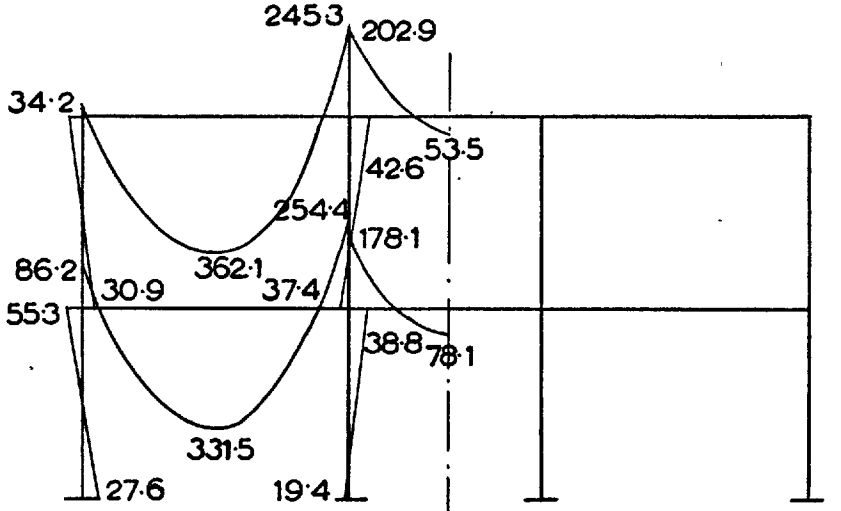


O. L. D.
(CASE 2)

LOADING CONDITION I



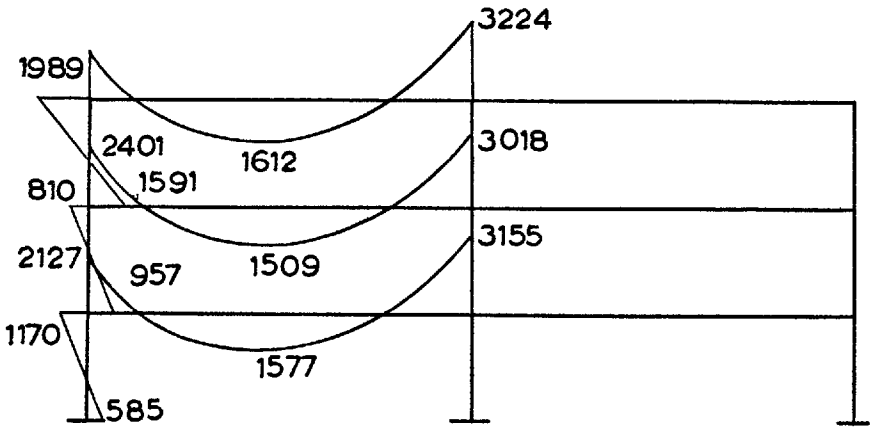
U. S. D



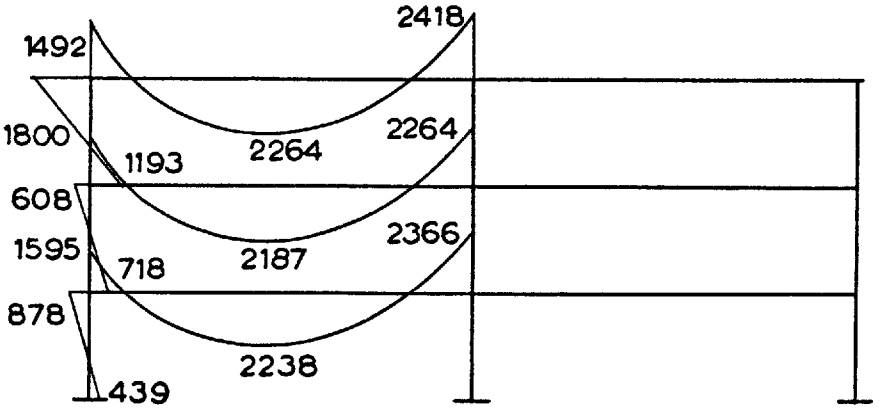
O. L. D.
(CASES 1 & 2)

LOADING CONDITION II

FIG. 6.6 B.M. DIAGRAMS EXAMPLE 3



U. S. D.

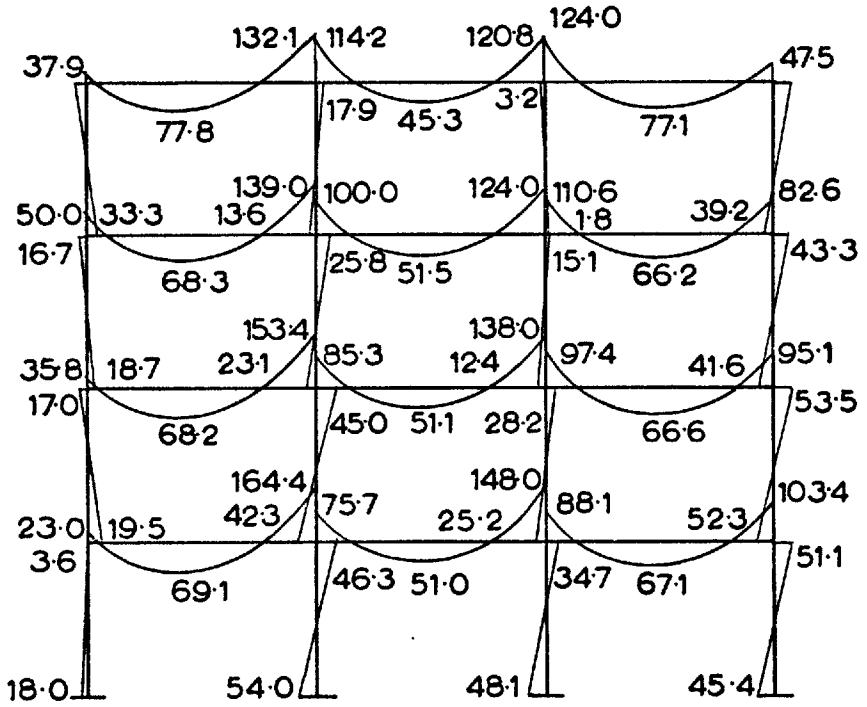


O. L. D.
(CASES 1 & 2)

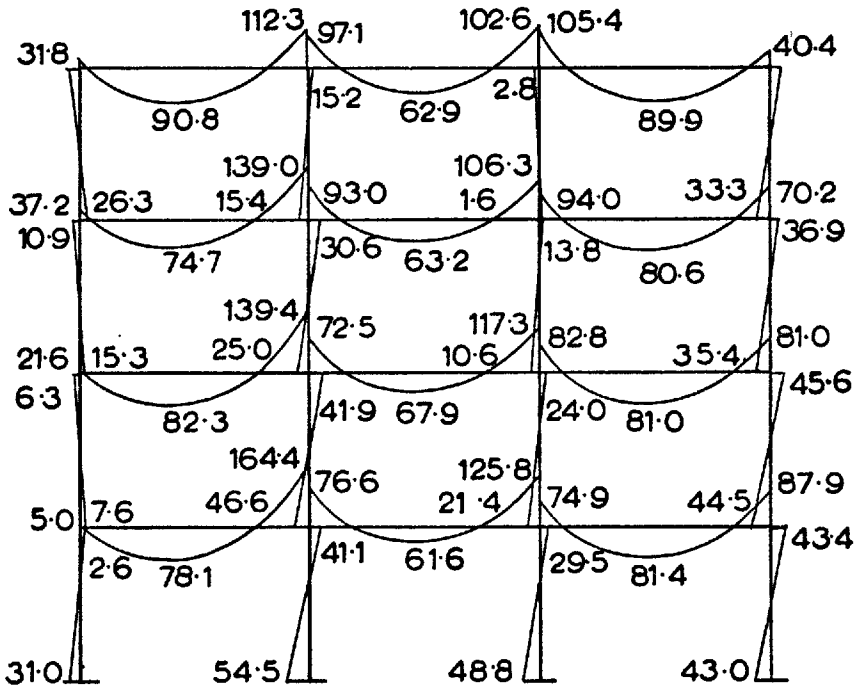
LOADING CONDITION II

FIG. 6.7 B.M. DIAGRAMS EXAMPLE 4

(units - kN m)



U. S. D.

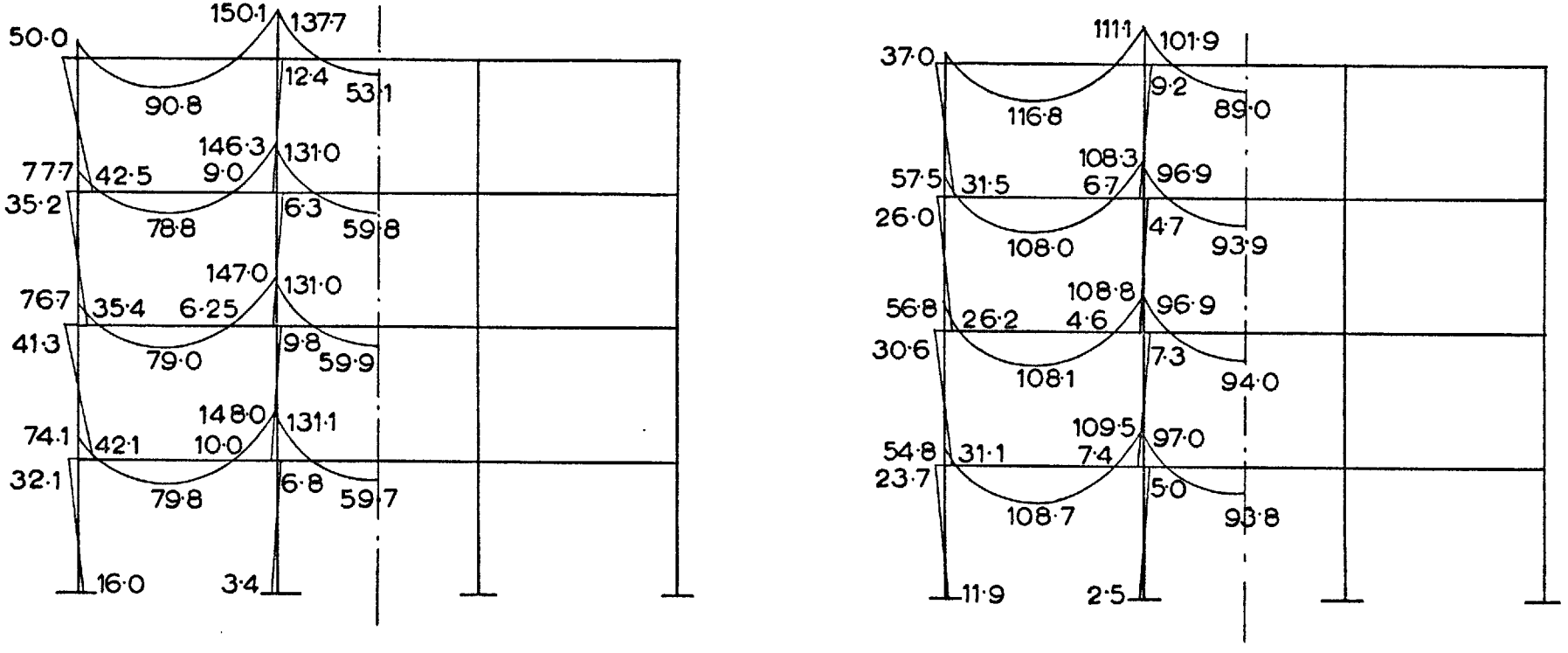


O. L. D.
(CASE 2)

LOADING CONDITION I

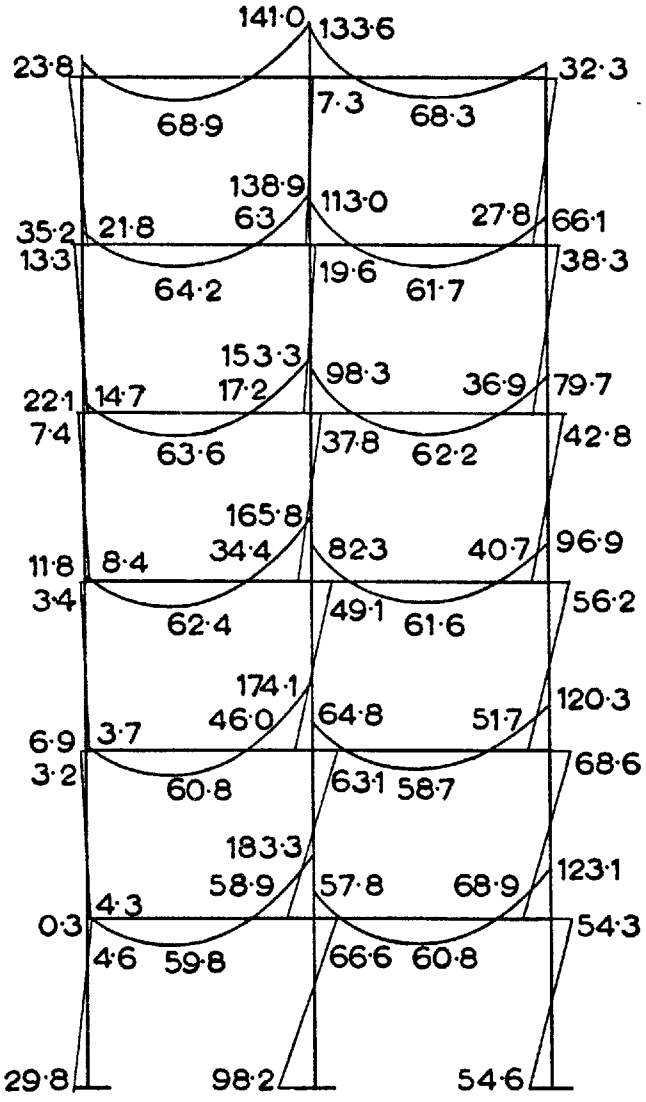
FIG. 6.8 (a) B.M. DIAGRAMS EXAMPLE 5

(Units – kN m)

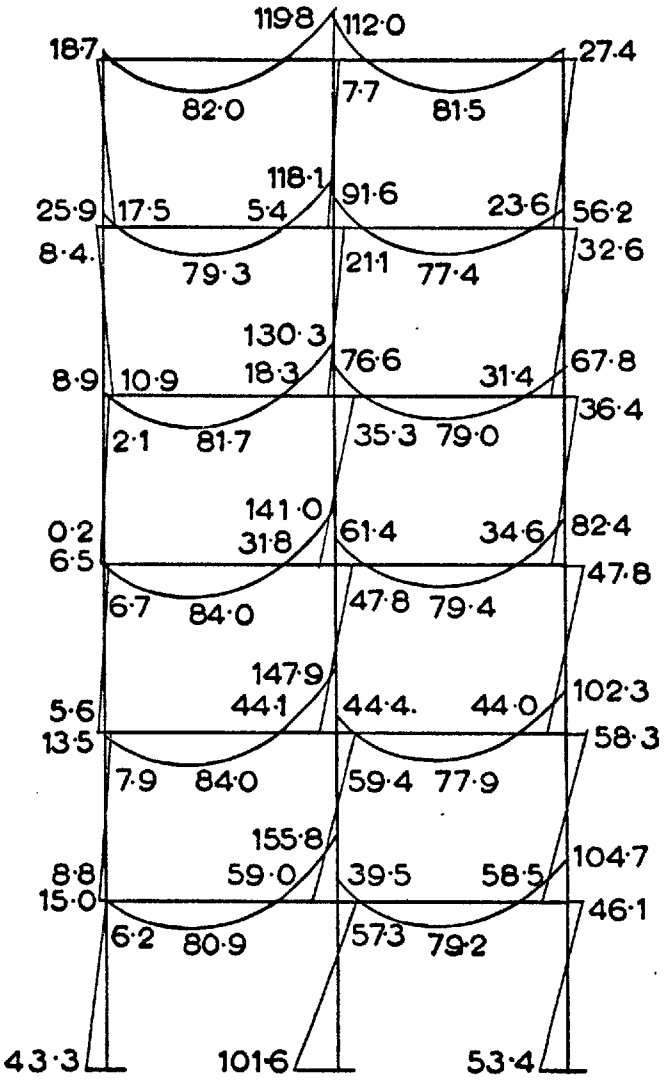


LOADING CONDITION III

FIG. 6.8 (b) B. M. DIAGRAMS EXAMPLE 5
(Units – k N m)



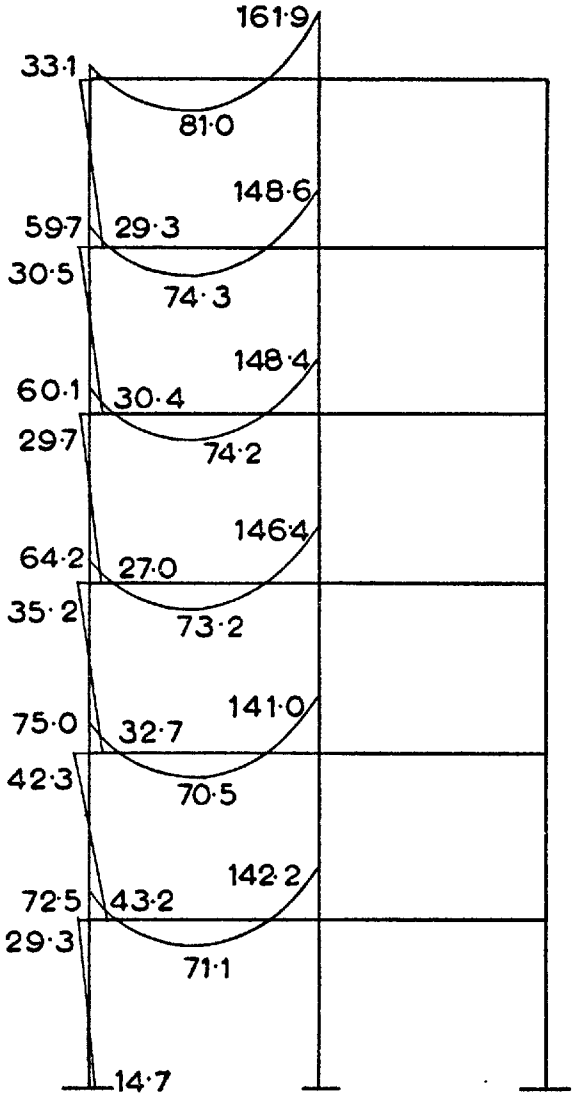
U. S. D.



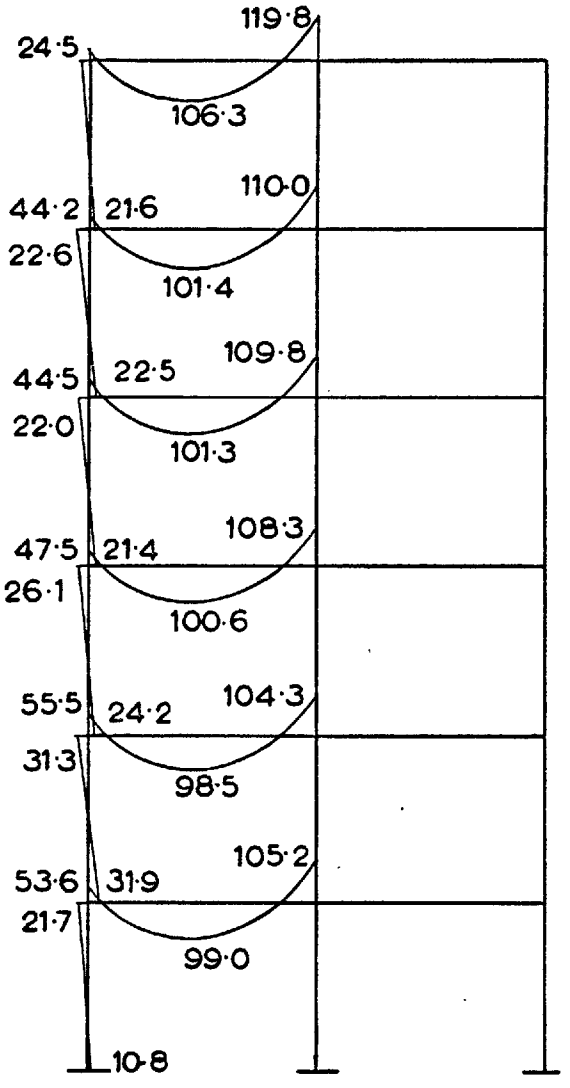
O. L. D.
(CASE 2)

LOADING CONDITION I

FIG. 6.9 (a) B. M. DIAGRAMS EXAMPLE 6
(Units kN m)



U. S. D.

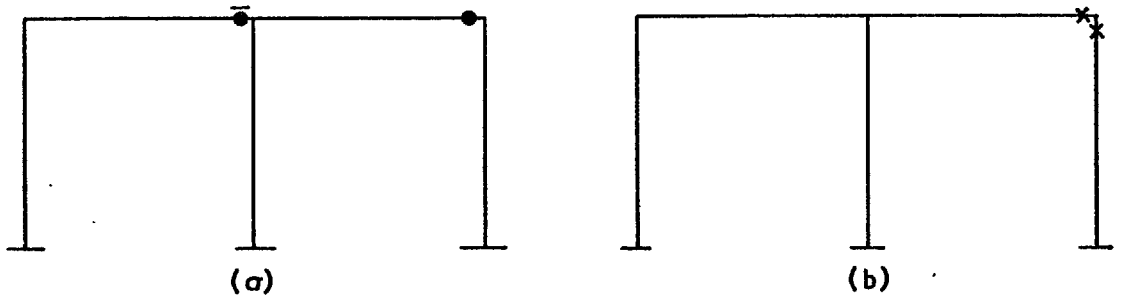


O. L. D.

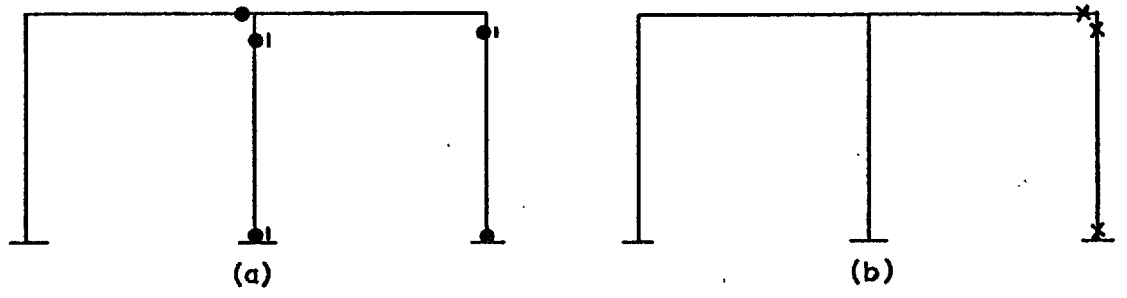
LOADING CONDITION II (CASES 1 & 2)

FIG. 6.9 (b) B. M. DIAGRAMS. EXAMPLE 6

(Units kN m)

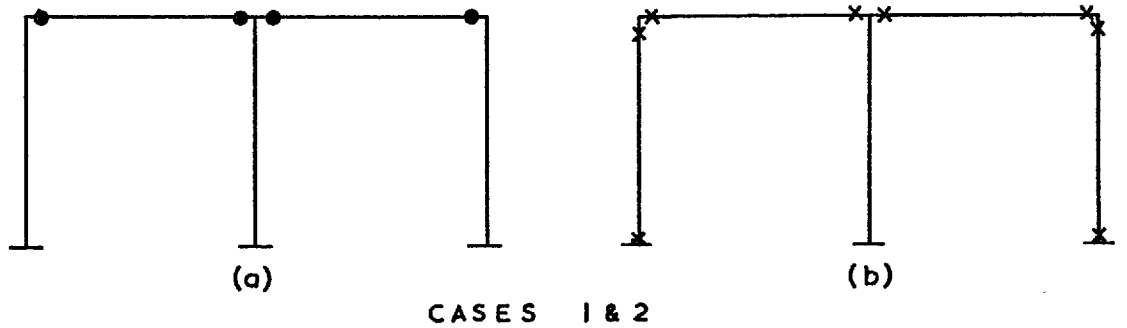


CASE 1

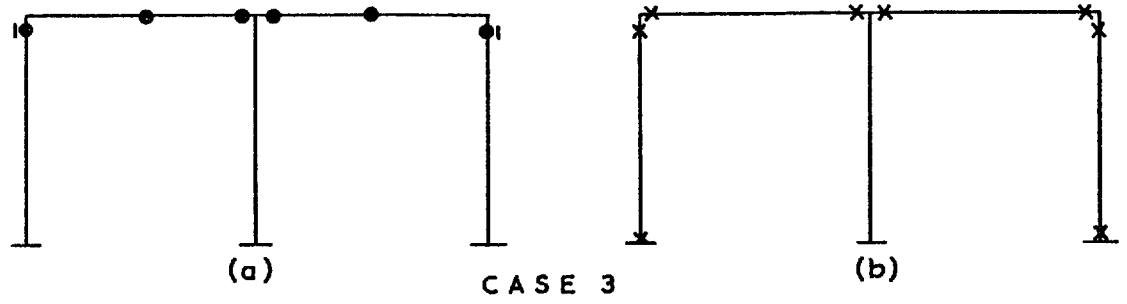


CASES 2 & 3

LOADING CONDITION I



CASES 1 & 2



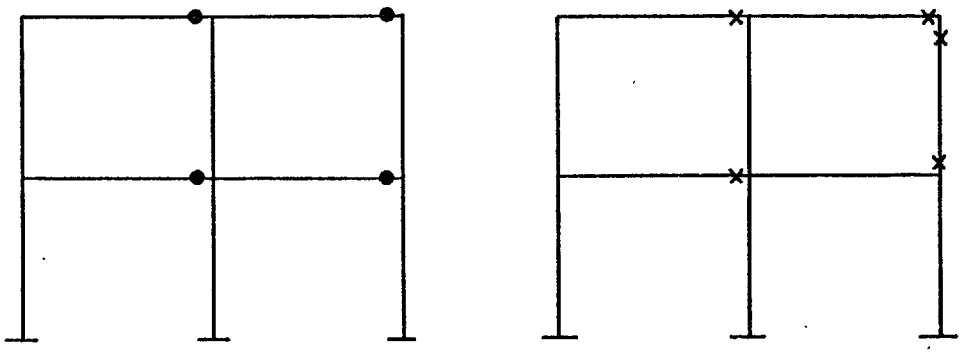
CASE 3

LOADING CONDITION II

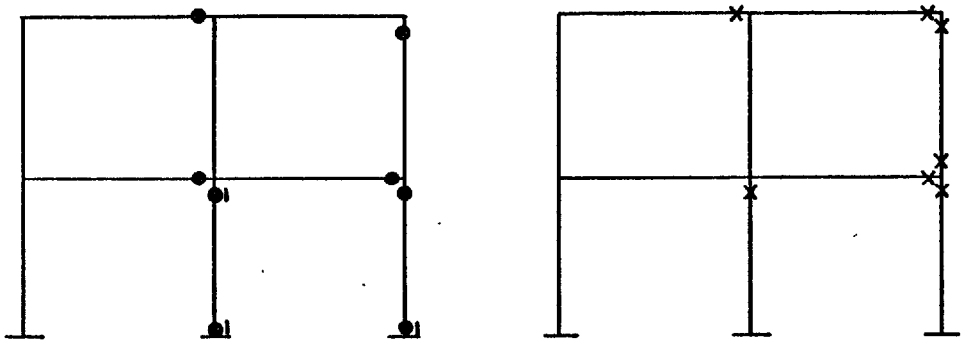
KEY : (a) ● _ Plastic hinge $\bar{\bullet}$ _ $\theta^{v} = \theta_p^{v}$

(b) x _ Serviceability condition , $x_d^j = L^j$

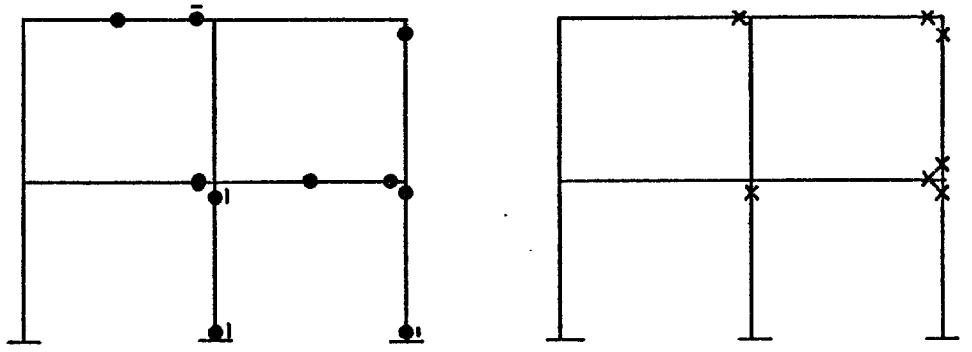
FIG. 6.10 EXAMPLE 1



(a) CASE 1 (b)

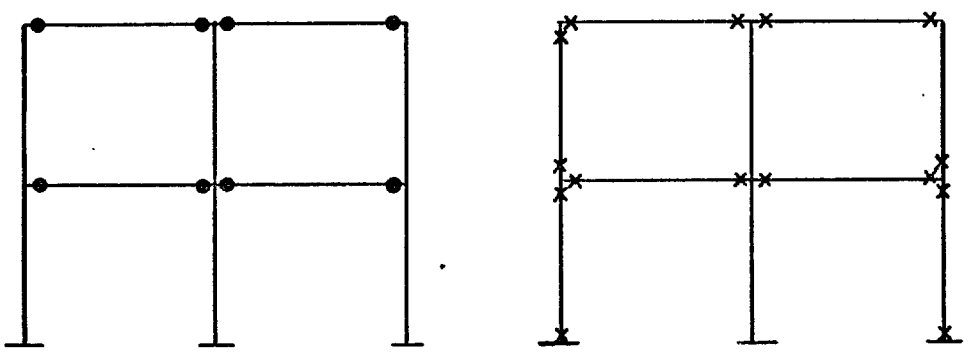


(a) CASE 2 (b)



(a) CASE 3 (b)

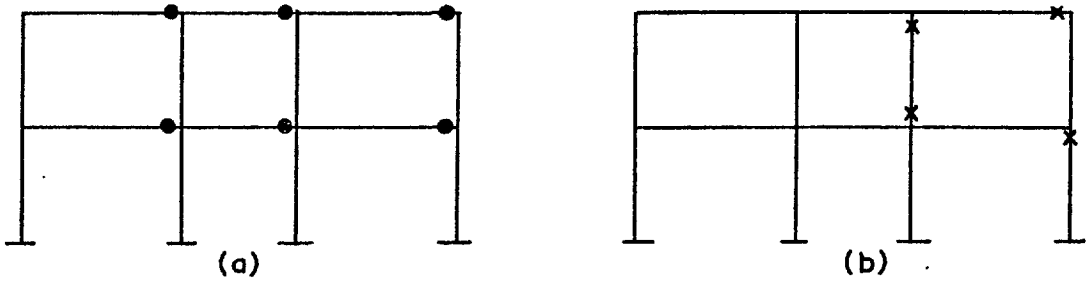
LOADING CONDITION I



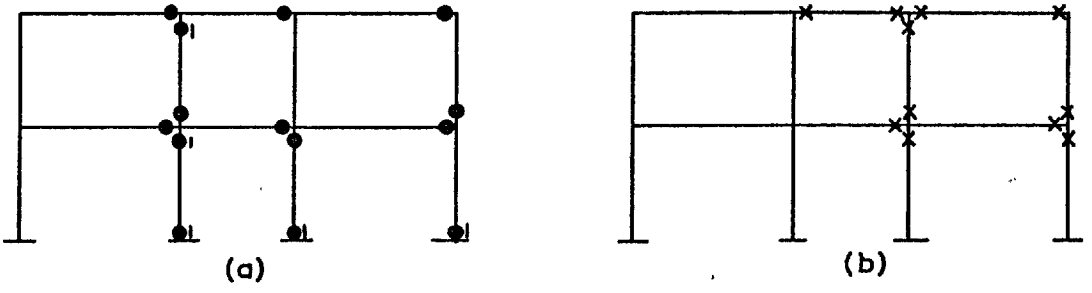
CASE 1 & 2

LOADING CONDITION II

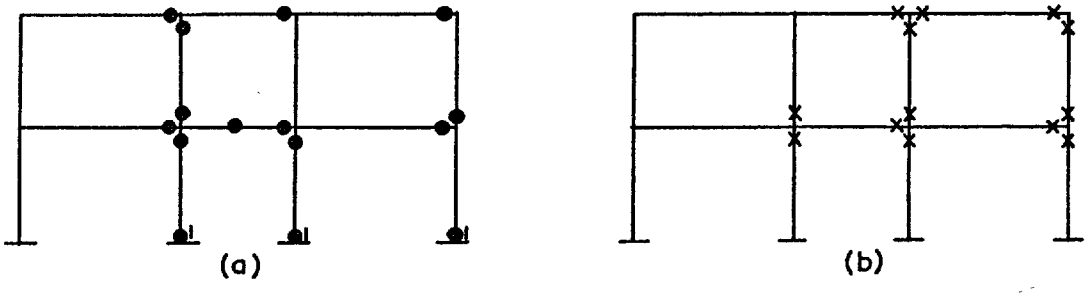
FIG. 6.11 EXAMPLE 2



CASE 1

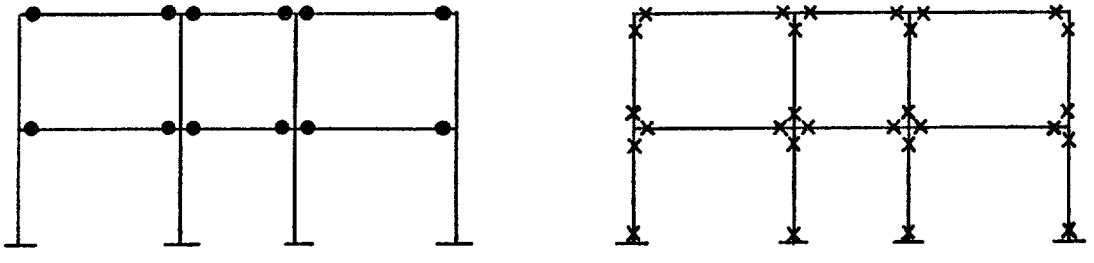


CASE 2



CASE 3

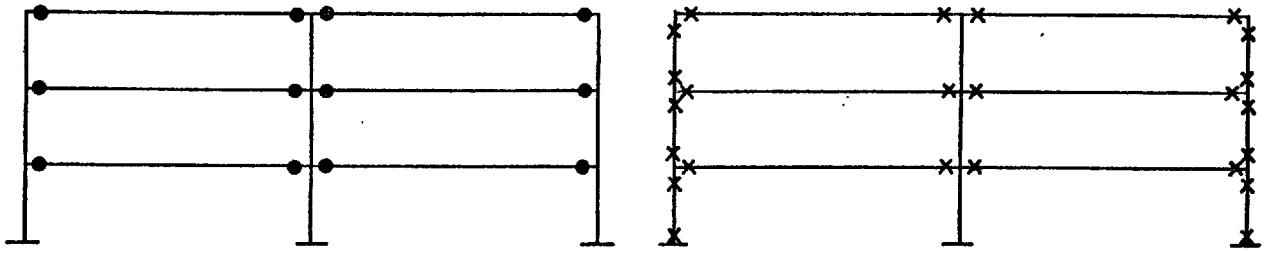
LOADING CONDITION I



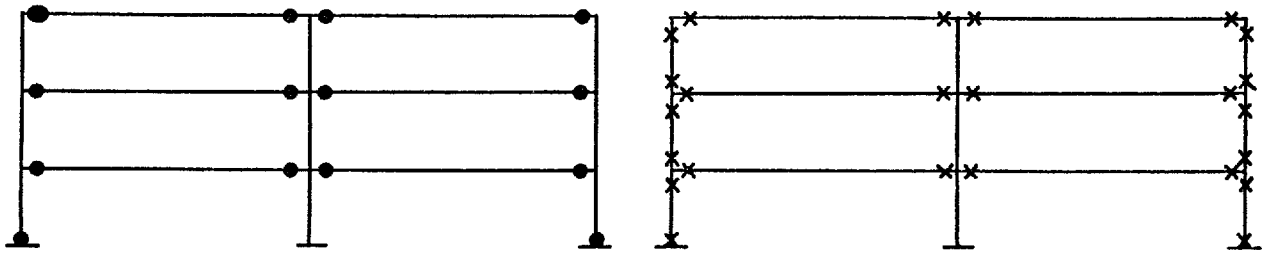
CASES 1 & 2

LOADING CONDITION II

FIG. 6.12 EXAMPLE 3



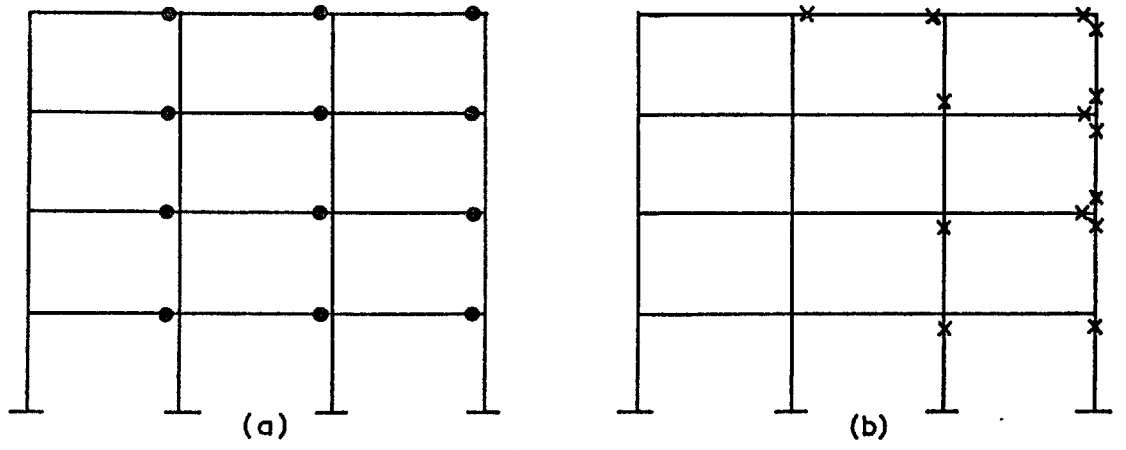
CASE 1



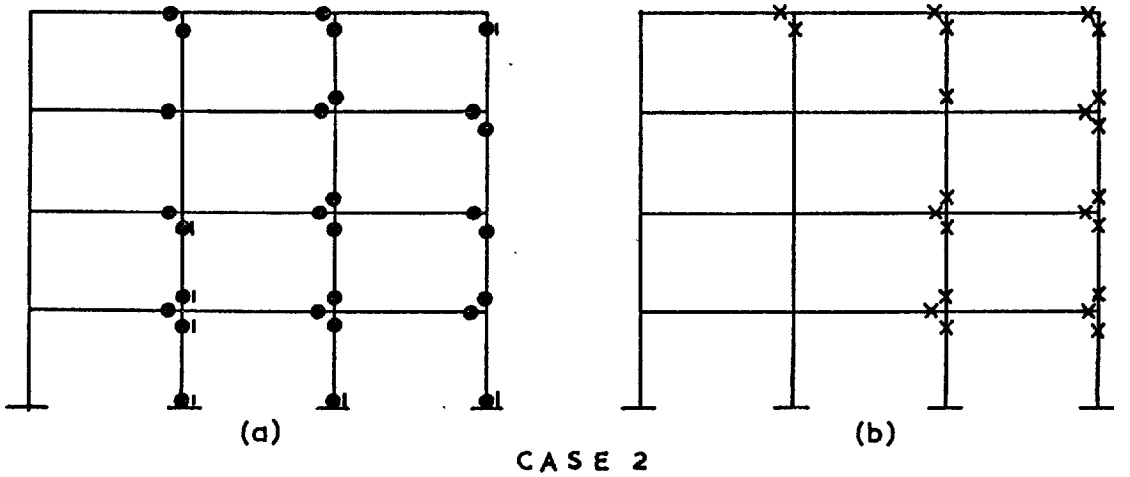
CASE 2

LOADING CONDITION II

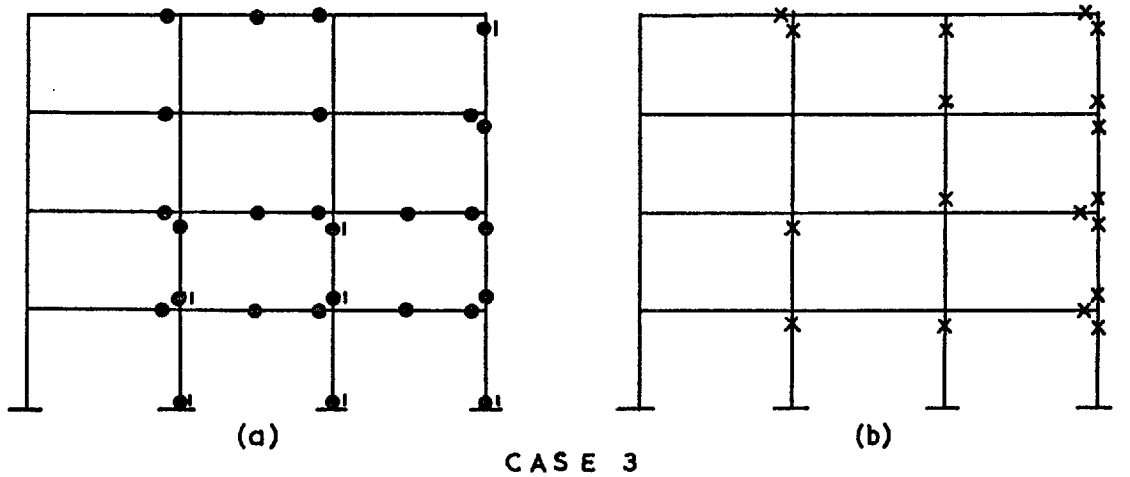
FIG. 6.13 EXAMPLE 4



CASE 1

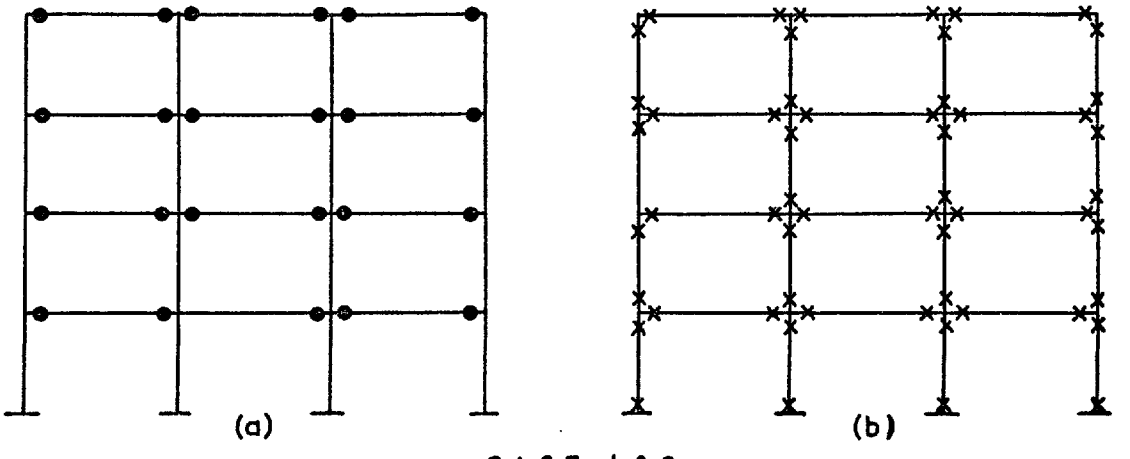


CASE 2



CASE 3

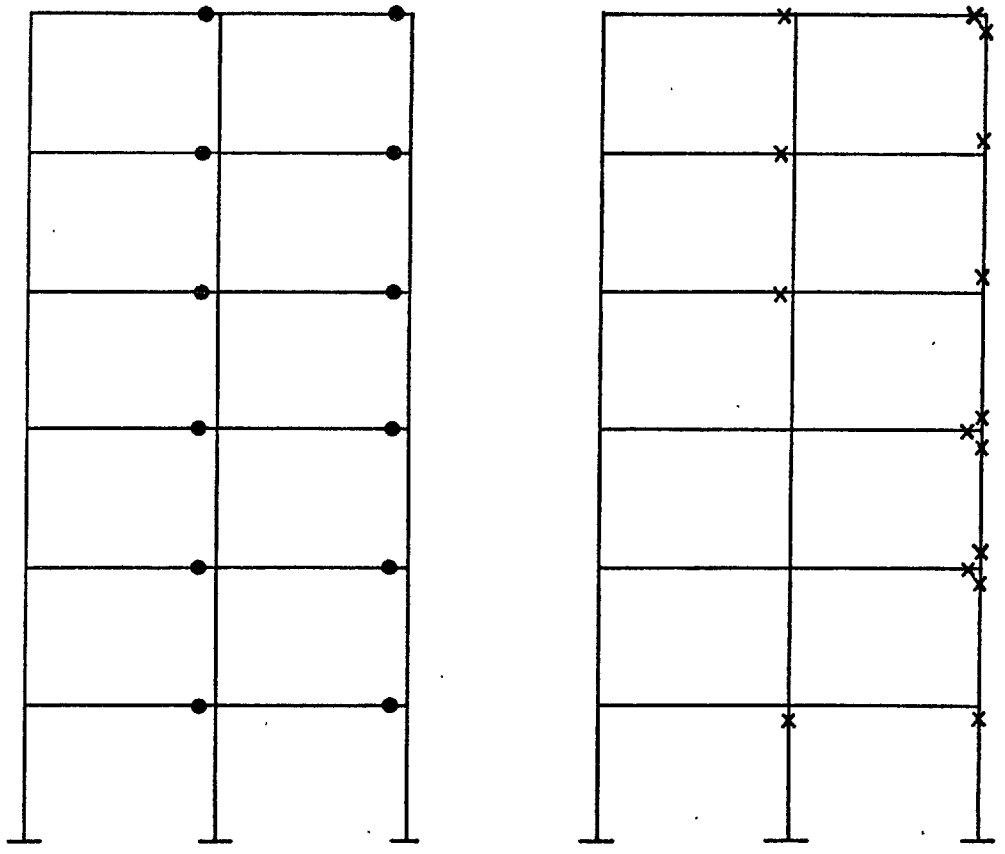
LOADING CONDITION I



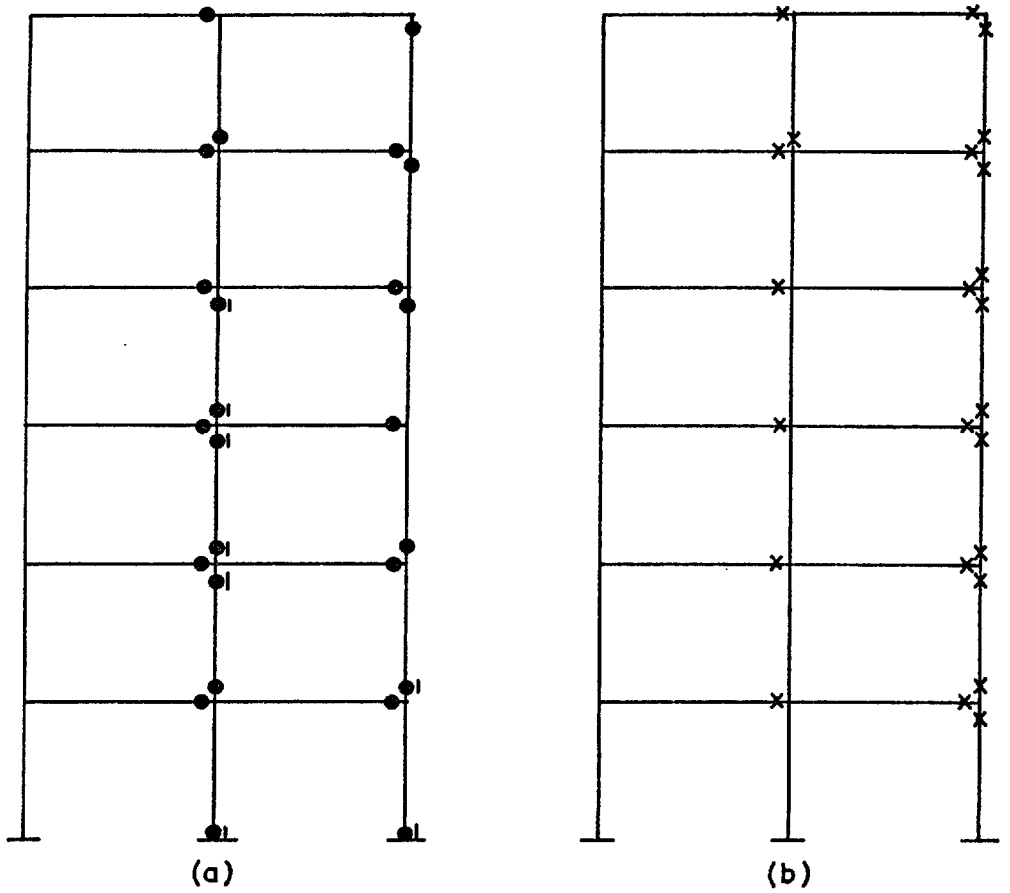
CASE 1 & 2

LOADING CONDITION II

FIG. 6.14 EXAMPLE 5

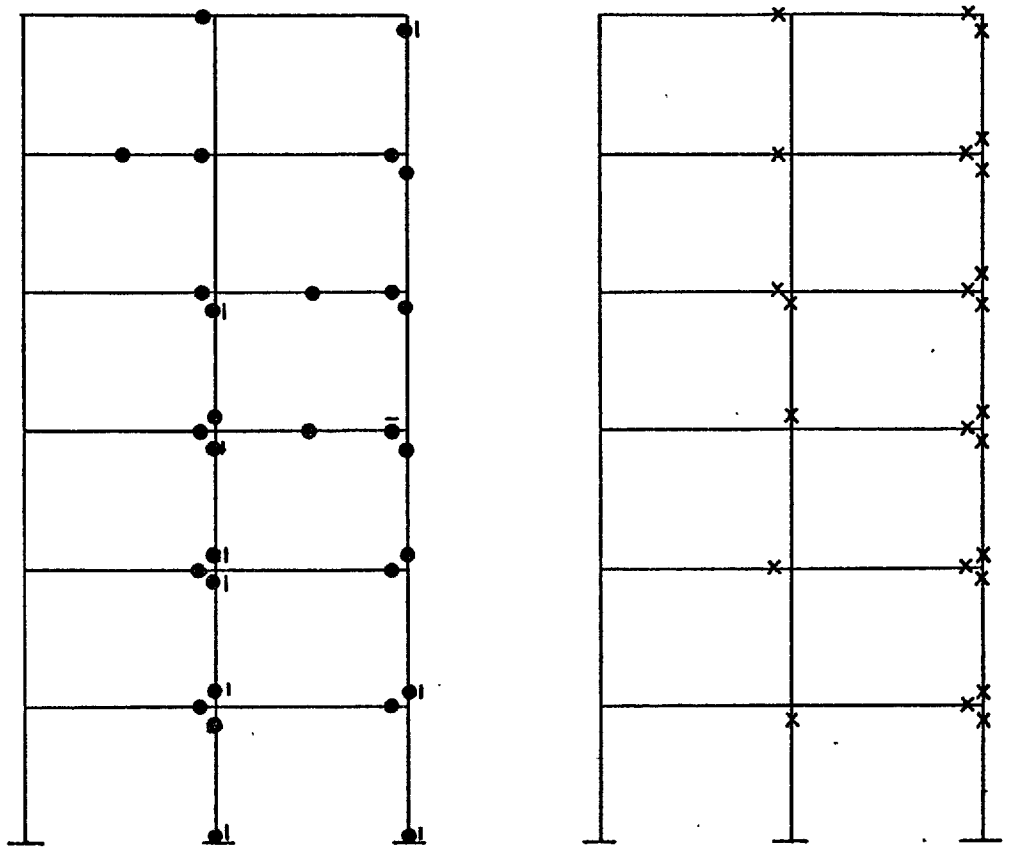


CASE 1



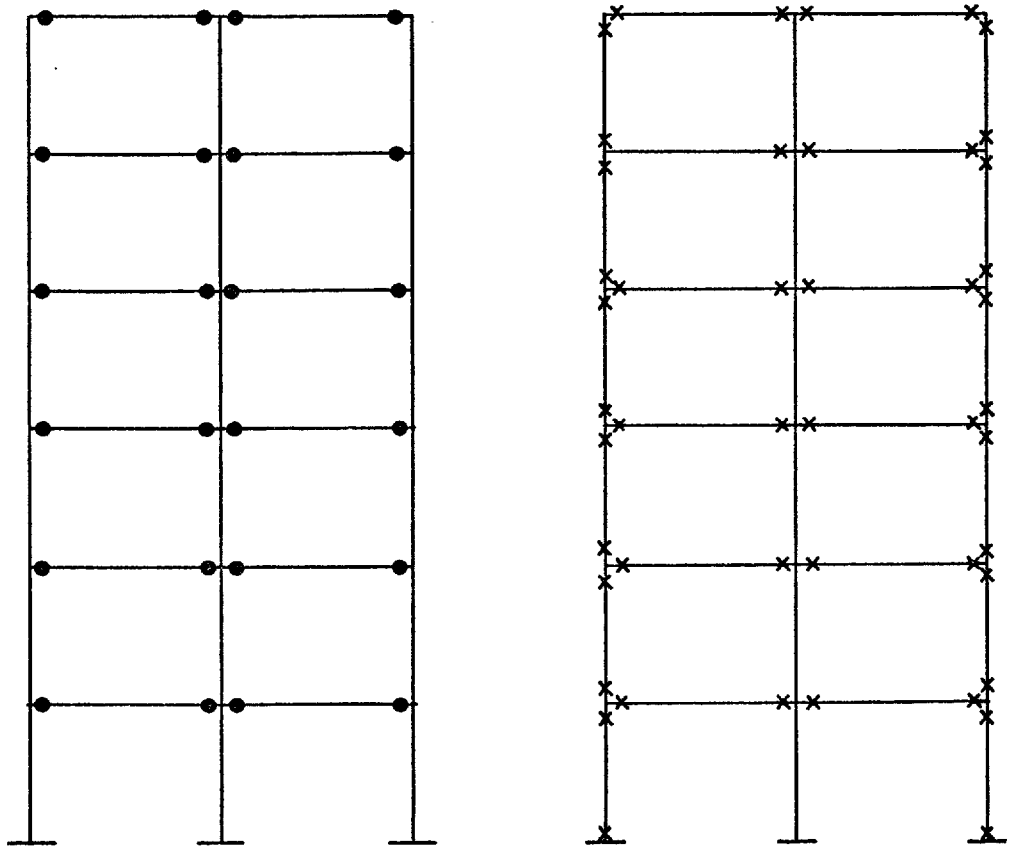
CASE 2

FIG. 6.15(a) EXAMPLE 6



(a) CASE 3 (b)

LOADING CONDITION I



CASE 1 & 2

LOADING CONDITION II

FIG. 15 (b) EXAMPLE 6

TABLE 6.8. COMPARISON OF ULTIMATE STRENGTH AND OPTIMAL DESIGNS

Example	Loading condition	Case	Vol. of steel U.S.D. V_U cm^3	Vol. of steel O.L.D. V_O cm^3	Percentage ecorromy
1	I	1	19,390	18,162	6.34
		2	19,390	17,096	11.83
		3	19,390	17,096	11.83
	II	1	11,138	9,785	12.14
		2	11,138	9,785	12.14
2	I	1	40,504	37,709	6.90
		2	40,504	36,656	9.50
		3	40,504	36,614	9.60
	II	1	28,752	24,703	14.08
		2	28,752	24,703	14.08
3	I	1	64,860	61,635	4.97
		2	64,860	59,517	8.24
		3	64,860	58,873	9.23
	II	1	74,401	59,403	20.16
		2	74,401	59,403	20.16
4	II	1	703,933	618,652	12.12
		2	703.933	618,652	12.12
5	I	1	76,774	71,914	6.33
		2	76,774	70,038	8.77
		3	76,774	69,225	9.83
	II	1	67,210	56,137	16.48
		2	67,210	56,137	16.48
6	I	1	129,821	120,778	6.97
		2	129,821	117,457	9.52
		3	129,821	116,804	10.03
	II	1	78,129	64,671	17.23
		2	78,129	64,671	17.23

The number of plastic hinges for optimal solution is found in most of the cases to be less than α, the indeterminacy number for a frame. It has also been observed that permissible values of rotation have been reached at some of the column hinges for cases 2 and 3 of hinge pattern under loading condition I. This emphasizes the need for the inclusion explicitly of the limited ductility constraints in O.L.D.

Table 6.8 gives the percentage economy of optimal limit design for the six frames for the three cases of hinge pattern under two loading conditions. The percentage economy is calculated with respect to the steel requirement for U.S.D. of sections for actions obtained from the elastic analysis for factored loads. It has been observed that the percentage economy depends on the geometry, loading condition and choice of hinge pattern. For loading condition I the percentage economy for case 1 of hinge pattern is found to be less than that for other cases of hinge pattern. This is due to the limited redistribution of moments resulting from the restricted choice of plastic hinges. For cases 2 and 3 of hinge pattern under loading condition I economy of upto 10 percent has been noted. Savings of steel of upto 20 percent have been observed for loading condition II.

In general it has been noticed that the savings of steel for loading condition II are higher than that for loading condition I. The area of steel, hence the volume, for the sections is proportional to the bending moment at the corresponding sections. In loading condition I with the development of plastic hinges a reduction in the value of moment is found at the ends of beams but this cannot be said of column sections. But for loading condition II, for symmetrical frames, there is an overall redistribution of moments resulting in a reduction of moment for beam ends and column sections. Hence in the later case the steel requirements also become less. Also in the case of loading condition II there is no difference in optimal solution due to different choice of hinge pattern for the three cases.

6.6. EFFECT OF VARIATION OF FLEXURAL RIGIDITY OF BEAMS

It has been observed from the tests conducted on T-beams subject to varying nature of moments along the beam that the EI distribution is non-uniform and that for the calculation of end rotations an equivalent EI

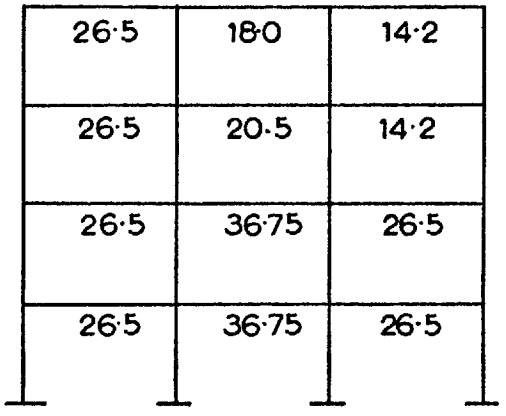
could be used. A simplified procedure has been suggested in section 5.7.4 for the computation of equivalent EI values.

In order to examine the effect of variation of flexural rigidity of beams on the optimal limit design, the examples 5 and 6 have been reworked using the equivalent EI values for beams. It may be noted that the calculation of equivalent EI values using the charts presented in section 5.7.4 require a knowledge of the ratio of moments and the ratio of flexural rigidities (at limit L_1) of the ends and mid-span sections. For the design examples these values have been obtained from the design of sections based on the analysis discussed in section 6.5. The equivalent EI values thus computed are shown in Fig.6.16. The results of analysis using the equivalent EI values for beams are discussed below.

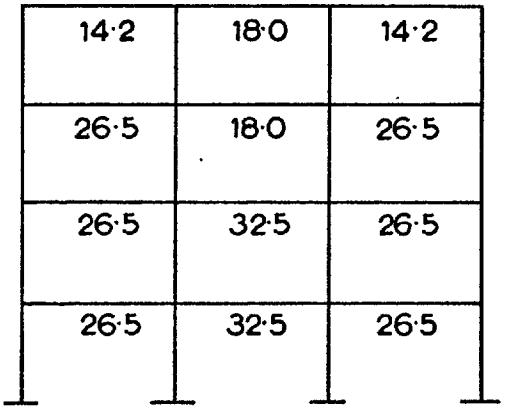
The frames have been analysed for three cases of hinge pattern under two loading conditions using the O.L.D. program described in Chapter 4. The bending moment diagrams for O.L.D. and for the U.S.D. are plotted in Figs. 6.17 to 6.18. The position of plastic hinges as obtained for optimal design are shown in Figs. 6.19 to 6.20.

The bending moment values are compared with the values obtained from analysis discussed in section 6.5 based on uniform EI values of beam sections and the results for some of the critical sections are given in Tables 6.9(a) and 6.9(b). It can be observed from these Tables that there is considerable difference in the magnitude of moments for some of the sections due to difference in the EI values of beams used in the analyses and the amount of variation depends on the geometry, loading condition, type of hinge pattern and the position of sections. For sections such as 2, 3 in Example 5 and 1, 2 in Example 6 an increase of about 10 percent in the value of moment is noted. But for beam end sections such as 6 in Example 5 and 3 in Example 6 a decrease of about 15 percent is noted. In the case of columns a reduction of about 15 percent is observed in the value of moment for sections such as 42 and 6 in Examples 5 and 6 respectively.

The plastic hinge pattern shown in Figs. 6.19 and 6.20 for the O.L.D. using equivalent EI values for T-beams are similar to that obtained for the O.L.D. discussed in the previous section. However, due to increased flexural rigidity of beams in the present analysis the inelastic rotations of beam hinges have been found to be less than the corresponding values for the O.L.D. using the uniform EI values of beam sections.



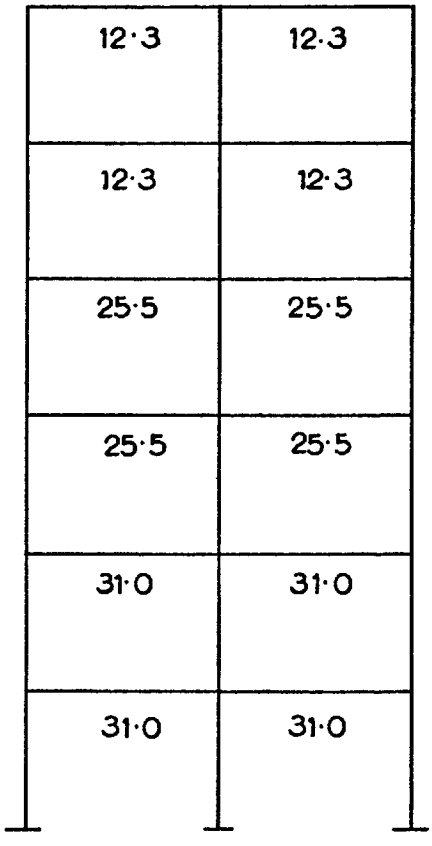
LOADING CONDITION I



LOADING CONDITION II

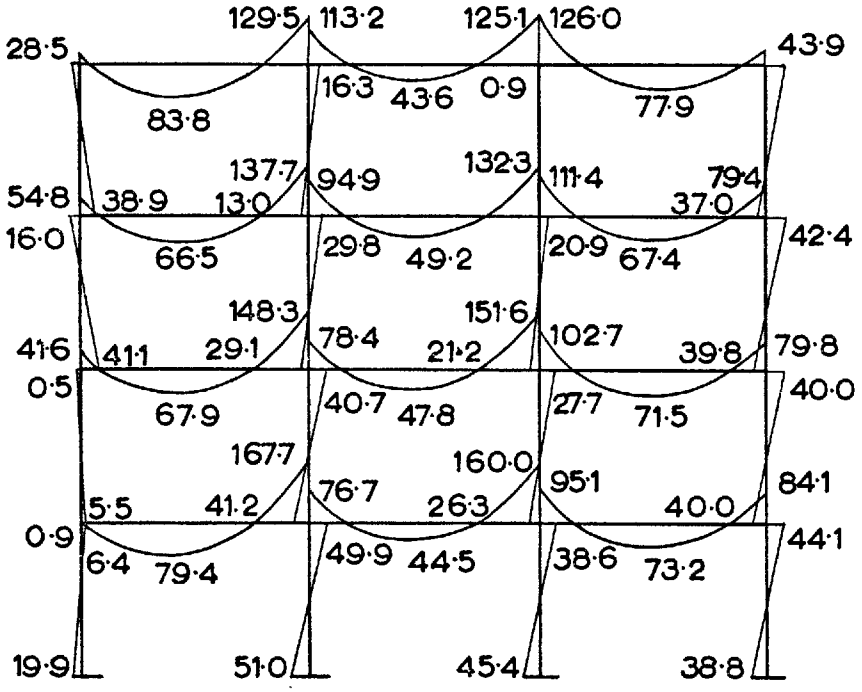
EXAMPLE 5

units - N mm^2 x 10^{12}

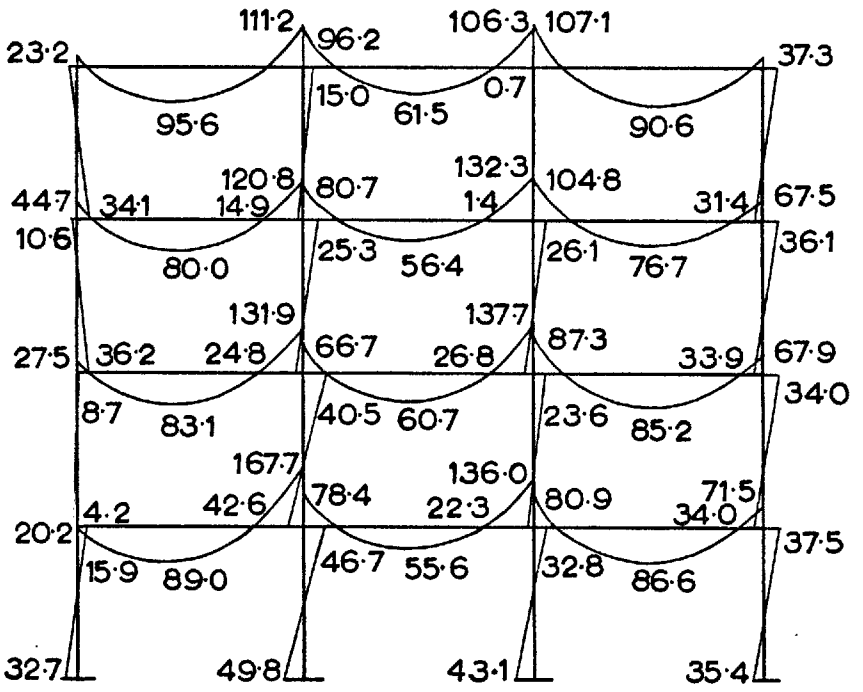


EXAMPLE 6

FIG. 6.16 E I VALUES FOR BEAMS



U.S.D.

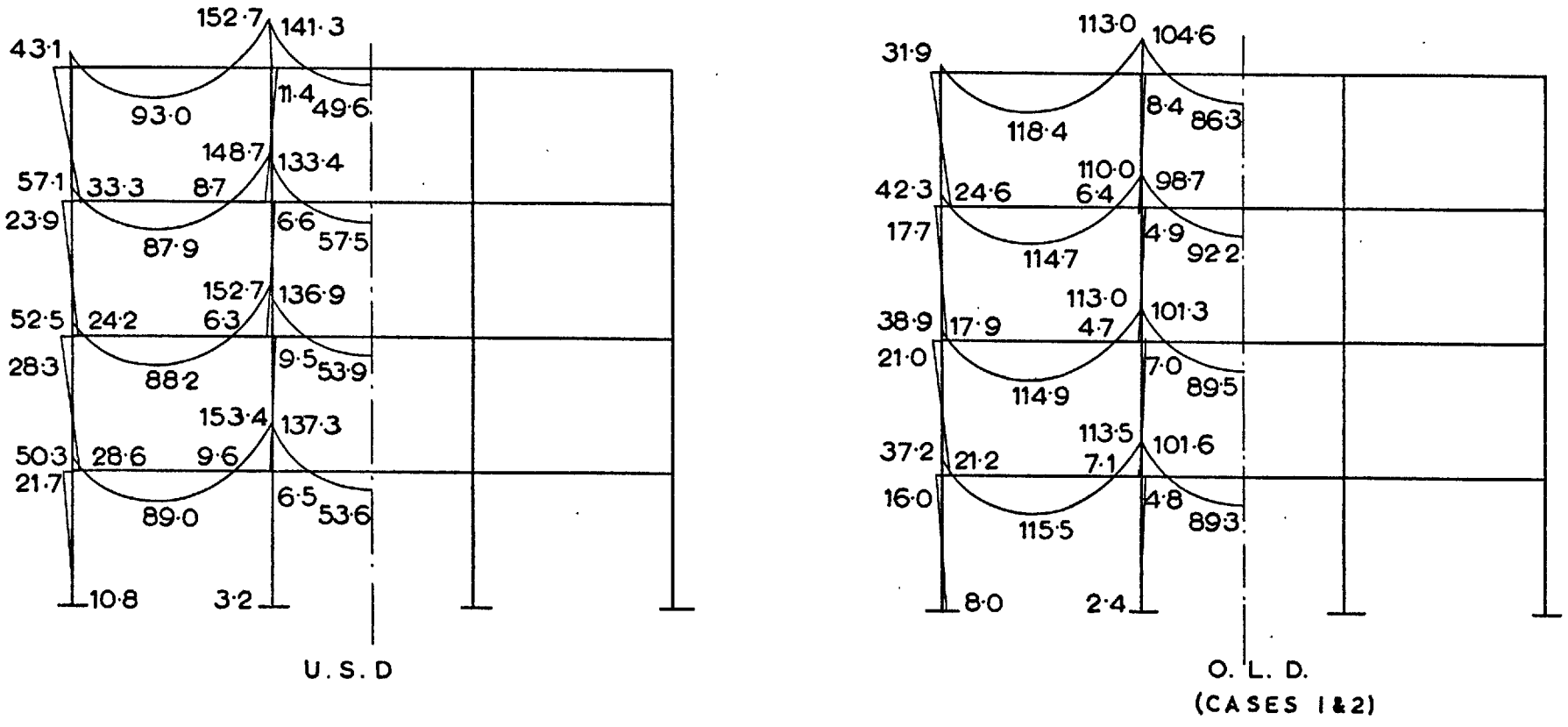


O.L.D.
(CASE 2)

LOADING CONDITION I

FIG. 6.17 (a) B.M. DIAGRAMS EXAMPLE 5

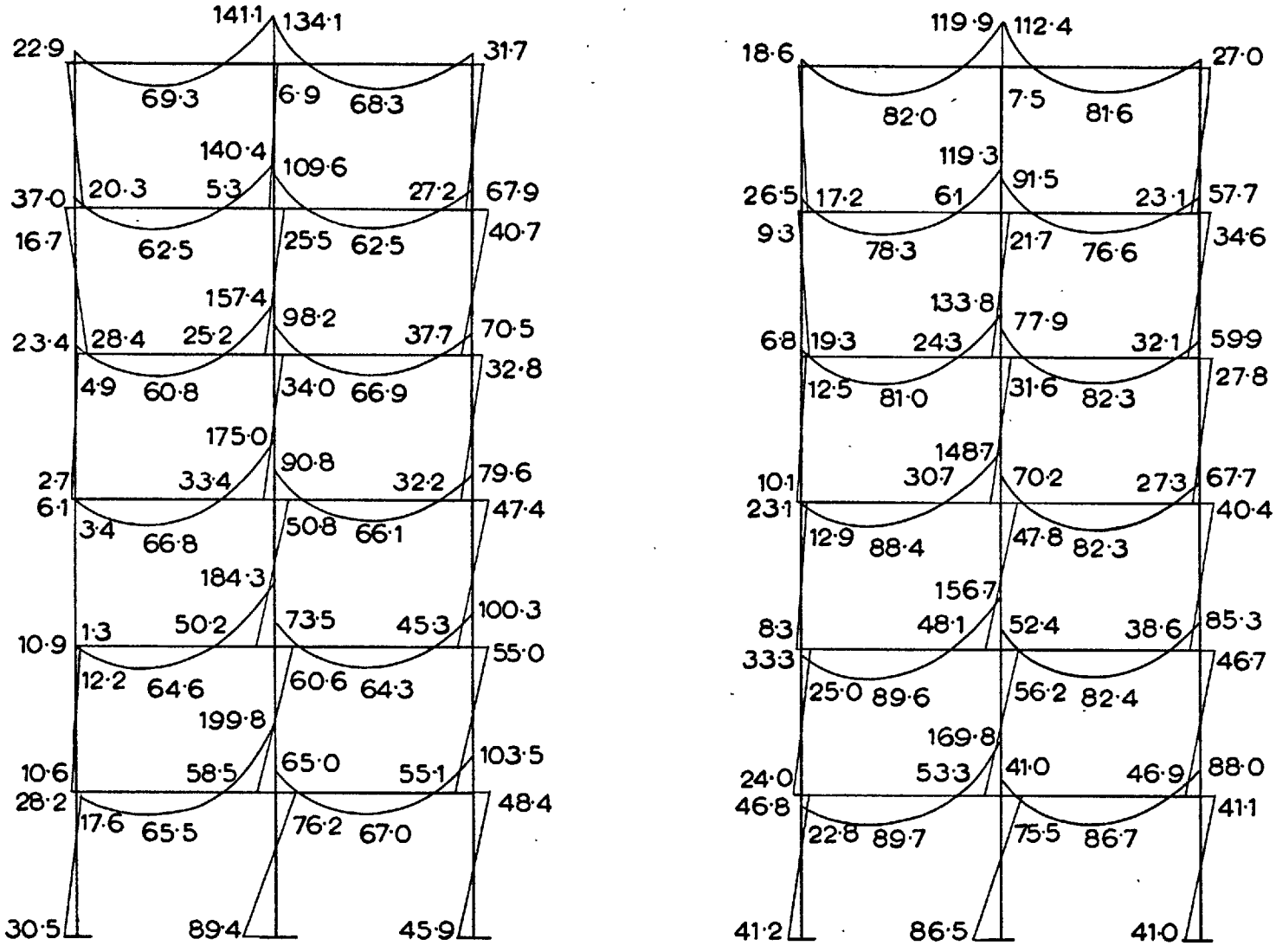
(units - kN m)



LOADING CONDITION III

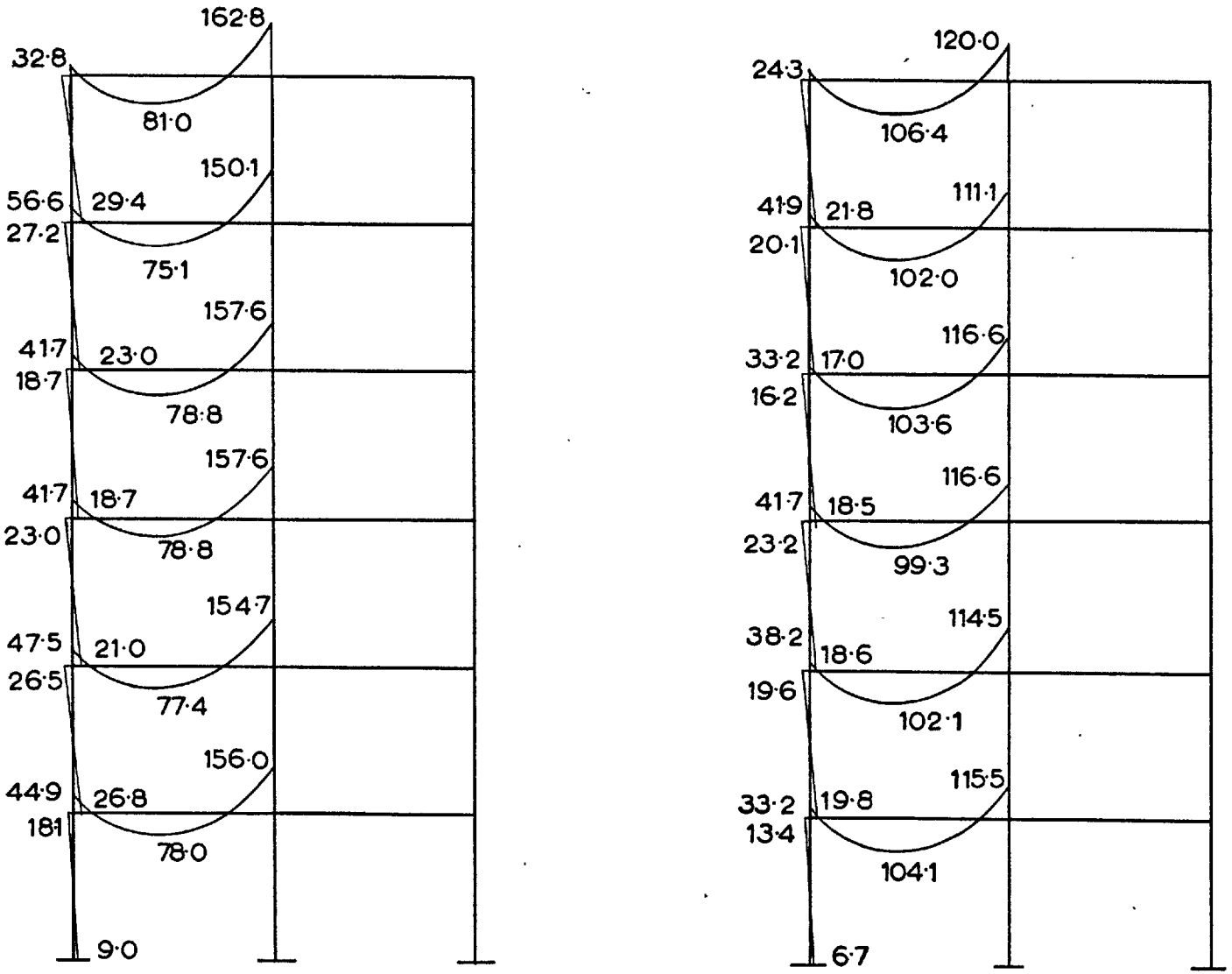
FIG. 6.17 (b) B.M. DIAGRAMS. EXAMPLE 5

(units - kN m)



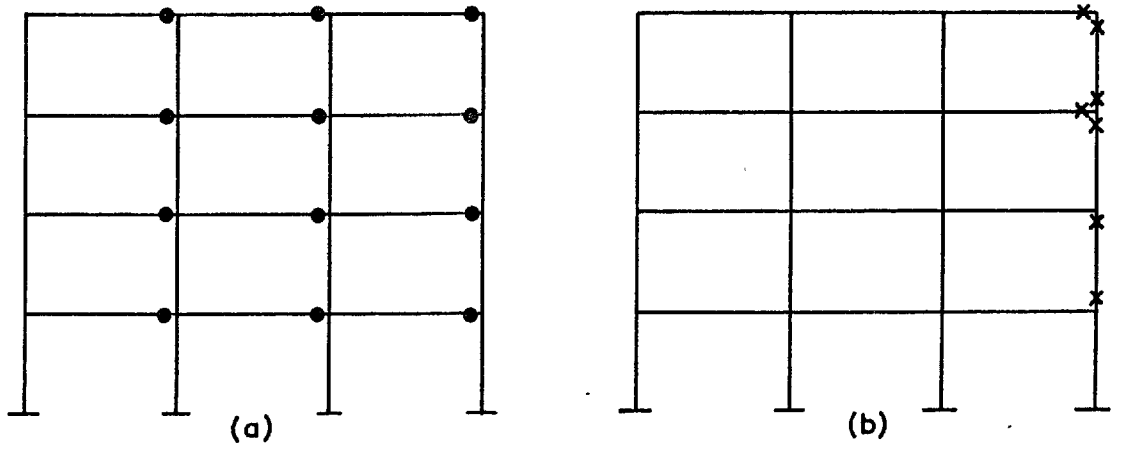
LOADING CONDITION I

FIG. 6.18 (a) B.M. DIAGRAMS. EXAMPLE 6

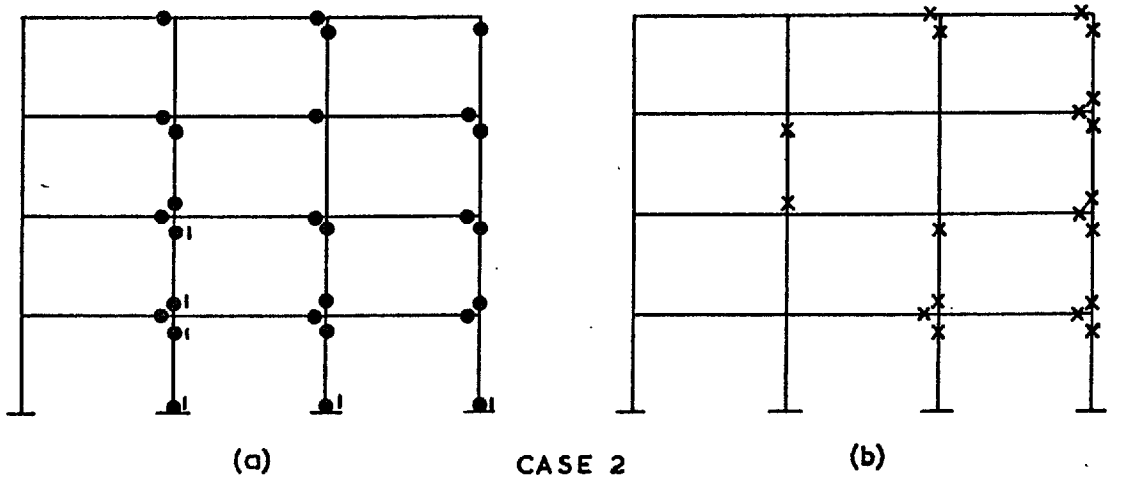


LOADING CONDITION II

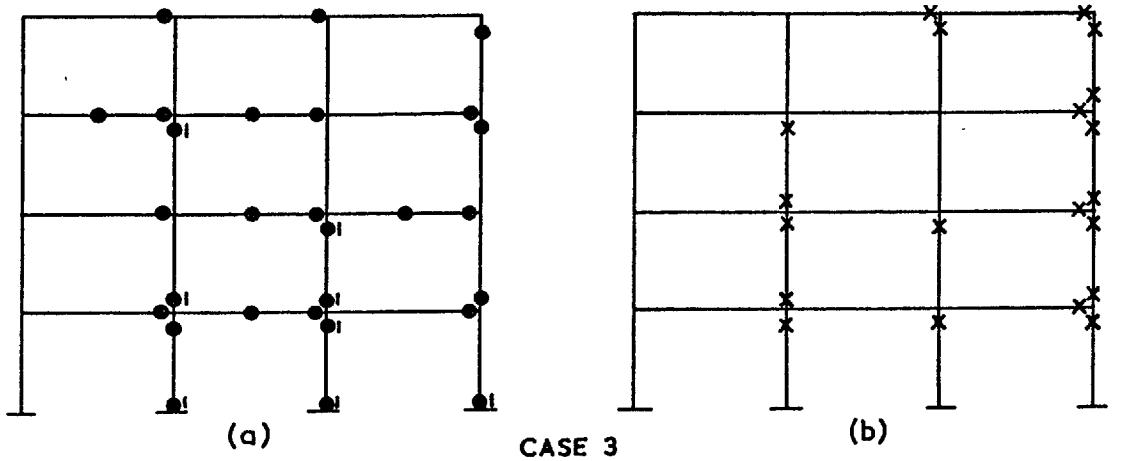
FIG. 6.18 (b) B.M. DIAGRAMS. EXAMPLE 6



CASE 1

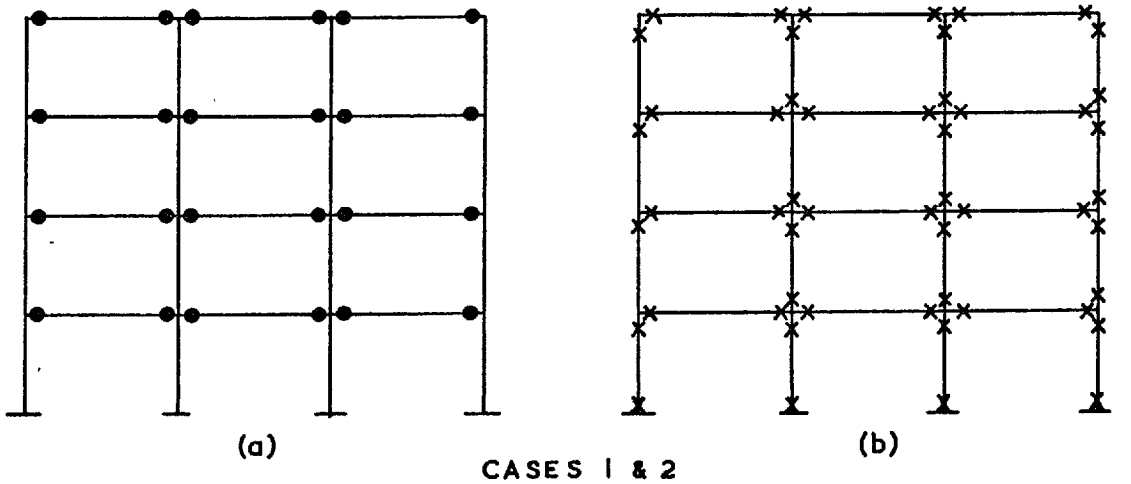


CASE 2



CASE 3

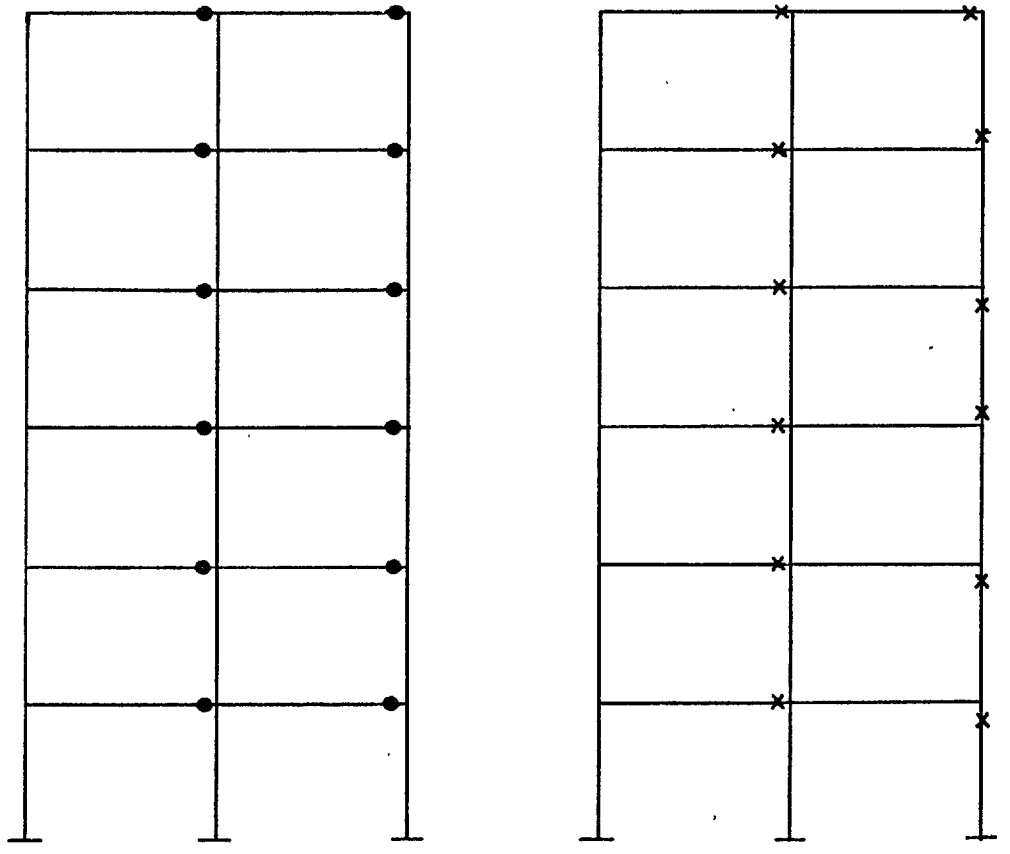
LOADING CONDITION I



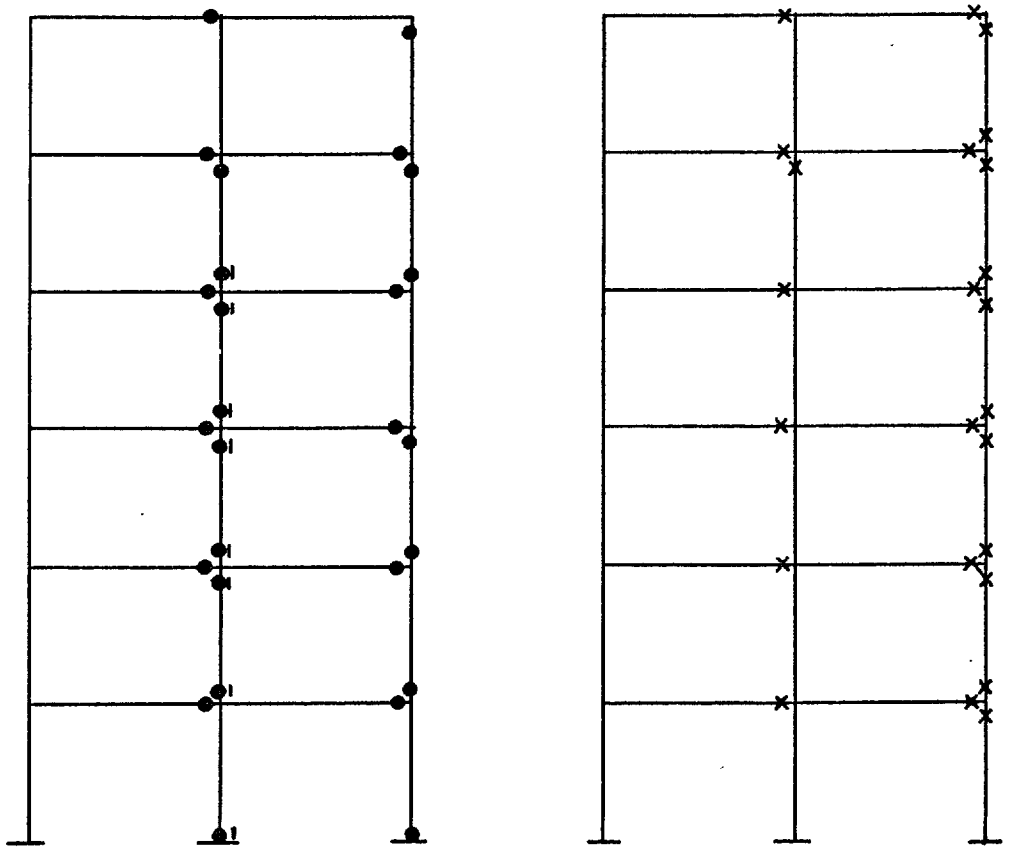
CASES 1 & 2

LOADING CONDITION II

FIG. 6.19 EXAMPLE 5

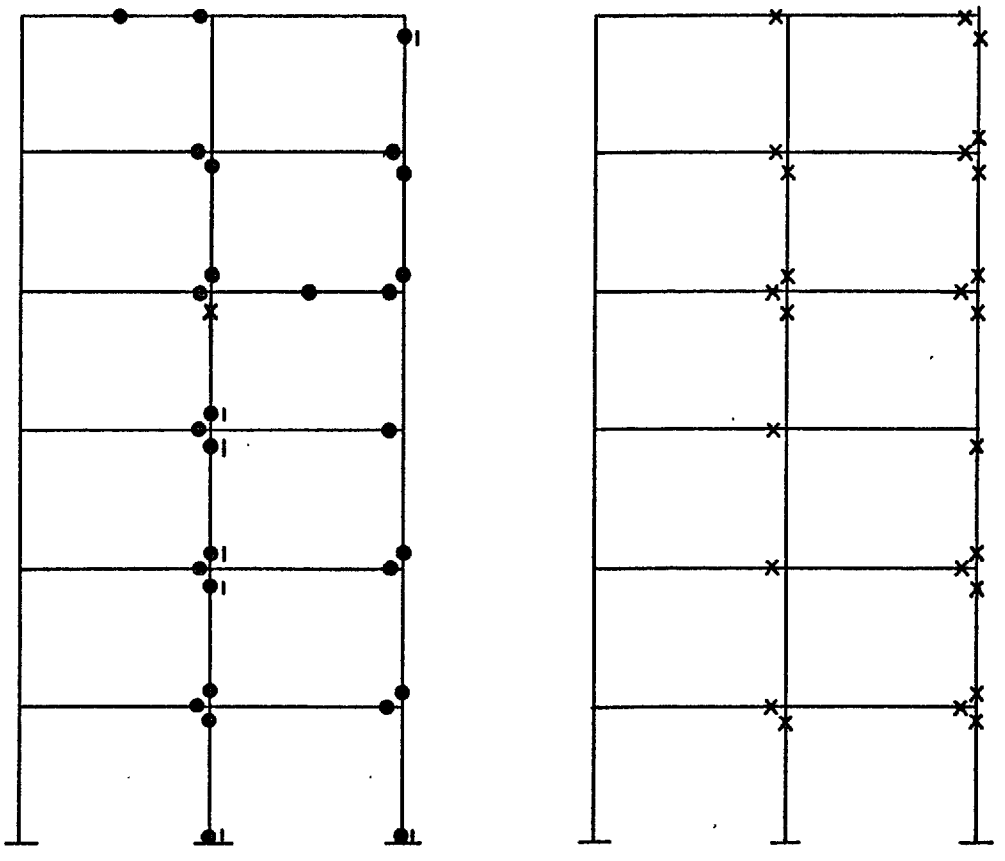


CASE 1



CASE 2

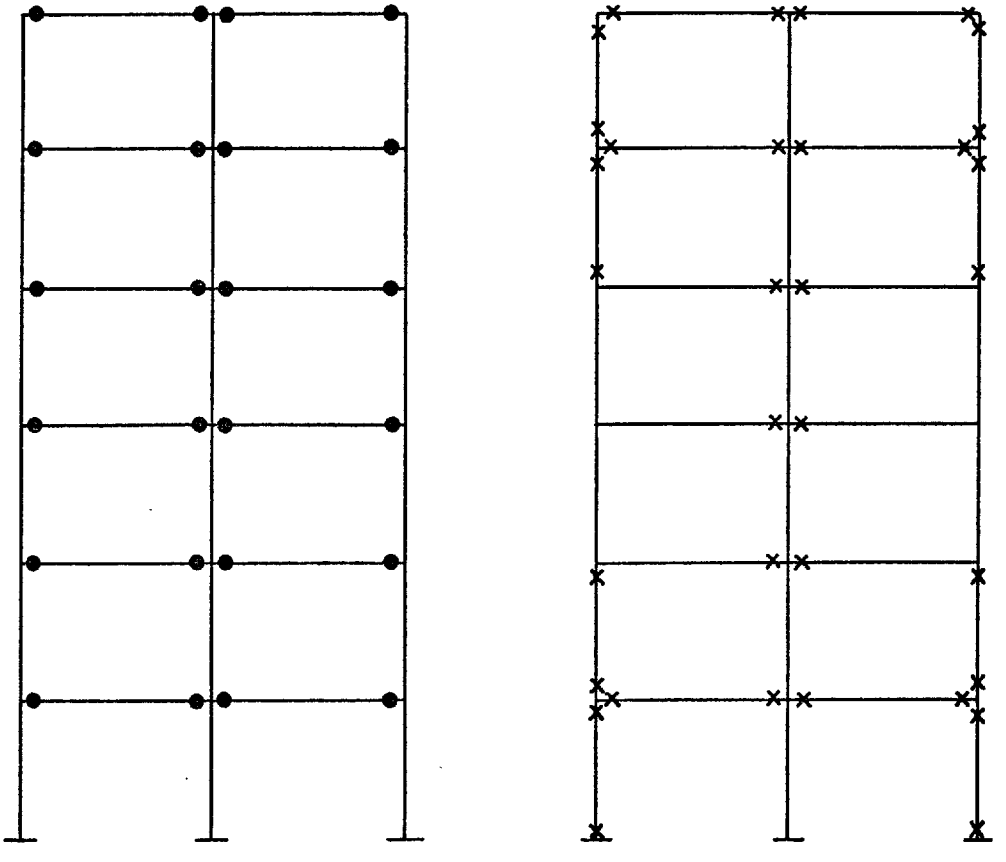
FIG. 6.20 (a) EXAMPLE 6 (CONTD.)



(a) (b)

CASE 3

LOADING CONDITION I



CASE 1

LOADING CONDITION II

FIG. 20(b) EXAMPLE 6

TABLE 6.9(a) RATIO OF MOMENTS $\frac{M^j_{dT}}{M^j_{dR}}$. EXAMPLE 5

Section	Loading Condition I				Loading condition II	
	U.S.D.	O.L.D.			U.S.D.	O.L.D. Cases 1 & 2
		case 1	case 2	case 3		
1	1.020	1.052	1.020	1.020	1.036	1.036
2	1.149	1.098	1.140	1.143	1.115	1.062
3	1.081	1.051	1.081	1.096	1.049	1.047
4	0.872	0.928	0.902	0.869	0.897	0.951
6	0.813	0.803	0.813	0.813	0.679	0.679
7	1.091	1.101	1.064	1.064	1.115	1.062
5	0.945	0.924	0.914	0.900	0.954	0.954
42	0.863	0.871	0.863	0.863	0.676	0.676
19	0.990	0.959	0.869	0.897	1.016	1.016
20	0.974	0.983	1.071	0.928	1.115	1.062
21	1.068	1.251	1.244	1.175	1.017	1.018
22	0.965	0.864	0.892	0.940	0.961	0.981
24	0.961	0.961	0.961	0.961	0.735	0.735
25	1.018	0.931	0.950	0.999	1.115	1.062
54	1.153	1.125	0.828	0.839	1.046	1.047
58	0.979	0.979	0.979	0.979	0.678	0.678
66	0.924	0.924	0.924	0.924	0.861	0.861

TABLE 6.9(b). RATIO OF MOMENTS $\frac{M^j_{dT}}{M^j_{dR}}$. EXAMPLE 6

Section	Loading condition I				Loading condition II	
	U.S.D.	O.L.D.			U.S.D.	O.L.D. Cases 1 & 2
		case 1	case 2	case 3		
1	1.090	1.041	1.090	1.064	1.100	1.100
2	1.095	1.151	1.109	1.142	1.097	1.052
3	0.841	0.819	0.841	0.841	0.619	0.619
5	0.911	0.886	0.851	0.856	-	-
6	0.840	0.814	0.765	0.807	0.617	0.617
13	1.042	1.007	1.055	1.022	1.077	1.077
14	1.083	1.090	1.053	1.057	1.076	0.987
15	0.821	0.832	0.821	0.826	0.651	0.879
50	1.036	1.022	0.999	1.100	-	-
52	0.844	0.862	0.844	0.844	0.654	0.892
25	1.010	1.010	1.011	1.010	1.010	1.010
26	0.974	0.971	0.988	1.029	1.010	1.006
27	1.028	1.011	1.028	1.028	0.947	0.948
62	1.300	1.213	1.027	0.946	-	-
64	1.062	1.031	1.060	1.060	0.891	0.891

TABLE 6.10. COMPARISON OF DESIGNS FOR THE EFFECT OF VARIATION OF FLEXURAL RIGIDITY OF BEAMS

Example	L.C.	Case	$(V_U)_T$ cm^3	$(V_O)_T$ cm^3	Percentage economy $\frac{(V_U)_T-(V_O)_T}{(V_U)_T} \times 100$	$\frac{(V_U)_T}{V_U}$	$\frac{(V_O)_T}{V_O}$	$\frac{(V_O)_T}{V_U}$
5	I	1	71,357	67,541	5.35	0.93	0.94	0.88
		2	71,357	64,661	9.38		0.92	0.84
		3	71,357	63,595	10.88		0.92	0.83
	II	1 & 2	59,137	51,116	13.56	0.88	0.91	0.76
6	I	1	122,465	114,400	6.59	0.94	0.95	0.88
		2	122,465	110,253	9.97		0.94	0.85
		3	122,465	109,591	10.51		0.94	0.84
	II	1 & 2	64,163	57,158	10.92	0.82	0.88	0.73

Table 6.10 gives the percentage economy for O.L.D. using the equivalent EI values for beams. As has been discussed earlier, the percentage economy depends on the geometry, loading condition and choice of hinge pattern. Savings of steel of upto 13.5 percent have been noted. It has also been observed that for loading condition II the percentage economy is less than that obtained for similar conditions using uniform EI values for beams. This is due to the favourable distribution of bending moment for the U.S.D. using equivalent EI values for beams and the resulting decrease in the volume of steel required, as discussed below.

The ratios of volume of steel required using equivalent EI values, $(V_0)_T$ and $V_U)_T$ and uniform EI values for beams, V_0 and V_U, for the U.S.D. and O.L.D. are given in Table 6.10. In general it has been observed that the volume of steel required in design using equivalent EI values is less than that required using uniform EI values of beams. Comparing the volume of steel required for O.L.D. using equivalent EI values and U.S.D. using uniform EI values it is noted that savings of steel of upto 16 percent for loading condition I and 25 percent for loading condition II can be obtained using equivalent EI values.

6.7. INSTABILITY CONSIDERATION IN O.L.D.

The secondary moments caused by the action of axial loads on the deformation of frame members are sometimes important enough to affect the overall bending moment distribution and the stability of the frame as a whole. The instability effects become more pronounced in the limit design of reinforced concrete frames when a number of plastic hinges are allowed to form in the structure. This is because the resultant reduction of overall stiffness may render the frame unstable at an earlier stage (53). A comprehensive investigation (53) has been carried out recently on the instability effects of reinforced concrete sway frames. Based on this study a design procedure has been suggested (53, 54), for incorporation in the simplified limit method, to allow for the instability effects by means of a magnification factor to the lateral loads. This approach has been found suitable for use in O.L.D.

The magnification factor β_e for the elastic stage is given by,

$$\beta_e = \frac{1}{1 - \bar{p}_T \cdot \dfrac{(2 - \frac{1}{m})(2 - \frac{r_f}{1 + \bar{K}_b}) + \dfrac{6y}{\bar{s}(1 + \bar{c})}}{12y}} \qquad (6.12)$$

Equation (6.12) is applicable as long as no plastic hinges are formed in the frame. When plastic hinges are assumed to form there is a reduction in the stiffness of the structure and consequently an increase in the magnification factor. The corresponding plastic magnification factor is given by,

$$\beta_p = \frac{1}{1 - \bar{p}_T \dfrac{2(2 - \frac{1}{m}) + \frac{6y}{\bar{s}(1 + \bar{c})}}{12y}} \qquad (6.13)$$

The total magnification factor β_d at the design load is greater than the corresponding value of β_e and less than β_p. The following expression was found to give a satisfactory combination of two factors,

$$\beta_d = \beta_e + \frac{(\lambda_c - 1)}{\lambda_c} (\beta_p - \beta_e) \qquad (6.14)$$

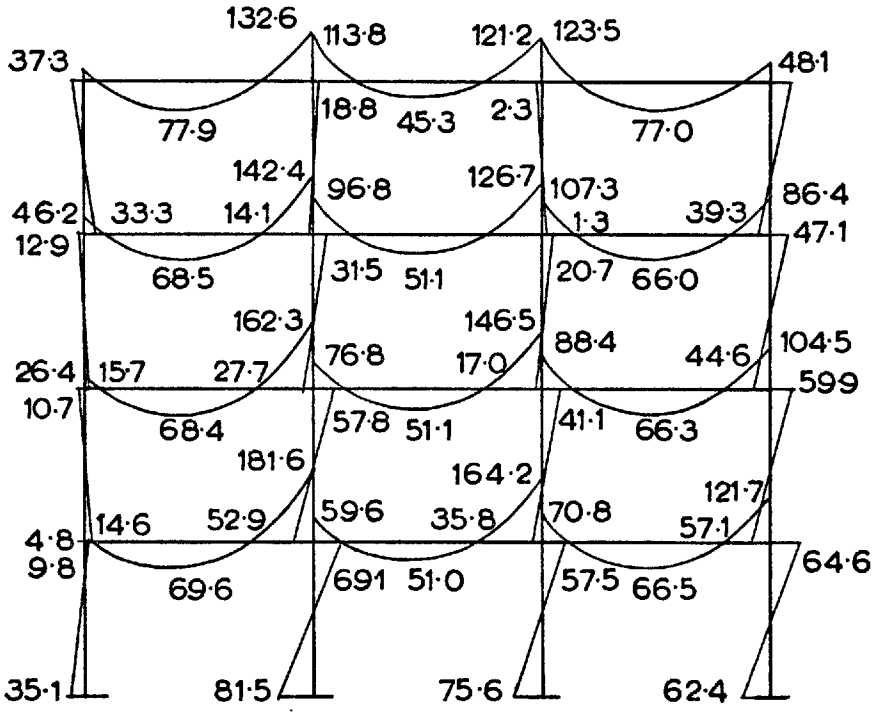
The value of $\bar{p}_T$ to be used in equations (6.12) and (6.13) is that corresponding to the design load. For concrete members the value of $\frac{P_T H^2}{\Sigma EI_c}$ is usually small enough so that little error is involved if the first order values of the stability functions (i.e. $\bar{s} = 4.0$ and $\bar{c} = 0.5$) are used.

The magnification factors to the lateral loads are worked out for the design examples 5 and 6, and the details of calculations are presented in Table 6.11. It may be observed that the magnification factors for some of the storey shears are as high as 1.55. This is due to the low values of the flexural rigidity of columns (calculated at limit L_1 for critical section) resulting from low percentage of high strength steel reinforcement used.

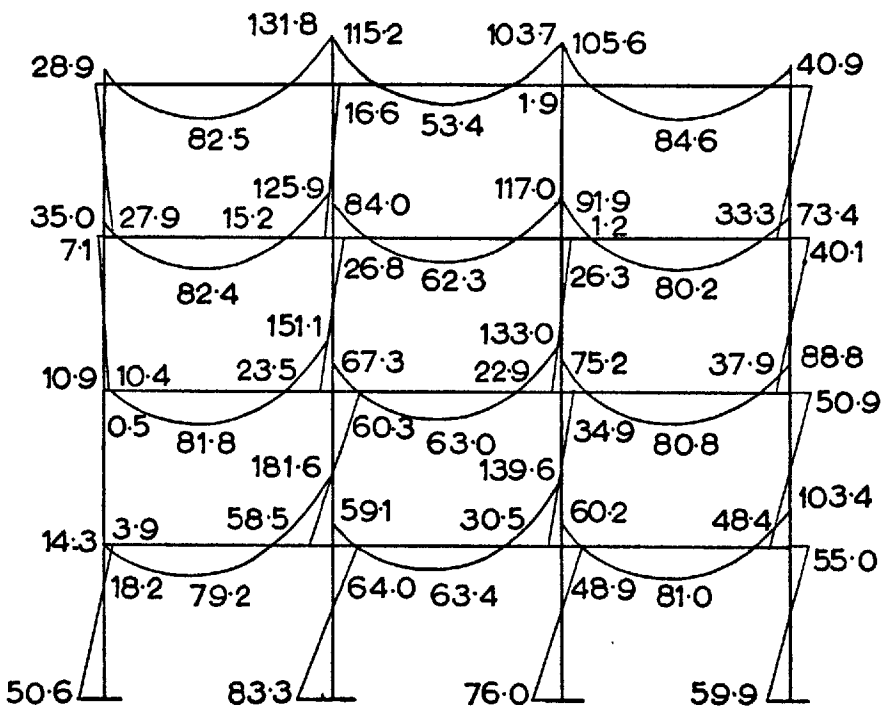
The frames have been analysed for loading condition I with the magnitude of lateral loads increased by the magnification factors. The bending moment diagrams for O.L.D. and U.S.D. are plotted in Figs. 6.21 and 6.22. The position of plastic hinges for O.L.D. are shown in Figs. 6.23 and 6.24.

TABLE 6.11. CALCULATION OF MAGNIFICATION FACTORS

Example	Storey	m	EI_{ce} x10^{12} Nmm^2	EI_{ci} x10^{12} Nmm^2	EI_{bi} x10^{12} Nmm^2	EI_{be} x10^{12} Nmm^2	P_T kN	$\bar{p}_T$	y	$\frac{r_f}{1+\bar{K}_b}$	β_e	β_p	β_d
5	1	4	4.5	7.0	12.0	12.0	2605	1.81	1.78	0.78	1.49	1.82	1.55
	2	3	4.0	7.0	12.0	12.0	1954	1.42	2.00	0.88	1.30	1.46	1.33
	3	2	3.5	4.5	12.0	12.0	1303	1.30	2.29	0.65	1.25	1.33	1.27
	4	1	3.5	4.0	12.0	12.0	651	0.70	2.29	0.57	1.10	1.12	1.10
6	1	6	5.5	13.0	12.0	12.0	2640	1.76	1.59	1.18	1.39	1.94	1.50
	2	5	5.5	10.0	12.0	12.0	2200	1.68	1.59	0.91	1.45	1.85	1.53
	3	4	4.0	7.0	12.0	12.0	1760	1.56	2.18	0.88	1.33	1.52	1.37
	4	3	3.0	6.0	12.0	12.0	1320	1.76	2.91	1.00	1.30	1.46	1.33
	5	2	3.0	4.0	12.0	12.0	880	1.41	2.91	0.67	1.25	1.31	1.26
	6	1	2.5	3.5	12.0	12.0	440	0.83	3.49	0.70	1.10	1.12	1.10



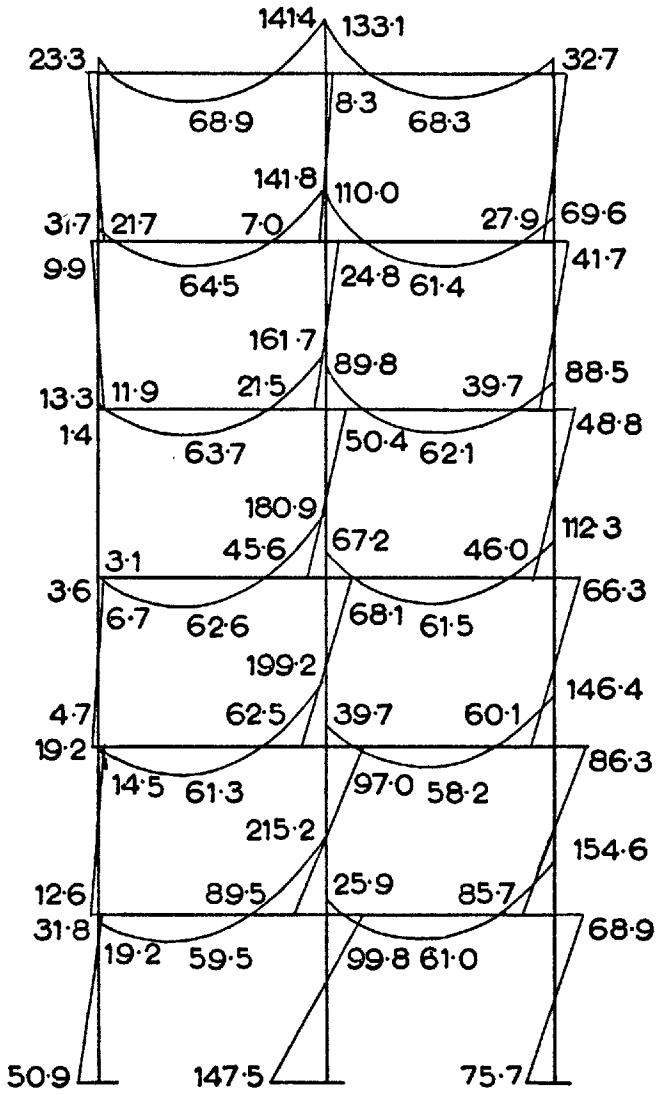
U.S.D.



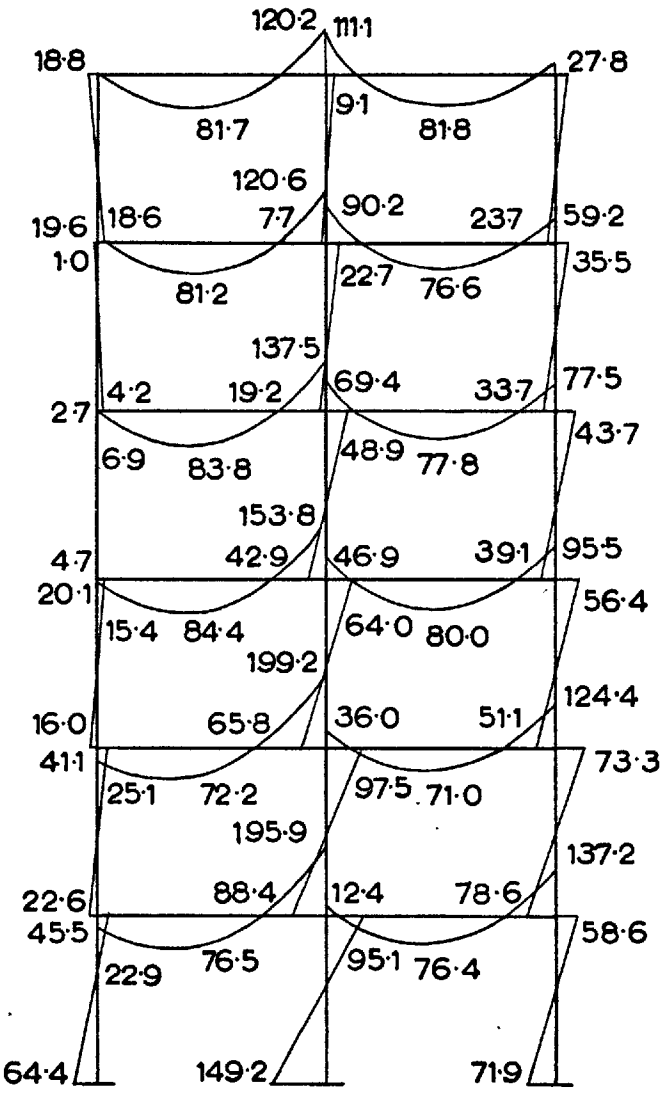
O. L. D.
(CASE 2)

LOADING CONDITION I

FIG. 6.21 B.M. DIAGRAMS EXAMPLE 5
(units – kN m)



U. S. D

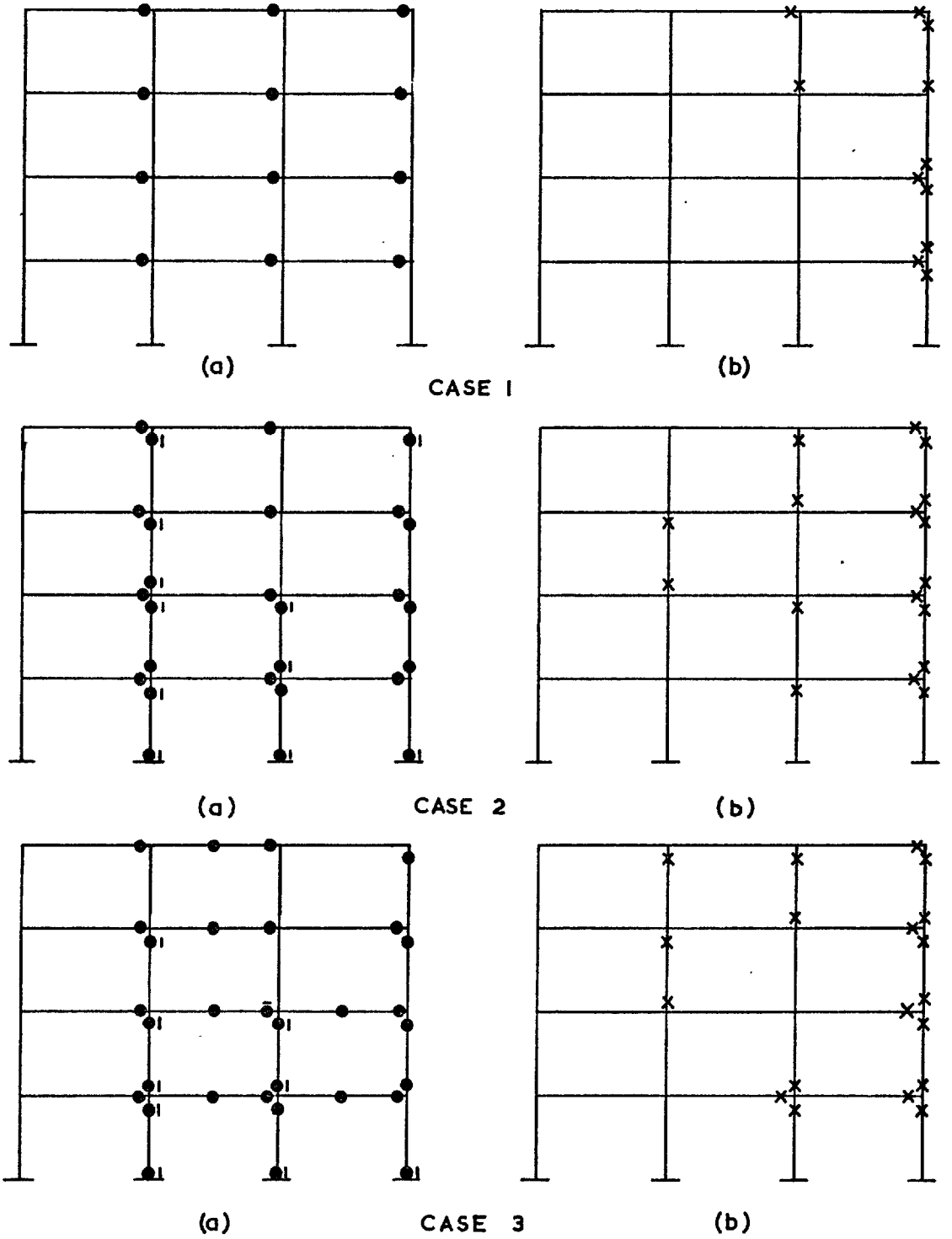


O. L. D.

(CASE 2)

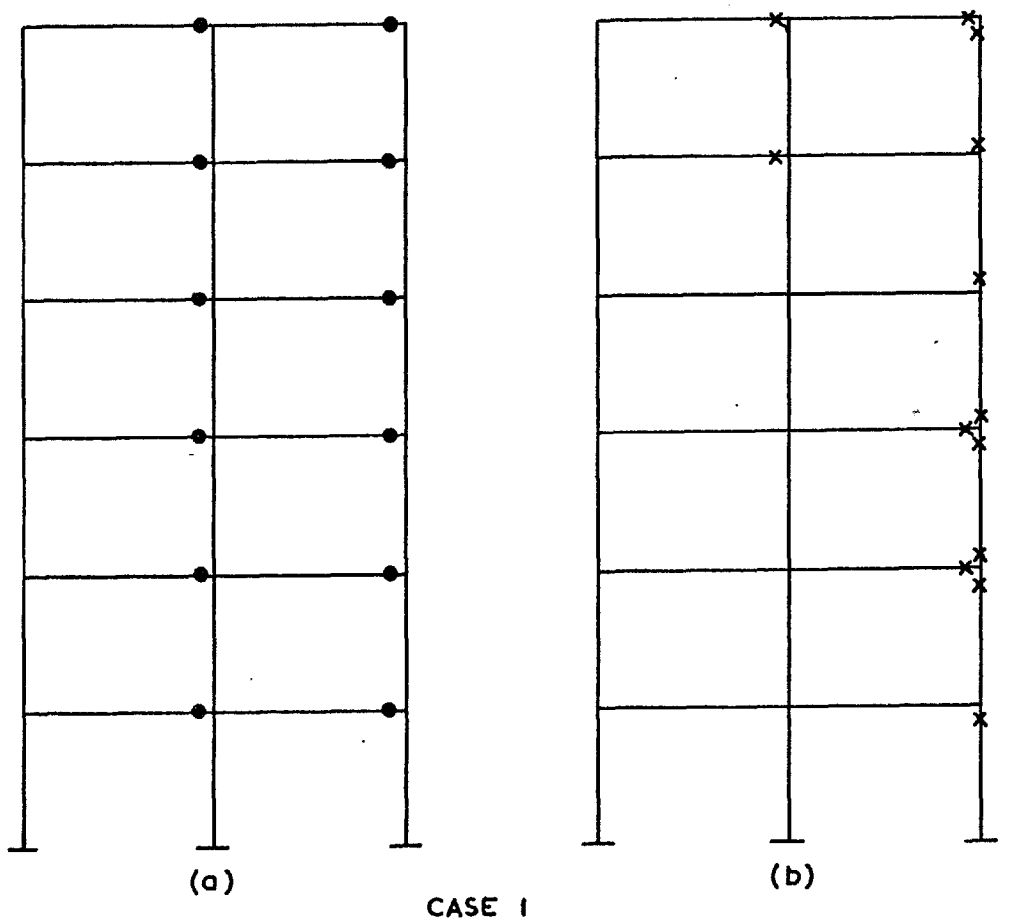
LOADING CONDITION I

FIG. 6.22 B. M. DIAGRAMS EXAMPLE 6



LOADING CONDITION I

FIG. 6.23 EXAMPLE 5



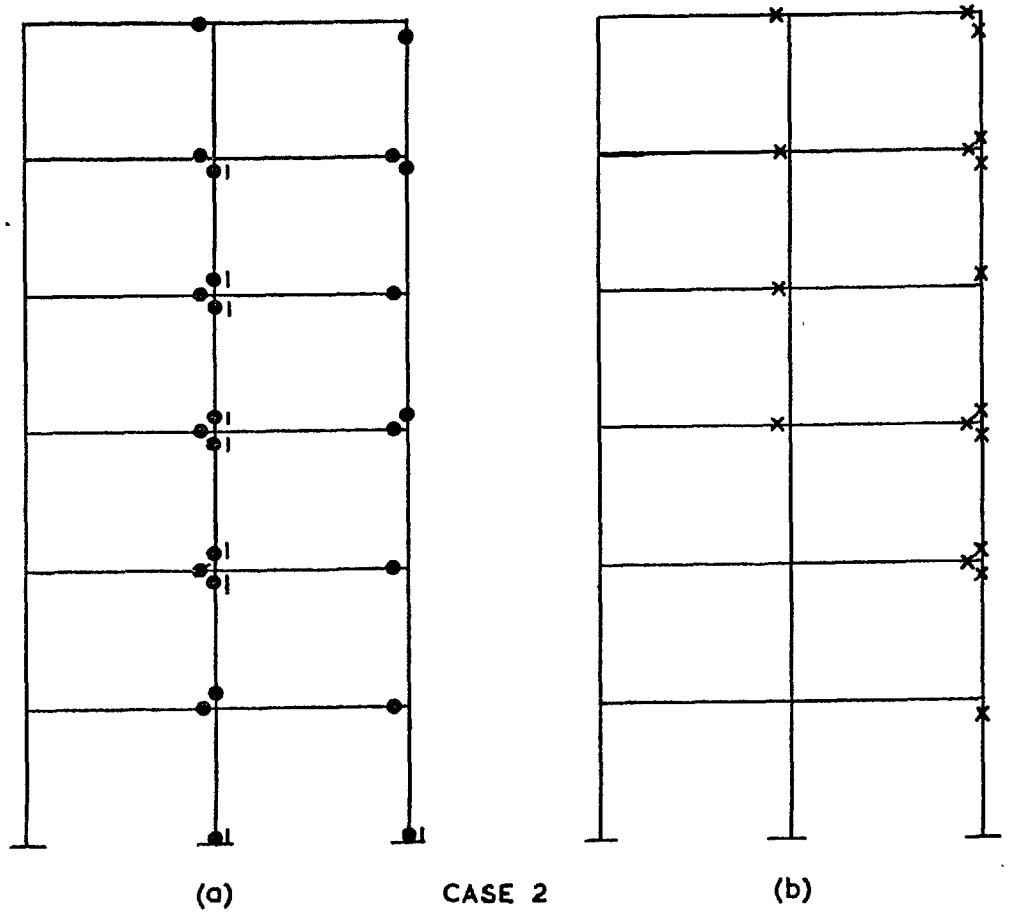
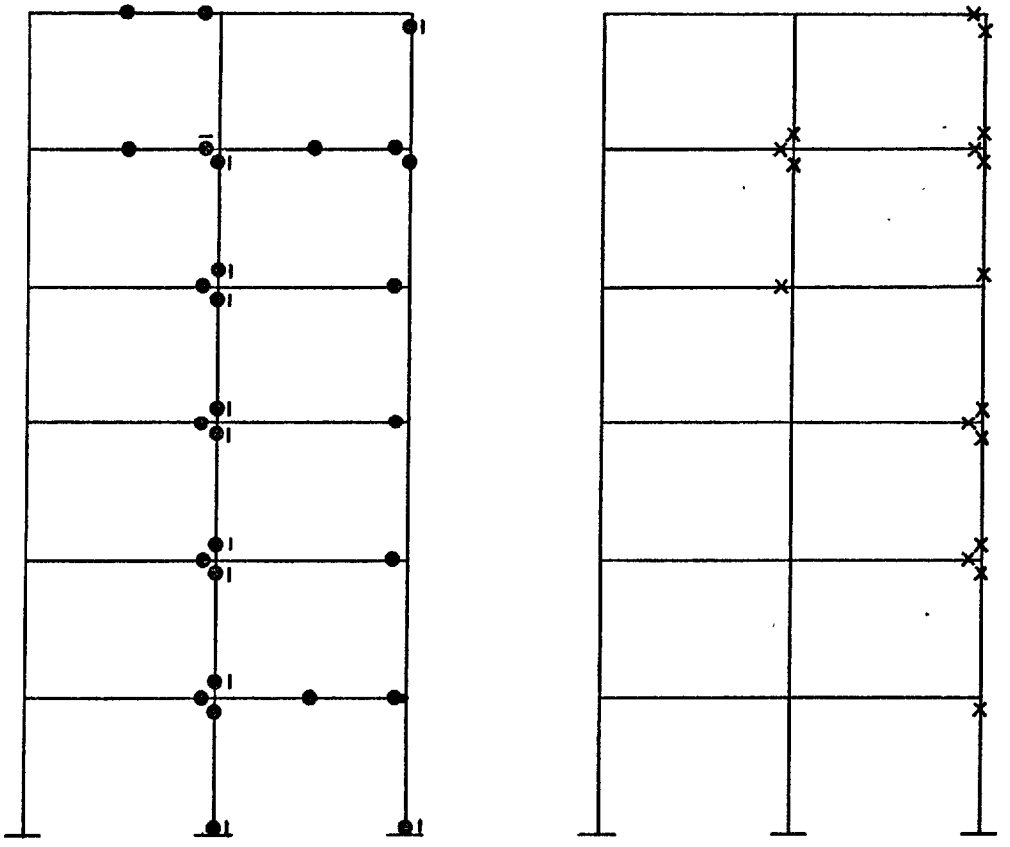


FIG. 6.24(a) EXAMPLE 6



(a) CASE 3 (b)

LOADING CONDITION I

FIG. 6.24 (b) EXAMPLE 6

TABLE 6.12. INSTABILITY CONSIDERATION IN O.L.D.

Example	L.C.	Case	$(V_U)_S$ cm^3	$(V_0)_S$ cm^3	Percentage economy $\frac{(V_U)_S-(V_0)_S}{(V_U)_S} \times 100$
5	I	1	95,804	90,438	5.6
		2	95,804	87,640	8.5
		3	95,804	86,712	9.5
6	I	1	164,862	154,342	6.4
		2	164,862	152,063	7.8
		3	164,862	150,856	8.5

Table 6.12 gives the percentage economy for O.L.D. compared to U.S.D. and savings of steel of upto 9.5 percent have been noted.

CHAPTER SEVEN

SUMMARY AND CONCLUSIONS

7.1. SUMMARY

Limit design methods for reinforced concrete frames must satisfy the following three criteria: (1) Compatibility and limited ductility (2) Equilibrium and (3) Serviceability. For optimal limit design the additional requirement is the satisfaction of a selected optimality criterion.

A study of the various limit design methods has shown that they are based on the satisfaction of two of the three criteria stated above. Compatibility methods satisfy the compatibility and limited ductility, and equilibrium condition of the frames. The final design is to be checked separately for the serviceability requirements under working loads. Serviceability methods are based on the limit equilibrium conditions of the governing collapse mechanisms and the serviceability requirements of the frames. It has been pointed out that due to low values of inelastic rotation capacity of some of the critical sections especially in columns carrying heavy axial loads, premature failure may occur before the formation of a collapse mechanism as assumed in the serviceability methods.

The simplified limit method of Baker for the analysis of moments under ultimate load by trial and adjustment procedure has been discussed. For the cases of large frames, it has been observed that this procedure may present problems for convergence of solution. Hence, a computer oriented procedure has been proposed to the simplified limit method. By the modified procedure the frame is analysed in successive steps by adjustment of rotations to obtain the solution that satisfies the compatibility, limited ductility and parity conditions of the frame.

Based on the above study a computer program has been developed for the ultimate load analysis of reinforced concrete frames for different cases of hinge pattern under two loading conditions. The program is based on the generalised compatibility equation due to Munro since it places no restriction as to the location of plastic hinges. The program includes the proposed modified procedure to the simplified limit method

and has facility to determine the moment redistribution at all the critical sections for the specified cases of hinge pattern.

Three reinforced concrete frames have been worked out using the ultimate load analysis program. It has been noted that the proposed procedure by adjustment of rotations yields rapid convergence of solution. The position of plastic hinges as obtained by the ultimate load analysis program for case 2 of the hinge pattern compared well with the plastic hinge pattern at failure obtained by the inelastic stage-by-stage analysis of frames. It has been observed that the amount of moment redistribution in frames depends on the geometry, loading condition, plastic hinge pattern and inelastic rotation capacity of plastic hinge sections. The ultimate load analysis program has been found useful to rationally determine the distribution of moment for any desired plastic hinge pattern.

Limit design methods discussed earlier do not include all the design criteria and the economical merits of the solution are not specifically known. In the present work a linear programming method has been proposed for the optimal limit design of reinforced concrete frames. The optimal frame design problem is to determine the value of design bending moment at all the critical sections such that the optimality, compatibility and limited ductility, equilibrium and serviceability criteria are satisfied. One important simplification which has assisted the process of linearisation is the assumption of known concrete sizes and hence the optimality criterion is confined to minimization of volume of steel reinforcement. The serviceability requirements are satisfied by placing a lower bound for the values of the yield safety parameters. Expressions have been derived for the constraints associated with optimality, compatibility and limited ductility, equilibrium and serviceability criteria of the frame. The optimal limit design problem has been formulated in the standard form of linear programming so that simplex algorithm can be applied for solution.

A computer program has been developed for the formulation and solution of the optimal limit design problem. The program analyses a frame for three different cases of hinge pattern, under each of the two loading conditions, to satisfy specific design requirements. As the linear programming formulation does not include constraints for mechanism conditions of the frame, a computer oriented procedure has been suggested for the position of plastic hinges for cases 2 and 3 of the hinge pattern. The suggested procedure has been shown to be efficient.

Tests conducted on eight T-beams subjected to negative moments at the ends and positive moment near midspan have been described. The experimental results of moment-curvature relations for various sections are compared with the theoretical relations. Based on the study of EI distribution of the test specimens two models have been proposed. Model type 1 has been suggested for use in a rigorous analysis of frames which considers the non-uniform EI distribution for the members. Simplifying assumptions have been made for Model type 2 to derive expressions for the equivalent EI values for T-beams to be used in the calculation of end rotations in frame analysis. The test results have been compared with the calculated values of end rotations using equivalent EI values.

The application of the proposed optimal limit design to practical designs has been illustrated by the examples of six reinforced concrete multi-storey frames. The results of analysis for the distribution of moments and the plastic hinge pattern for optimal solution are discussed. It has been observed that at optimal solution stage the inelastic rotation in some of the column hinges have reached the permissible values. Hence, the need for the inclusion explicitly of the limited ductility constraints in optimal limit design has been emphasized. The economical merits of the optimal limit design are compared with the ultimate strength design based on elastic analysis for factored loads. Savings of steel of upto 10 percent under loading condition I and of upto 20 percent under loading condition II have been noted. In order to study the effect of flexural rigidity of T-beams, two of the design examples have been reworked using the proposed equivalent EI values for beams. The results of this analysis are discussed. For the frames susceptible to instability effects the use in optimal limit design of the magnification factor for lateral loads recommended by a recent investigation has been illustrated by two design examples.

7.2. CONCLUSIONS

The following conclusions can be drawn from the results of this investigation:

1. a) For the ultimate load analysis of reinforced concrete plane frames based on simplified limit method, the proposed modified procedure by adjustment of rotations provides rapid convergence of solution.

b) The ultimate load analysis program developed here offers the designer facility to analyse a frame for different cases of hinge pattern depending on his requirements. The amounts of moment redistribution for different cases of hinge pattern are known from the output of the program. This result will be useful to design the sections such that no plastic hinge appears under working loads as one of the serviceability requirements.

c) The examples of frames presented here illustrate that the recommended design procedure for the ultimate load design of reinforced concrete frames is efficient and practical. However, this design method requires a separate check for serviceability requirements under working load and the economical merits of the design are not specifically known.

2. The proposed linear programming formulation of optimal limit design based on optimality, compatibility and limited ductility, equilibrium and serviceability criteria as the governing constraints, presents a rational unified method for limit design of reinforced concrete frames.

3. The formulation lends itself to computer programming and such an Optimal Limit Design Program developed here offers the following advantages:

a) Additional design constraints that may be necessary from practical considerations, such as symmetry in design, may be included in the program.

b) Any Code Specification for the design of concrete sections which could be approximated to piece-wise linear relationships may be incorporated in the program.

c) Different choice of plastic hinge pattern to satisfy specific design requirements can be analysed by suitable use of the plastic hinge indicator.

4. a) The flexural rigidity, EI, distribution along T-beams subjected to negative moments at the ends and positive moment near midspan is non-uniform and that due to inelastic behaviour of the three critical sections, the support and midspan sections, the curvatures at these sections are markedly increased with a consequent reduction in their flexural rigidities. This significant reduction in flexural rigidity is concentrated over a distance on either side of critical sections depending on the spread of inelastic behaviour to the adjacent sections.

b) The simplified design procedure suggested here can be used to determine the equivalent EI value for T-beams and this EI_e value can be used for the calculation of end rotations of T-beams in frame analysis.

5. a) The percentage economy of steel reinforcement for the optimal limit design compared to ultimate strength design depends on the geometry, loading condition and choice of plastic hinge pattern.

b) The variation of flexural rigidity of beams due to T-beam action has considerable influence on the distribution of bending moment and on the percentage economy of optimal design. Additional savings have been noted by using equivalent EI values for T-beams.

c) For the cases of sway frames susceptible to instability effects the magnification factor to lateral loads suggested by a recent investigation can be used in optimal limit design.

c) Practical design examples show significant savings in flexural steel reinforcement by the use of the proposed optimal limit design method.

7.3. RECOMMENDATIONS FOR FUTURE RESEARCH

The present work has shown the application of linear programming technique to the development of an optimal limit design method for reinforced concrete frames which considers various design criteria of interest. Further research is required on several areas of this subject and they are briefly described in the following:

1. Limit design of reinforced concrete frames may require consideration of several loading schemes. Extension of the proposed method to deal with these situations requires further work to express the mechanism criteria of the frame as one of the governing constraints.

2. The optimality criterion selected in this study was the minimisation of the total volume of steel reinforcement. If the overall minimum material cost is to be achieved the objective function should include the cost of concrete and shear reinforcement in addition to the longitudinal reinforcement. Further research is required to include these factors in the optimality criterion.

3. The flexural rigidity of reinforced concrete members forms an important parameter in the deformation calculations. Further experimental investigation is needed on continuous T-beams and columns to study the EI values to be used in the optimal limit design of frames.

4. The serviceability criteria for the optimal limit design was expressed through the yield safety parameters for critical sections. Experimental investigation is very much needed in this area to study the behaviour under working loads of reinforced concrete frame members and to specify the limits for the various serviceability criteria. This work would enable to stipulate safe lower bound values for the yield moment factors for the critical sections.

5. A comprehensive programme of research is required for the development of a non-linear analysis program that predicts cracking, stress pattern and deformations of frames under various stages of loading and for experimental investigation on frames to verify the analytical methods. This study would provide the facility to verify the adequacy of the simplified models for the parameters discussed above and to check the assumptions made in the development of optimal limit design methods.

REFERENCES

1. Baker, J.F., Horne, M.R. and Heyman, J. — "The Steel Skeleton", Vol. 2, Cambridge University Press, 1956.

2. Hodge, P.G. — "Plastic Analysis of Structures", McGraw-Hill Book Co., New York, 1959.

3. Neal, B.G. — "Plastic Methods of Structural Analysis", Chapman and Hall Ltd., London, Second Edition, 1963.

4. Heyman, J. — "An Approach to the Design of Tall Buildings", Proceedings, The Institution of Civil Engineers, London, V.17, December 1960, pp.431-454.

5. Heyman, J. — "Plastic Design of Frames", Vol. 2. Applications, Cambridge University Press, 1971.

6. Horne, M.R. — "Plastic Theory of Structures", Nelson, London, 1971.

7. Baker, A.L.L. — "The Ultimate Load Theory Applied to the Design of Reinforced and Pre-stressed Concrete Frames", Concrete Publications Limited, London, 1956.

8. Baker, A.L.L. — "Ultimate Load Theory for Concrete Frame Analysis", Transactions, American Society of Civil Engineers, V.127, Part II, 1962, pp. 561-596.

9. Report of the Research Committee. — "Ultimate Load Design of Concrete Structures", The Institution of Civil Engineers, London, 1964, p. 104.

10. Baker, A.L.L. and Amarakone, A.M.N. — "Inelastic Hyperstatic Frames Analysis", Proceedings, International Symposium on Flexural Mechanics of Reinforced Concrete, Miami, Florida, 1964, ACI Special Publication SP-12, pp. 85-142.

11. Baker, A.L.L. "Fully Plastic Analysis and Design", Paper presented at the ASCE - IABSE International Conference on Planning and Design of Tall Buildings, Lehigh University, Bethlehem, Pennsylvania, August 21-26, 1972.

12. Baker, A.L.L. "Limit-State Design of Reinforced Concrete", Cement and Concrete Association, London, 1970.

13. Baker, A.L.L. "The Inelastic Space Frame", Concrete Publications Ltd., London, 1967.

14. Amarakone, A.M.N. "Limit Design of Reinforced Concrete Skeletal Structures", Ph.D. Thesis, University of London, 1966.

15. Macchi, G. "A Proposal of Analysis on the Theory of Imposed Rotations", Bulletin d'Information, CEB, No. 21, 1960, pp. 121-158.

16. Sawyer, H.A., Jr. "Design of Concrete Frames for Two Failure Stages", Proceedings, International Symposium on Flexural Mechanics of Reinforced Concrete, Miami, Florida, 1964, ACI Special Publication SP-12, pp.405-437.

17. Petcu, V. "The Optimum Redistribution Principle", The Indian Concrete Journal, V.35, No. 7, July 1961, pp. 259-260.

18. Cohn, M.Z. "Limit Design Solutions for Concrete Structures", Journal of the Structural Division, Proceedings of the American Society of Civil Engineers, V.93, No. ST 1, February 1967, pp. 37-57.

19. Cohn, M.Z. "Limit Design of Reinforced Concrete Frames", Journal of the Structural Division, Proceedings of the American Society of Civil Engineers, V. 94, No. ST 10, October 1968, pp. 2467-2483.

20. Cohn, M.Z., Burnett, E.F.P. and Grierson, D.E. "Safety, Serviceability and Efficiency of Limit Design for Reinforced Concrete Beams and Frames", Publications, International Association for Bridge and Structural Engineering, V.29-I, 1969, pp. 17-32.

21. Cohn, M.Z. and Grierson, D.E. "Further Results on the Equilibrium Method of Limit Design", Proceedings, The Institution of Civil Engineers, London, V.46, June 1970, pp. 143-168.

22. Cohn, M.Z., et al. "Application of Limit Design to Reinforced Concrete Building Structures", Proceedings, The Institution of Civil Engineers, London, Supplement (xvii), Paper 7335 S, 1970, pp. 375-414.

23. Charnes, A. and Greenberg, H.J. "Plastic Collapse and Linear Programming", American Mathematical Society, Abstract No. 506, 1951.

24. Dorn, W.S. and Greenberg, H.J. "Linear Programming and Plastic Limit Analysis of Structures", Quarterly of Applied Mathematics, Vol. XV, 1959, pp. 155-167.

25. Charnes, A., Lemke, C.E. and Zienkiewicz, O.C. "Virtual Work, Linear Programming and Plastic Limit Analysis", Proceedings, Royal Society, London, Series A, V. 251, 1959, pp. 110-116.

26. Grierson, D.E. and Gladwell, G.M.L. "Collapse Load Analysis Using Linear Programming", Journal of the Structural Division, Proceedings of the American Society of Civil Engineers, V. 97, No. ST 5, May 1971, pp. 1561-1573.

27. Neal, B.D. and Symonds, P.S. "The Calculation of Collapse Loads for Framed Structures", Proceedings, The Institution of Civil Engineers, London, Part III, No. 1, 1952, pp. 58-71.

28. Cohn, M.Z., Ghosh, S.K. and Parimi, S.R. "A Unified Approach to the Theory of Plastic Structures", Solid Mechanics Report Series, University of Waterloo, Report No. 78, May 1971, p. 30.

29. Foulkes, J.D. "Minimum Weight Design and the Theory of Plastic Collapse", Quarterly of Applied Mathematics, V. 10, January 1953, pp. 347-358.

30. Foulkes, J.D. "The Minimum Weight Design of Structural Frames", Proceedings, Royal Society, London, Series A, V. 223, 1954, pp. 482-494.

31. Livesley, R.K. "The Automatic Design of Structural Frames", Quarterly Journal of Mechanics and Applied Mathematics, V.8, No. 3, September 1956, pp. 257-278.

32. Kawai, T. "Plastic Analysis and Minimum Weight Design of Multi-Storey Plane Frames", Guest Lectures, 1965, Summer Conference on Plastic Design of Multi-Storey Frames, Lehigh University, 1966, Fritz Engineering Laboratory Report 273-46, pp. 21-56.

33. Rubinstein, M.F. and Karagozian, J. "Building Design Using Linear Programming", Journal of the Structural Division, Proceedings of the American Society of Civil Engineers, V. 92, No. ST 6, December 1966, pp. 223-245.

34. Toakley, A.R. "The Optimum Plastic Design of Unbraced Frames", Civil Engineering Transactions, The Institution of Engineers, Australia, V. CE 11, No. 2, October 1961, pp. 111-116.

35. Horne, M.R. and Morris, L.J. "Optimum Design of Multi-Storey Rigid Frames", Paper presented at the International Symposium on Computers in Optimisation of Structural Design, University of Wales, Swansea, January 1972.

36. Munro, J. "The Elastic and Limit Analysis of Planar Skeletal Structures", Civil Engineering and Public Works Review, V. 60, No. 706, May 1965, pp. 671-677.

37. Munro, J. "The Stress Analysis and Topology of Skeletal Structures", Concrete Structures and Technology Research Report, CSTR 14, Imperial College, London, March 1965.

38. Munro, J and Smith, D.L. "Linear Programming Duality in Plastic Analysis and Synthesis", Paper presented at the International Symposium on Computer-Aided Structural Design, University of Warwick, July 1972.

39. Cohn, M.Z. and Grierson, D.E. "Optimal Design of Reinforced Concrete Beams and Frames", Final Report, 8th IABSE Congress, 1968, pp. 215-226.

40. Grierson, D.E. "Optimal Design of Reinforced Concrete Frames", Ph.D. Thesis, University of Waterloo, Ontario, Canada, 1968.

41. Cohn, M.Z. and Grierson, D.E. "An Automatic Approach to the Analysis of Plastic Frames Under Fixed and Variable Loading", The Structural Engineer, V. 49, No. 7, July 1971, pp. 291-297.

42. Grierson, D.E. and Cohn, M.Z. "A General Formulation of the Optimal Frame Problem", Transactions ASME, Journal of Applied Mechanics, June 1970, pp. 356-360.

43. Burnett, E.F.P. "The Ultimate Load Design of Statically Indeterminate Concrete Structures", M.Sc. Thesis, University of London, 1962.

44. Burnett, E. "Flexural Rigidity, Curvature and Rotation and their Significance in Reinforced Concrete Design", Magazine of Concrete Research, V.16, No. 47, June 1964, pp. 67-72.

45. Amarakone, A.M.N. and Yu, C.W. "Flexural Stiffness of R.C. Members for Ultimate Load Design", Civil Engineering and Public Works Review, November 1965, pp. 1637-1641.

46. Burnett, E.F.P. and Yu, C.W. "Reinforced Concrete Linear Structures at Ultimate Load", Proceedings, International Symposium on Flexural Mechanics of Reinforced Concrete, Miami, Florida, 1964, ACI Special Publication SP.12, pp. 29-52.

47. Palmer, B.E. "The Ultimate Strength of Reinforced Concrete Space Frames", Ph.D. Thesis, University of London, 1968.

48. Chan, W.W.L. "An Investigation into the Characteristics of Plastic Hinges in Reinforced Concrete", Ph.D. Thesis, University of London, 1954.

49. Mattock, A.H. "Rotational Capacity of Hinging Regions in Reinforced Concrete Beams", Proceedings, International Symposium on Flexural Mechanics of Reinforced Concrete, Miami, Florida, 1964, ACI Special Publication SP.12, pp. 143-181.

50. Corley, W.G. "Rotational Capacity of Reinforced Concrete Beams", Journal of the Structural Division, Proceedings of the American Society of Civil Engineers, V.92, No. ST 5, October 1966, pp. 121-146.

51. Soliman, M.T.M. "Ultimate Strength and Plastic Rotation Capacity of Reinforced Concrete Members", Ph.D. Thesis, University of London, 1966.

52. Burnett, E.F.P. and Trenberth, R.J. "Column Load Influence on Reinforced Concrete Beam-Column Connection", ACI Journal, V.69, No. 2, February 1972, pp. 101-109.

53. Nahhas, U. "The Inelastic Behaviour of Reinforced Concrete Sway Frames with Special Reference to Instability", Ph.D. Thesis, University of London, 1970.

54. Nahhas, U. and Yu, C.W. "The Elastic-Plastic Design of Reinforced Concrete Sway Frames against Instability", Proceedings, The Institution of Civil Engineers, London, V.53, Part 2, June 1972, pp. 41-56.

55. Livesley, R.K. "Matrix Methods of Structural Analysis", Pergamon Press Ltd., London, 1964, pp. 230-258.

56. Winter, G., Urquhart, L.C., O'Rourke, C.E. and Nilson, A.H. "Design of Concrete Structures", McGraw-Hill Book Co., New York, Seventh Edition, 1964, pp. 392-393.

57. Dunham, C.W. "Advanced Reinforced Concrete", McGraw-Hill Book Co., New York, 1964, pp. 222-226.

58. Dantzig, G.B. "Linear Programming and Extensions", Princeton University Press, Princeton, 1963.

59. Hadley, G. "Linear Programming", Addison-Wesley Publishing Co., Reading, Mass. 1962.

60. ACI "Causes, Mechanism and Control of Cracking in Concrete", ACI Publications, SP-20, 1968.

61. Morice, P.B. "Linear Structural Analysis", Thames and Hudson, London 1959.

62. British Standards Institution Draft British Standard Code of Practice for the Structural Use of Concrete, British Standards Institution, London, 1970.

63. CEB Recommendations for an International Code of Practice for Reinforced Concrete, Cement and Concrete Association, London, 1965.

64. Regan, P.E. and Placas, A. "Limit-State Design for Shear in Rectangular and T-Beams", Magazine of Concrete Research, V. 22, No. 73, December 1970, pp. 197-208.

65. Hognestad, E., Hanson, N. and McHenry, D. "Concrete Stress Distribution in Ultimate Strength Design", ACI Journal, V.52, No. 4, December 1955, pp. 455-479.

66. Rüsch, H. "Researches Toward a General Flexural Theory for Structural Concrete", ACI Journal, V.57, No. 1, July 1960, pp. 1-28.

67. Sargin, M. "Stress-Strain Relationships for Concrete and the Analysis of Structural Concrete Sections", Study No. 4, Solid Mechanics Division, University of Waterloo, Ontario, Canada, 1971, p. 167.

68. Macchi, G. "Non-Linear Analysis and Limit Design", Theme Report, ASCE-IABSE International Conference on Planning and Design of Tall Buildings, Lehigh University, Pennsylvania, August 1972, Reports Vol. III - 22, pp. 1-20.